IMPACT OF CLIMATE CHANGE ON HYDROLOGY AND WATER RESOURCES IN THE UPPER ZAMBEZI RIVER BASIN

By

George Zayeqa Ndhlovu

A thesis submitted in fulfilment of the requirements for the degree

Doctorate of Engineering in Civil Engineering

In the

Department of Civil Engineering

Of the

Faculty of Engineering, Built Environment and Information Technology

Of the

Central University of Technology, Free State, South Africa

Supervisor: Prof YE Woyessa

Co-supervisor: Dr SV Raghavan

November 2019

DECLARATION

I declare that all the work written in this thesis is my own and where other materials are used, they have been duly acknowledged. The thesis is submitted by me for the degree *Doctorate of Engineering in Civil Engineering* at the Central University of Technology, Free State, Bloemfontein. It is my own independent work and has not been submitted by me to another university and/or faculty in order to obtain a degree. I further cede copyright of this thesis in favour of the Central University of Technology, Free State, Bloemfontein. I, George Zayeqa Ndhlovu, further declare that:

(a) This thesis does not contain other people's data, writings, pictures, graphs or other information unless specifically acknowledged as being sourced from other researchers or persons.

(b) This thesis does not contain text, graphics or tables copied and pasted from the Internet, unless specifically acknowledged, and the source being detailed in the thesis and in the references sections.

George Zayeqa Ndhlovu

Signature: _____

Date: November 2019

Bloemfontein, South Africa

ABSTRACT

According to the Inter-Governmental Panel on Climate Change (IPCC), the Southern African region is regarded as one of the most vulnerable regions in Africa. The Zambezi River Basin (ZRB), the largest basin in Southern Africa is characterised by spatial and temporal rainfall variability, and in some cases, scarce water resources. Climate change is likely to affect nearly every aspect of human well-being; from agricultural productivity and energy use to flood control, municipal and industrial water supply to wildlife management. There are few studies focussed on hydrology and climate change at a local catchment scale in the ZRB, therefore, this research sought to investigate the severity of the impacts of climate change on hydrology and water resources for the purposes of evaluation for sustainable planning and management of the resources. The review of water resources linkage to climate variability showed occurrences of floods,droughts,uneven distribution of water resources,rising temperatures and high evapotranspiration rates. The technology of using Climate Forecasting System Reanalysis (CFSR) data to estimate water resources in data scarce regions such as Southern Africa showed results that were satisfactory. Providing Regional Climate Impact Studies (PRECIS) model results proved to be reliable with a sufficient model skill that predicted an increase in rainfall and temperature while predicting a decrease in other areas within the same basin. The results from six downscaled bias-corrected Global Climate Models (GCM) were focussed on 2020-2050.The results under RCP4.5 climate scenario, predicted a seasonal increase in rainfall,runoff and water yield in December, January and February (DJF) while the changes in the rest of the seasons were generally insignificant. The annual rainfall was predicted to decrease by 0.7% while water yield and runoff would increase by 5% and 6%, respectively. The results

under RCP8.5 climate scenario predicted seasonal increases of runoff at 211% and rainfall at 35% indicating a strong likelyhood of occurrence of an extreme flood event. Annual statistics show a significant increase of 65%, 40% and 19% in runoff, water yield and rainfall, respectively. The basin under RCP4.5 climate scenario is predicted with insignificant changes with baseline in monthly, seasonal and annual flow regime. The majority of GCMs under RCP8.5 climate scenario indicate 4-8% increase in streamflow while the intra-annual and inter-annual streamflow variability will increase by a considerable margin. There is also a significant increase in seasonal streamflow that ranges between 34 - 134%. The future climate change impact studies need to focus on RCP4.5 and RCP8.5 for 2050-2100 in order to assess and evaluate any possible future impact on hydrology and water resources.

ACKNOWLEDGEMENTS

Many thanks go to specific individuals and institutions for their role in the completion of my studies. I wish to acknowledge Professor Yali Woyessa, my supervisor for his unwavering support. His knowledge, expertise and supervision throughout the research has been much appreciated. Thank you to Dr SV Raghavan, my co-supervisor, for his guidance and general support. Also, Mr David Heinn, Dominic Kuetz and Van Rooyen Mauritz for all the IT support and technical assistance in running the experiments on Linux machines and operations. I also thank my wife, Mercy and our three daughters for their encouragement, love, patience and support during my studies.

Further acknowledgements go to the Rectorate and relevant functionalities from Central University of Technology, Free State, for the support rendered; the Central University of Technology, National Research Foundation and the Department of Higher Education and Training (DHET) for the financial support given to help me complete my studies.

Many thanks also go to the Government of the Republic of Zambia (GRZ) through Ministry of Water Resources, Sanitation and Environmental Protection, Water Resources Management Authority (WARMA) and Zambia Meteorological Department (ZMD) for their support and for facilitating the provision of the necessary data.

Finally, and above all, I wish to give thanks to the Lord, my God for He is good and His love endures forever (Ps 136:1).

TABLE OF CONTENTS

Page

DECLARATION II
ABSTRACT III
ACKNOWLEDGEMENTS V
TABLE OF CONTENTS VI
LIST OF TABLES X
LIST OF FIGURES XI
LIST OF APPENDICES XIV
LIST OF ABBREVIATIONS XVI

CHAPTER 1 : INTRODUCTION 1

1.1 BACKGROUND 1
1.2 PROBLEM STATEMENT 4
1.3 AIM AND OBJECTIVES 6
1.4 SCOPE OF STUDY 7
1.5 STRUCTURE OF THE THESIS 7

CHAPTER 2 : LITERATURE REVIEW 11

2.1 CLIMATE CHANGE 11
2.1.1 Climate Sensitivity 12
2.1.2 Climate Change Modelling 13
2.1.3 Methodologies for Climate Change Impact Assessments 14
2.1.4 Dynamical and Statistical Downscaling Techniques 18
2.1.5 Model Validation and Evaluation 18
2.1.6 Downscaling GCM Projections to Regional Scale 20
2.1.7 Representative Concentration Pathways 22
2.1.8 Bias Corrections 24
2.1.9 Uncertainty 26
2.2 HYDROLOGY AND WATER RESOURCES 27
2.2.1 Gridded Climate Data 28
2.2.2 Flood Frequency Analysis 32
2.2.3 Flow Duration Curves 33
2.2.4 Hydrological Modelling 34
2.2.5 Model Calibration and Validation 35

2.2.6 Hydrological models commonly used in climate change Impact studies. 35
2.2.7 Water Resources Management 39

CHAPTER 3 : RESEARCH METHODOLOGY 42

3.1 DESCRIPTION OF THE ZAMBEZI RIVER BASIN.....42
3.1.1 Description and Location of Kabompo River Basin 44
3.2 BIOPHYSICAL DATA 45
3.3 CLIMATE CHANGE MODELLING.....46
3.3.1 Regional Climate modelling using PRECIS Model.....47
3.4 HYDROLOGICAL MODELLING USING SWAT MODEL 50
3.4.1 Estimation of Water Yield 51
3.4.2 Calibration, uncertainty and sensitivity analysis 51
3.5 EVALUATION OF CLIMATE CHANGE IMPACT ON HYDROLOGY AND WATER RESOURCES....54

CHAPTER 4 :STATUS OF HYDROLOGY, WATER RESOURCES AND CLIMATE VARIABILITY 56

4.1 INTRODUCTION 56
4.2 MATERIALS AND METHODS 58
4.3 CLIMATE VARIABILITY IN THE ZAMBEZI RIVER BASIN 59
4.4 HYDROLOGY OF THE ZAMBEZI RIVER BASIN.....61
4.5 WATER RESOURCES IN THE ZAMBEZI RIVER BASIN 63
4.6 LAND USE/COVER OF THE ZRB.....64
4.7 CLIMATE CHANGE AND WATER RESOURCES IN THE ZRB.....65
4.7.1 Drought 66
4.7.2 Floods 68
4.8 CONCLUSION 69

CHAPTER 5 : HYDROLOGICAL MODELLING USING GRIDDED CLIMATE DATA.....71

5.1 . INTRODUCTION.....71
5.2 MATERIALS AND METHODS 72
5.2.1 Data sets.....72
5.2.2 SWAT Model set up 75
5.2.3 Performance Indices 77
5.3 RESULTS AND DISCUSSION.....79
5.3.1 Comparison of observed and CFSR rainfall data.....79
5.3.2 Calibration, uncertainty and sensitivity analysis 86
5.3.3 Land use/cover.....90
5.3.4 Soil.....92

5.3.5 Calibration and validation 94
5.3.6 Uncertainty Analysis 96
5.3.7 Goodness-of-Fit 97
5.3.8 Simulation of stream flow and water yield 99
5.4 CONCLUSION 104

CHAPTER 6 : REGIONAL CLIMATE MODELLING 106

6.1 INTRODUCTION 106
6.2 DOMAIN AREA 108
6.3 MATERIALS AND METHODS 108
6.3.1 Precis Experiment Set Up 110
6.3.2 Procedure for Estimation of Climate Change Impact 112
6.4 RESULTS AND DISCUSSION 113
6.4.1 Validation of PRECIS Experiment Results 114
6.4.2 Time Series of Future Climate 120
6.4.3 Future Climate Change under RCP4.5 (2020-2050) 126
6.4.4 Future Climate Change under RCP8.5 (2020-2050) 130
6.5 CONCLUSIONS 134

CHAPTER 7 : MODELLING IMPACT OF CLIMATE CHANGE ON CATCHMENT WATER BALANCE 137

7.1 INTRODUCTION 137
7.2 MATERIALS AND METHODS 138
7.2.1 Description of the GCMs 138
7.2.2 GCM Projections and Data Source 140
7.2.3 Prediction of Changes in Hydrology & Water Resources 141
7.2.4 Modelling Climate Change Impact Using SWAT 142
7.3 RESULTS AND DISCUSSION 143
7.3.1 Comparisons of Means for PRECIS, CRU,GCM Ensemble and Observed Climate Data 143
7.3.2 Impact of Climate Change on Catchment Water Balance 149
7.3.3 Baseline Seasonal Catchment Water Balance 153
7.3.4 Future Changes in Catchment Water Balance under RCP4.5 155
7.3.5 Future Changes in Catchment Water Balance under RCP8.5 159
7.3.6 Analysis of Water Balance under RCP4.5 and RCP8.5 165
7.4 CONCLUSION 167

CHAPTER 8 : ASSESSMENT OF IMPACT OF CLIMATE CHANGE ON STREAMFLOW 171

8.1 INTRODUCTION 171
8.2 MATERIALS AND METHODS 172
8.2.1 Hydrological Statistics 173
8.3 RESULTS AND DISCUSSION 173
8.3.1 Simulated Streamflow under three Climate Scenarios 175
8.3.2 Monthly Streamflow Analysis 177
8.3.3 Seasonal Flow Analysis 184
8.3.4 Intra-Annual Flow Analysis 185
8.3.5 Intra-Annual and Inter-Annual Streamflow Variability 187
8.3.6 Analysis of Flood Frequency in a changing Climate 190
8.3.7 Variability of streamflow under Flow Duration Curves 194
8.4 CONCLUSION 199

CHAPTER 9 : CONCLUSION AND RECOMMENDATIONS 201

9.1 INTRODUCTION 201
9.2 HYDROLOGICAL MODELLING WITH ALTERNATIVE TECHNOLOGY 202
9.3 PRECIS EVALUATION OF CLIMATE CHANGE IMPACTS 203
9.4 EVALUATION OF IMPACT OF CLIMATE CHANGE ON WATER BALANCE 205
9.5 ANALYSIS OF IMPACT OF CLIMATE CHANGE ON STREAMFLOW 207
9.6 GENERAL RESEARCH FINDINGS 208
9.7 RECOMMENDATIONS FOR FUTURE RESEARCH 209

REFERENCES 211

APPENDICES 229

LIST OF TABLES

TABLE 2.1 SOME HYDROLOGICAL MODELS USED IN CLIMATE CHANGE STUDIES.....38
TABLE 3.1 PERFORMANCE RATING FOR RECOMMENDED STATISTICS (MORIASI ET AL.2007).....53
TABLE 4.1 WATER USE/CONSUMPTION IN ZRB.....64
TABLE 4.2 IMPACT OF CLIMATE CHANGE INDUCED FLOODS 2000-2009.....68
TABLE 5.1 ESTIMATED COEFFICIENT OF VARIATION.....85
TABLE 5.2 GLOBAL SENSITIVITY OF PARAMETERS.....89
TABLE 5.3 LAND USE TYPES ACCORDING TO THE SWAT CLASSIFICATION.....92
TABLE 5.4 BASIN SOIL COVERAGE PERCENTAGE.....94
TABLE 5.5 FITTED PARAMETER VALUES.....98
TABLE 5.6 STATISTICAL INDEX FOR CALIBRATION (1982-1997) AND VALIDATION (1998-2005).....99
TABLE 7.1 SUMMARY OF GCMS USED IN THE STUDY.....140
TABLE 7.2 ANNUAL CHANGES UNDER RCP 4.5.....159
TABLE 7.3 ANNUAL CHANGES UNDER RCP 8.5.....165
TABLE 7.4 ANNUAL WATER BALANCE CHANGES.....167
TABLE 8.1 MEAN CVS BASED ON SIX GCMS.....189

LIST OF FIGURES

FIGURE 2.1 THE CONCEPT OF SPATIAL DOWNSCALING (SOURCE:VINER,2012) 21
FIGURE 3.1 LOCATION OF ZAMBEZI RIVER BASIN AND KABOMPO RIVER BASIN.....43
FIGURE 3.2 CLIMATE CHANGE MODELLING PROCESS.....49
FIGURE 3.3 OVERVIEW OF THE SWAT PROCESS 54
FIGURE 4.1 LOCATION OF THE LARGEST MAN-MADE RESERVOIRS IN THE WORLD 57
FIGURE 4.2 COMPARISONS OF MAP AND PET IN THE UPPER ZRB 60
FIGURE 4.3 COMPARISONS OF MAP AND PET IN THE MIDDLE ZRB.....60
FIGURE 4.4 COMPARISONS OF MAP AND PET IN THE LOWER ZRB 61
FIGURE 4.5 COMPARISONS OF MAP AND MAR IN THE ZRB 62
FIGURE 4.6 MEAN SUB-BASIN FLOWS IN THE ZRB (DATA SOURCE: WORLD BANK,2010).....62
FIGURE 4.7 MEAN DECADAL TEMPERATURE RISE (SOURCE:YOUNG ET AL. 2010).....66
FIGURE 4.8 TOTAL NUMBER OF PEOPLE AFFECTED IN THE ZAMBEZI RIPARIAN STATES 67
FIGURE 5.1 DIGITAL ELEVATION MODEL OF THE KRB 75
FIGURE 5.2 THE SUB-BASINS OF THE KRB 77
FIGURE 5.3 DISTRIBUTION OF CFSR AND GROUND WEATHER STATIONS 80
FIGURE 5.4 SPATIAL DISTRIBUTION OF ANNUAL RAINFALL FOR CFSR (A) ANDOBSERVED (B).....81
FIGURE 5.5 RELATIONSHIP BETWEEN CFSR AND OBSERVED MEAN MONTHLY RAINFALL 82
FIGURE 5.6 COMPARISON OF AVERAGE MONTHLY CFSR AND OBSERVED RAINFALL.....83
FIGURE 5.7 CFSR AND OBSERVED ANNUAL RAINFALL (1982-2013).....84
FIGURE 5.8 COMPARISON OF CV OF OBSERVED AND CFSR SEASONAL RAINFALL 1982-2013 86
FIGURE 5.9 KRB LAND-USE/LAND COVER FOR 2010 91
FIGURE 5.10 SPATIAL DISTRIBUTION OF SOIL IN KRB 93
FIGURE 5.11 CALIBRATED OF SWAT MODEL.....95
FIGURE 5.12 VALIDATED OF SWAT MODEL 95
FIGURE 5.13 COMPARISONS OF CALIBRATED AND VALIDATED OF SWAT MODEL.....96
FIGURE 5.14 MONTHLY SIMULATED AND OBSERVED FLOW VERSUS MONTHLY RAINFALL 100
FIGURE 5.15 COMPARISON OF ANNUAL WATER YIELD AND CFSR ANNUAL RAINFALL 101
FIGURE 5.16 AVERAGE MONTHLY CFSR RAINFALL AND WATER YIELD (1982-2013) 102
FIGURE 5.17 WATER YIELD VARIABILITY MAP (1982-2013).....103
FIGURE 6.1 DOMAIN AREA USED IN PRECIS EXPERIMENT 108
FIGURE 6.2 CLIMATE CHANGE MODELLING PROCESS WITH PRECIS 110
FIGURE 6.3 COMPARISON OF PRECIS MODEL AND OBSERVED RAINFALL IN MM/DAY. 116
FIGURE 6.4 COMPARISON OF PRECIS AND OBSERVED TEMPERATURE IN ^{O}C 119
FIGURE 6.5 MONTHLY COMPARISON OF PRECIS BASELINE AND CRU OBSERVED TEMPERATURE121
FIGURE 6.6 COMPARISON OF PRECIS AND CRU OBSERVED BASELINE MONTHLY RAINFALL 122

FIGURE 6.7 COMPARISON OF DAILY PRECIS BASELINE AND CRU RAINFALL IN A MONTH 123
FIGURE 6.8 MONTHLY PRECIS PRECIPITATION MODEL BIASES 124
FIGURE 6.9 MONTHLY TEMPERATURE PRECIS MODEL BIASES 125
FIGURE 6.10 PREDICTED FUTURE SEASONAL RAINFALL BASED ON RCP4.5 127
FIGURE 6.11 PREDICTED FUTURE SEASONAL TEMPERATURE BASED ON RCP4.5 129
FIGURE 6.12 PREDICTED FUTURE SEASONAL RAINFALL BASED ON RCP8.5 131
FIGURE 6.13 PREDICTED FUTURE SEASONAL TEMPERATURE BASED ON RCP8.5 133
FIGURE 7.1 LOCATION OF WEATHER STATIONS 144
FIGURE 7.2 COMPARISONS OF AVERAGE MONTHLY TEMPERATURE 145
FIGURE 7.3 COMPARISONS OF AVERAGE MONTHLY RAINFALL 146
FIGURE 7.4 COMPARISONS OF TEMP AND RAINFALL FOR OBSERVED AND ENSEMBLE MEANS 147
FIGURE 7.5 MONTHLY OBSERVED VS ENSEMBLE BASELINE RAINFALL 148
FIGURE 7.6 SIMULATED ENSEMBLE AND THE MEAN FOR BASELINE RAINFALL AND WATER YIELD150
FIGURE 7.7 SIMULATED ENSEMBLE AND THE MEAN FOR BASELINE RAINFALL AND RUNOFF 151
FIGURE 7.8 SIMULATED ENSEMBLE AND THE MEAN FOR BASELINE MONTHLY ET 153
FIGURE 7.9 SEASONAL WATER BALANCE OF THE BASELINE PERIOD 154
FIGURE 7.10 MONTHLY CHANGES IN CATCHMENT WATER BALANCE UNDER RCP4.5 156
FIGURE 7.11 AVERAGE MONTHLY CHANGES UNDER RCP4.5 157
FIGURE 7.12 SEASONAL CHANGES UNDER RCP4.5 158
FIGURE 7.13 MONTHLY CHANGES IN CATCHMENT WATER BALANCE UNDER RCP8.5 160
FIGURE 7.14 AVERAGE MONTHLY CHANGES UNDER RCP8.5 163
FIGURE 7.15 SEASONAL CHANGES UNDER RCP8.5 164
FIGURE 8.1 BASELINE AND FUTURE TEMPERATURE VARIABILITY 174
FIGURE 8.2 (A) SIMULATED ENSEMBLE AND THE MEAN FOR STREAMFLOW UNDER BASELINE 175
FIGURE 8.2 (B) SIMULATED ENSEMBLE AND THE MEAN FOR STREAMFLOW UNDER RCP4.5 176
FIGURE 8.3 STREAMFLOW SIMULATIONS BASED ON INDIVIDUAL GCMS 178
FIGURE 8.4 MONTHLY ENSEMBLE MEAN STREAMFLOW 182
FIGURE 8.5 ENSEMBLE MEAN STREAMFLOW CHANGES 183
FIGURE 8.6 COMPARISONS OF CHANGE IN SEASONAL FUTURE STREAMFLOW 184
FIGURE 8.7 INTRA-ANNUAL STREAMFLOW SIMULATIONS BASED ON SIX GCMS UNDER RCP4.5 186
FIGURE 8.8 MONTHLY STREAMFLOW FOR SIX GCMS UNDER RCP8.5 186
FIGURE 8.9 ENSEMBLE MEAN ANNUAL FLOWS 187
FIGURE 8.10 COMPARISONS OF CVS 189
FIGURE 8.11 COMPARISONS OF FLOOD FREQUENCY CURVES FOR TWO PERIODS 192
FIGURE 8.12 FLOW DURATION CURVES FOR ENSEMBLE STREAMFLOW UNDER BASELINE 195
FIGURE 8.13 FLOW DURATION CURVES FOR ENSEMBLE STREAMFLOW UNDER RCP45 196

FIGURE 8.14 FLOW DURATION CURVES FOR ENSEMBLE STREAMFLOW UNDER RCP8.5.....197
FIGURE 8.15 FDC FOR PERCENTAGE CHANGE IN AVERAGE ENSEMBLE UNDER RCP8.5.....198

APPENDICES

APPENDIX A TABLE A1 KABOMPO SUB BASIN AREAS 229
APPENDIX B FIGURE B1 THE EXTRACTED BASIN FROM MOSAIC DEM 232
APPENDIX C TABLE C1 CALIBRATION FLOW DATA 1982-1997 234
APPENDIX C TABLE C2 VALIDATION FLOW DATA 1998-2005…….. ……..237
APPENDIX D TABLE D1 GRIDDED RAINFALL FROM CFSR 238
APPENDIX E PRECIS (RCM) AVERAGE CLIMATE DATA 1975-2005 242
APPENDIX E TABLE E1 PRECIS (RCM) AVERAGE TEMPERATURE DATA 1975-2005.....242
APPENDIX E TABLE E2 PRECIS (RCM) AVERAGE PRECIPITATION DATA 1975-2005 242
APPENDIX F CRU (OBSERVED) DATA 1975-2005.....243
APPENDIX F TABLE F1 CRU TEMPERATURE (^{O}C) DATA 1975-2005.....243
APPENDIX F TABLE F2 CRU PRECIPITATION 1975-2005.....243
APPENDIX G FIGURE G1 GRAPHICAL RAINFALL COMPARISONS FOR MAM & JJA.....244
APPENDIX G FIGURE G2 GRAPHICAL RAINFALL COMPARISONS FOR SON & DJF.....245
APPENDIX H FIGURE H1 GRAPHICAL TEMP COMPARISONS FOR MAM & JJA 246
APPENDIX H FIGURE H2 GRAPHICAL TEMP COMPARISONS FOR SON & DJF 247
APPENDIX I SIMULATED RAINFALL FOR BASELINE AND RCP 4.5.....248
APPENDIX I TABLE I1 SIMULATED RAINFALL FOR BASELINE AND RCP 4.5.....248
APPENDIX I TABLE I2 SIMULATED RAINFALL FOR RCP 8.5 (MM) 249
APPENDIX J TABLE J1 SIMULATED RUNOFF FOR BASELINE 249
APPENDIX J TABLE J2 SIMULATED RUNOFF FOR RCP 4.5 AND RCP 8.5 (MM).....250
APPENDIX K TABLE K1 SIMULATED WATER YIELD FOR BASELINE (MM).....251
APPENDIX K TABLE K2 SIMULATED WATER YIELD FOR RCP 4.5 (MM).....251
APPENDIX K TABLE K3 SIMULATED WATER YIELD FOR RCP 8.5 (MM).....252
APPENDIX L COMPARISON OF CLIMATE VARIABLES OBSERVED AND BASELINE 252
APPENDIX L TABLE L1 COMPARISON OF CLIMATE VARIABLES OBSERVED AND BASELINE.....252
APPENDIX M TABLE M1 SIMULATED STREAMFLOW BASED ON ACCESS1-0 253
APPENDIX M TABLE M2 SIMULATED STREAMFLOW BASED ON P-CNRM-CM5 253
APPENDIX M TABLE M3 SIMULATED STREAMFLOW BASED ON P-IPSL-CM5A-LR 254
APPENDIX M TABLE M4 SIMULATED STREAMFLOW BASED ON P-MIROC5……..255
APPENDIX M TABLE M5 SIMULATED STREAMFLOW BASED ON MPI-ESM-MR 255
APPENDIX M TABLE M6 SIMULATED STREAMFLOW BASED ON MRI-CGCM3-MR.....255
APPENDIX N TABLE N1 RANKED SIMULATED STREAMFLOW FOR SIX GCM.....256
APPENDIX O TABLE O1 ESTIMATED COEFFICIENT OF VARIATION FOR EACH GCM 257

LIST OF ABBREVIATIONS

AEP	Annual Exceedance Probability
AMS	Annual Maximum Series
CORDEX	Coordinated Regional Downscaling Experiment
CSIR	Council for Scientific and Industrial Research
ESRI	Environmental Systems Research Institute
EV 1	Extreme Value Type 1
FDC	Flow Duration Curve
GEV/LM	General Extreme Value using Linear Moments
GEV/PWM	General Extreme Value using Probability Weighted Moments
GCM	General Climate model
GCD	Gridded Climate Data
GIS	Geographical Information Systems
GOF	Goodness-of-Fit
GRZ	Government of the Republic of Zambia
HRU	Hydrological Research Unit
IDW	Inverse Distance Weighted
IPCC	Inter-Governmental Panel on Climate Change
KRB	Kabompo River Basin
LP3/MM	Log-Pearson Type III using Method of Moments
LN/MM	Log Normal using Method of Moment
PRECIS	Providing Regional Climate Impact Studies
RCP	Representative Concentration Pathways
RCM	Regional Climate Model
SADC	Southern Africa Development Community
SARDC	Southern African Research and Documentation Centre
USAID	United States Aid for International Development
WARMA	Water Resources Management Authority
WCRP	World Climate Research Programme
WRC	Water Research Commission
ZAMCOM	Zambezi Watercourse Commission
ZMD	Zambia Meteorological Department
ZRB	Zambezi River Basin

CHAPTER 1 : INTRODUCTION

1.1 Background

The impact of climate change on hydrology and water resources is a topical issue in the scientific world that has attracted a substantial body of research (Zhang & Wurbs, 2018; Kusangaya et al. 2014; Kaluarachchi & Smakhtin 2008; Inter-Governmental Panel on Climate Change (IPCC), 2007). Climate change affects temperature and precipitation, subsequently altering the water resources and hydrology cycle (Djebou & Singh, 2017; Trenberth, 2011). There is a huge complexity of the impact of climate change on the livelihood of the global population. There is also a strong likelihood that the occurrence of extreme events such as floods and droughts will increase under the climate change phenomena (IPCC, 2013). The changing climate in the African continent has made the continent particularly vulnerable because of its low adaptive capacity and vulnerability (Niang et al. 2014; Naidoo, 2013; Callaway, 2004).

According to the IPCC (2007), the Southern African region is regarded as one of the most vulnerable regions in Africa. The region is characterised by spatial and temporal rainfall variability and in some cases, also scarce water resources. The Zambezi River Basin (ZRB) in Southern Africa is one such example with the most variable climates of any major river basin in the world, which includes an extreme range of conditions across the basin and through time (Hamududu & Killingtveit, 2016; Beilfuss, 2012). The Mean Annual Precipitation (MAP) ranges from 100mm in the west to 1500mm in the northern and eastern parts (Water Research Commission

(WRC), 2011). Climate change is likely to affect nearly every aspect of human well-being, from agricultural productivity and energy use to flood control, municipal and industrial water supply to wildlife management (River et al. 2016; Niekerk Van et al. 2010).

Southern Africa has continued to experience variable climates, which has now been exacerbated by climate change effects (Naidoo, 2013). Temperatures in Africa are projected to increase at a rate of 1.5 to 2 times the global average (Council for Scientific and Industrial Research (CSIR), 2017). The setting in of climate change impacts has worsened the situation in the ZRB as availability of water resources in time and space has been drastically affected due to the high frequency of extreme events such as floods and droughts.

Further more the changing climate has also altered the hydrology of the region to the extent where all water dependent sectors such as energy, agriculture, mining, municipal water supply, tourism and environment are experiencing shortages, which affect the productivity and overall performance of the economy. The major river basins in the region have already formed the governmental transboundary river basin organisations through the Southern Africa Development Community (SADC) in order to enhance cooperation and benefit-sharing. The existence of these structures provides the region with an opportunity to address the challenges of climate change effectively and in an integrated manner.

Some of the worst-hit sectors include energy and agriculture. Energy sectors where most of the hydropower dams were operating with low levels of water, led to the low

production of electricity and eventually power rationing programmes such as load shedding had to be implemented. This has been the case for Kariba dam in the ZRB, which has shared benefits between Zambia and Zimbabwe. Agriculture is also adversely affected leading to food insecurity as both irrigated and rain-fed agriculture was not undertaken at expected capacities and thus reduced production. The situation culminates into food shortages in the region. The wildlife in the Okavango River Basin was equally affected as many sources of water had dried up, forcing the wildlife to walk long distances in search of water and in the process died.

The temporal and spatial variability of water resources in the region is a source of concern to many countries whose rural population entirely depend on water resources for their livelihood. The economies in the region have also been affected negatively due to climate change effects (i.e. droughts, floods and heatwaves).

Many institutions have already begun research studies, although there has not yet been a conclusion and detailed analysis on climate change impact studies for the region (World Bank, 2010; Southern African Research and Documentation Centre (SARDC), 2007). There is, therefore, a need for more research in the field of climate change and water resources in the region and on local level (basin-scale) to understand the detailed climatic variables and hydrological interactions (Schulze, 2000). Therefore, this study was undertaken as a response to the prevailing situation in the ZRB with a focus on Kabompo River Basin (KRB). It is envisaged that the knowledge generated from such studies, would greatly contribute to the body of knowledge and help to address the situation through adaptation and mitigation strategies..

1.2 Problem Statement

The land surface temperatures across the ZRB and the rest of Southern Africa have increased by 0.5°C during the last 50-100 years, while the global sea level has risen by 19cm between 1901 and 2010 (IPCC, 2014). The IPCC (2007) has categorised the Zambezi as the river basin exhibiting the “worst” potential effects of climate change among 11 major African basins, due to the resonating effect of an increase in temperature and a decrease in rainfall. According to Zambezi Watercourse Commission (ZAMCOM) et al. (2015), an increased incidence of malaria in parts of the basin and a shift in farming practices, for example, can be attributed to changes in temperature, rainfall and a rise in sea level.

The ZRB is home to about 40 million people that depend on water resources for agriculture, mining, industrial and domestic water supply, thus hydro-electricity generation and tourism makes a significant contribution to the economies of the riparian states. Lately, this basin has been experiencing periodic effects of climate change (e.g., floods and droughts).

These effects are often devastating and worsen the poverty levels of the people, especially in rural communities where alternatives for livelihood are few. In the ZRB, the demands on water, energy and food have become more pronounced during the past few years. With the impressive socio-economic development in riparian states, the pressure on water, energy and food security resources has increased. Challenges such as climate change consequences put additional pressure on the river and its resources. There is a paucity of data and limited knowledge on climate change impacts in the ZRB, which makes it difficult for governments and stakeholder

participation to adapt and mitigate these negative impacts. The following research gaps were identified:

- The recent studies in ZRB, emphasise that more research is needed for assessing the impact of climate change (Hamududu & Killingtveit, 2016; Niang et al. 2014; World Bank, 2010a).
- There is research and knowledge gaps on climate change impacts in hydrology and water resources for the ZRB (Kusangaya et al. 2014; Niang et al. 2014).
- Climate change impact studies have mostly been undertaken in developed countries while few studies have been conducted in developing countries, particularly Africa (Amede et al, 2014; Manase, 2010).
- No focused studies on the severity of climate change impacts in the ZRB have yet been concluded (SARDC, 2007).
- Most assessments of climate change impacts have been primarily undertaken at macro and regional scales, masking the complex hydrological interactions at the local catchment scale (Schulze, 2000).

In view of the research gaps highlighted above, a case study focussed on KRB was designed to investigate the impacts of climate change on hydrology and water resources in the ZRB. The research would generate new knowledge for adaptation and mitigation and provide baseline information to governments and stakeholders for policy review.

1.3 Aim and Objectives

Climate change impacts on hydrology and water resources were explored in this study to assess the complex hydrological interactions at a local scale in detail and generate new knowledge. The hydrological responses of the KRB to climate change was analysed, while trends in annual and seasonal temperature, precipitation and streamflow was identified. The severity of impacts of climate change at KRB scale was analysed and the results would be shared and transfered to other sub-basins within the ZRB. In order to investigate the impact of climate change on hydrology and water resources for adaptation and mitigation strategies, the following objectives were considered:

- Assessment of the hydrology and water resources in the KRB using alternative technology to conventional methods of using ground observed data which is scarce in the region.

- Conducting experiments for Regional Climate Modelling, using Providing Regional Climate Impact Studies (PRECIS) model to generate high-resolution climate scenarios for climate change impact studies on a local scale.

- Investigating hydrological responses to climate change using six downscaled bias-corrected Global Climate Models (GCMs) which involved the analysis of the catchment's water balance.

- Evaluating streamflow regime based on the six downscaled bias-corrected GCMs through hydrological modelling in the KRB.

1.4 Scope of Study

The study analysed a wide range of interrelated impacts of climate change on hydrology and water resources at a local catchment scale.This was in response to the research gaps identified in section 1.2. The study reviewed the assessments done on water resources with its linkage to climate variability in the basin; applied alternative technology for estimation of water resources in a data scarce region; Conducted four experiments for generation of a high resolution climate scenario through Regional Climate Modelling and analysed six statistically downscaled bias-corrected, GCMs for impact studies on streamflow regime and other water balance components in KRB.

Some of the limitations of the study included scarcity of the observed data within the KRB to use for model parameterisation,calibration and validation, the uncertainity in regional climate modelling and the statistically downscaled bias-corrected GCM results in impact assessments made it difficult to strongly conclude.

It is envisaged that the research results, will enhance capacity building, information sharing, decision-making, policy direction and provide baseline information for future research.

1.5 Structure of the Thesis

The structure of the thesis consists of Chapter one being a general introduction to the study while Chapter two is about the review of relevant literature used in the thesis. Chapters three provided the general methodology used in the research and

chapters four to eight include, specific introductions to the chapters, detailed materials and methods used in the chapters, results and discussions, as well as conclusions and Chapter nine is about a general conclusion of the research, as discussed in all the chapters. Several references are made to different appendices, which are included at the end of the document.

Chapter one is a general introduction that highlighted details on the background and analysed the problems in the ZRB and Southern Africa at large. Furthermore, the research gaps present in the area of study have also been highlighted while indicating the significance of the research. This chapter also elaborates on the overall and specific objectives of the thesis itself.

Chapter two provides a review of the relevant literature concerning factors that impacts climate change on hydrology and water resources. It includes; a review on flood frequency analysis, flow duration curves, hydrological modelling,hydrological models,gridded climate data, including Regional Climate Modelling in Southern Africa, downscaling techniques, bias correction and water resources management.

Chapter three encompasses the general research methodology used in the study and provides an overview of the materials and methods used for the entire research. Each chapter contains a detailed description of the materials and methods used.The chapter has also shown the study area in the Southern Africa.

Chapter four provides an overview of the status of water resources of the ZRB, with climate, hydrology, geological and geomorphology of the basin. It shows the

linkages of climate and water resources, land use and land cover, as well as the socio-economic aspects.

Chapter five involves the use of gridded climate data for hydrological modelling in data-scarce regions such as the KRB. The chapter demonstrates the practical solution and introduces an alternative to conventional methods of assessment of water resources using ground observed data. The chapter also displays the spatial distribution of water resources through the created maps in GIS.

Chapter six provides a discussion about the procedures for the four experiments undertaken with regional climate modelling through the PRECIS model for Southern Africa and further evaluation of the generated data for climate change impact studies. Regional climate modelling focussed on the application of the PRECIS Model, downscaling techniques and analysis of climate variables such as precipitation and temperature for the region.

Chapter seven deals with modelling climate change impact on catchment water balance components specifically rainfall, runoff and water yield and elaborates on particular details concerning the preparation of input model data, SWAT model application on the study area, analysis of hydrological variables and temporal and spatial variability of water resources.

Chapter eight involves evaluation of climate change impact on streamflow regime for the historical and future periods. Hydrological modelling is performed by using a

SWAT calibrated model and streamflow is simulated based on the six bias-corrected and downscaled GCMs projections.

Lastly, the thesis concludes with a ninth chapter that encompasses a conclusion, as well as recommendations. It also includes a summary of all the major findings and the newly generated knowledge is highlighted. These findings and other related information, including major opinions and recommendations are available for public consumption. A proposition of future research areas has also been made

.

CHAPTER 2 : LITERATURE REVIEW

2.1 Climate Change

Climate change is an alteration in the mean climate and or climate variability that perseveres for a prolonged period (Sivaramanan, 2015; Adedeji at al. 2014; Riedy, 2011). Climate change and global warming, refers to the rise in average surface temperatures on earth due to natural and anthropogenic activities (Sivaramanan, 2015; IPCC, 2014). An overwhelming scientific consensus maintains that climate change is due primarily to the human use of fossil fuels, which releases carbon dioxide and other greenhouse gases into the atmosphere. The gases trap heat within the atmosphere, which can have a range of effects on ecosystems, including rising sea levels, severe weather events and droughts that render landscapes more susceptible to wildfires (Davis-Reddy & Vincent, 2017; Handmer et al. 2012).

In order to anticipate future climate change, it is necessary to project how greenhouse gases will change in the future. A range of emission scenarios have been developed in the IPCC Special Report on Emissions Scenarios (SRES) that reflect several different ways in which the world might develop and the consequences for population, economic growth, energy use and technology (Thorpe, 2005; Jones et al. 2004).

The recent anthropogenic emissions of greenhouse gases into the atmosphere are the highest in history because of evidenced human influence on the climate system (IPCC, 2014). This has led to widespread impacts of climate change on human and

natural systems. The climate system has warmed up undeniably since the 1950s and there are unprecedented observed changes over decades, centuries to millennia. The sea levels have risen; snow and ice have continued to melt while the atmosphere and ocean have warmed up tremendously (Davis et al. 2017; IPCC, 2014). The frequency of occurrence of extreme events such as droughts, floods and cyclone activity has increased and also been cited as evidence of a changing climate (Bell et al. 2018; Kusangaya et al. 2013).

According to the African Climate Policy Centre (ACPC) (2011), climate variability is one of the causes of the prevailing poverty, food insecurity and the weak economic growth in Africa today. The African continent has been identified as particularly vulnerable to the changing climate due to its envisaged low adaptive capacity and vulnerability (Callaway, 2004).

2.1.1 Climate Sensitivity

Climate sensitivity is defined as the level of warming that corresponds to increases in carbon dioxide (CO_2) from the atmosphere. It is widely known as the stable global average surface temperature alteration following a multiplying CO_2 concentration in the atmosphere (Cain et al. 2019; Yu & Boer, 2014; Randall et al. 2007). There is a linear relationship between radiactive forcing and climate response that permits some components of climate change to be assessed from radiactive forcing estimates alone, minus the use of GCM simulations (Yu & Boer, 2014). According to Yu & Boer (2014), Climate sensitivity and response can be explored through three components listed as follows:

(i) The ratio amongst global mean forcing and global mean temperature response which is not dependant on the nature of the forcing and its geographical array.

(ii) The absence of a relationship between Geographical array of forcing and geographical array of temperature response and

(iii) The significant summation of response arrays whereby the addition of the temperature response arrays for a number of various forcings is almost the response array of the addition of the forcings. The energy budget of the system is used to analyse the climate sensitivity resulting from local contributions.

2.1.2 Climate Change Modelling

Climate models are defined as a mathematical representation of physical, biological and chemical fundamentals of the climate system (Gettelman & Rood, 2016; Goosse et al. 2010). These laws are complex; the equations derived from them must be solved numerically. Therefore, climate models are used to provide spatial and temporal solutions that are discretised. The results obtained from the models are averages over regions, whose coverage rely on specific times and the resolution of the model (Flato et al. 2013; Goosse et al. 2010). Climate change modelling is achieved through two major methods and these are Global climate modelling and Regional climate modelling.

Estimating the effect of green house emissions on the global climate, requires GCMs to be employed. GCMs consist of a scale, which is typically a few hundred kilometres in resolution. In order to study the impact of climate change, however, it is necessary to predict changes on much finer scales (Gettelman & Rood, 2016; White, 2014). One such technique entails the use of Regional Climate Models (RCMs), which have the potential to improve the representation of the climate information; this is important for assessing a country's vulnerability to climate change (Trzaska & Schnarr, 2014; Keller, 2007; Jones et al. 2004).

2.1.3 Methodologies for Climate Change Impact Assessments

Several methods have been devised to assess the impact of climate change on global or regional scale.The most widely used method is the Change Factor Methodology (CFM) also known as delta change factor methodology (Vavrus et al. 2015; Trzaska & Schnarr, 2014; Hamududu, 2012; Anandhi et al., 2011a). More complex methods also exist but they are not commonly used. Even though change factor methodologies are widely used, to determine the future climate scenarios,there are no procedures available in the literature that can be used to select the most appropriate methodology for various application (Anandhi et al. 2011a). According to Hamududu, (2012) and Anandhi et al. (2011a), the CFMs commonly used include: Temporal scale,temporal resolution, mathematical formulation and or number of change factors which may be categorised as follows:

(i) The temporal scale and domain are the first type of CFM upon which calculations are based. The temporal scale is about timescales such as daily,monthly,seasonal, bi-annual and annual values that are used in the analysis. Whilst temporal domain denotes the both time of the year i.e January,winter or annual and the start and end date of a climate period (also known as time slice) such as observed historical,simulated historical and simulated future time series are used in the analysis. For example a simulated historical or observed historical period 1975-2005 can be compared with a simulated future time slice of 2020-2050. Overall, GCMs produce dependable results at reduced frequency temporal scales than at higher frequency temporal scales e.g the monthly, seasonal, and annual means of climate variable are better simulated than daily or hourly values (Anandhi et al., 2011a).

(ii) The arithmetic procedure is second type of CFM which is additive or multiplicative. The CFM in additive is calculated by finding the change of a GCM variable resulting from a recent climate simulation and a future climate scenario based on the identical GCM grid position. The calculated change (also sometimes called delta change) is then added to observed data to find the simulated future time series. The additive and multiplicative CFs involves estimation of means for baseline and future scenarios using equation (2.1) and (2.2) respectively.

$$\overline{GCM_b} = \sum_{i=1}^{N_b} \frac{GCM_{bi}}{N_b} \qquad 2.1$$

$$\overline{GCM_f} = \sum_{i=1}^{N_f} \frac{GCM_{fi}}{N_f} \qquad 2.2$$

where

GCM_{fi} and GCM_{bi} Represent values from future and baseline scenarios for a temporal domain

$\overline{GCM_f}$ and $,\overline{GCM_b}$ Mean values of the future and baseline climate

To calculate the CF for additive and multiplicative the following equation (2.3) and (2.4) are used

$$CF_{add} = \overline{GCM_f} - \overline{GCM_b} \qquad 2.3$$

$$CF_{mul} = \frac{GCM_f}{GCM_b} \qquad 2.4$$

To calculate local scaled futures values ($\mathbf{LSF}_{mul,i}$ and $\mathbf{LSF}_{add,i}$) by applying CF_{add} and CF_{mul} the following equations (2.5) and (2.6);

$$\mathbf{LSF}_{add\ i} = \mathbf{LOb_i} + \mathbf{CF}_{add} \quad 2.5$$

$$\mathbf{LSF}_{mul\ i} = \mathbf{LOb_i}\ x\ \mathbf{CF}_{mul} \quad 2.6$$

Where

$\mathbf{LOb}_i$ are observed values of the climate variable (at the ith time step) at an identical weather station, or are the averaged climate variables of a catchment for the selected temporal domain.

$\mathbf{LSf}_{add,i}$ and $\mathbf{LSf}_{mul,i}$ are time series of future climate scenarios of the variable obtained using additive and multiplicative CFM.

The method is mostly used for climate variables such as temperature (Hundecha et al., 2016; Anandhi et al., 2011a; Akhtar et al. 2008 ; Hay et al. 2000). it also adopts that the GCM gives a realistic approximation of the complete difference in the value of a specific variable irrespective of the GCM's current climate simulation accuracy.

Change Factor (CF) with a multiplicative factor is comparable to CF with additive factor. However the major difference is that multiplicative factor uses ther ratio instead of calculating arithmetic change, between the future and current GCM simulations; the CF ratio is then used to multiply observed values (instead of additing

to). The method also makes an assumption that the GCM gives a realistic approximation of the relative difference in the value of a variable, and mostly applied for rainfall (Hundecha et al., 2016; Akhtar et al., 2008). Literature available does not show clear standards on when to use the additive CF or multiplicative CF for some meteorological variables such as wind speed and solar radiation.

(iii) The classification of the third CFMs is based on number of change factors such as single and multiple CFs. All values of the variable in Single CFs are computed individually, irrespective of scale (Anandhi et al., 2011a; Akhtar et al. 2008). Whilst multiple CFs are computed independently for various scales of the variable (Hundecha et al., 2016) e.g, computation of independent CFs for percentile such as 0-15,15-30 etc corresponding to a particular climate. Literature doesnot show clear procedures on suitable number of CF identity.

(iv) Detailed assessment is the fouth guidelines that involve the menthods described above and use downscalled,bias corrected data. Downscalling is done from GCM to produce recent climate and future climate ensembles which are then used in hydrological modelling for hydrology and water resources studies. Investigating a variety of possible impacts of climate change on hydrology and water resources in detail requires step by step approach. The steps of evaluation of ensemble simulations are imperative for reasonable future climate scenarios for impact studies. This detailed approach with the use of ensembles reduces uncertainity and the results may be more acceptable.

2.1.4 Dynamical and Statistical Downscaling Techniques

Dynamical downscaling is a comprehensive methodology that uses physical models of the climate system, which enables modelling of the dynamics of the physical systems that characterise the climate of a region (Mancosu, 2015). The two main modelling techniques employed are the Atmospheric General Circulation Model (AGCM) and RCM. Statistical downscaling, on the other hand, refers to a statistical approach based on formulated relationships between the large-scale and local-scale climate scenarios calibrated with historical data (Jacobeit et al. 2014; Katz et al. 2002). These statistical relationships are then applied to the large-scale climate variables from an Atmospheric Oceanic General Circulation Model (AOGCM) projection to estimate the corresponding local and regional characteristics. Statistical downscaling is based on the assumption that the statistical relationship between large scale GCM outputs and fine-scale observational data for the current climate will remain constant in the future climate (Farzan et al. 2013; Katz et al. 2002).

Statistical/dynamical is a combined approach that uses statistical methods for a large-scale climate scenario and RCM high-resolution climate scenarios. The approach has been developed with two variants. The first variant uses a RCM driven by observed boundary conditions from certain well-defined large-scale weather situations. The AGCM simulation is the second variant that is then decomposed into a sequence of these weather situations and the high-resolution surface climate is inferred from the corresponding RCM simulations (Lopes, 2009; Fuentes & Heimann, 2000).

2.1.5 Model Validation and Evaluation

Evaluation is the practice of recognising a model and its capabilities for a specific purpose. It is the process of establishing the value of a model and the objective is really to find out what value a model has (by evaluation). Whilst validation is the means of determining or examining reality of a model (Gettelman & Rood, 2016b).

A climate model is evaluated by simulating the climate of a specific period in the system with a model and then making comparisons of that simulation against a set of observations. Model evaluation also entails comparison of various models.

The guideline to model valuation is to collect,understand and analyse observations and their uncertainty, and then match the model as thoroughly as possible to the observations. Obtaining various statistics (mean, variability) right is important. Which statistics are important will depend on the application (Gettelman & Rood, 2016b).

Prediction of a future climate based on the model results can be either accurate or inaccurate. Climate change impact study results can be sensitive to the meteorological data used and therefore evaluation of RCM results is essential for interpretation of the results (Schoetter & Hoffmann, 2012).

This applies to both weather prediction and climate prediction. It is therefore important to critically analyse the model. Weather forecasts are made for a couple of days or weeks and can quickly and easily be evaluated with observed weather and it can be based on the length of time; statistics can be gathered about the performance of a particular model or a forecast system (Wiston & Km, 2018).

However, in climate change simulations, models are used to make projections of possible future changes over different time scales such as decades, generations or centuries. Such periods will have no precise previous similarities. It is, therefore, necessary to build confidence in a model by analysing its performance of the simulations of the historical record; such opportunities are much more limited than those available for weather prediction (Randall et al. 2007; WMO, 2000).

2.1.6 Downscaling GCM Projections to Regional Scale

The most advanced tools for projecting future climate change scenarios are considered to be GCMs that have been used extensively in the studies of climate change. However, GCMs have coarse spatial resolutions, which require downscaling to regional or local scales (Trzaska & Schnarr, 2014; Kusangaya et al. 2014; Jones et al. 2004). Normally, downscaling is based on spatial and temporal climate projections. Spatial downscaling is performed when extracting finer-resolution spatial aspects of the climate projection from a course resolution GCM output such as 1000km grid cell to GCM output to a 100km resolution.

Temporal downscaling is performed when fine-scale temporal information is extracted from a course-scale temporal resolution GCM output such as daily rainfall time series from a monthly rainfall time series (Trzaska & Schnarr, 2014). Figure 2.1 represents the spatial downscaling.

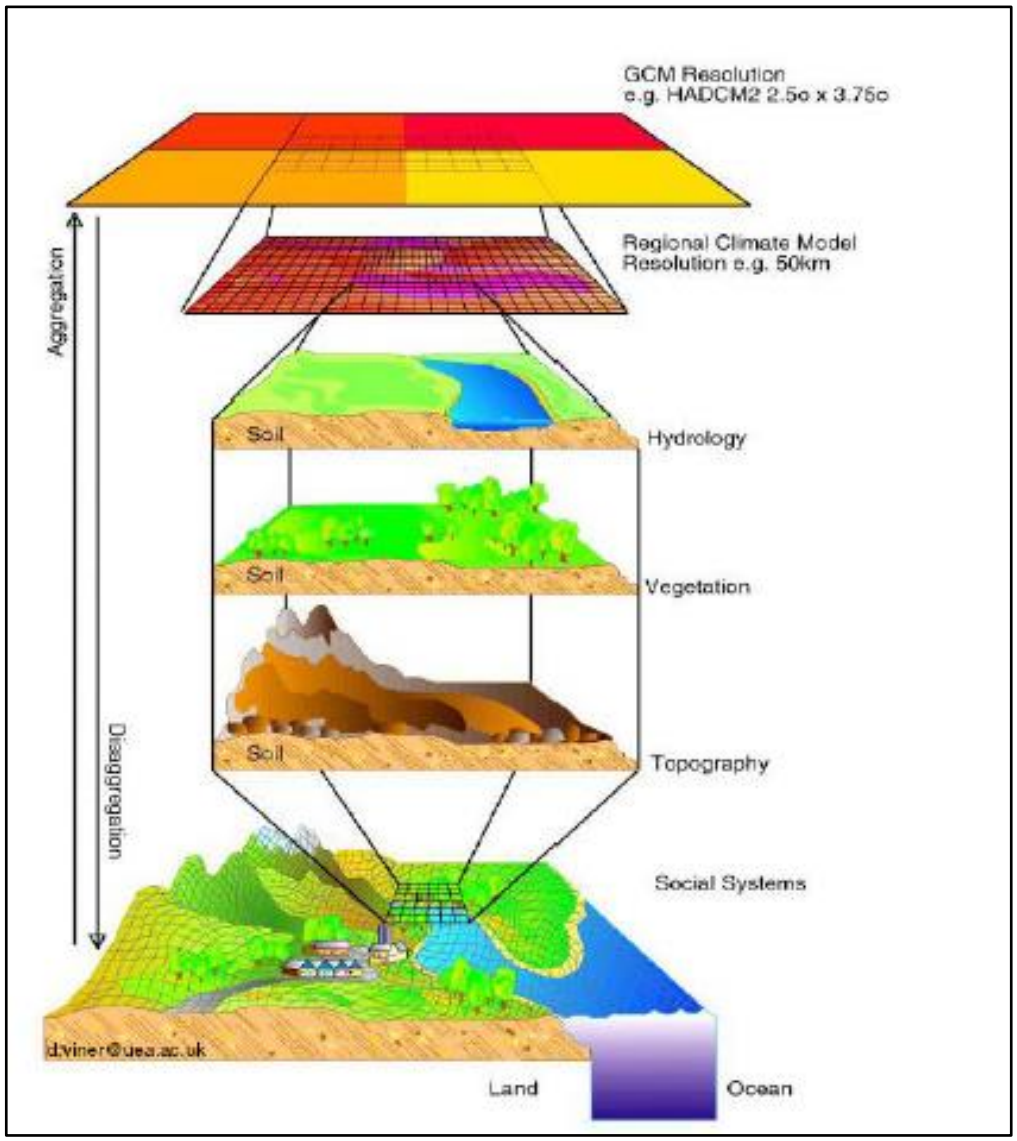

Figure 2.1 The concept of spatial downscaling (Source:Viner,2012)

Downscaling GCM outputs is achieved through dynamic and statistical downscaling. It is computationally expensive to undertake dynamic downscaling and may not be practical to use, especially for predictions from several models required at a particular spatial resolution. Furthermore, the outputs from RCMs may still have some biases which will need to be removed especially if the data will be used for hydrological modelling (Giorgi et al. 2001; Chen & Roads, 1999).

It is computationally efficient to undertake statistical downscaling and feasible for spatial downscaling and bias correction for multiple GCM outputs. Several studies have shown that both dynamic and statistical downscaling techniques have similar skills. Statistical downscaling is based on observed relationships between the current climate and future climate for a specific GCM; the result can be used to validate the results of the RCMs (Kusangaya et al. 2014; Giorgi et al. 2001).

In Southern Africa, downscaled climate change data is available with the Coordinated Regional Downscaling Experiment (CORDEX) programme, which was founded by the World Climate Research Programme (WCRP). This initiative emanated from the need for downscaled climate data. The objective of the CORDEX-Africa is to develop a coordinated framework for improved regional climate projections that will meet the growing demand for high resolution downscaled projections. Thus, the generated data is used by the scientific community for impact and adaptation studies (Dosio & Jürgen, 2016; Kusangaya et al. 2014).

2.1.7 Representative Concentration Pathways

Representative Concetration Pathways (RCP) is a set of scenarios that have been adopted by climate researchers to provide possible future scenarios for the evaluation of the atmospheric composition (Meinshausen et al. 2011; Moss et al. 2010). Scenarios are detailed descriptions of how the future is likely to unfold in social, economic, technological and environmental, emissions of greenhouse gases and aerosols, and climate (Moss et al. 2010; Zhang et al. 2007).

The earlier scenario-based projections of the atmospheric composition have been complimented by RCPs and in some cases superseded, for example the SRES. The RCPs are used to drive the climate model simulations planned as part of the World Climate Research Programme's Fifth Coupled Model Intercomparison (CMIP5) (Meinshausen et al. 2010). There are four RCPs that have been developed as climate scenarios and these include RCP2.6 as the lowest range, RCP4.5 and RCP6.0 as the middle range and RCP8.5 as the highest range. The global mean surface temperature has been projected to range from 1.5°C for the lowest range of the four RCPs to 4.5°C for the highest RCP up to 2100 (Vuuren, 2011; Meinshausen et al. 2010).

These four RCPs describe various possible future climates that largely depend on future greenhouse gases emissions into the atmosphere. The four RCPs are numbered based on the possible range of climate forcing values for the future year of 2100 (2.6, 4.5, 6.0, and 8.5 W/m^2, respectively) (Vuuren et al. 2011). Figure 2.2 illustrates the four RCPs trajectories.

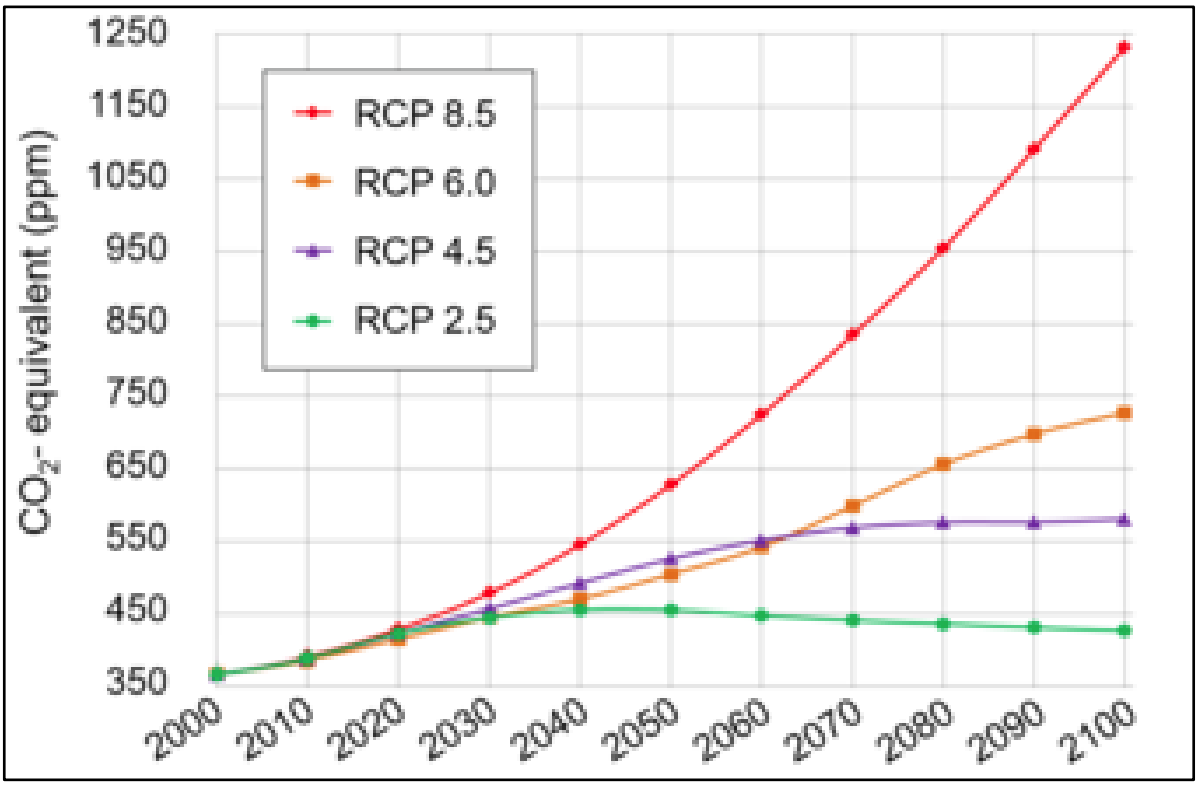

Figure 2.2 IPCC AR5 Greenhouse Gas Concentration Pathways (Source: IPCC, 2013 – WikiCommons)

(All forcing agents' atmospheric CO_2-equivalent concentrations (in parts-per-million-by-volume (ppmv)) according to the four RCPs used by the fifth IPCC Assessment Report to make predictions).

The RCP4.5 is a middle pathway scenario that correlates well with the recently released guidelines of lower greenhouse gas emission by the international community. It is, therefore, a good case sensitive scenario in light of the new guidelines. RCP 8.5 is a high emission scenario, which provides possibly the highest impact on climate change. In view of the above-mentioned factors, RCP 4.5 and RCP 8.5 are mostly selected to provide a possible complete range of impacts (Khan et al. 2018).

2.1.8 Bias Corrections

The study of climate change and its impact is mostly based on the simulated outputs from the GCM and the RCM driven by greenhouse gases and aerosol emission

scenarios such as the RCP4.5 and RCP8.5. There are, however, limitations in the studies of climate change, especially pertaining to hydrological modelling because of the scale mismatches between the climate model output and the spatial scale at which the hydrological models operate (Baimoung et al. 2014).

Though regional climate models are reliable tools for simulating regional and local finer-scale climate conditions, they still have systematic errors, particularly the small-scale patterns of daily precipitations that mostly rely on model resolution and selected parameters. Considering the above, RCMs are found to be inadequate for direct use in climate change impact and adaptation assessment studies (Fowler et al. 2007).

However, this challenge is no longer an issue because of the use of various bias-correction techniques to RCM outputs to render them suitable for the impact studies (Baimoung et al. 2014). Among the most applied techniques, Quantile Mapping (QM) is a technique that alters the value of a model by mapping quantile of the distribution of the model to the quantile of the observed data (Casanueva et al. 2019; Feigenwinter et al. 2018).

Another technique used is known as Cumulative Distribution Function transform (CDF-t), which undertakes that the baseline (historical) plot linking the model and observed cumulative distribution functions applies to the future period. The intermediate quantile matching, which preserves the GCM, predicted change at each quantile estimated in which the future minus the baseline is used as the basis for calculation (Jo et al. 2019; Lian-yi et al. 2018; Pierce et al. 2015).

2.1.9 Uncertainty

The GCM projections of future climate scenarios are dependent on uncertainties emanating from various sources (Hosseinzadehtalaei, 2017). The future projections of climate extremes have larger uncertainties because of the complexities of simulating extremes. Climate change uncertainty is better quantified with a larger ensemble size of independent climate models (Hosseinzadehtalaei, 2017).

Comparisons between many models have shown that averaged near-surface temperatures will increase in the next two decades in response to increased greenhouse gas emissions. Nevertheless, the magnitude of the increase will differ from one model to another. Furthermore, various models project opposite changes in climate variables such as rainfall in certain regions indicating uncertainty of the future climate change projections even when advanced models are utilised (Trzaska & Schnarr, 2014). According to Trzaska & Schnarr (2014), the following are the four major uncertainties present in climate projections:

- The future levels of emissions emanating from human activities and natural forcings, such as volcanic eruptions.
- Uncertainty arising from model errors due to imperfect model representations of climate processes.
- Uncertainty due to inaccurate knowledge of the prevailing climate conditions that are used as initial conditions for projections.
- Uncertainty due to the complexity of representing inter-annual and decadal variability in long-term projections.

The future greenhouse gas emissions evolution has a high level of uncertainty due to demographic, technological and socio-economic dynamics. GCMs are driven by alternatives of greenhouse gas emission scenarios with a view of obtaining a variety of possible future outcomes and models need initial conditions not perfectly known to start projections.

Adjusted initial conditions are used as a starting point to perform projections for obtaining a series of simulations, also known as an “ensemble.” There is no model that perfectly simulate all climate processes. Simulations from several models are produced and a multi-model ensemble mean is considered as the most probable future climate path. The variability of GCM individual simulations in a multi-model ensemble indicates a degree of uncertainty (Hosseinzadehtalaei, 2017).

2.2 Hydrology and Water Resources

Current research in most of the hydrological studies seeks to enhance our ability to understand and predict the impacts of climate change and land use on the water balance, groundwater levels, streamflows variability and the water quality ranges from hillslopes to catchments. Many applications in hydrology to practical problems of design and forecasting need the use of hydrological models (Fatichi et al. 2016; Dingman, 2002).

Catchment hydrology is being altered by climate change through variations of extreme events such as floods, droughts, heatwaves and windstorms. The complexity of river catchments with dynamic systems requires the development of

a better understanding of how these systems will be altered with climate change impacts (Pletterbauer et al. 2018; Murthy, 2012).

2.2.1 Gridded Climate Data

Gridded climate data (GCD) is the data developed from simulated and satellite remotely sensed data sources. The data has potential to be an alternative of the observed climate data (conventional climate data) for streamflow simulation and other uses (Mou et al. 2017). It is also defined as a multiple year global gridded representations known as reanalysis datasets (Tomy & Sumam, 2016).

Gridded climate data also referred to as reanalysis products which combine available measured data with a current atmospheric (or more recently) model to develop the finest approximation of the condition of the atmosphere and land surface (Decker et al. 2012). Gridded climate data are mainly used for different applications in the global community due to paucity of complete direct observation e.g using gridded climate data to drive land surface models,explore the climate system,through boundary conditions and regional modelling (Decker et al. 2012). Some of reanalysis datasets (gridded climate data) used in different parts of the world include:

(i) Asian Precipitation Highly-Resolved Observational Data Integration towards Evaluation of Water Resources (APHRODITE). It was produced by the Research Institute for Humanity and the Meteorological Research Institute of the Japan Meteorological Agency. APHRODITE is a long-term daily precipitation product that covers the period 1951 to 2007, and is based on observed data collected from thousands of gauge stations in different countries and government agencies.

APHRODITE is located into the following regions; Middle East, Russia, Monsoon Asia and Japan. For example, APHRODITE V1101 (Monsoon Asia) utilises a resolution of 0.25° (Mou Leong Tan et al. 2017).

To overcome the challenge of data scarcity, the CFSR of the NCEP and APHRODITE are readily accessible for any geographical location on earth at a daily time-scale for periods 1979-2014 (Mou et al. 2017; Decker et al. 2012)

(ii) National Centers for Environmental Prediction Climate Forecast System Reanalysis (NCEP-CFSR). The CFSR is the latest dataset from NCEP that span from 1979 to the current, and the period 2001/02 is used for this analysis. The CFSR is the third generation reanalysis data that can be accessed at https://globalweather.tamu.edu. The analysis utilises the Global Forecast System (GFS) as its atmospheric model with a horizontal resolution of T382 (~38km) with 64 vertical layers (Saha et al. 2010).

The CFSR uses the NOAH land surface model with four vertical layers while the rest of reanalyses utilise observed seas surface temperatures to force the atmospheric CFSR incorporates a complete coupled ocean model, the Geophysical Fluid Dynamics Laboratory Modular Ocean Model (GFDL MOM) version 4 (Decker et al. 2012) . The atmospheric analysis has a cycle of 6 hour and applies the gridpoint numerical interpolation method such as in MERRA. The assimilation of land surface happens has a cycle 24 hours and utilises observed precipitation. The CFSR products are founded on a sprectral model which includes

the parametrisation of all main physical processes as elaborated in depth by (Worqlul et al., 2017; Kistler et al. 2001; Kalnay et al. 1995).

(iii) Precipitation Estimation from Remotely Sensed Information using Artificial Neural Network-Climate Data Record (PERSIANN-CDR). PERSIANN-CDR was developed from the PERSIANN algorithm using Gridded Satellite Infrared Data (GridSat-B1), a standardised and mapped geostationary satellite dataset (Mou et al. 2017). PERSIANN-CDR makes available daily precipitation data spanning from 1983 to the current for coverage area lying within latitudes 60° S–60° N at a spatial resolution of 0.25°. The artificial neural network was trained using the NCEP phase four hourly precipitation information. The Global Precipitation Climatology Project (GPCP) monthly version 2.2 modifies the product (Mou Leong Tan et al. 2017).

(iv) Modern-Era Retrospective Analysis for Research and Applications (MERRA-2) is second-generation reanalysis product designed to update retrospective analysis of the whole era of satellite from NASA beginning from 1979 to present (Bosilovich et al. 2015). In general MERRA-2 incorporates many updates of the global simulation and assimilation of data systems. The major difference between MERRA and other products lies in the size of coverage area and the time scale of the documented information. MERRA-2 documents most of the results of the model at its built in coverage scale per hour (Molod et al. 2015; Rienecker et al. 2008).

(v) ERA 40 is the reanalysis for second generation of meteorological data spanning from September 1957 to August 2002 with 1991-2001 used in the current study.The ERA-40 was established by the European Centre for Medium-Range Weather

Forecasts (ECMWF) in conjuction with many other institutions and organisations (Uppala et al. 2005). ERA-40 datasets may be accessed from http://dss.ucar.edu/pub/era40. ERA-40 uses dynamical model version cycle 23R4 from ECMWF, with 60 vertical levels at a horizontal resolution of T159 (125 km).

The data for both the atmosphere and the land surface was assimilated into the system using a 3DVar methodology analysed at 6 hours per cycle. It uses data comparable to those utilised by MERRA and other reanalyses but with difference is that ERA-40 does not comprise observed 2-m air temperature (and relative humidity) from weather observation stations throughout the analysis cycle (six-hourly) of the land surface (Decker et al. 2012; Uppala et al. 2005).

(vi) The current ECMWF reanalysis is ERA-Interim which spans from 1989 to present (upto 2002 is used in the present work). ERA-Interim uses modernised version of the ECMWF forecasting model with a horizontal resolution of T213 (80 km) (Decker et al. 2012). Despite this higher resolution than ERA-40, ERA-Interim is the only reanalysis product that integrates the whole four-dimensional variational data assimilation (4DVar) (Decker et al. 2012; Simmons et al. 2006).

(vii) Global Land Data Assimilation System (GLDAS) was produced through corroborative efforts by scientists from National Aeronautics and Space Administration (NASA) Goddard Space Flight Centre (GSFC) and the National Oceanic and Atmospheric Administration (NOAA) National Centres for Environmental Prediction (NCEP) (Rodell et al. 2004). The GLDAS utilises the new generation of ground and space based observation systems which make available

data to force the simulated land surface states. Several different datasets may be accessed from http://disc.sci.gsfc.nasa.gov/hydrology/data-holdings that are available for use in weather and climate research (Decker et al., 2012; Rodell et al. 2004).

(viii) NCEP–NCAR. The NCEP–NCAR reanalysis (NCEP) is a regularly used dataset that spans from 1948 to 2009 with the present period used as 1991-2006 and is the oldest gridded climate product included in this research.Data is accessible at http://dss.ucar.edu/pub/reanalysis/. The NCEP global atmospheric spectral model is used as the dynamical atmospheric model which became operational in 1995 with 28 vertical levels and a horizontal resolution estimated to be 210km (Kalnay et al.1995). The NCEP–NCAR uses the Oregon State University land surface model which has two vertical layers and a 3DVar approach is utilised to assimilate the observations into the model just like with the process in MERRA (Decker et al. 2012).

2.2.2 Flood Frequency Analysis

Flood frequency analysis is an important statistical technique in hydrology that is used to determine the nature and magnitude of the peak streamflow (Ganamala & Pitta, 2017). The purpose of flood frequency analysis is to relate the peak flood with a probability of exceedance. Many methods have been developed for this purpose and range from statistical distribution fitting to simulation approaches (Odry, 2017).

Some of the basic reasonable distributions suitable for modelling include Lognormal (LGIII), Extreme Value Type 1 (EV 1 or Gumbel), Extreme Value Type II, Pearson type II and Log Pearson Type III (LPIII) distributions (Alias & Takara, 2012). Most

studies have focused on fitting a probability distribution such as Generalised Extreme Value (GEV) from the Annual Maximum Series (AMS) to the hydrological sample data (Katz et al. 2002). Although the distribution fitting technique is widely used, the availability and amount of historical discharge data at a specific location of interest remains a challenge (Odry, 2017). The extrapolation of flood frequency curves in hydrological processes is also a well-known problem (Katz et al. 2002).

2.2.3 Flow Duration Curves

Flow Duration Curves (FDC) are determined and plotted to analyse streamflow regime and percentage flow exceedances (Mülle & Thompson, 2015; Ngongondo et al. 2013). FDC is important in hydrology as it reveals much of the stream flow temporal variability and its shape is a function of different factors.

An FDC with a steep slope throughout shows variability of streamflow, which is mostly caused by rainfall producing quick runoff to the stream. A curve with a flat slope indicates a significant contribution of base flow to the streamflow originating from springs or diffuse inflow along the stream. Policy and regulation of streamflow through management of discharge from reservoirs can also result in a flat curve of the FDC. High stream flows are caused by quick runoff of the rainfall and will have a steep slope at the upper end of the stream. Nevertheless, the high flows can also be reduced by riverbanks consisting of permeable alluvium.

The topography and geology of the basin are the major causes of the distribution of low flows in the middle part of the FDC. The lowest flows can also be strongly influenced by the uptake of water by riparian forests such as phreatophytes along the riverbanks to produce a sharp dip at the lower end of an FDC. The shape of

FDC has continued to be a matter of research because of the many factors that influence it (http://www.dunnhydrogeo.com/home/flow-duration-curves-nt).

2.2.4 Hydrological Modelling

Developments in integrated hydrological modelling in the modern years has brought innovations in calibration, validation and uncertainty analysis tools and the presence of grid technology for model performance, which leads to the construction of more, detailed, robust and complete models (Christos et al. 2016; Abbaspour et al. 2010).

These models account for processes such as water quantity and quality, soil, climate, land use, agricultural management and nutrient cycling in a coupled single package (Rouholahnejad et al. 2014; Loliyana & Patel, 2014). Climate system is a principle driving force of the hydrological cycle because it is the source of precipitation, maximum/minimum air temperature, solar radiation, wind speed and relative humidity, which control the water balance.

Therefore, hydrological modelling targets simulation of hydrological processes that include canopy storage, surface runoff and infiltration. While in the subsurface, the processes include lateral flow from the soil, return flow from shallow aquifers, tile drainage, shallow aquifer recharge, capillary rise from shallow aquifer into the root zone and deep aquifer recharge (Abbaspour et al. 2015).

The other processes include moisture redistribution in the soil profile and evapotranspiration. Vegetation growth must be considered in the hydrological model, as evapotranspiration is imperative in water balance and management

operations of irrigation system (Faramarzi et al. 2009). Hydrology and water quality is largely affected by fertilisation.

2.2.5 Model Calibration and Validation

The objective of the calibration process is to reduce the error sources until they become insignificant (Loliyana & Patel, 2014; Andréassian et al. 2012; Refsgaard & Storm, 1996). According to Refsgaard and Storm (1996), the various sources of errors in hydrological simulation may arise from the following factors:

- Systematic errors from input data such as rainfall, temperature and evapotranspiration.
- Systematic errors in recorded or observed data such as river water levels, discharge data, groundwater levels or other data used in simulation.
- Errors originating from non-optimum values.
- Errors from an incomplete or bias model structure.

A calibrated model can be deemed valid if it is tested against data different from those used during calibration. Therefore, model validation entails confirming that a site-specific model can produce simulation results within the acceptable limits of accuracy specified in the performance criteria for a particular study (Andréassian et al., 2012; Refsgaard & Storm, 1996).

2.2.6 Hydrological models commonly used in climate change Impact studies.

Hydrological models are deemed to be an essential, required tool for water and environment resources management (Christos et al. 2016; Devia et al. 2015; Wheater, 2008) They are principally utilised for predicting the behaviour of a natural

or artificial systems and enhance understanding of different hydrological processes. Every hydrological model has its own individual features and specific applications. Some of them are comprehensive and utilise dynamics of fundalmental hydrological processes and are a function of space and time (Devia et al. 2015; Wheater, 2008; Gupta et al. 1998).

The most important inputs needed for each hydrological model are precipitation data and catchment area**.** Besides these inputs a model would also require, catchment characteristics such as catchment topography, soil moisture content, vegetation cover, soil properties and characteristics of ground water aquifer may also be considered. The hydrological model that gives results close to reality with the use of least parameters and model complexity is considered to be the best model (Devia et al. 2015; Wheater, 2008). Hydrological models are categorised based on model input parameters and the level of physical principles utilised in the model. Models may be categorised as lumped and distributed subject to the model parameters as a role of space and time and deterministic and stochastic models based on the other principles.

Hydrological models are widely and significantly categorised as empirical model, conceptual models and physically based models (Devia et al. 2015; Wheater, 2008). An empirical model is described as observation oriented models that only extract information from the existing dataset without regarding the characteristics and processes of hydrological system and therefore these models are also known as data driven models. Conceptual models describe every element of hydrological processes. It comprises a number of interconnected reservoirs that symbolises the

physical components in a watershed in which they are recharged by precipitation, infiltration and percolation and are drained by evaporation, runoff, drainage etc.

Whilst physically based models are mathematically idealized representation of the reality also known as deterministic models that include the principles of physical processes. It uses state variables which are measurable and are functions of both time and space. The hydrological processes of flow of water are symbolised by finite difference equations at doesn't need extensive hydrological and meteorological data for their calibration (Farmer & Richard, 2016; Devia et al. 2015; Wheater, 2008)

An effective hydrological modelling process depends on availability of quality data which require evaluation for setting up,calibrating,validating of a hydrological model. Availability of continuous quality data is mostly a challenge in Southern Africa and that hinders the use of many different hydrological models which largely rely on such data. Most hydrological models used in climate change impact studies require comprehensive data sets to be used for optimisation of a model. Table 2.1 shows some hydrological models commonly used in climate change impact studies.

Table 2.1 Some hydrological models used in climate change studies

Hydrological Model	Description of a Model	Time Resolution	References
TOPMODEL	It is a semi distributed, conceptual rainfall runoff model, has advantage of topographic information related to runoff generation, considered as a physically based model, main aim is to compute storage deficit or water table depth at any location. Can be used in catchments with shallow soil and moderate topography.	Hourly,Daily	(Jeziorska & Niedzielski, 2018; Devia et al. 2015)
Hydrologiska Byrans Vattenavdelning model (HBV)	It is a semi distributed, conceptual,hydrological model. Can simulate snow accumulation and snow melt.Groundwater recharge ,runoff and actual evaporation are simulated as functions of actual water storage	Daily, monthly	(Bergström, 2006; Johansson et al. 2003; Bergström et al. 2001)
Soil Water Assessment Tool (SWAT) Model	Complex,physically based model, efficient in performing long term simulations and is able to describe water and sediment circulation, vegetation growth and nutrients circulation.	Hourly,Daily, monthly	(Guzman et al. 2015;Arnold et al. 2012; Neitsch et al. 2005;Arnold et al. 2012)
MIKE Systeme Hydrologique European (SHE)	It is a physically based model,requires extensive model data and physical parameters, can simulate surface and ground water movement, interactions, sediment, nutrient and pesticide transport.	Hourly	(Sandu & Virsta, 2015) (Butts & Graham, 2005; Zhang et al. 2008)

Thornthwaite Monthly water balance model	It is a numerical, Conceptual model,It's a water balance model,It undertakes water budgeting.Its driven by graphical user interface.One of the oldest models	Monthly	(Westenbroek et al. 2010; McCabe & Markstrom, 2007)
Variable Infiltration Capacity(VIC) model	A semi distributed, grid based, hydrology model, uses both energy and water balance equations performs well in moist areas	Daily	(Devia et al. 2015; Gao et al. 2010)
Water Resources Simulation Model WRSM/Pitman Model	Conceptual lumped monthly rainfall-runoff, semi distributed model.	Monthly	(Kapangaziwiri et al. 2013; Ndiritu, 2009; Pitman & Bailey, 2005)
HSPF model Hydrological Simulation Program-FORTRAN (HSPF)	A semi distributed deterministic, continuous and physically based model	Hourly	(Javan et al. 2013)
WBM (Water Balance – Monthly Global model (uncoupled to GCM)	Spatially distributed, hydrology model. Originally designed for more temperate climates	Monthly	(Fekete et al. 2002)
Identification of unit Hydrographs And Component flows from Rainfall,Evaporation and Streamflow data (IHACRES)	It a metric conceptual, Parameterically efficient rainfall-runoff model,uses a transfer function/Unit hydrograph method for catchment scale,continuous simulation.	Daily	(Dye and Croke, 2003;Croke & Littlewood, 2005)

2.2.7 Water Resources Management

Millions of people in Southern African depend on water resources from 14 transboundary river basins for their livelihoods. The region already faces numerous challenges that range from water-stressed river basins emanating from inadequate rainfall, water management challenges, population growth, lack of adequate infrastructure and water storage, as well as poor institutional capacity.

Furthermore, renewable freshwater is unevenly distributed across rivers, lakes and groundwater. Climate change occurring with higher temperatures, decreased precipitations, rising frequency and intensity of extreme events and sea-level rise is already worsening the impacts on water supply and shortages in the region. Decreasing rainfall may lead to reduced runoff and eventually result in some rivers, streams, reservoirs drying up. The communities that depend on these water resources may be more vulnerable and will need adaptation and mitigation strategies (USAID, 2011). Scarce water resources require enhanced Integrated Water Resources Management (IWRM) (Sukereman, 2015; Claassen, 2013; MEWD, 2008).

A conceptual advancement of IWRM that seeks to incorporate land use is important in emphasising Integrated Land and Water Resources Management (ILWRM). A water decision is also a land-use decision, thus highlighting their interdependence.

IWRM plans are currently executed at a national (country) scale and in some cases at a basin scale, in response to the World Summit for Sustainable Development (WSSD) operation strategy of Johannesburg in 2002. It has been emphasised that

L in IWRM be included in the operation strategies of water resources for sustainable development (Rockstrom & Falkenmark, 2006).

CHAPTER 3 : RESEARCH METHODOLOGY

3.1 Description of the Zambezi River Basin

The four largest river basins in Africa are Congo, Nile, Niger and Zambezi. The ZRB located in Southern Africa is the fourth largest among the four basins found in Africa. It has a surface area of 1,390,000km^2, which represents about 4.5% of the area of the African continent and is shared by eight countries (http://www.fao.org/3/W4347E/w4347e0o.htm).

The Zambezi River stretches through a distance of 3000km from Kalene Hills in Northwestern Zambia at an elevation of 1500m above sea level to the delta in the lower Zambezi in Mozambique (Teodoru et al. 2015).

The ZRB has 42.5% surface area on Zambian territory, which is the largest among the eight countries and therefore this research will focus on the Kabompo River Basin (KRB), one of the 13 sub-basins of the ZRB found in Zambia. KRB is located on the Upper ZRB and will be used as a case study in the analysis of climate change and impacts on hydrology and water resources for the entire ZRB. Figure 3.1 illustrates the location of ZRB and KRB in Southern African region.

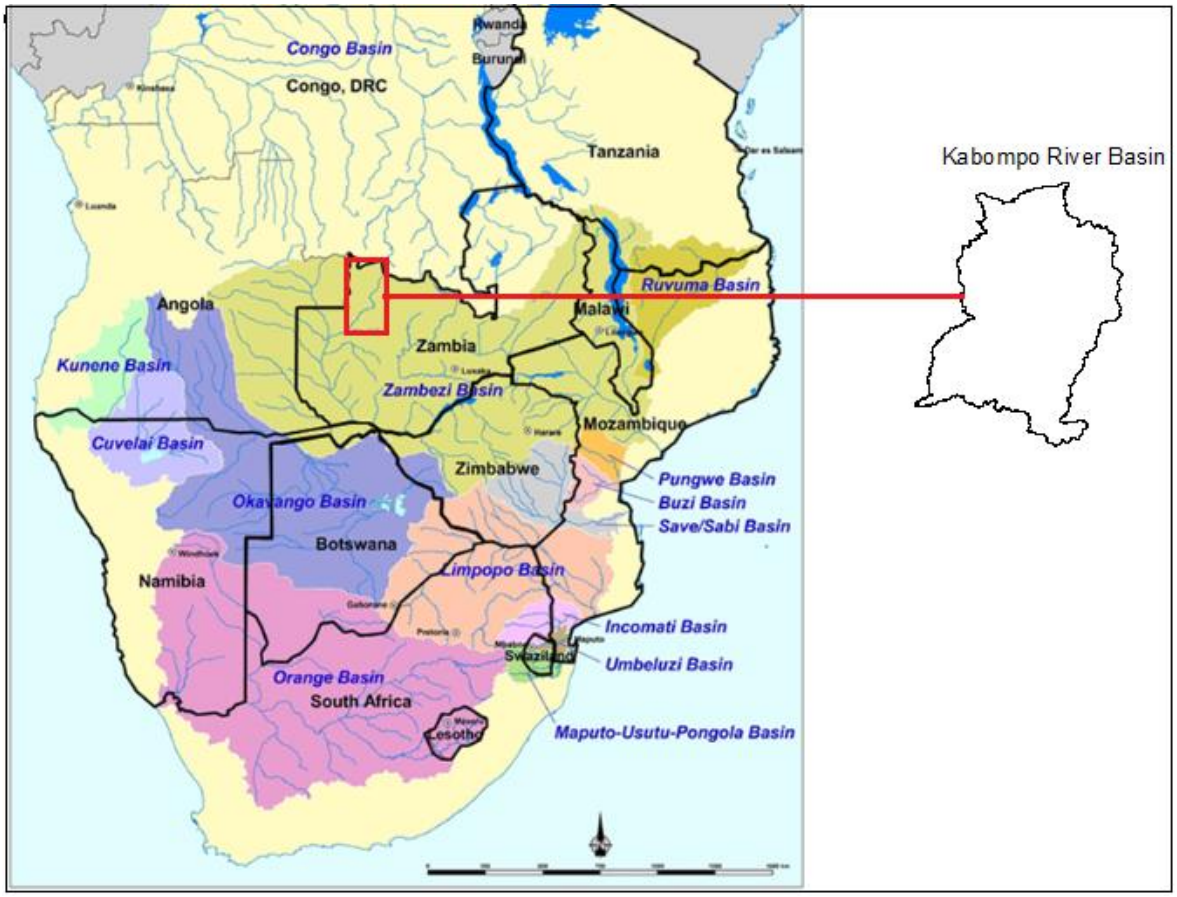

Figure 3.1 Location of Zambezi River Basin and Kabompo River Basin (Source: http://cridf.net/why-we-work-in-southern-africa).

The temporal and spatial variability of water resources in the ZRB is a function of rainfall and temperature climate variables. The basin experiences variable average annual rainfall ranging from 1500mm to 100mm, from northern to southwestern parts respectively (WRC, 2011).

The time series data for temperatures across the ZRB show variations in accordance with elevation. July is the coldest month with Mean monthly

temperatures of less than 14ºC for higher elevation areas in the south of the basin to more than 22°C for the low elevation areas around the delta in Mozambique. October and November are the warmest months with mean daily temperatures varying from 23°C in the highest elevation areas to 31°C in the lower parts of the Zambezi valley (ZAMCOM et al. 2015).

3.1.1 Description and Location of Kabompo River Basin

Figure 3.1 also shows the KRB with a delineated surface area of 72 082km^2 and part of the UZRB located between 14^O 15" 07.29'S, 23^O 08' 27.44" E and 17^O 36' 17.21'S, 25^O 48' 28.39"E. KRB has the highest MAP of 1200mm, high Mean Annual Runoff (MAR) and high river flows that makes a significant contribution of surface and ground water resources in the entire UZRB. KRB is one of the six basins in the UZRB which has deep, well-drained Kalahari sands covering the entire region (Beilfuss, 2012). The basin has wooded savannahs as the predominant land use.

The basin has high potential for both rain-fed and irrigated agriculture productivity and important sites for hydro electric power generation such as Chikata falls in Kabompo district, Kabompo gorge (under construction), Nyamwezi falls, Muzhila falls in Mwinilunga district. The basin is also a home of West Lunga National Park and big mines such as Lumwana mine, one of the largest mines in Africa, Kalumbila mine and Zabesha mine.

The estimated population based on Zambia 2010 census of the basin stands at 700,000 people with high poverty levels who rely on water resources for their liveliwood.There are seven rural towns (Districts) found in the basin namely: Mwinilunga,Ikelengi, Kabompo, Mufumbwe, Zambezi, Solwezi and Kasempa.

In view of the hydrological and social economical factors mentioned above,the KRB was identified to be strategic and hence chosen as a case study to demonstrate the impact of climate change on hydrology and water resources in the UZRB.

3.2 Biophysical Data

The research involved the collection of biophysical data such as land use/land cover, vegetation,Hydrological soils, topographical, climate and river discharge. Gridded climate data (Reanalysis data) such as Climate Forecasting System Reanalysis (CFSR) and other variables were also used in the studies for the KRB basin. CFSR data was selected for modelling because it is a third generation reanalysis dataset (newest among NCAP) and had the highest horizontal resolution of approximately 38km among the reviewed hydrological models in chapter two.The CFSR data set was also readily available in a SWAT format with adequate coverage of the study area. Detailed specific data for Regional Climate modelling, and Hydrological Modelling may be found in the subsequent chapters.

The Soil Water Assessment Tool (SWAT) model was selected for hydrological modelling because of its capability of long term simulations and wide aplication in climate change impact studies (Abbaspour et al. 2019; Gassman et al. 2007). It was therefore used in the simulation of hydrological processes for the catchment to estimate water resources using gridded climate data. The model was further used with downscaled, bias-corrected GCM projections to analyse hydrological responses for climate change. SWAT model results were calibrated and validated

with observed data obtained from the Zambia Meteorological Department (ZMD) and Water Resources Management Authority (WARMA).

3.3 Climate Change Modelling

The first approach was based on four experiments using the PRECIS model, which is a regional climate model that provides historical and future climate scenarios. The first approach involved the use of PRECIS, a regional climate model to generate a high-resolution climate scenario over the study area in order to identify and quantify the climate change impact in precipitation, temperature and other variables important for climate change impact studies.

The second approach to climate change modelling was based on six downscaled,bias-corrected,GCM projections based on the historical period 1975-2005 while the future period under RCP4.5 and RCP8.5 covered 2020-2050 for the KRB. The historical period 1975-2005 was chosen to be the baseline period (The recent past climate) because of availability of the required climate data. Further more Many climate change impact studies are conducted using a recent baseline period such as 1961-1990 and 1975-2005 (Krinner et al. 2013; Ferrise et al. 2011). The 19th centuary is mostly preferred baseline period due to insignificant anthropogenic effects on global climate.

The climatic variables from the two climate scenarios (RCP4.5 and RCP8.5) were used differently to quantify the impact of climate change for the KRB. The second approach involved the use of six downscaled and bias-corrected GCM outputs for hydrological modelling using the SWAT model. The GCM projections were used as

input data in the SWAT model in order to determine the impact on hydrology and water resources management.

3.3.1 Regional Climate modelling using PRECIS Model

PRECIS is a land surface and atmospheric model of limited area with a high-resolution that can be performed on any part of the earth. Dynamic downscaling was performed with the PRECIS model from Hadley Centre Global Environment Model version 2-Earth System (HadGEM2-ES) GCM over the historical (baseline) and future climate periods (Bodas-salcedo et al. 2014). The Hadley centre, UK developed the PRECIS model, which is the current version of the RCM with HadRMP3 based on HadAM3P, an updated version of the atmospheric component of the newest Hadley centre, coupled with the Atmosphere Ocean Global Circulation Model (AOGCM), HadCM3 (Macadam & Janes, 2017; Nandozi et al. 2012). Therefore, HadRM3P is a PRECIS, RCM based on the UK Met Office's HadCM3 GCM. Dynamic downscaling was achieved through the method of nesting HadRM3P into the HadGEM2-ES GCM to represent the atmospheric physics with a high-resolution grid box of a limited area (Brienen et al. 2010).

The model is developed on the dynamical flow, clouds, precipitation, radiative processes and the atmospheric sulphur cycle, the land surface and the deep soil. The hydrostatic version of the PRECIS model is the atmospheric component, which is based on the full primitive equations. The atmosphere consists of 19 vertical levels with the lowest at ~50m and the highest at 0.5hPa while the horizontal resolution is 0.44° × 0.44° with a time step of 5 minutes to maintain numerical stability (Judit et al. 2008; Jones et al. 2004). Solar radiation provides remote processes with external forcing that determines the climate of a particular local region. The composition of

the atmosphere affects radiation and various responsive processes within the global climate system. A regional climate model requires boundary conditions as inputs to provide the remote forcing of the regional climate and coherent information on atmospheric composition (Simon et al. 2015).

Regional Climate Modelling through PRECIS was conducted over the study area in order to provide high-resolution climate scenarios for a historical and future period under RCP4.5 and RCP8.5 with a focus on 2020-2050. The generated recent climate simulation was compared with observed values to validate the model and used as a baseline to provide climate change projections for the study area.

Four experiments were conducted to generate high-resolution climate scenarios, namely Reanalysis, Historical (baseline), RCP4.5 and RCP8.5 climate scenarios. The experiment results provided data specific to the study area to help generate new knowledge from the climate impact studies.

Figure 3.2 illustrates climate change modelling process as a methodological approach followed in the research.

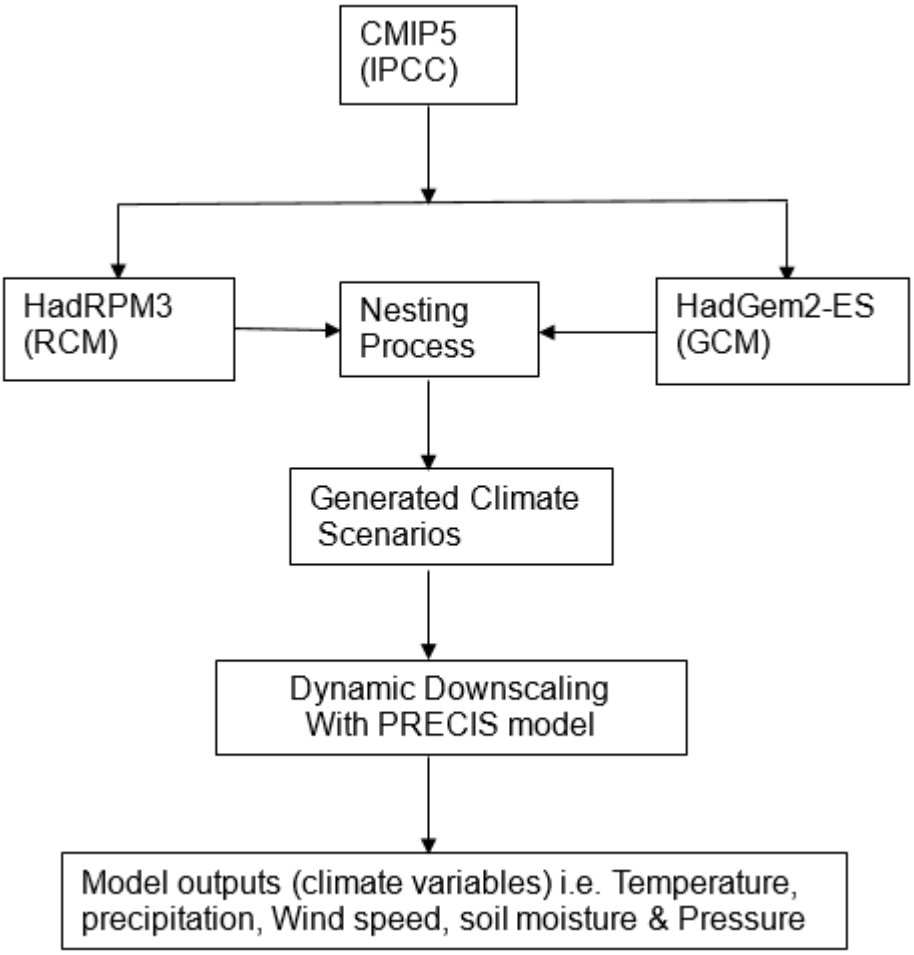

Figure 3.2 Climate change modelling process

Figure 3.2 illustrates the climate change modelling process with PRECIS model followed during the experiments. The process involved dynamic downscaling of the HadRM3P, RCM which was nested to HadGEM2-ES GCM. Both RCM and GCM were sourced from CMIP5, IPCC. The PRECIS model outputs included precipitation, temperature, pressure, soil moisture and wind speed.However in this research focus was on precipitation and temperature model outputs.

The research focused on the assessment of generated RCM projections from the PRECIS model experiments and the six downscaled and bias-corrected GCMs

projections. The forcing data generated covered the entire ZRB in Southern Africa and is therefore useful for further research in other areas within the basin to explore the impact of climate change.

3.4 Hydrological Modelling Using SWAT Model

SWAT model is a physically based and semi-distributed model that operates on a continuous daily time step and it was designed to predict the impact of management on water, sediment and agricultural chemical yields in ungauged catchments (Gassman et al. 2007;Neitsch et al. 2005). The Soil and Water Assessment Tool (SWAT) model, is well recommended and the most widely used hydrological model in the world (Abbaspour et al. 2019; Wang et al. 2019; Mehan et al. 2017). The SWAT model is considered user-friendly and easy to access, as it is readily available(Habte et al. 2013).

In the SWAT model, surface runoff volume is estimated with the modified Soil Conservation Service (SCS) Curve Number (CN) method (Mohammad, 2016). Peak runoff indicates the erosive power of a storm and is used in the prediction of sediments loss (Rostamian, 2010). The peak runoff rate is calculated in the SWAT model by using the modified rational method (Chow et al. 1988). Whilst the Kinematic Storage model is used to simulate lateral flow. The return flow is approximated by creating a shallow aquifer (Arnold et al. 1998). The Muskingum method is used to predict channel flood routing.

The water balance (Neitsch et al. 2005) equation that comprises the hydrological components in the SWAT model is described in Equation (3.1).

$$SW_t = SW_0 + \sum_{i=1}^{t} \left(R_{day} - Q_{surf} - E_a - W_{seep} - Q_{gw}\right) \quad 3.1$$

Where: SW_t final soil water content (mm); SW_0, initial soil water content on day i (mm); R_{day}, amount of precipitation on day i (mm); Q_{surf}, amount of surface runoff on day i (mm). Whilst $E_{a.}$, amount of evapotranspiration (ET) on day i (mm); W_{seep}, amount of water entering the vadose zone from the soil profile on day i (mm); Q_{gw}, amount of return flow on day i (mm).

3.4.1 Estimation of Water Yield

Water yield is one of the most important parameters used in the evaluation of water resources management in the basin under study. It is the summation of water leaving the HRU and entering the main channel during a time step (Arnold et al. 2011). Water yield of a sub-basin is evaluated by the SWAT model using the following Equation (3.2):

$$Wyld = Qsurf + Qgw + Qlat - Qloss \quad 3.2$$

Where: Wyld is the measure of the water yield (mm), Qsurf is the surface runoff (mm), Qgw is the groundwater contribution to streamflow (mm), Qlat is the lateral flow contribution to stream (mm) and Qloss is the transmission losses (mm) from the tributary in HRU by means of transmission through the bed (Fredrick & Manoj, 2018).

3.4.2 Calibration, uncertainty and sensitivity analysis

Calibration and uncertainty analysis is conducted using different methods, which include Parameter Solution (PARASOL), Adaptive Clustering Covering (ACCO), General Algorithm (GA), multi-start (M_Simplex), SWAT-CUP (Includes GLUE, SUFI2, MCMC, PARASOL and PSO). The uncertainty analysis is based on local errors and clustering. Calibration of models brings about some uncertainty in predictions, which can be categorised as conceptual model uncertainty, input uncertainty and parameter uncertainty (Abbaspour, 2015).

The most widely used method of the uncertainty estimation is the Sequential Uncertainty Fitting 2 (SUFI-2) together with the SWAT Calibration Uncertainty Programme (SWAT-CUP). The method is used to carry out parameterisation, sensitivity analysis, uncertainty analysis, calibration and validation of hydrological variables on daily and monthly time steps. The calibration process is made easier in SUFI-2 as it is semi-automated and can be conducted within a short period of time (Mehan et al. 2017).

The performance of the model for simulating streamflow based on monthly and daily measured flows has been classified into four categories, which depend on the threshold of the Modified Nash Sutcliff Efficiency (MNE) and Percent Bias (PBIAS) values (Moriasi et al. 2007). Table 3.1 shows the general performance ratings and the recommended statistics.

Table 3.1 Performance rating for recommended statistics (Moriasi et al.2007)

Category of MN	Category of PBIAS	Class
0.75 < MN ≤ 1.0	PBIAS < ±10	Very Good
0.65 < MN ≤ 0.75	±10 ≤ PBIAS < ±15	Good
0.5 < MN ≤ 0.65	±15 ≤ PBIAS < ±25	Satisfactory
MN ≤ 0.5	PBIAS ≥ ±25	Unsatisfactory

Besides the quantitative statistics in Table 3.1, hydrographs for observed and simulated flows are plotted to compare and enhance understanding of the base flow recession and other hydrograph characteristics (Daggupati et al. 2015). Figure 3.3 illustrates the hydrological modelling process using SWAT.

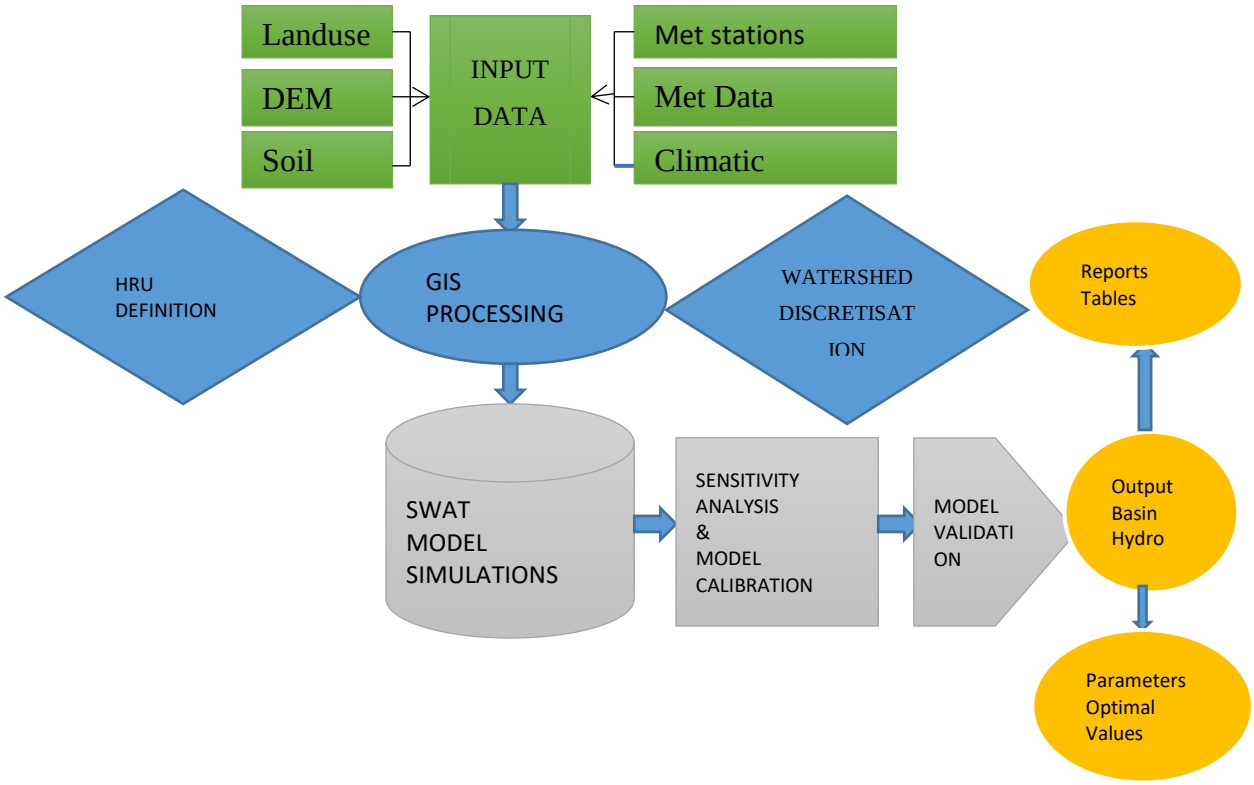

Figure 3.3 Overview of the SWAT process

Figure 3.3 illustrates the SWAT modelling process. The prevailing philosophy of modelling demands that models be described in a transparent manner that show the routine performance of calibration, validation, sensitivity and uncertainty analysis. Calibration is based on the model structure, model inputs, analyst's assumptions, calibration algorithm and calibration data while uncertainty analysis is used to evaluate the strength of the calibrated model (Abbaspour et al. 2015).

3.5 Evaluation of climate change impact on hydrology and water resources

The hydrological model results for the current water resources and the projected future water resources were analysed and integrated. A review of the current hydrology and water resources and its linkage to climate variability was undertaken

to establish a baseline. The current water resource was simulated with the use of the SWAT model and based on CFRS climate data. The future water resources were simulated using the calibrated SWAT model for all the GCM data.

Change Factor Methodology (CFM) a widely used method as described in chapter two was applied for climate change quantification (Trzaska & Schnarr, 2014; Hamududu, 2012; Anandhi et al.; Chen et al, 2011) in order to evaluate the changes in hydrology as simulated by SWAT based on the six GCMs. Impact assessments were done for the catchment water balance on temporal and spatial resolution, catchment streamflow variability and other climate and hydrological variables.

The PRECIS model outputs were used to identify climate change signals and the quantification based on monthly, seasonal and annual time scales. The major climate variables evaluated included precipitation and temperature. The PRECIS experiments generated data for the entire ZRB in Southern Africa.

The data generated under PRECIS experiments were for the period 1960-2009 for historical scenario while reanalysis scenario was from 1980-2009 and the future period under RCP4.5 and RCP8.5 covered 2020-2100. However the studies only focussed on the future period of 2020-2050. The PRECIS model utilised pressure, temperature, vapour, sea and ice as boundary conditions for Regional Climate modelling. The generated results were compared and validated with observed data from the same KRB over the same period.

CHAPTER 4 :STATUS OF HYDROLOGY, WATER RESOURCES AND CLIMATE VARIABILITY

4.1 Introduction

The assessment of the current status of water resources in ZRB and its linkage to climate variability is the first step in understanding the basin challenges,gaps and creates a baseline for studies. In view of climate change in the region, the need to assess the impact begins with a knowing the status of the hydrology and water resources by reviewing the available information for the region. Climate variability affect hydrology and water resources differently depending on time scale. The basin hydrology and water resources need to be continuously assessed in order to determine the availability and quality in a changing climate. This leads to formulation of adaptation and mitigation strategies.

In this chapter, an attempt is made to review the status of hydrology and water resources situation in the ZRB in order to identify linkages and gaps for future interventions. The overview of the changing climate is also heighted with evidence of climate change presented for most of riparian states.

In a bid to jointly manage the Zambezi transboundary river basin, the riparian states formed the Zambezi Water Course Commission (ZAMCOM), following the ratification of SADC protocol on water in June 2011 (ZEO-Zambezi-environment Outlook, 2012).

The ZRB is normally split into three distinct major river reaches. The first river reach is the upper ZRB that starts from the source at Kalene Hills up to the Victoria Falls. The second reach is the middle ZRB, which starts from the Victoria Falls to Cahora Bassa Gorge and the third reach is the lower ZRB, starting from Cahora Bassa Gorge to the Zambezi Delta and ending into the Indian Ocean.

The basin has two largest man-made reservoirs in the world and these are namely Kariba and Cahora Bassa. Lake Malawi (a natural lake) and Victoria Falls which is one of the seven wonders in the world are also sites for a hydroelectric power generation and irrigated agriculture. Figure 4.1 shows Lake Malawi, Victoria Falls, Kariba and Cahora Bassa reservoirs in the ZRB.

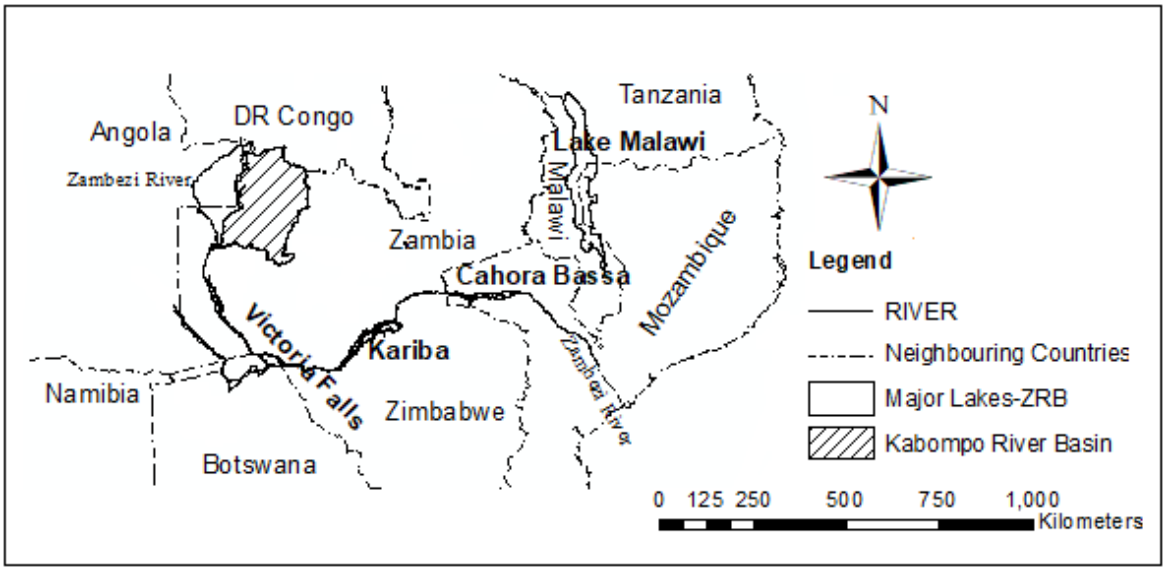

Figure 4.1 Location of the largest man-made reservoirs in the world

The variable climate in the basin directly affects the temporal and spatial variability of water resources in the region and therefore requires constant monitoring and evaluation in order to enhance integrated water resources management. The effects

of climate change are exacerbating the already poor water resources situation in ZRB. The previous decade has seen the availability of water resources in time and space drastically affected due to the high frequency of extreme events such as floods and droughts.

The challenges of extreme events are well known and include loss of lives, displacement of people, low agricultural productivity, low hydropower generation, increased malaria incidence cases, poor ecosystems and increased environmental problems. These challenges have adversely affected the performance of some economies in the SADC (SARDC, 2007).

Specific information on the climate change impact can be obtained through Regional Climate Modelling, which provides enhanced understanding of adaptive water resources management. Understanding the status of hydrology and water resources in ZRB and its linkage to climate variability is the necessary step in modelling and projection of future scenarios of water availability.

4.2 Materials and Methods

The methods used in this chapter included both quantitative and qualitative approaches. The methods applied involved a review of relevant literature such as books,written reports,research articles, conference proceedings and other periodicles and data collection from various sources within and outside the basin; validation and verification of the water resources in the basin. The data collected included time series data such as rainfall, temperature,water use statistics, river discharges and water levels. The other data included decadal temperature change,

areas affected by floods. While qualitative data included areas affected by floods, droughts, indications and evidence of climate change.

4.3 Climate Variability in the Zambezi River Basin

The MAP varies from 1200mm to 800mm in the Upper ZRB,1050mm to 700mm in the middle ZRB and about 1100mm to 900mm in the lower ZRB. The temperature differs significantly across the basin in accordance with Topography. The codest month is July with mean monthly temperatures of less than 14^{o}C while October is the hottest month with mean daily temperatures of 31°C in the lower parts of the Zambezi valley (ZAMCOM et al. 2015).

The Potential Evapotranspiration (PET) also varies considerably across the basin from more than 1700mm per year in the Middle ZRB to less than 1400mm per year in the Upper ZRB. The Potential Evapotranspiration in many parts of the ZRB is twice as high as the Precipitation totals and this affects the overall basin water balance (ZAMCOM et al. 2015; World Bank, 2010).

The Upper ZRB has six sub-basins while the Middle ZRB has four and the lower ZRB has three. Figures 4.2, 4.3 and 4.4 illustrate the distribution of the Mean Annual Precipitation (MAP) and the Potential Evapotranspiration (PET) for the three main river reaches. The data covered a period of about 50 years up until 2006 (Data source: World Bank, 2010; Builfuss & Santos, 2001).

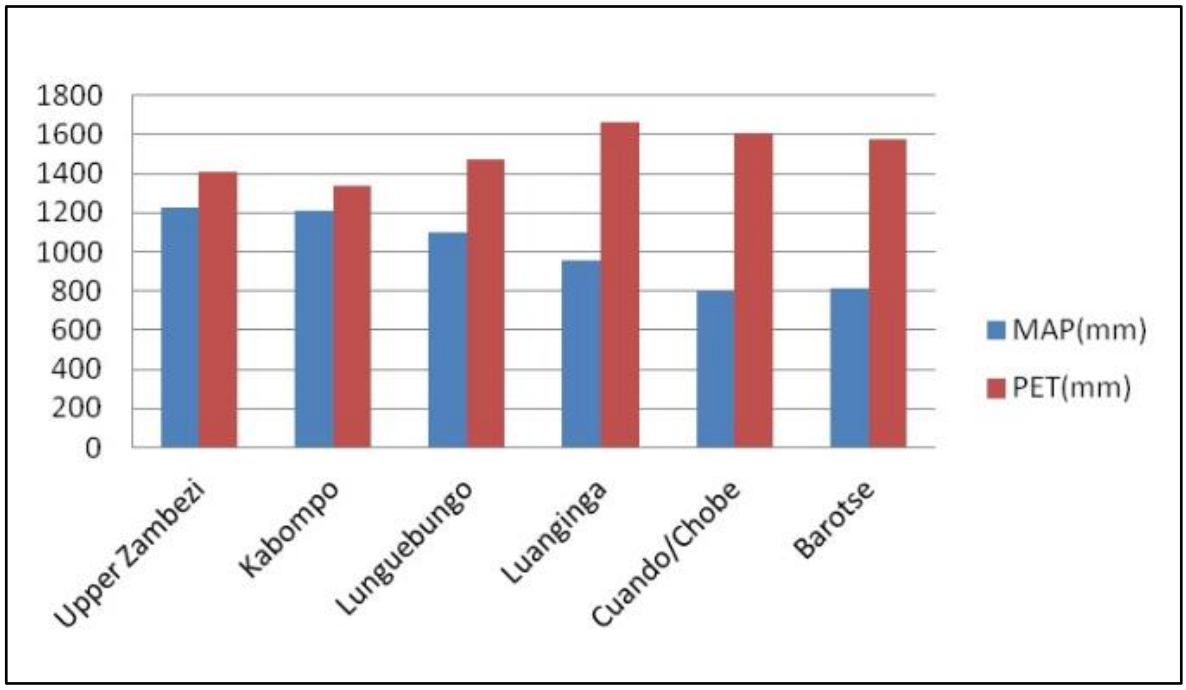

Figure 4.2 Comparisons of MAP and PET in the Upper ZRB

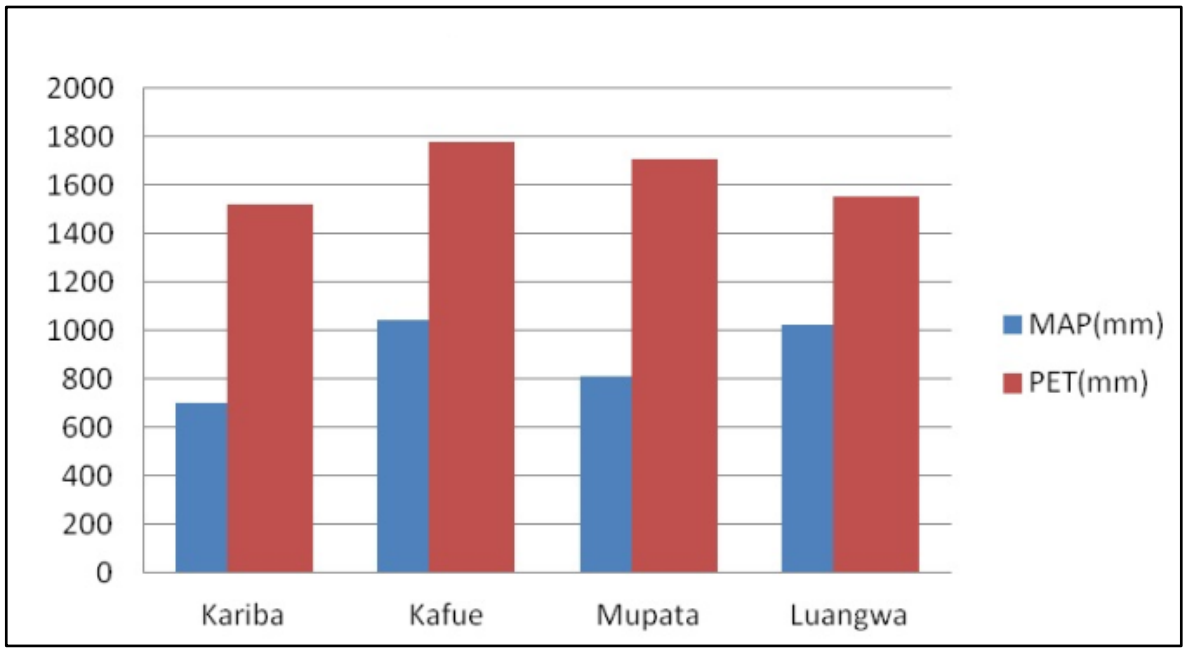

Figure 4.3 Comparisons of MAP and PET in the Middle ZRB

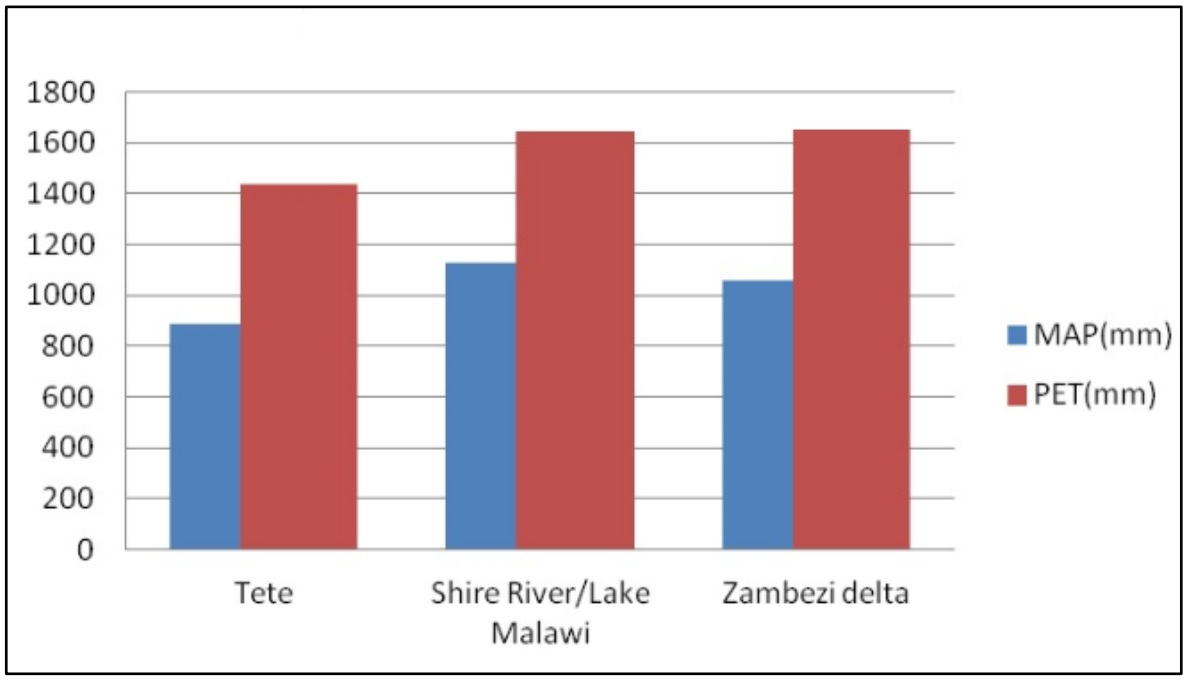

Figure 4.4 Comparisons of MAP and PET in the Lower ZRB

4.4 Hydrology of the Zambezi River Basin

The magnitude of the Zambezi River with all its tributaries has an average discharge of 2,600 m^3/s of water into the Indian Ocean; the same range as the Nile at 2,830 m^3/s and the Rhine at 2,200 m^3/s (Beck ; Bernauer, 2011). Rainfall is the principal source of all the available ground and surface water resources in the basin. The runoff coefficient is very low in the basin and averages less than 10% of the MAP (Beilfuss, 2012; World Bank, 2010). The basin experiences droughts and floods with a frequency of a decade.

Figure 4.4 shows less than 10% of the precipitation in the basin contributing to the natural (unregulated) flow of the Zambezi River into the Indian Ocean. The MAP and Mean Annual Runoff (MAR) indicate significant differences and thus more than 90% of the MAP in the basin evaporates and returns to the earth's atmosphere.

Therefore, the temporal and spacial variability of the available water resources in the basin is very significant (ZAMCOM et al. 2015).

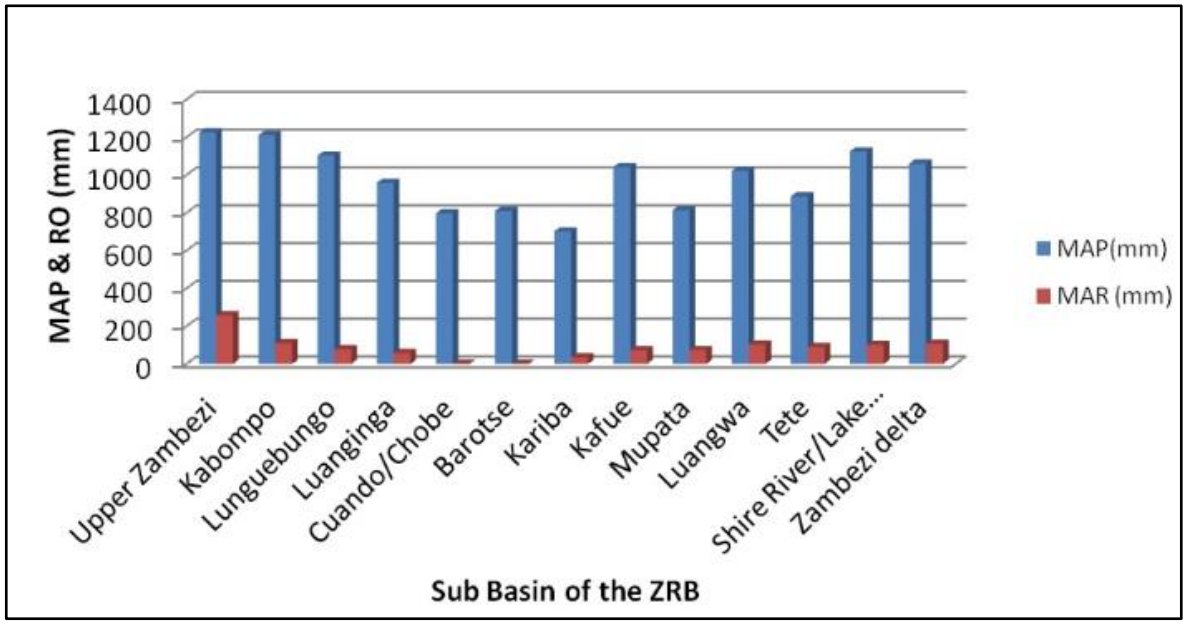

Figure 4.5 Comparisons of MAP and MAR in the ZRB

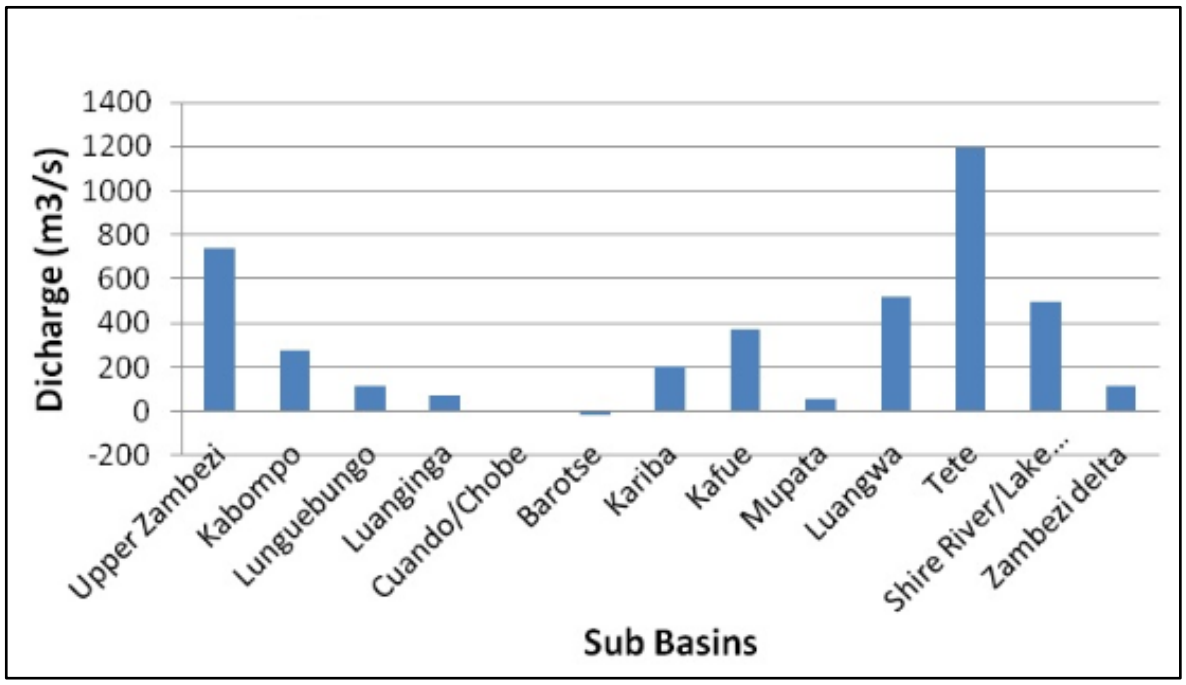

Figure 4.6 Mean Sub-Basin Flows in the ZRB (Data source: World Bank,2010)

Figure 4.6 illustrates that the highest flows were recorded in Tete sub-basin, which is found in the Lower ZRB while the Cuando/Chobe and Barotse contributed negligible flows to the entire basin. The flow regime of the basin also shows a higher contribution in the Upper and Lower ZRB than the Middle. The highest flow contribution to the river emanates from the Lower ZRB, leading to high potential for flooding because of general lower elevations (low lying areas that are prone to flooding).

4.5 Water Resources in the Zambezi River Basin

Water resources have become more vulnerable to climate change effects than ever before.The level of vulnerability varies in time and space throughout the basin. Vulnerability of water resources is mostly caused by floods, droughts, pollution sources such as on site sanitation,effluent discharges from waste water treatment plants in urban areas, industrial and mining effluents and agricultural pesticides,hebicides and other anthropogenic activities.

Surface water resources such as rivers, streams, reservoirs and lakes are more vulnerable than groundwater resources. The ZRB has more surface water resources in the lower ZRB and Upper ZRB than in the Middle ZRB. Botha & Cloot (2004), estimates that 75% of the fresh water on earth is frozen in glaciers, while approximately 0.33% is held in rivers, streams, reservoirs, lakes and the remaining 24.67% is groundwater. Therefore, groundwater needs to be further explored to augment surface water for mostly municipal water supply.

The largest water user in the basin has remained Hydro-Electricity Power (HEP) generation through evaporation from reservoirs. About 5000MW hydropower generation capacity is installed on the ZRB and an additional 13000MW of hydropower potential has been identified (World Bank, 2010). Table 4.1 illustrates the water use in the ZRB.

Table 4.1 Water use/consumption in ZRB

Consumptive Water Uses/Sector	Percentage (%)
HEP (evaporation)	83
Environmental/flood releases	6
Irrigated agriculture	7
Mining	1
Urban domestic consumption	1

(Source: Euroconsult Mott MacDonald, 2008)

4.6 Land Use/Cover of the ZRB

The anticipated development in energy and agriculture in a bid to increase HEP and agricultural production poses a challenge of changing land use and land cover significantly and may come at a cost of conservation of ecosystems and wildlife. When land use changes, hydrology is changed with its ecosystem.

Woyessa et al. (2011) argue that the impact of land use changes on water resources have multiple agents that directly or indirectly influence the land use decision-making process. Therefore, the ZRB should consider all factors at play in the land use decision-making process to ensure a balance is found between the development of energy, agriculture and the conservation of the ecosystem that will help to achieve poverty alleviation and contribute to economic development.

The other major land use has been the Miombo woodlands, which are the most extensive dry deciduous forests in the world, covering a substantial area of the KRB (Naidoo et al. 2013). However, the land use has been altered with the developments on the river systems such as changes in land use in the flood plains.

4.7 Climate Change and Water Resources in the ZRB

Studies carried out in Southern Africa on water resource management and climate change, indicated that hydrological systems and water resources would be altered resulting in the reduced availability of water (Cessford & Burke, 2005). Climate change in the basin has already begun to increase the variability of rainfall, as well as the occurrence of extreme events such as droughts, floods and heat waves.

Figure 4.7 illustrates the evidence of climate change recorded in the riparian countries.

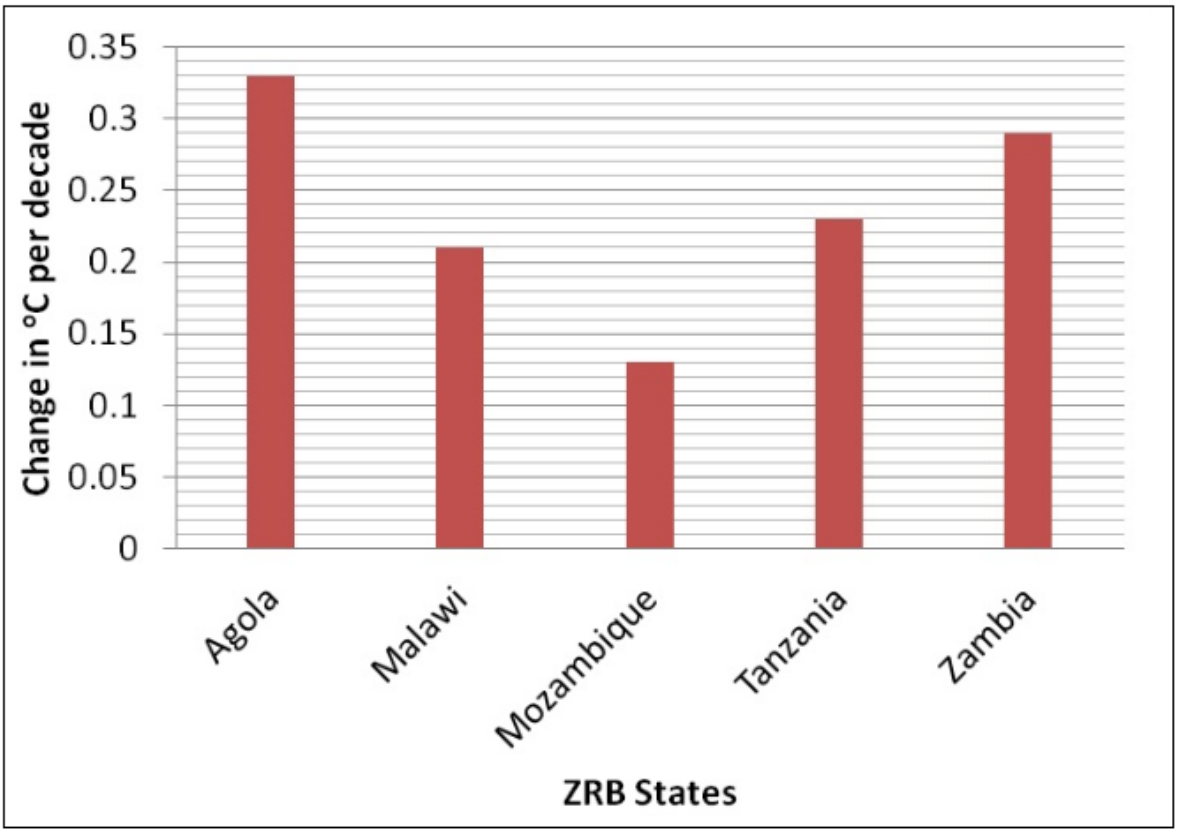

Figure 4.7 Mean decadal temperature rise (Source:Young et al. 2010)

Figure 4.7 illustrates that the observed trend in some Southern African countries between 1960 and 2006 with an increase in the mean annual temperature. Figure 4.7 also shows that Angola's mean annual temperature has increased with an average rate of 0.33^{o}C per decade, while Malawi's average increase rate was 0.21^{o}C per decade in the same period (SADC, 2014; Beilfuss, 2012; Young et al. 2010).

4.7.1 Drought

Droughts and floods drastically affect the availability of water resources. The climate change induced droughts has affected nearly all water consumption/uses in the basin such as energy, agriculture, municipal water supply, tourism, environment and mining. The biggest water use in the basin is in HEP generation through evaporation

from reservoirs. The water levels in reservoirs for hydropower generation become low in the basin to an extent where power generation is reduced, triggering shortages and affecting the economies adversely. The climate change induced drought between 2000-2009 killed about 500 people in Malawi and 58 people in Angola and affected about 30 million people in the riparian states (ZAMCOM et al. 2015). Figure 4.8 illustrates the distribution of people affected by country.

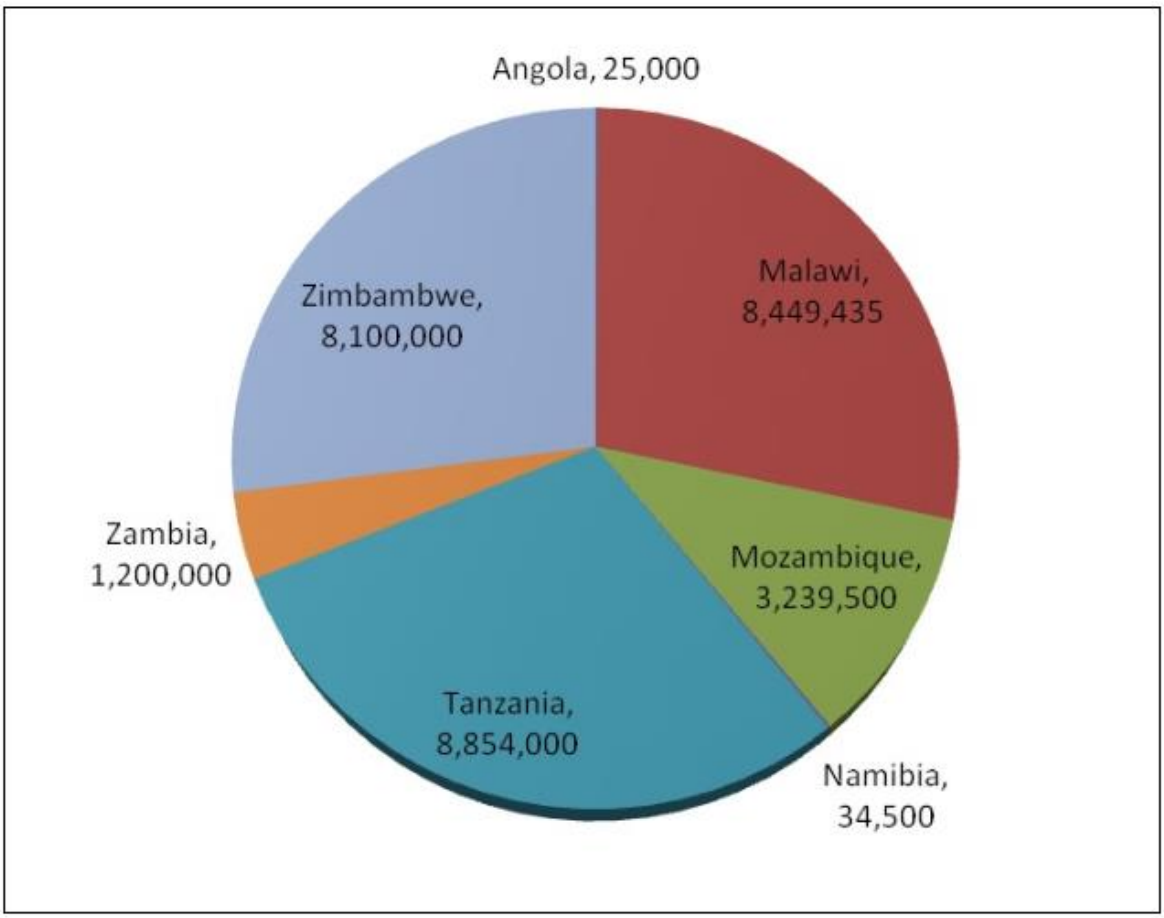

Figure 4.8 Total number of people affected in the Zambezi riparian states (Source: ZAMCOM et al. 2015)

The recent droughts in 2015/2016 affected the power generation at Kariba North and South banks where generation was reduced from 540MW to 305MW translating

into about 43% (Ipsos, 2015).This is due to the entire basin largely depending on hydropower with very few alternatives. The agricultural sector was equally affected, as most of the riparian states could not grow enough food, which led to food insecurity and famine. Tourism was also affected by the reduced flow as the Victoria Falls could not flow as required and wildlife in Namibia, Botswana and Zimbabwe were all affected due to the drought conditions. The drought also affected the groundwater levels where most of the boreholes and wells in rural areas dried up, forcing communities to walk long distances to fetch water for domestic purposes.

4.7.2 Floods

When above normal rains are experienced in the basin, floods occur; has a frequency of about once every 10 years. The climate change induced floods between 2000 and 2009 have killed 1,885 people while those affected were 12.1 million. Table 4.2 illustrates the magnitude of the problem in the basin by country.

Table 4.2 Impact of climate change induced floods 2000-2009

Country	People Killed	Total Affected
Angola	297	591509
Botswana	3	148392
Malawi	91	1223435
Mozambique	1012	6225126
Namibia	148	474300
Tanzania	162	96750
Zambia	60	3024633
Zimbabwe	112	331000
Total	1885	12115145

Source: ZAMCOM et al. 2015

Floods also destroy the public infrastructure such as roads, bridges, buildings and settlements in the region, which worsens the poverty levels. The agricultural sector is also adversely affected as most of the crop fields tend to be destroyed by floods reducing the yield and thus creating food insecurity.

Furthermore, the malaria prevalence tends to increase during floods, affecting a large population and leading to death. Water quality is also affected for both ground and surface water resources across the basin as much of the runoff transports pollutants, debris and faecal matter, from most of the shallow deposit sites. The populations face considerable challenges to find potable water during the season.

4.8 Conclusion

The variability of water resources across the basin is a matter of concern and requires concerted efforts to establish linkages of cooperation at a regional basin level. The energy sector are the most affected, as hydropower generation was drastically reduced by about 40%; in Zambia at Kariba North Bank the reduction was from 540MW to 305MW. The trend was the same with Zimbabwe at Kariba South Bank (Ipsos, 2015).

The situation has been exacerbated by the effects of climate change. There is inadequate knowledge coupled with research gaps on climate change impact on a local sub-basin scale as the most scientific information is on a global scale. There is, therefore a need to localise the research on climate change in an attempt to understand the complex hydrological processes.

The ZRB like other basins in Southern Africa also lacks hydro-meteorological data to accurately assess the water resources due to few, poorly maintained, hydro-meteorological observation networks. Therefore, there is a need for more research to explore other alternatives of assessing water resources in data scarce regions in order to be able to accurately quantify the available water resources.

More research is also needed in groundwater resources for the region as there is little knowledge, but a lot of potential. Review of relevant literature has shown that there is more fresh water on earth frozen in glaciers, than what is held in rivers, streams, reservoirs, lakes and groundwater. The largest percentage of water held is groundwater and therefore needs to be further explored to augment surface water for municipal water supply.

Therefore Chapter five explores the possibilities of using alternatives other than using the conventional (traditional observed data) in estimating water resources in data scarce regions. More research and a detailed analysis of the technologies used is presented in an attempt to accurately quantify the water resources in the ZRB and enhance a policy review of adaptation and mitigation strategies.

CHAPTER 5 : HYDROLOGICAL MODELLING USING GRIDDED CLIMATE DATA

5.1. Introduction

The hydro-meteorological stations of many river basins in Southern Africa are inadequate, low resolution and a poorly maintained (Botai et al. 2015; Hughes, 2013; Euroconsult Mott MacDonald, 2008; Walker & Road, 2000; Desmond et al. 1997). This culminates into inadequate and scarcity of hydrological data sets leading to challenges of inaccurate estimation of water resources (Tan et al. 2017). Water resources assessments are key to the planning and development of water resources in any given river basin (World Bank Group, 2018). The effective assessment of water resources is achieved through a well-maintained hydro-meteorological observational network in a given river basin.

In view of the affore mentioned challenges, gridded climate data as alternative technology to the conventional ground observed data was explored in assessing the hydrology and water resources of the KRB.

Gridded climate data selected was Climate Forecast System Reanalysis (CFSR) as it is a high resolution,global reanalysis climate data set, captured through satellite imagery. The use of CFSR for the hydrological simulation in the ZRB has not been adequately investigated . Therefore the main objective of this chapter is to determine the suitability of CFSR in data scarce regions for hydrological modelling and estimation of water resources of the KRB.

The CFSR was used as input data in SWAT model to simulate hydrological processes in the basin. Calibration and validation of the model for observed and simulated flows were performed using the SWAT-CUP.

The statistics showed NS at 0.73, while R^2 was 0.73. The uncertainty analysis showed the P-factor at 0.75 and the R-factor at 0.75. The simulation results also indicate that there is adequate water yield at present across the KRB with potential to harness and utilise more than half of the water yield that is distributed across the basin.

Overall, this chapter confirms that the use of CFSR for hydrological modelling in data-scarce regions could be a useful tool to estimate the main hydrological parameters and water resources of an area with satisfactory accuracy.

5.2 Materials and Methods

5.2.1 Data sets

The datasets used included the gridded climate data, global land use and land cover processed from remotely sensed imagery and global soil classification data. These data were used as input into a SWAT hydrological model in conjunction with GIS.

Gridded climate data

Soil and land cover data are more reliable and accessible because of modern technological advancement in remote sensing. However, hydro-meteorological networks are still rarely available and inconsistent in data capturing. In this chapter,

The gridded climate data sources such as CFSR are readily available from the National Centre for Environmental Prediction (NCEP) and ECMWF Re-Analysis ERAs from the European Centre for Medium-Range Weather (ECMWF) is explored to find lasting solutions. The CFSR, which covered the entire basin was downloaded from Texas A & M University Global Weather database (https://globalweather.tamu.edu).

The data included Precipitation (mm), Temperature (^{o}C), Relative Humidity (Fraction), Solar Radiation (MJ/m^2) and Wind Speed (m/s). The CFSR was captured from 55 stations within the basin and covered a period of 34 years (1979 to 2013). The CFSR was compared with ground observed rainfall data from five stations covering a period of 34 years (1979 to 2013) in order to determine the relationship between the two data sets.

Land use /land Cover

Land use types and various vegetation affect the overland flow of water in different ways. Evapotranspiration (ET) and runoff are mainly affected by vegetation, while land use types for different slopes with varying crop types result in varying runoff volumes (Woyessa et al. 2011). The activities of land use/land cover and water resources management are co-dependent. Land erosion in a catchment leads to sedimentation in water resources and on-site nutrient loss and nutrient enrichment of water resources (Rahul et al. 2012).

The land use/land cover data sets were obtained from USGS (https://landcover.usgs.gov/global_climatology.php), which is a Moderate Resolution Imaging Spectroradiometer (MODIS) land cover type with a resolution of

500m x 500m. MODIS-based global land cover types are widely used in hydro-meteorological modelling. It was found that the Collection 5.1 (MCD12Q1) product has a substantial amount of inter-annual variability, with 40% of land pixels showing land cover change one or more times from 2001 to 2010 (https://landcover.usgs.gov).

The Basin Soils

The basin soil map was prepared in ArcGIS based on the United Nations Food and Agriculture Organisation (FAO) soil classification obtained from Ministry of Lands, Government of the Republic of Zambia (GRZ). The soil identification for the basin was performed using the FAO/United Nations Scientific Council (UNESCO) soil scientific description based on the pixels.

The Digital Elevation Model (DEM)

The DEM was obtained from the Shuttle Radar Topographical Mission (SRTM) with a resolution of 30m (https://earthexplorer.usgs.gov/), which is also the most widely used elevation data in the world. The basin DEM, which was masked from the pro-mosaic DEM has the highest elevation of 1568m while the lowest point is 1020m above sea level. Figure 5.1 illustrates the delineated KRB DEM with an area of 72 082km^2.

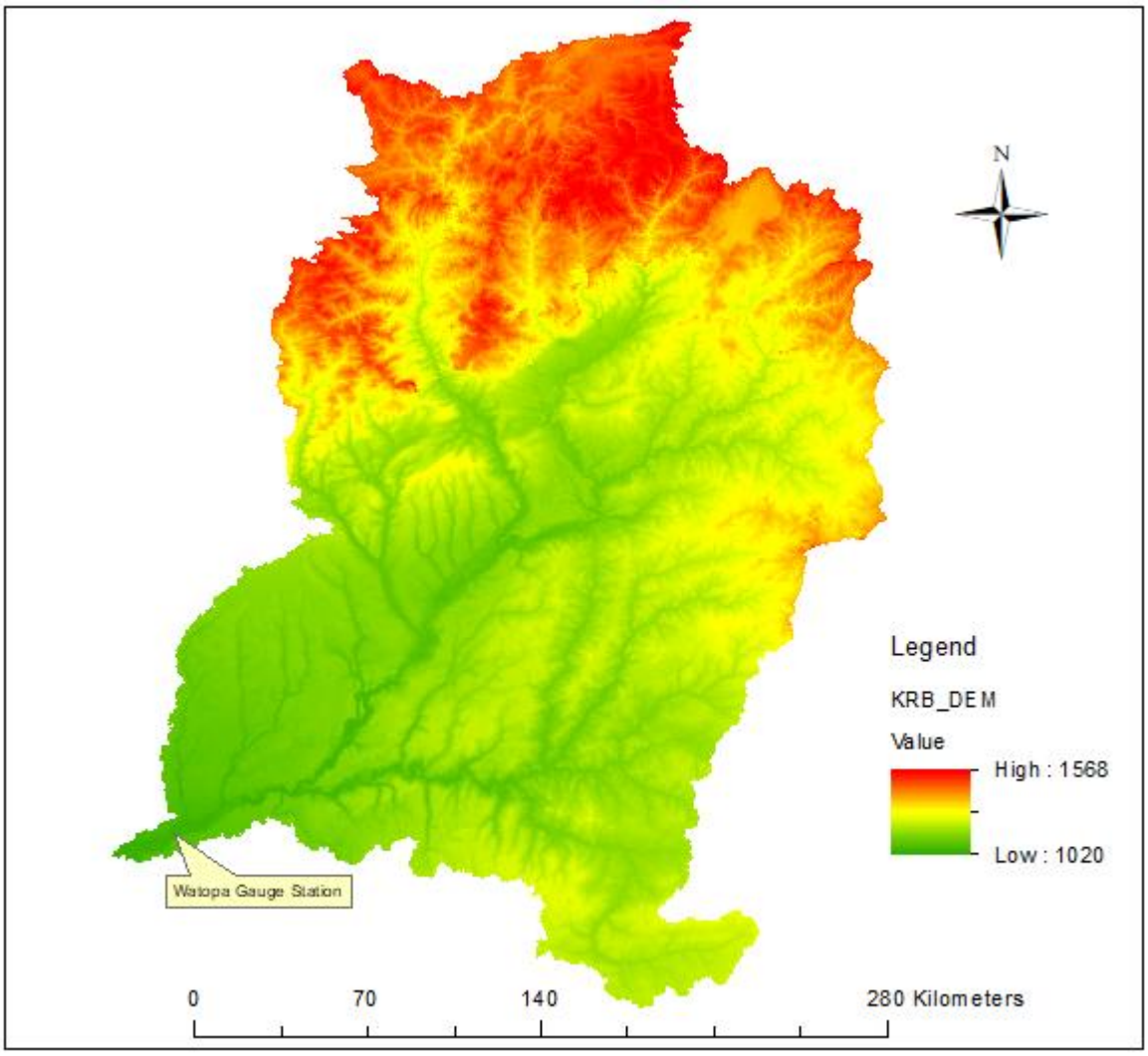

Figure 5.1 Digital elevation model of the KRB

Figure 5.1 illustrates the KRB with a delineated surface area of 72082km^2. It also shows the Watopa gauge station where observation flow data is captured.

5.2.2 SWAT Model set up

The model was set up and parameterised within ArcGIS interface (Arc SWAT 2012). A DEM of 30m resolution was used to delineate KRB with an area of 72 087km^2. The DEM was overlaid with soil and land use data, producing 102 sub-basins and 255 hydrological response units (HRUs). The HRUs are not spatially continuous but

are considered homogenous units with similar slope range, soil type and land use types and are the basic units for hydrological simulations.

The model simulations were undertaken for a period of 1979 to 2013. The first three years of simulations are used for initialising or warming up the model. Due to insufficient and unreliable flow measured data, only one gauging station with observed streamflow data was used for calibration and validation. About two-thirds of monthly flows (data points) from 1982 to 1997 of the observed data from this station (Watopa) was used for calibration and the remaining one-third from 1998 to 2005 was used for validation of the model. Figure 5.2 illustrates the subdivided KRB and the created HRUs.

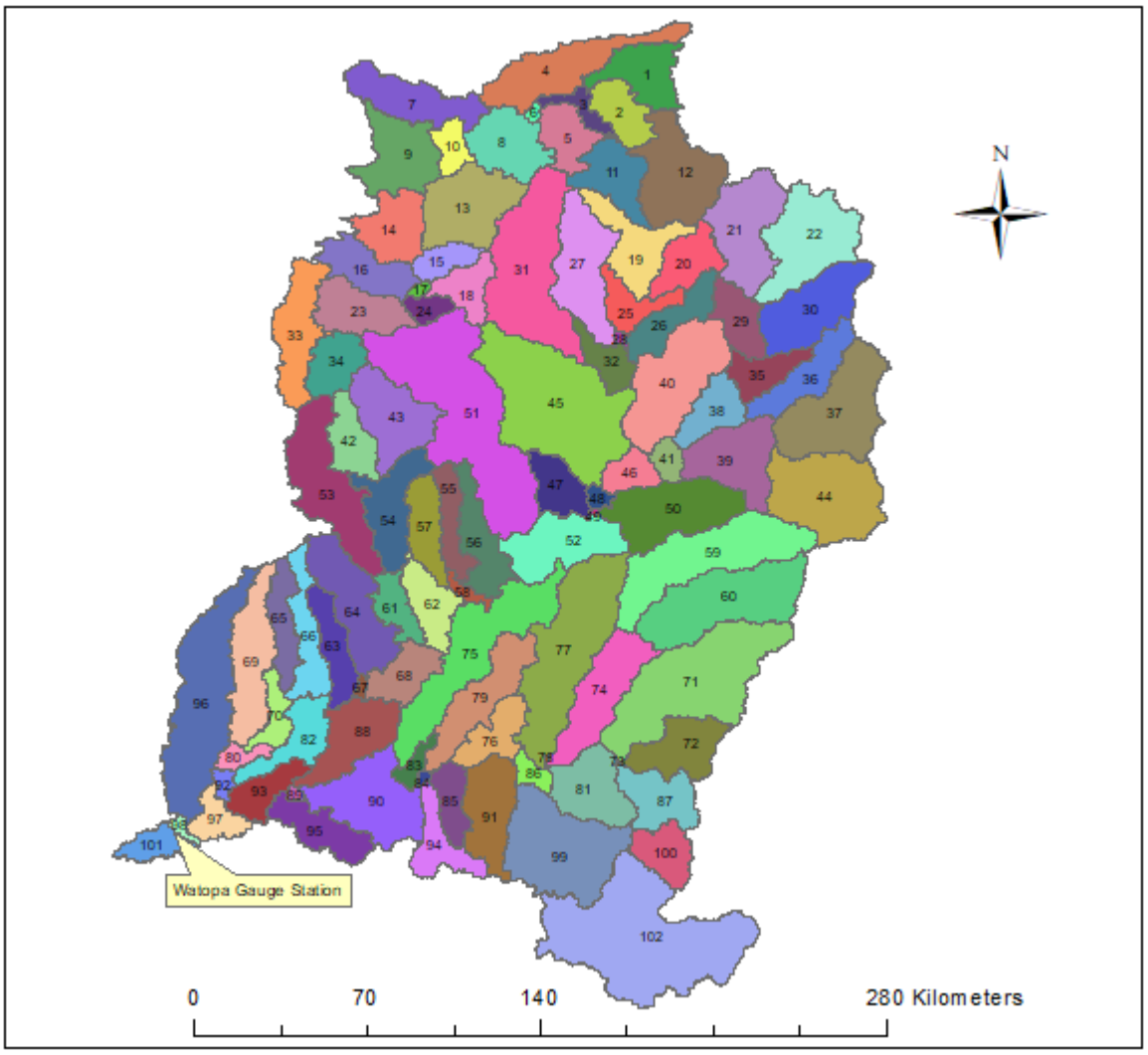

Figure 5.2 The sub-basins of the KRB

Figure 5.2 illustrates the 102 sub-basins with their numbers, which were further divided into 255 HRUs. Observed flow data were obtained from Watopa gauge station (shown on figure 5.2) on sub-basin number 98 for calibration and validation purposes. The sub basin areas are listed in, Appendix A, Table A1.

5.2.3 Performance Indices

The study considered four performance indices to evaluate the model performance, namely P-factor, R-factor, R^2 and NS. The R^2 and NS were used as a likelihood measure for the rainfall-runoff model (SWAT model) in the SUFI-2 approach

between the simulated and observed streamflow. The NS was calculated using the following Equation (5.1):

$$NS = 1 - \frac{\sum_{i=1}^{n}[yi - xi]^2}{\sum_{i=1}^{n}[xi - \bar{x}]^2} \quad (5.1)$$

Where: xi is the ground-based measurements; yi is the model predicted data; $\bar{x}$ is the mean of the ground-based measurements.

The P-factor, which is the percentage of measured data bracketed by the 95% prediction boundary, also referred to as 95PPU, was used to quantify all the uncertainties associated with the SWAT model. The P-factor and R-factor are linked to each other; a larger P-factor can only be obtained at the expense of a higher R-factor. The R-factor is calculated by the following Equation (5.2):

$$\text{R-factor} = \frac{\frac{1}{n}\sum_{i=1}^{n}\left(y^{M}_{ti,97.5\%,} - yi^{M}_{ti,2.5\%}\right)}{\sigma_{obs}} \quad (5.2)$$

Where: y_ (ti, 97.5 %,) ^M is the upper boundary of the 95UB; y_ (ti, 2.5%) ^M is the lower boundary of the 95UB and σ_obs is the standard deviation of the observed data.

5.3 Results and Discussion

5.3.1 Comparison of observed and CFSR rainfall data

Long-term gridded climate data are reliable data sets that can be used in the determination of climate change and in the development of adaptation and mitigation strategies in a river basin (Tan et al, 2017). Recent investigations revealed that the use of gridded climate data in the SWAT model produced streamflow simulations that are comparable to when conventional weather stations were used (Fuka et al. 2014; Grusson, 2017).

In addition, (Dile & Srinivasan, 2014) found that the application of CFSR data is comparable to conventional weather stations and that in data scarce regions CFSR could be recommended. CFSR data set covered the entire basin with a ground resolution of approximately 38km and Figure 5.3 illustrates the distribution of the CFSR precipitation locations and ground weather stations.

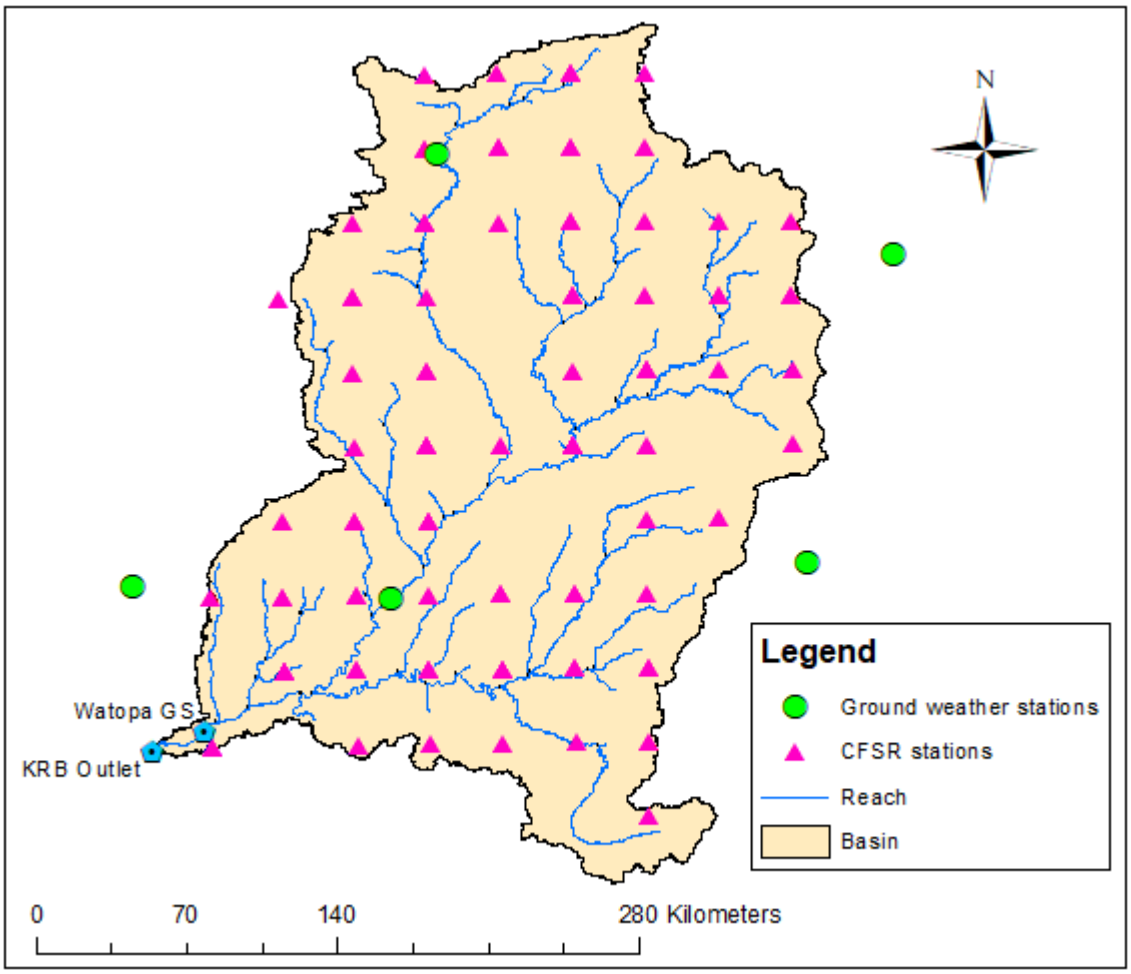

Figure 5.3 Distribution of CFSR and ground weather stations

As indicated in Figure 5.3, there are 55 CFSR stations (represented by pink triangles) while there are five ground weather stations (represented by green circles), with a ground resolution of approximately 150km.The observed flows were recorded at Watopa GS (Indicated in blue pentagon-shaped symbols).

The CFSR data is based on both historical and operational records of observations and newly reprocessed sets of observations produced at meteorological research centres around the world. CFSR assimilates observations from upper air balloon observations, aircraft observations and satellite observations. Since 1978, several records were combined for CFSR assimilation from National Centres for

Environmental Prediction (NCEP) and the European Centre for Medium Climate data (https://www.ecmwf.int/en/about).

Figures 5.4 (a) and (b) illustrates the spatial distribution of the annual rainfall based on sub-basins and HRUs for CFSR rainfall and ground observed rainfall, respectively.

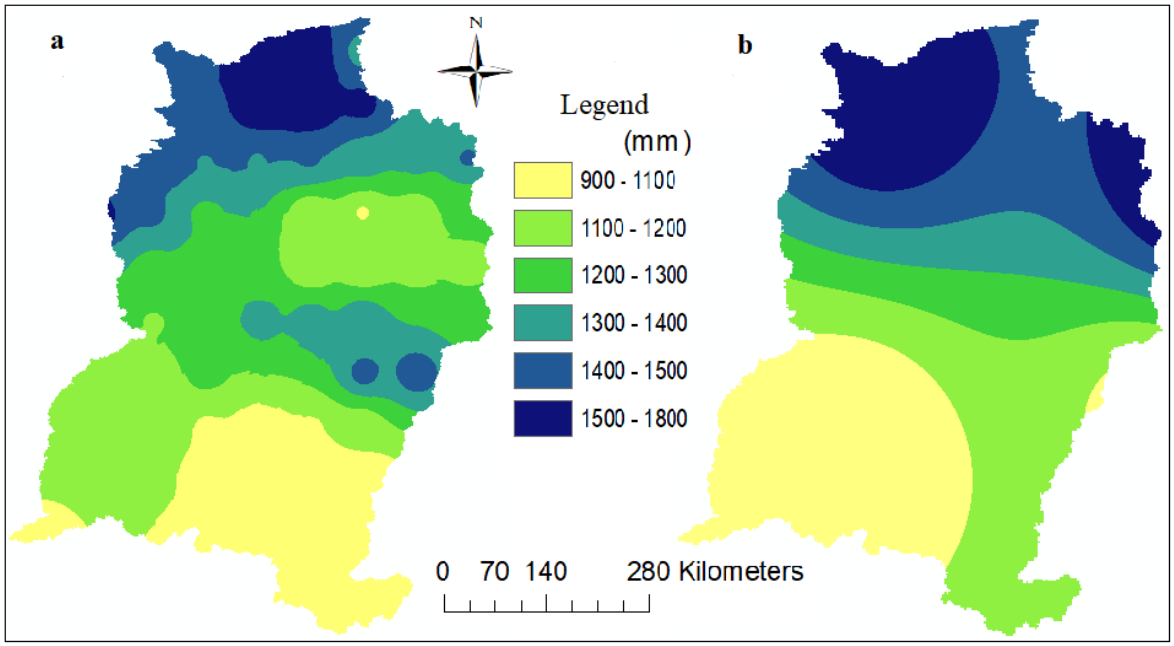

Figure 5.4 Spatial distribution of annual rainfall for CFSR (a) and observed (b)

The spatial distribution of CFSR rainfall in Figure 5.4 (a) clearly illustrates that more rainfall is received in the northern part of the basin and less in the southern part, which is confirmed by the observed spatial distribution of annual rainfall in Figure 5.4 (b) during the same period. The observed spatial distribution of annual rainfall was derived from five meteorological stations.

The CFSR data was further subjected to a trend analysis in order to determine its suitability for use in the SWAT model. A correlation coefficient was determined

between the observed monthly rainfall data considered suitable from ZMD for the basin area and the CFSR monthly rainfall data. Gridded rainfall data from CFRS is listed on Appendix D,Table D1.

The results shown in Figure 5.5 indicate a correlation efficiency of 97%, which confirms the reliability of the CFSR data for use in hydrological modelling.

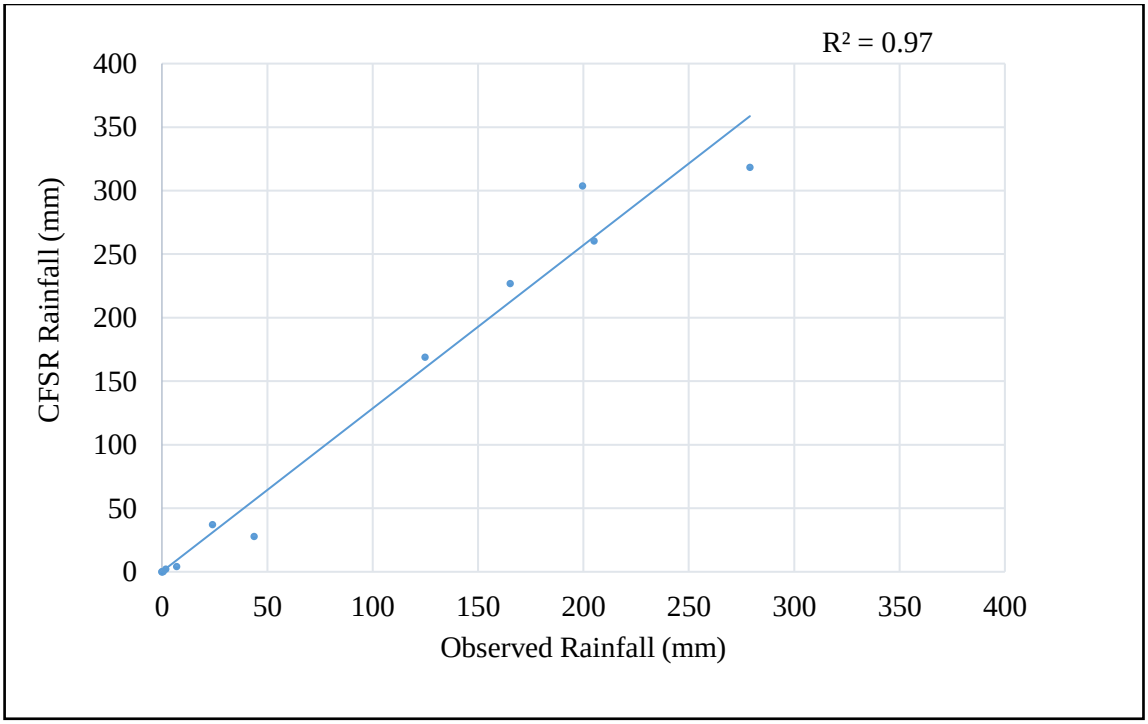

Figure 5.5 Relationship between CFSR and observed mean monthly rainfall

The mean monthly rainfall for both CFSR and observed rainfall is illustrated in Figure 5.6 and the graphical comparison indicates a strong correlation. The rainfall starts in September and increases every month until January when peak rainfall is recorded while there is no rainfall recorded between May and August for both data sets. However, the differences are also eminent in magnitude where CFSR data is slightly overestimating monthly rainfall for some months.

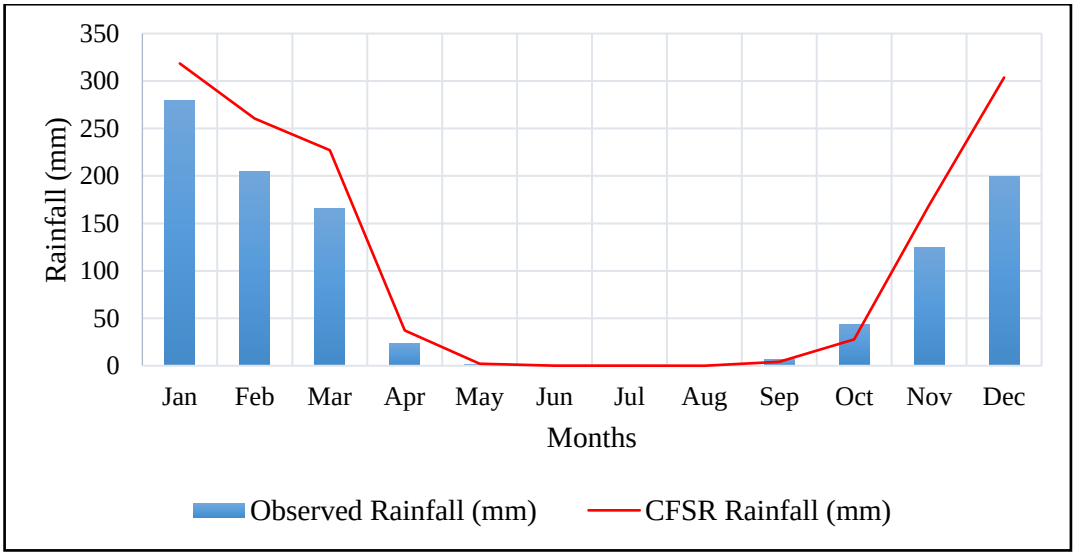

Figure 5.6 Comparison of average monthly CFSR and observed rainfall

The mean annual rainfall for both datasets is illustrated in Figure 5.7 with the mean annual rainfall from both datasets have similar patterns and trends with minor differences between the two curves. The available observed data was from 1982-2013 and hence only that period was obtained for CFSR annual rainfall to enable comparisons.There is however, a wide separation between 2007 and 2013 of the

curves perhaps due to some inherent errors in the observed data or a change in the rainfall regime.

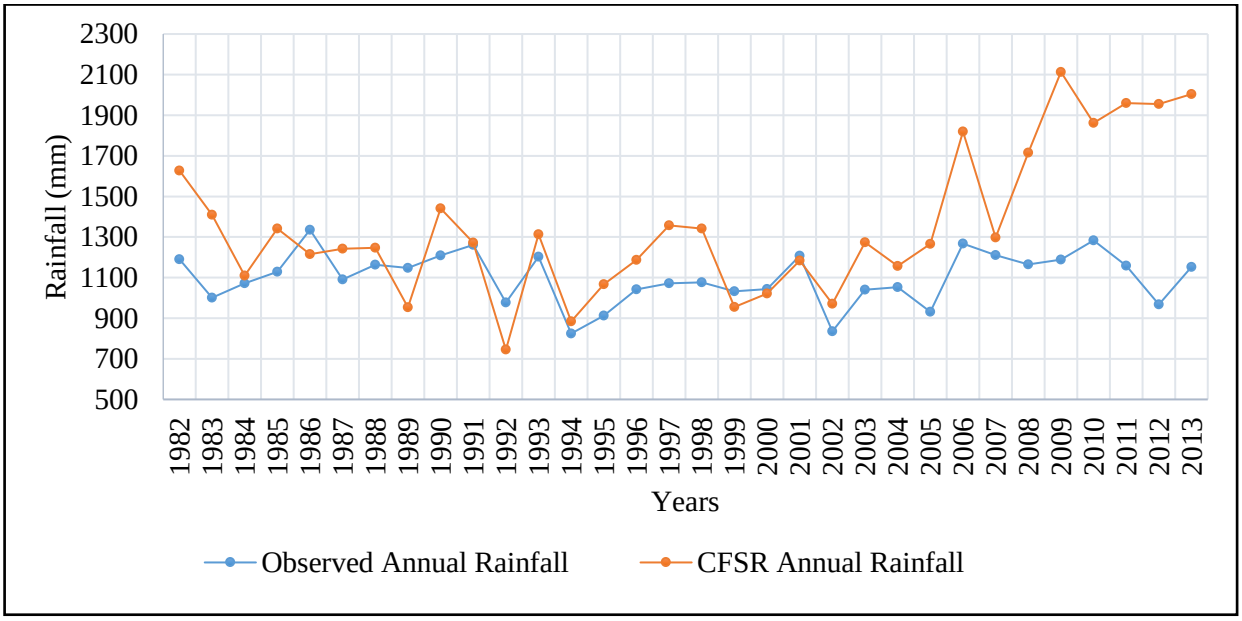

Figure 5.7 CFSR and observed annual rainfall (1982-2013)

Further analysis was performed to determine the Coefficient of Variation (CV) for the annual, monthly and seasonal rainfall for the two data sets. The CV was calculated for each period of analysis to measure the relative variability of datasets on a ratio scale and was used to study quality assurance by measuring the dispersion of rainfall data of a frequency distribution. Table 5.1 shows the results.

Table 5.1 Estimated Coefficient of Variation

Parameter	Observed	CFSR
Annual CV	0.115	0.262
Monthly CV	1.159	1.173
Seasonal CV		
DJF CV	0.195	0.103
MAM CV	1.393	1.362

The calculated annual, monthly and seasonal CV for CFSR and observed rainfall are comparable as seen in Table 5.1. The year is divided into four seasons, namely December, January and February (DJF) which is the typical rain season, March, April and May (MAM) which is the autumn, June, July and August (JJA), the winter season and September, October and November (SON) which is the summer season. DJF and MAM are rainy seasons in the basin that have matched well. The highest rainfall is recorded in DJF, followed by MAM, which forms the end season of rainfall.

Figure 5.8 shows a comparison of CVs for the CFSR and the observed rainfall datasets. The correlation coefficient of 97% shows that the gridded climate data are good enough to be used in hydrological modelling.

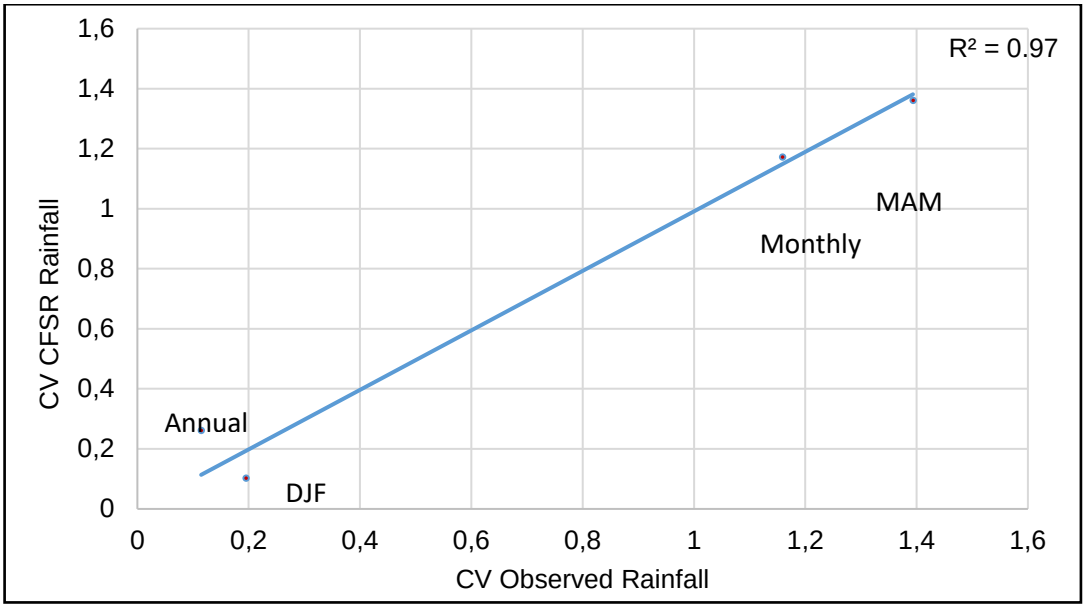

Figure 5.8 Comparison of CV of observed and CFSR seasonal rainfall 1982-2013

5.3.2 Calibration, uncertainty and sensitivity analysis

Model calibration and uncertainty analysis were performed with the SUFI-2 algorithm (Abbaspour et al. 2004; 2007) using the SWAT CUP software package. The results of the SWAT-CUP were useful in calibrating the model and estimating uncertainties and related assumptions in water resources modelling (Narsimlu *et al*. 2015). The algorithm calculates all the uncertainties of the parameters, conceptual model and other inputs in the form of a graph expressed as uniform distributions or ranges. Much of the observed data is captured within a threshold of 95% prediction uncertainty (95PPU) through the model iteration process. Latin hypercube sampling is used to calculate the 95PPU at 2.5% and 97.5% levels of cumulative distributions of an output variable.

Two indices, referred to as P-factor and R-factor (Abbaspour et al. 2004), were calculated in order to determine the Goodness-of-Fit (GOF). The P-factor represents the 95PPU for model simulation and the R-factor is the band representing observed

data including its error. The fraction of the observed data error, bracketed by the 95PPU band, is the P-factor and ranges from 0 to 1, where 1 is 100% bracketing of the observed data within the prediction uncertainty; the model simulation is perfect. A P-factor value of > 0.7 is often recommended to be adequate for simulation purposes, but the recommended values are largely dependent on the quality of the input parameters, calibration and validation data. While the R-factor is simply the ratio of the mean width of the 95PPU band and standard deviation of the measured variable, the preferred value is less than 1.5 based on the scale of the study (Abbaspour et al. 2015).

The P-factor and R-factor indices indicate the strength and performance of the calibration and validation. A bigger P-factor value can be obtained at the expense of a bigger R-factor value and, therefore, there must be a balance between the two. When acceptable R-factor and P-factor values are reached through iteration, the parameter ranges are considered calibrated parameters.

The sensitivity analysis was performed for 18 input parameters for KRB in the SWAT model. The large number of input parameters, representing various processes in the objective function of SUFI-2, improves enveloping of the observations in the model (Habte et al. 2013; Mehan et al. 2017). The parameters were selected and ranked through the global and local sensitivity analysis (Abbaspour et al. 2015). Global sensitivity analysis was determined by calculating the multiple regression of the Latin hypercube generated parameters against the objective function values.

The sensitivity of parameters in SUFI-2 is the estimate of the average changes in the objective function resulting from changes in each parameter when all other parameters are changing (Khalid et al. 2016). Table 5.2 indicates the sensitivity of parameters based on the global sensitivity analysis.

Table 5.2 Global Sensitivity of Parameters

Parameter Name	Description	t-Stat	P-Value
R__SOL_AWC (.).sol	Available water capacity of the soil layer (mm H_2O /mm soil)	-7.615	0.000
R__HRU_SLP.hru	Average slope steepness (fraction)	-2.171	0.030
R__SOL_BD (.).sol	Soil Bulk Density	-2.126	0.033
R__SOL_K (.).sol	Saturated hydraulic conductivity (mm/hour)	-2.032	0.042
V__GW_DELAY.gw	Groundwater delay (days)	-1.812	0.071
V__CH_K2.rte	Manning's n value for the main channel	-1.239	0.215
R__SLSUBBSN.hru	Average slope length (m)	1.057	0.291
R__OV_N.hru	Manning's n value for overland flow	-1.031	0.303
V__ALPHA_BNK.rte	Base flow alpha factor for bank storage (days)	-0.822	0.411
V__ALPHA_BF.gw	Base flow alpha factor (days)	-0.777	0.437
V__GWQMN.gw	Threshold depth of water in the shallow aquifer required for return flow to occur (mm)	0.5636	0.573
R__CN2.mgt	SCS runoff curve number	0.525	0.599
V__CH_N2.rte	Manning's n value for the main channel	-0.382	0.703
V__SURLAG.bsn	Surface runoff lag time (days)	-0.340	0.734
V__REVAPMN.gw	Threshold depth of water in the shallow aquifer for "revap" to occur (mm)	-0.314	0.753
R__SOL_ZMX.sol	Max depth from soil surface to rooting depth (mm)	-0.182	0.856
V__ESCO.hru	Plant uptake compensation factor	0.122	0.903
V__GW_REVAP.gw	Groundwater "revap" coefficient	0.036	0.971

Table 5.2 is the assessment of the sensitivity of parameters in SUFI-2 which was measured with the t-stat values and P-values. The parameters with larger absolute t-stat values are more sensitive while the P-values are used to determine the

significance of the sensitivity. When the P-value is close to zero the parameters are classified to have significance of the sensitivity.

SUFI-2 has 10 different objective functions, some of which include mean square error (MSE), Nash Sutcliff (NS), R^2 and Br2. The most widely used statistics in calibration and validation are R^2 and NS. The R^2 ranges from 0 to 1, where 0 shows non-correlation while 1 indicates a perfect correlation and provides an estimate of how well the variance of observed values are replicated by the model predictions (Krause et al. 2005).

The regression slope and intercept are equal to 1 and 0 respectively, although most of the published SWAT studies do not show the slope and intercept as a perfect fit. The NS values range from -∞ to 1 and provide a measure of how well the simulated output matches the observed data along a 1:1 line (regression line with slope equal to 1). The NS value of 1 shows a perfect fit between observed and simulated data. NS values ≤ 0 indicate that the observed data mean is a more accurate predictor than the simulated output. Both NS and R^2 are biased towards high flows (Arnold et al. 2012). In this study, Nash-Sutcliff (NS) was used as the objective function for discharge.

5.3.3 Land use/cover

The classification of land use for the basin was based on MODIS land cover type with a resolution of 500m x 500m. Figure 5.9 shows the land use/land cover for KRB.

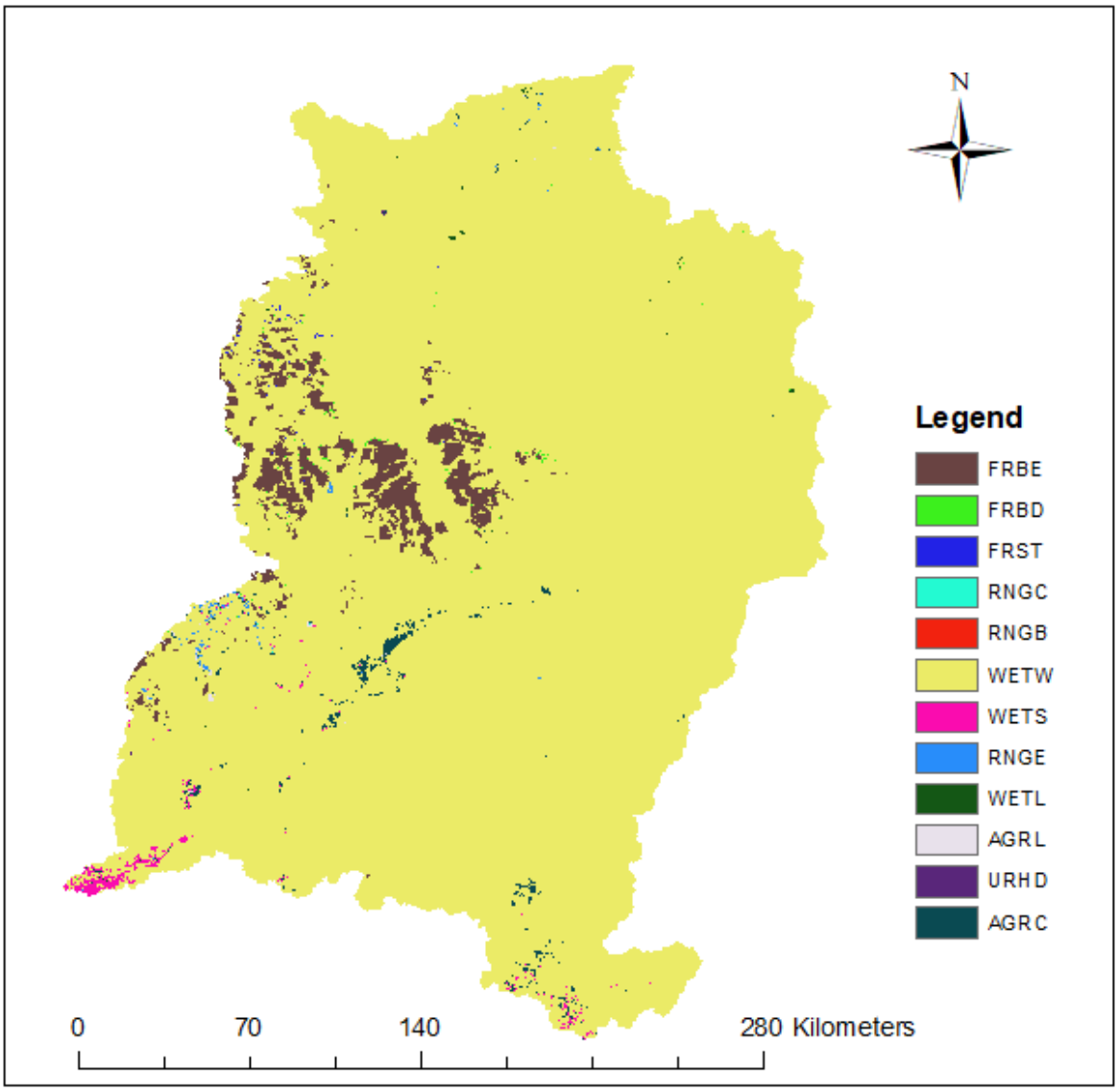

Figure 5.9 KRB land-use/land cover for 2010

The KRB land-use was grouped into 12 classes, with the woody savannahs being the predominant feature, which covers more than 90%, followed by evergreen broadleaf forest at 3.2% and the rest of the area is covered by landuse of less than 0.5%.Therefore the major influencing land use is woody savannahs. Table 5.3 shows land use/land cover for the basin based on 2010.

Table 5.3 Land use types according to the SWAT classification

Value	Description	Landuse	Area(%)
2	Evergreen Broadleaf Forest	FRBE	3.235
4	Deciduous Broadleaf Forest	FRBD	0.07
5	Forest-Mixed	FRST	0.051
6	Closed Shrub-lands	RNGC	0.002
7	Range Brush	RNGB	0.001
8	Woody Savannahs	WETW	95.624
9	Savannahs	WETS	0.355
10	Range-Grasses	RNGE	0.085
11	Wetlands-Mixed	WETL	0.04
12	Agricultural Land-Generic	AGRL	0.038
13	Urban and Built-Up	URHD	0.005
14	Agriculture Land-Close grown	AGRC	0.493
Total			100%

The KRB is divided into sub-basins, which are further subdivided into HRUs in order to classify the watershed conditions. The SWAT model reflects differences in evapotranspiration for various crops and soils based on the subdivision of the watersheds. The land use is, therefore an important data input into the SWAT model. Data sets with land use use types that account for more than 20% of the area in HRU are included in order to help address differences between the resolution of data sets (Coutu & Vega, 2007).

5.3.4 Soil

The KRB has eight identified soil types according to FAO/UNESCO soil classification of which arenosols are predominant with 30% basin coverage. The arenosols are commonly Kalahari sands, extending up to one-metre depth with sand

content of more than 70%, a clay and silt content of less than 10%, low nutrient content and low water retention capacity. Figure 5.10 illustrates the soil distribution across the basin.

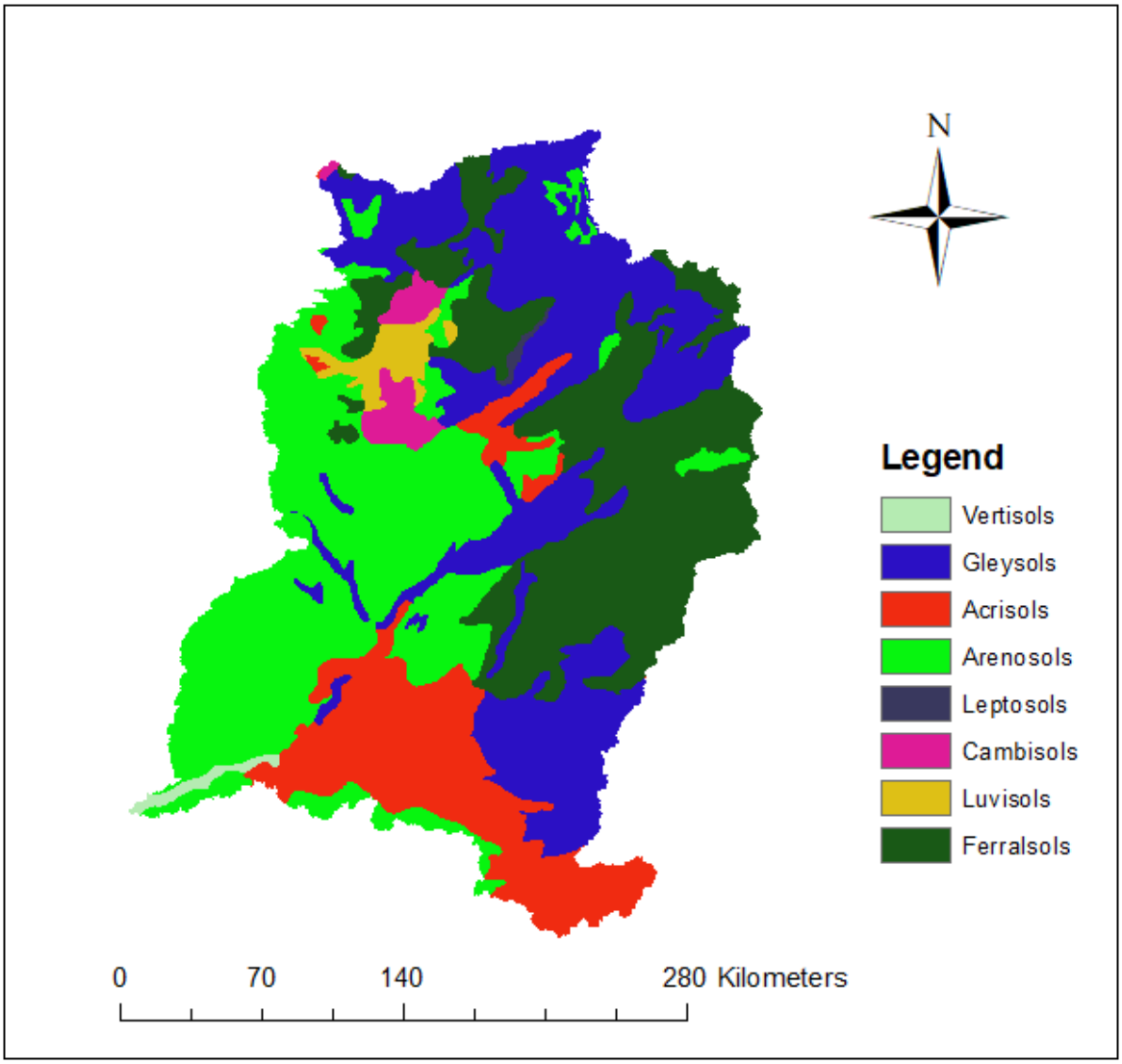

Figure 5.10 Spatial distribution of soil in KRB

Table 5.4 Basin soil coverage percentage

Soil Name	Texture	Basin Coverege (%)
Luvisols	Loam	1.77
Leptosols	Clay-Loam	0.0
Vertisols	High clay content	0.53
Gleysols	Loam	27.12
Acrisols	Loam	14.80
Cambisols	Loam	1.86
Arenosols	Sands	29.57
Ferralsols	Clayey soils	24.35
Luvisols	Loam	1.77

Source: (http://www.fao.org/soils-portal/soil-survey/soil-maps-and-databases/en/)

5.3.5 Calibration and validation

The SWAT model outputs were subjected to calibration by using SWAT_CUP with SUFI2. The model calibration was performed for the period 1979-1997, with an initial three years being used as a warm-up. The model was validated with the flow data from 1998-2005.The performance of the model calibration was found to be good with R^2 at 0.73 while NS was 0.73. Figures 5.11 and 5.12 show the graph with 95PPU for the calibration and validation, respectively.

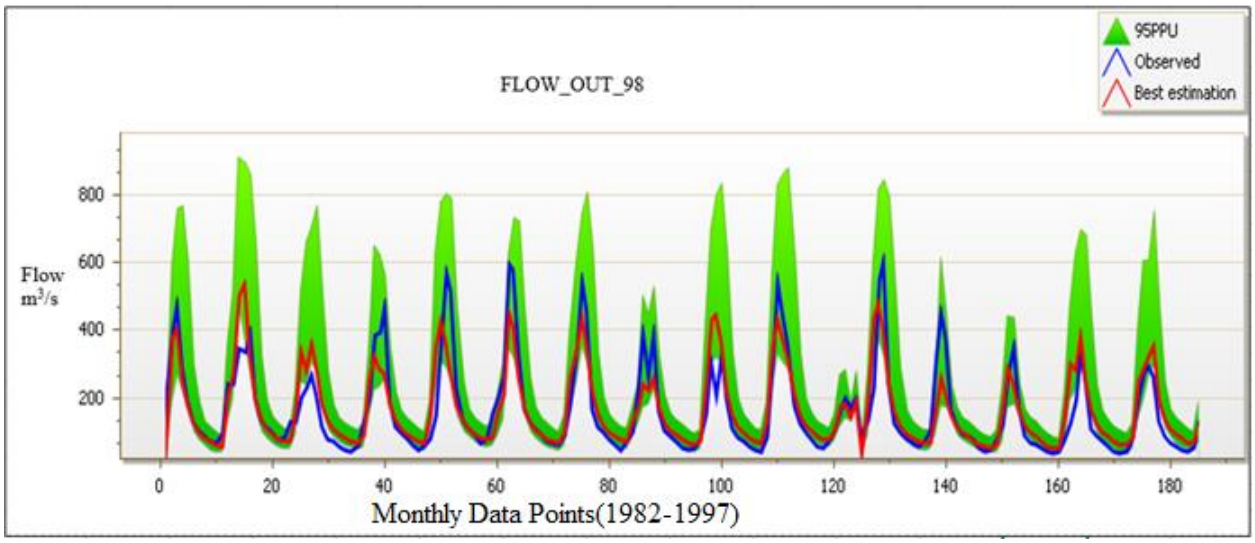

Figure 5.11 Calibrated of SWAT Model

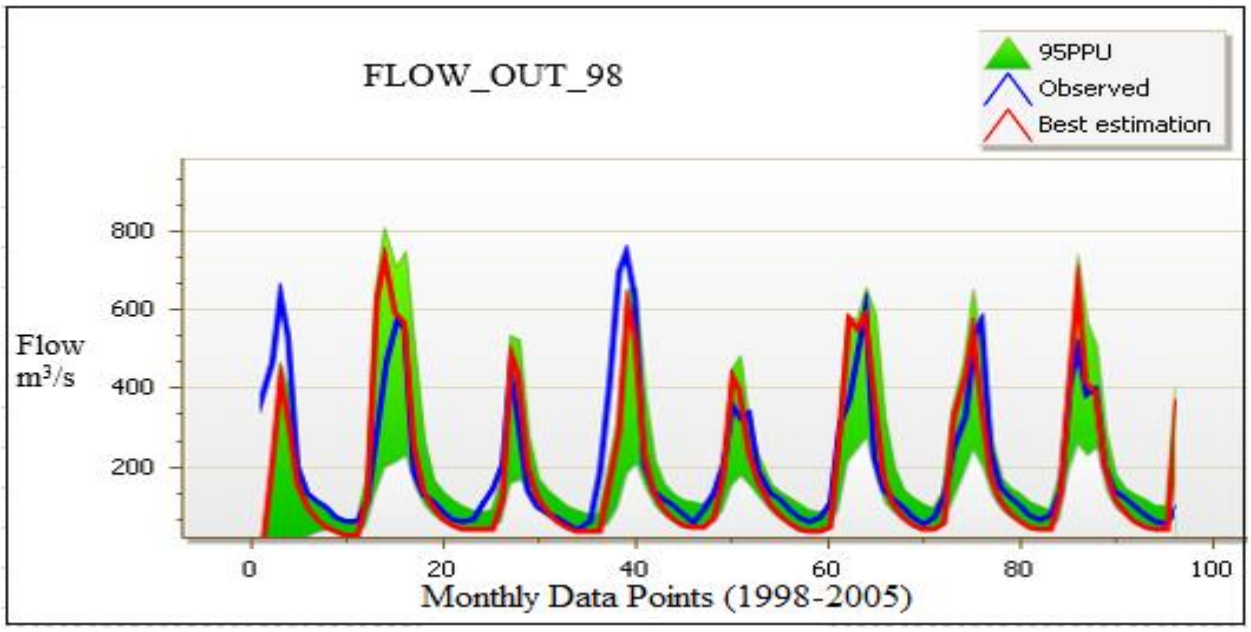

Figure 5.12 Validated of SWAT model

The comparisons of the calibrated and validated results are shown in Figure 5.13.

The data for calibration and validation is listed in Appendix C,Table C1 and C2.

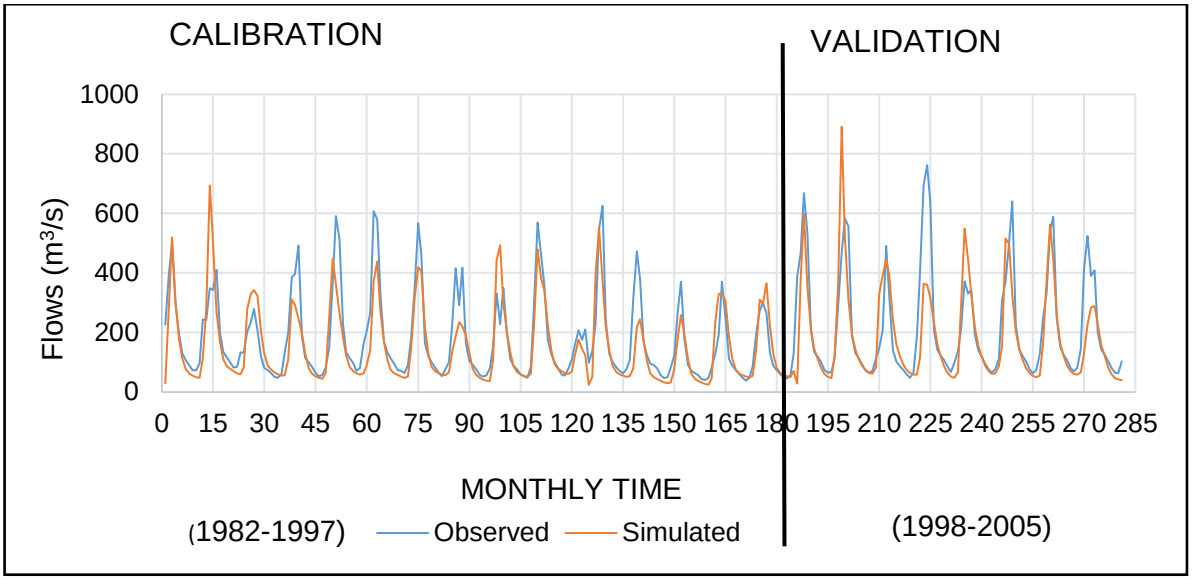

Figure 5.13 Comparisons of calibrated and validated of SWAT model

5.3.6 Uncertainty Analysis

Monthly time steps data were used to determine the performance indices for the model parameters. The calibration results in Figure 5.11 revealed that there were consistency and a close match between observed and simulated flows between 1982 to 1997. While the validated results in Figure 5.12 indicated a consistency in simulation of the stream flows between 1998 and 2005, the observed and simulated peak flow showed some mismatches probably due to the large area of the basin with limited gauging stations.

Figures 5.11 and 5.12 also show that the 95PPU was well bracketed during the calibration period from 1982 to 1997, with a P-factor of 0.75 and the R-factor at 0.75 while during the validation period from 1998 to 2005, the values changed to 0.73 and 0.55, respectively. The P-factor of 0.75 obtained during calibration and 0.73 during validation indicate that most of the observed and simulated data are bracketed with 95PPU. The slight decrease in P-factor from 0.75 to 0.73 during validation indicates the level of uncertainties in input variables, such as rainfall. The

measured data used for calibration and validation of model predictions is widely accepted with uncertainty inherent.

However, the model performance evaluation seldom includes the measurement uncertainty inherent due to data paucity on uncertainty inherent on measured input data (Harmel & Smith, 2007).

5.3.7 Goodness-of-Fit

The Goodness-of-Fit (GOF) was measured using R^2 and NS (Nash & Sutcliffe, 1970) between observed and simulated flow. The NS values, after calibration and validation, were found to be 0.73 and 0.64, respectively, which indicate that the results are good. A value of 0.6 is considered good for hydrologic evaluations performed on a monthly time step.

The coefficient of determination (R^2), after calibration and validation, was found to be 0.73 and 0.70, respectively, which indicate that the results are good since it exceeds 0.6 (Moriasi et al. 2007; Arnold et al. 2012; Tan et al. 2017). Table 5.5 shows the fitted parameter values.

Table 5.5 Fitted parameter values

Par No	Parameter Name	Fitted Value	Min_Value	Max_Value
1	R__CN2.mgt	-0.515517	-0.549675	-0.485105
2	V__ALPHA_BF.gw	-0.135606	-0.190592	-0.132034
3	V__GW_DELAY.gw	482.561829	478.066803	488.693329
4	V__GWQMN.gw	3.649851	3.511368	3.82972
5	R__SOL_AWC (...).sol	0.165577	-1.988471	0.496013
6	R__HRU_SLP.hru	0.443559	0.338701	0.524949
7	V__GW_REVAP.gw	0.105361	0.098434	0.11652
8	V__ESCO.hru	0.495606	0.489305	0.518885
9	R__OV_N.hru	19.204071	19.126938	27.697338
10	V__CH_N2.rte	0.267918	0.246142	0.268896
11	R__SOL_K (...).sol	0.074562	0.020596	0.159326
12	R__SLSUBBSN.hru	0.624561	0.565059	0.660875
13	V__SURLAG.bsn	26.83889	26.71983	27.194176
14	V__ALPHA_BNK.rte	0.032703	0.022104	0.051628
15	R__SOL_ZMX.sol	0.054973	0.024473	0.057517
16	V__REVAPMN.gw	487.243347	479.313232	496.294189
17	V__CH_K2.rte	4.76998	4.463252	7.561514
18	R__SOL_BD (...).sol	-0.579658	-0.595719	-0.486459

The most sensitive parameters were CN2 and Soil-AWC, while parameters such as R-soil _BD, were less sensitive. Robust calibration was performed with 500 iterations per simulation. Global sensitivity analysis was used in order to determine

the sensitivity of the parameters in SUFF-2. The statistics of GOF are summarised in Table 5.6.

Table 5.6 Statistical index for calibration (1982-1997) and validation (1998-2005)

Index	Calibration	Validation
Coefficient of determination (R2)	0.73	0.70
Nash and Sutcliffe Coefficient (NS)	0.73	0.64
P-factor	0.75	0.73
R-factor	0.75	0.55

The statistics in Table 5.6 indicate a good model performance at calibration with NS of 0.73 and R^2 of 0.73 while for validation the parameter values were 0.64 and 0.70, respectively. Sensitivity analysis also indicates that most of the observed and simulated data were bracketed by the 95PPU (P-factor) at 0.75 during calibration.

However, at the validation phase a slightly lower value of 0.73 was obtained probably due to the inherent uncertainty of measured data. Good results were also obtained for calibration with R-factor of 0.75 and validation with R-factor of 0.55. This shows that the thickness of uncertainty band was reduced and provided more confidence in the produced results (see Figures 5.11 and 5.12). The results also show that the use of CFSR in data scarce regions could be reliable and effective.

5.3.8 Simulation of stream flow and water yield

Simulation of streamflow for any river basin is an important result in hydrological modelling as it is used in water resources management. The simulated flows in KRB were graphically compared with the observed flow during and after the calibration period in order to determine their suitability for use in water resources management.

Figure 5.14. illustrates the rainfall with simulated and observed flows.

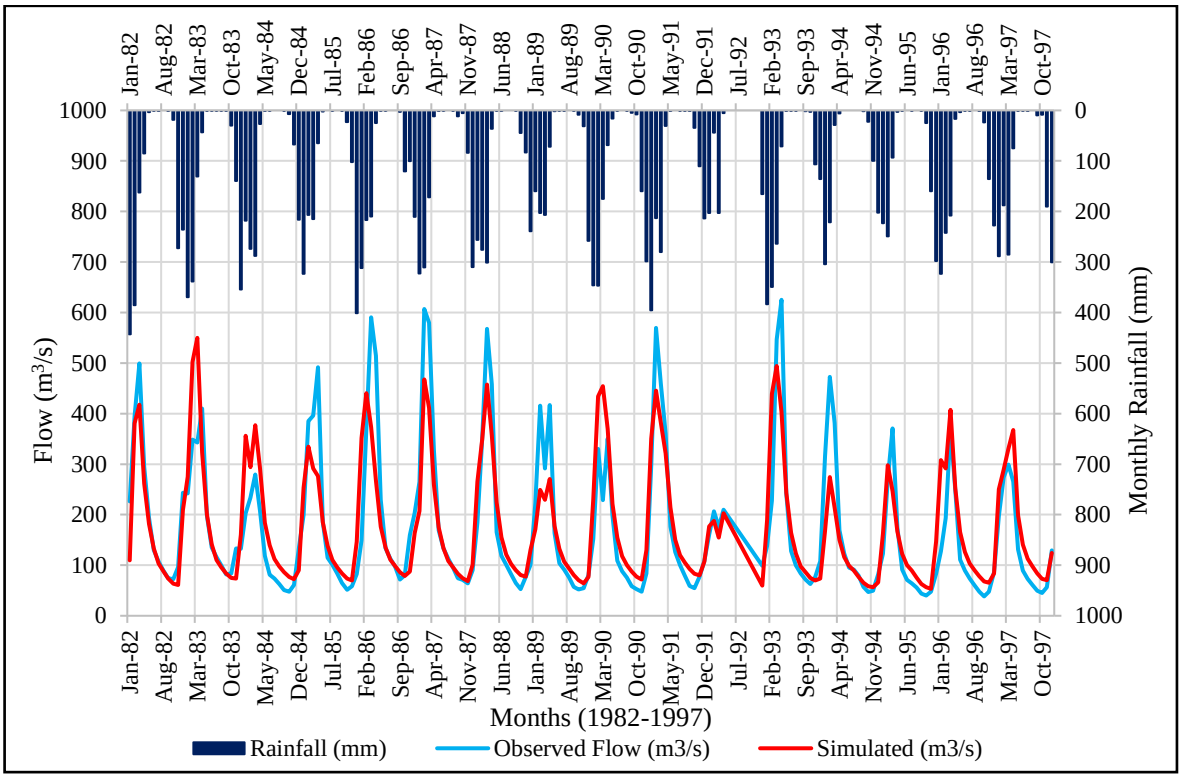

Figure 5.14 Monthly simulated and observed flow versus monthly rainfall

The simulated flows compare well with observed flows, as indicated in Figure 5.14. The trend and streamflow regime are the same for monthly and seasonal time scales. The simulated peak and low flows agree well with observed peak and low flows. However, variations exist in flow magnitude at the peak and low flows. The simulated flows underpredict the peak and low flows in some months. In general, the simulated flows are well accepted and reliable based on the graphical comparisons and the statistics obtained in Table 5.7.

Further comparisons were done with simulated and observed flows against the average monthly rainfall. The comparisons in Figure 5.14 illustrate that the rainfall peaks for each month also corresponds to the simulated and observed peak flows

while periods of lowest and or no rainfall also correspond to low simulated and observed flows. The matching of the rainfall and simulated peaks further shows the rainfall-runoff relationship and the KRB response time to a rainfall input event. The simulated flows are therefore reliable and suitable for use in hydrology and water resources management.

The SWAT model simulated water yield for the period of 1982-2013 compares relatively well and Figure 5.15 illustrates the CFSR annual rainfall and annual water yield across the basin.

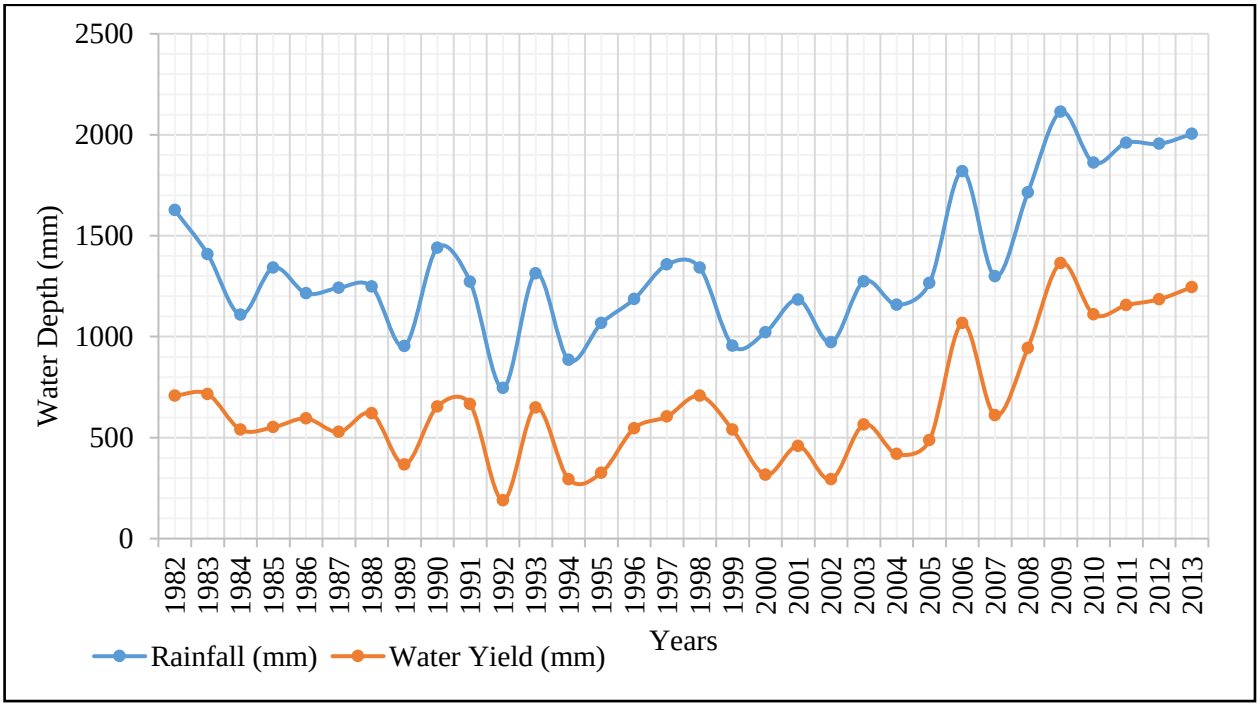

Figure 5.15 Comparison of annual water yield and CFSR annual rainfall

As illustrated in Figure 5.15, the water yield varies with corresponding variability of rainfall in the basin. There has been sufficient water yield over the years with the lowest being 200mm recorded in 1992 and the highest being 1400mm recorded in 1982. The year 1992 was characterised by drought while floods occurred in 1982.

Figure 5.16 illustrates CFSR monthly rainfall and water yield obtained after analysis.

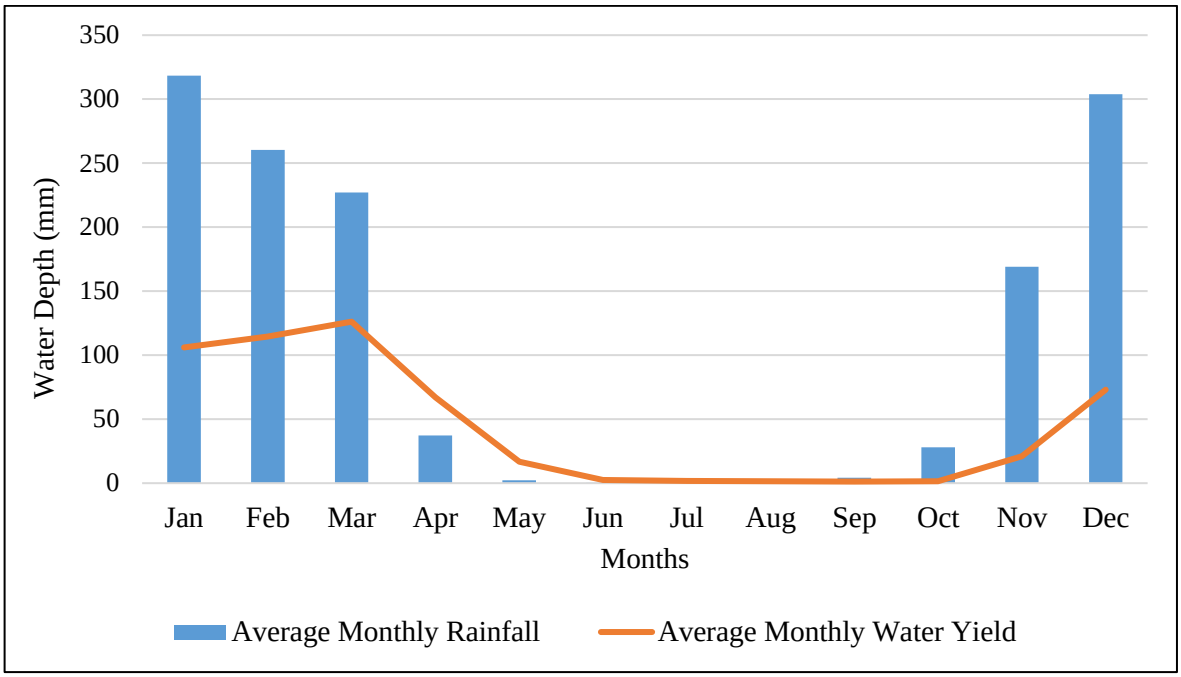

Figure 5.16 Average monthly CFSR rainfall and water yield (1982-2013)

Figure 5.16 shows the mean monthly water yield that follows the rainfall trend, which is high between January and March, recedes between April to June and dry between June and September. The rainfall begins to rise sharply from October to December, which is a rainy season in the basin. The water yield hydrograph is a delayed response to rainfall input in the basin and from January to June and October to December there is adequate yield. However, from May to October, there is almost zero water yield and during this time the river flow in the basin is at its lowest.

Water yield was further analysed based on its spatial distribution in the basin and the water yield variability map was created as shown in Figure 5.17.

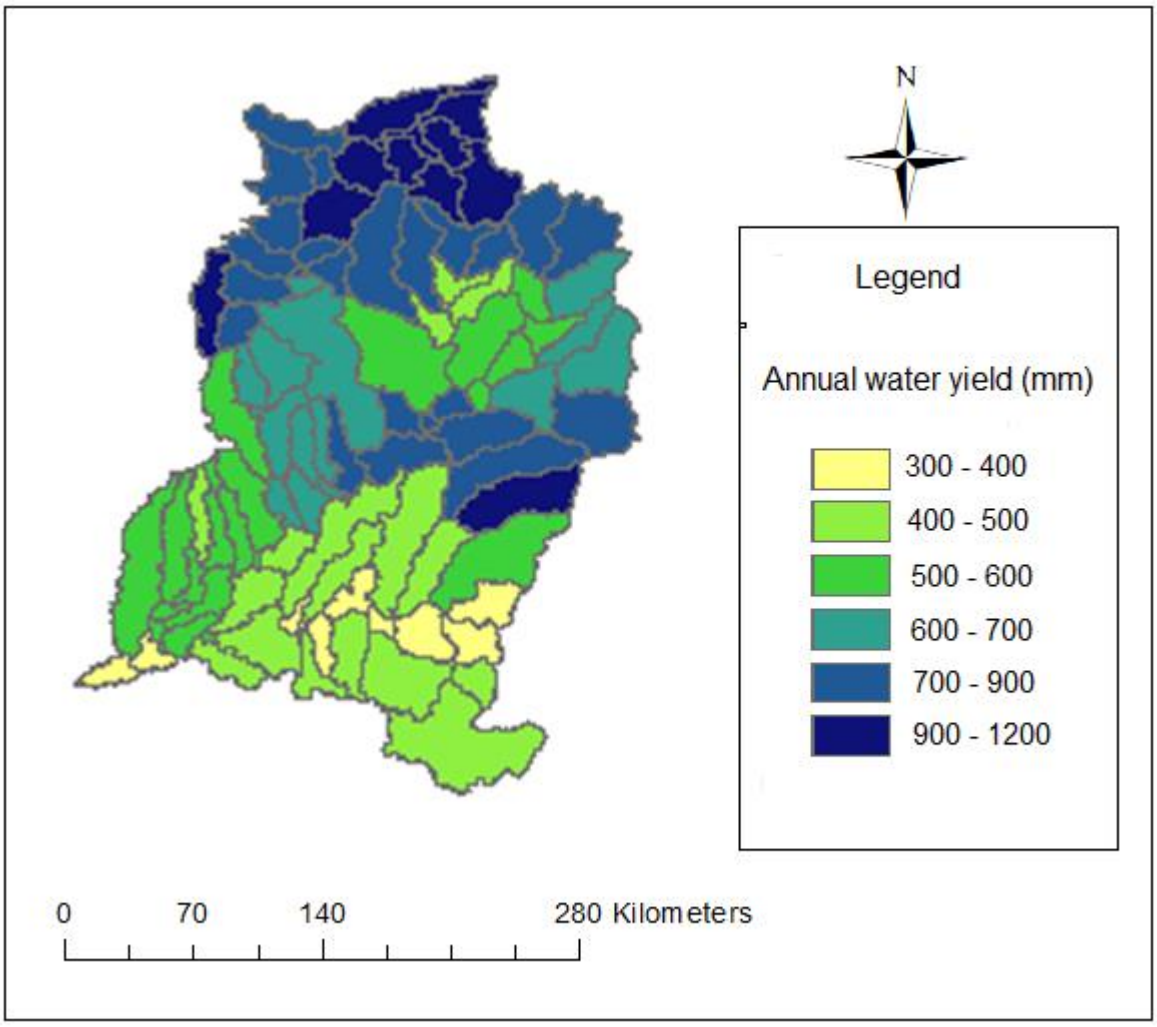

Figure 5.17 Water yield variability map (1982-2013)

Figure 5.17 indicates the spatial variability of the Mean Annual Water Yield (MAWYLD) across the entire basin. The northern part of the KRB has the highest water yield ranging from 820 to 1011 mm while the lowest is found in the southern part of the KRB ranging from 363 to 413mm.

Water resources are analysed in the context of blue and green water flows in a basin and its spatial variability across the basin. The blue water is the estimated water yield and the deep aquifer recharge while green water storage is soil moisture, which

has been broadly identified as very important for water resources management (Schuol et al. 2008; Rockstrom & Falkenmark, 2006).

The green water can better be used to boost agricultural production in the KRB because nearly all seasons have sufficient green water, except for the winter and spring season (July-September). There is also good rainfall in the KRB that is normally converted to runoff and can further be harnessed through construction of water conservation structures that can serve as a source of water for winter and spring farming.

5.4 Conclusion

The use of gridded climate data (CFSR) has proved to be reliable and perhaps an appropriate alternative in data scarce regions. Automatic calibration and validation with SWAT-CUP SUFI-2 have proved effective in producing calibrated parameters. The southern African region has particularly been a data scarce region, which has hampered research on a large scale, but with the use of alternative technology, water resources would be well-assessed and effective management can be envisaged.

The simulated results with NS as the objective function showed that calibrated results were good at 0.73 and R^2 was found to be good at 0.73 while the uncertainty analysis was obtained with a P-factor (95PPU) at 0.75 and the R-factor of 0.75 values which were very good within the accepted standard. The quantitative statistics show that the model results are satisfactory and may be used in basins with similar characteristics.

The spatial distribution of water yield showed uneven distribution with some areas experiencing water stress while other areas have excess water, which tends to flow out of the basin due to underutilisation and limited water conservation structures. The estimated water resources provide insight into the water balance of the basin where various water demands from different water use sectors can be assessed. The mean annual water yield ranging from 362 to 1011mm across the sub-basin forms part of the green water that can be used to enhance agricultural productivity.

The basin has potential of water resources to be harnessed where more than half of the generated runoff appears to flow out of the basin without any form of conservation. Furthermore, these water resources could be used to boost irrigated agriculture, which can improve the livelihood and reduce poverty levels.

The water resources in the ZRB have already begun to be altered by climate change impact, as highlighted in Chapter three while the basin is poorly informed because of inadequate knowledge at the local basin scale. In order to investigate, analyse and quantify climate change impact at a basin, scale experiments were conducted through Regional Climate Modelling by using the PRECIS model. Therefore, chapter six deals with Regional Climate modelling that was performed to generate a high-resolution climate scenario for climate change impact studies.

CHAPTER 6 : REGIONAL CLIMATE MODELLING

6.1 Introduction

The study of the impact of climate change utilises data and information generated by GCM (Raghavan et al. 2014). The GCMs currently in use are very course and as a result, are unable to adequately deal with local forcings. The GCM with coarse resolution can only produce results that may be considered as a rough estimate of climate change consequences at the local scale (Judit et al. 2008). Generating future climate scenarios using GCMs for local regions of interests does not produce realistic results due to large horizontal resolution of 150km-500km (Baimoung et al. 2014; Brienen et al. 2010; Zhang et al. 2006; Jones et al. 2004). There are also difficulties in computational capacities and representations of local physical processes (Giorgi, 1990).

RCMs at a higher resolution (10–50 km) are widely used in climate research (Raghavan et al. 2014; Marengo et al. 2009). Better estimations of the future climate scenarios may be achieved by nesting RCM in GCMs since the horizontal resolution of the models is much finer than GCM (Judit et al. 2008).

This chapter aims at demonstrating the usefulness of downscaling large-scale climates over the Southern African region from which one can study possible future climate change and also utilise the outputs of the regional climate model for impact assessment on hydrology and water resources at a local catchment scale.

The output of RCMs is then commonly used as input data for hydrological models in order to analyse the hydrological processes of the study area. Similar studies have been carried out (Kling et al. 2014; Kim et al. 2013). Results from high-resolution Regional Climate Models such as PRECIS, MM5, WRF have also shown to be credible (Zhang et al. 2006; Tadross et al. 2005).

Regional Climate Modelling was, therefore conducted through experiments to investigate and predict the climate change impact on a local scale. Four experiments were performed using the PRECIS model, which is a Regional Climate Model for generating high-resolution climate scenarios. Experiments were undertaken on a defined domain of KRB within the ZRB.

PRECIS model was used to downscale the GCM HadGEM2-ES over the baseline and future climate periods. The evaluation of the model was performed using the Era-Interim Reanalyses (1980-2010). While the historical simulations of the GCM were performed from 1960-2005, future simulations spanned the period 2020-2021, using both RCP 4.5 and RCP 8.5 scenarios.However the focus time slice for this study was 2020-2050.

The results generated indicate that the PRECIS model was able to simulate the climate of the region well. The climatic variables such as precipitation and temperatures were particularly analysed climate change impact in terms of coverage area and magnitude, which hold strong implications for adaptive measures over this region.

6.2 Domain area

The target area in Figure 6.1 is the domain area excluding the rim thickness of eight grids where the experiment was conducted and it was designed to capture the entire ZRB, Eswatini and some parts of South Africa. The region of interest was also the Region of Validation (ROV) and the focus geographical area for the research where the KRB is situated with surrounding areas in the northern parts of Zambia.

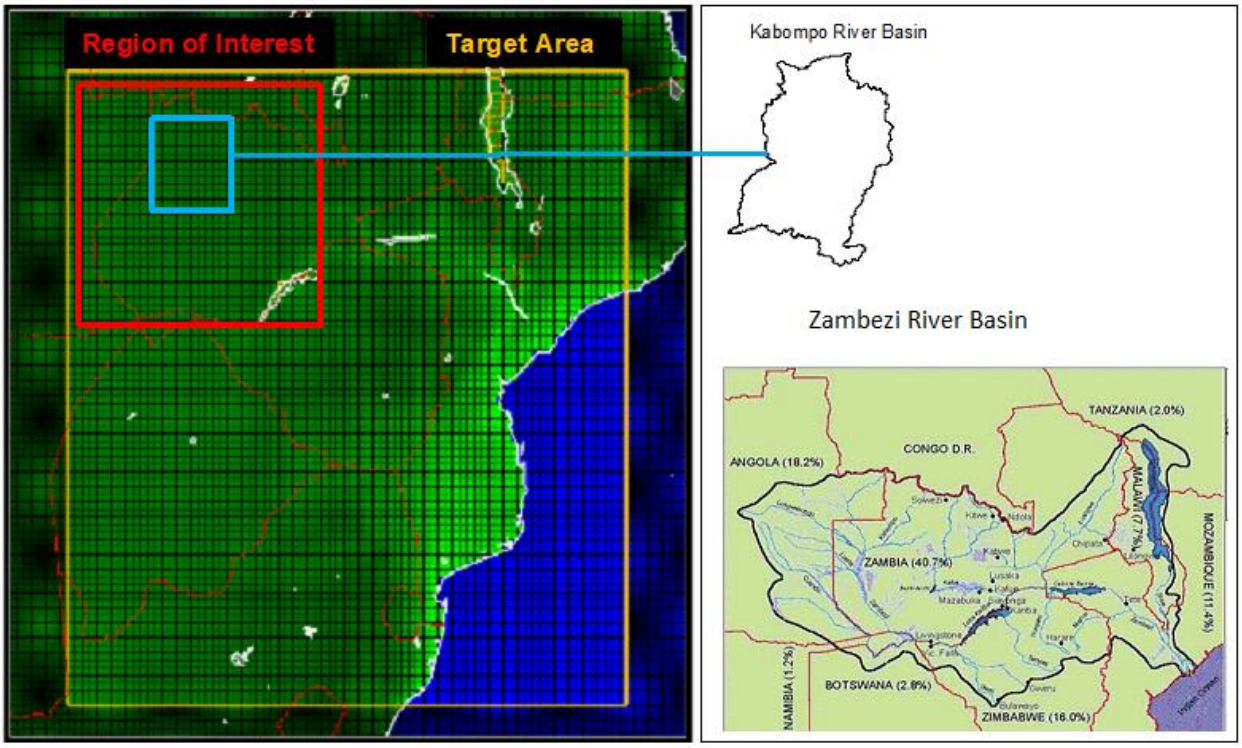

Figure 6.1 Domain area used in PRECIS experiment
(Source:Zambezi River Authority, 2000 - Zambezi River Basin)

6.3 Materials and Methods

Four experiments were conducted using the PRECIS RCM for the defined domain in Southern Africa covering the KRB. The lateral boundary conditions included surface pressure, winds, relative humidity and temperature while surface boundary

conditions included sea surface temperature (SST) and sea ice, which were all defined for the domain area.

The RCM and GCM used in the experiments are part of the Coupled Model Intercomparison Project (CMIP5). The CMIP5 is an international data bank for climate model outputs established to facilitate assessments of future climate projections and to evaluate performance of the climate models. The collection of model outputs is also used to improve the people's understanding of the climate process and responses (Sheffield et al. 2013).

The evaluation of the model was performed on the ROV using the Era-Interim Reanalyses for the period 1980-2009. While the historical simulations of the GCM were performed over the period 1960-2005 with a focus on 1975-2005,future simulations spanned the period 2020-2050, under both RCP4.5 and RCP8.5 scenarios. Figure 6.2 illustrates detailed climate change modelling process used in the generation of high-resolution climate scenarios.

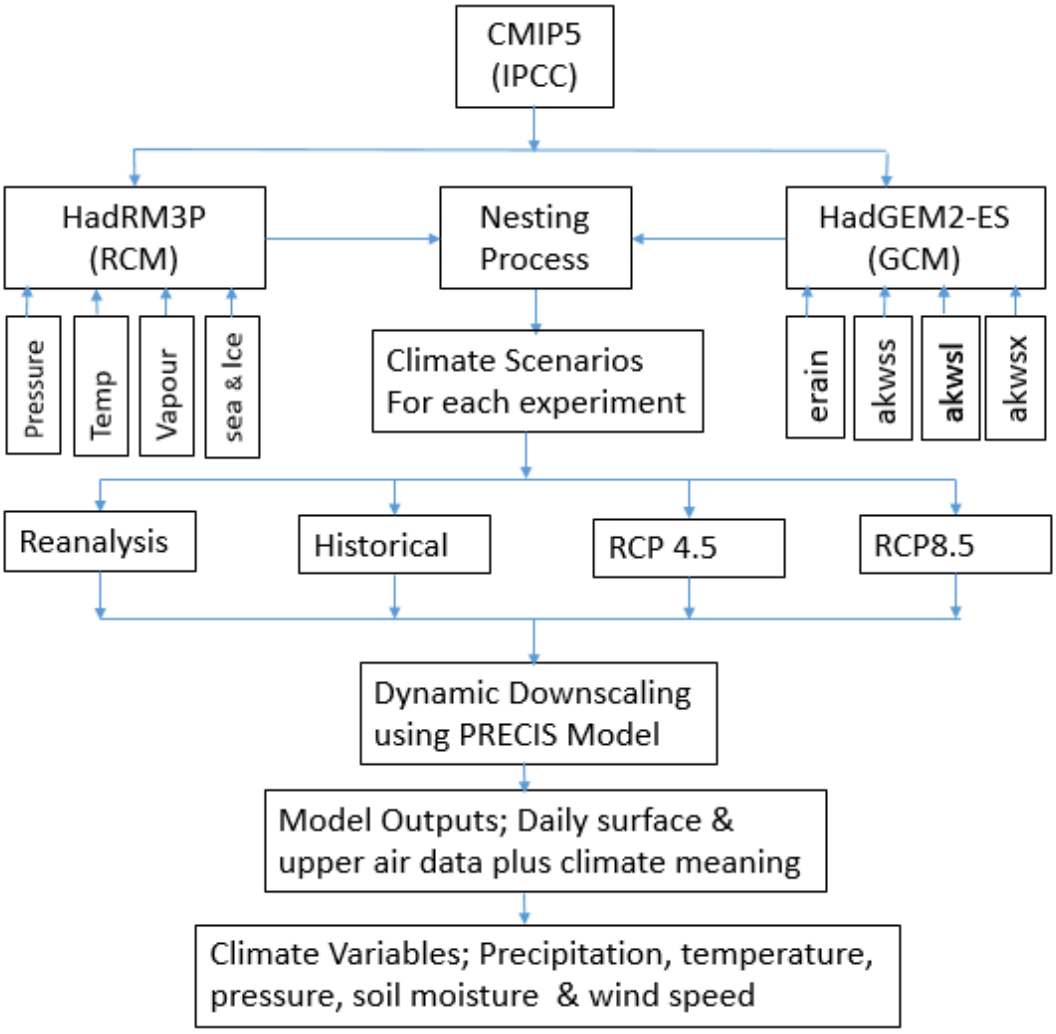

Figure 6.2 Climate change modelling process with PRECIS

6.3.1 Precis Experiment Set Up

The PRECIS model was set up to create high-resolution climate scenarios for Southern Africa that included the study area in the ZRB. The experiment was performed on a defined domain area, which was large enough to completely include the ZRB and other geographical features such as mountains, which could influence the weather and climate system on the local scale. The experiment was defined with surface and lateral boundary conditions of the domain area. Lateral boundary conditions (LBCs) consisted of surface pressure, temperature, water vapour and wind while surface boundary conditions included the sea and ice.

The experiment was conducted with the Linux operating system and took seven months (September 2017 to April 2018) to be completed because the domain was large and the computational capacity was inadequate and low. The experiments were set up with a high resolution of 0.22^{o} x 0.22^{o} (25km x 25km) under reanalysis, historical and future climate scenarios. The major outputs of the experiments included daily surface and upper-air data plus climate meaning. Each experiment was identified with a unique Run Identifier (Run ID). Several national and international projects in Europe have used RCMs to better estimate regional climate change and project climate scenarios for climate change impacts studies (Marengo et al. 2009).

Experiment one under Reanalysis Scenario

Experiment one was conducted to evaluate the model output in order to have confidence in its performance for predicting the future climate scenarios (Macadam and Janes, 2017). According to Gettelman & Rood, (2016b), the purpose of a model evaluation is to determine how well it represents the present climate before it can be used to make projections for the future. The experiment was, therefore, performed for validation of the results with observed climate variables. The experiment ran under the Gregorian calendar that covered the period 1979-2009 (32 years, 1 month and 0 days) with RCM as HadRM3P while the GCM was ERA-Interim (erain).

Experiment two under Historical Scenario

Experiment two was conducted to generate baseline scenario that could be used as a reference for determining change in climate variables with future climate

scenarios. The experiment was driven by CMIP5 historical scenarios covering the period 1959-2010 (50 years, 1 month and 0 days) with RCM as HadRM3P while the GCM was HadGEM2-ES (akwss).

Experiment three under RCP4.5 Scenario

Experiment three was conducted to generate a future climate scenario under RCP4.5, which is a medium emission scenario. The experiment was driven by CMIP5 RCP4.5 scenario covering a period of 94 years, 1 month and 0 days (2005-2099) with RCM as HadRM3P while the GCM was HadGEM2-ES (akwsl).

Experiment four under RCP8.5 Scenario

Experiment four was conducted to generate a future climate scenario under RCP8.5, which is a high emission scenario. The experiment was driven by CMIP5 RCP8.5 scenario covering a period of 95 years, 1 month, 0 days (2005-2100) with RCM as HadRM3P while the GCM was HadGEM2-ES (akwsx).

6.3.2 Procedure for Estimation of Climate Change Impact

The estimation of climate change impact is based on the change factor methodology elaborated in chapter two.

(a) CRU observed climates were obtained for 1975-2005 as a historical period (baseline).

(b) PRECIS baseline climate generated from historical experiment for 1975-2005 using the HadGEM2-ES (akwss) GCM as driving boundary condition.

(c) PRECIS future climate covered 2020-2050 using RCP4.5 and RCP8.5 climate scenarios as driving condition and HadGEM2-ES providing lateral boundary data.

(d) The future climate scenario for impact study was therefore calculated as:

Value of observed climate (a) plus (Value of PRECIS future climate(c) minus value of PRECIS baseline climate(b).

The impact of the future climate scenario was assessed by comparing the impact of baseline climate against the impact of the future climate scenario and mathematically it can be written as:

• Baseline climate impact = Impact model run using baseline climate

(a - above)……..(X)

• Future climate impact = Impact model run using future climate scenario

(d-above)…….(Y)

Future impact …… X - Y

6.4 Results and Discussion

The experiments conducted over the entire PRECIS domain area over Southern Africa generated results and future time series data such as precipitation, temperature, wind speed, pressure and soil moisture covering the period 2020-2100. However, for this research, the focus was on KRB (study area) within the region of interest with a time slice of 2020-2050.

The generated data and results from the four experiments were analysed and plotted for the region of interest encompassing the study area with a spatial variability of climate variables. The major climate variables analysed were average precipitation (mm) and average temperature (^{o}C). The results were validated with the observed data from Climate Research Unit (CRU) of East Anglia for the same length of period.

In general, the results indicate that precipitation will slightly increase under the RCP4.5 while there will be a large increase under RCP8.5 with a considerable temporal and spatial variability for the future period. Temperature also shows a rising trend with temporal and spatial variability under both future climate scenarios. The results were analysed based on KRB seasonal climatology defined as follows: December, January, February (DJF) which is a typical rainy season, March, April, May (MAM), which is the autumn season, June, July, August (JJA) being the winter season and September, October, November (SON), which is the summer season.

6.4.1 Validation of PRECIS Experiment Results

The model results must be compared with observations in the ROV (Macadam and Janes, 2017; Gettelman & Rood, 2016b). Such comparisons can highlight problems which may be hidden by the complexity of a model (Randall et al. 2007). All the figures for comparisons are based on the ROV, which was the region of interest. The PRECIS model results for re-analysis covered the period from 1980-2009 and was compared to the observed data from CRU to validate the experiment results (Macadam and Janes, 2017; Jones et al. 2004). The CRU observed data was downloaded from http://www.cru.uea.ac.uk/cru/data/hrg/cru_ts_2.10 and processed for comparisons with the PRECIS generated results. The graphical comparisons between PRECIS reanalysis and baseline period are listed on Appendix G and H.

Validation of Rainfall Results

The results from the PRECIS model under reanalysis were plotted for seasonal rainfall and compared with CRU observed rainfall based on the same season and length of period. Figure 6.3 illustrates the comparisons based on the four seasons.

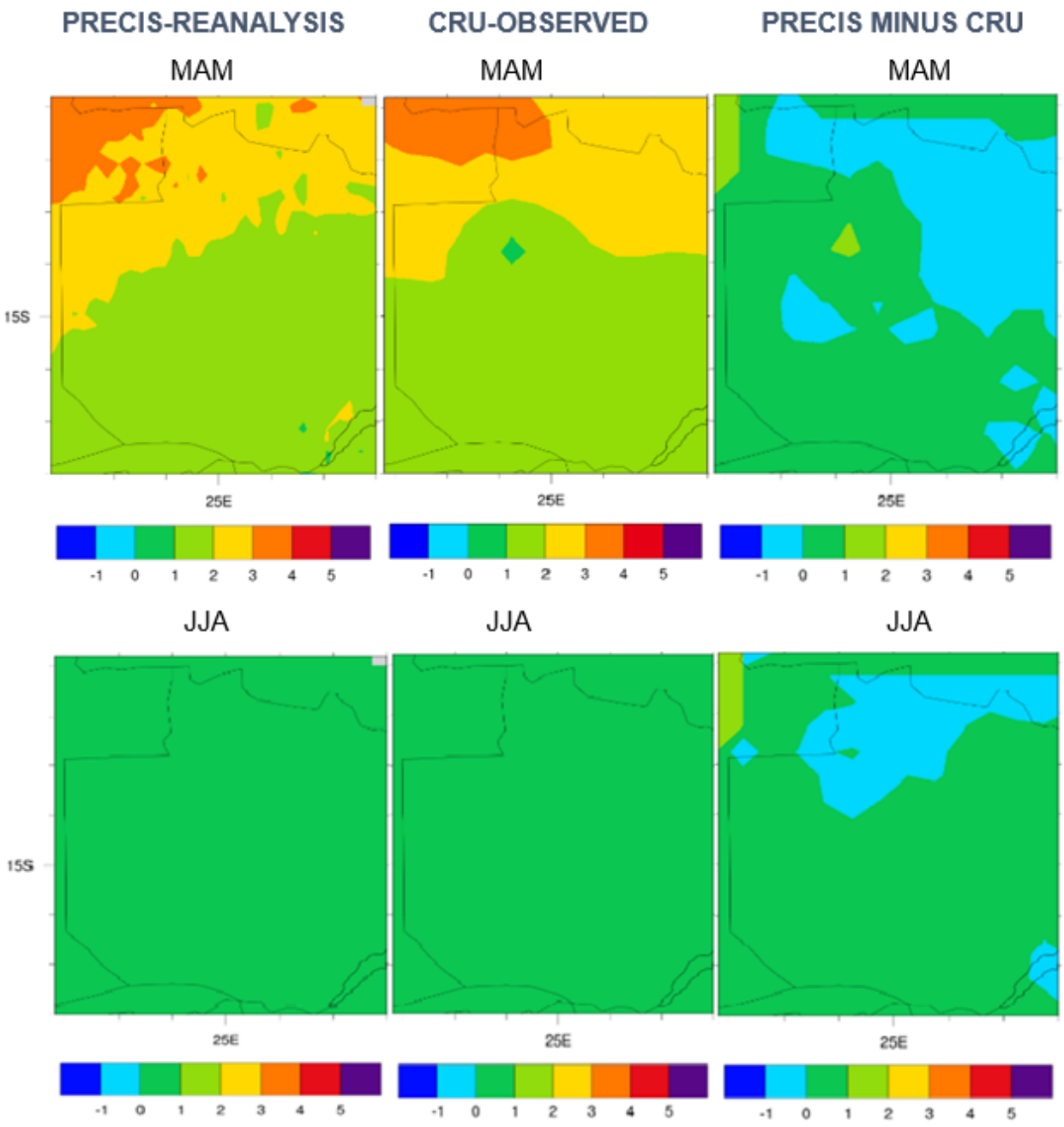

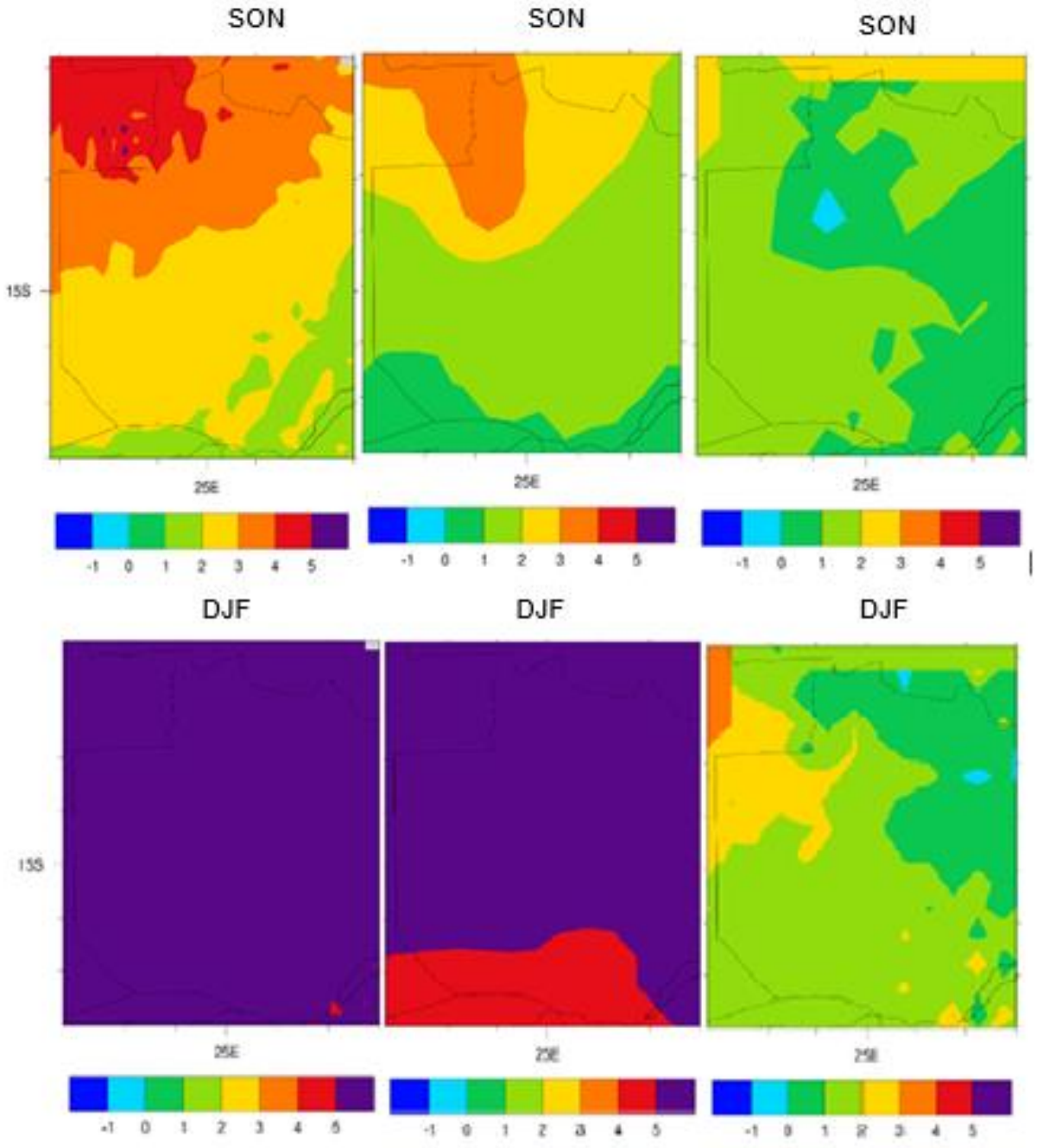

Figure 6.3 Comparison of PRECIS model and observed rainfall in mm/day.

The graphical comparisons in Figure 6.3 illustrates that MAM has a very close match of magnitude of rainfall with its temporal and spatial variability across the defined region of the interest. The PRECIS model simulates more rainfall in the northern part than in the southern part and this is confirmed by the CRU observed rainfall, which also show that the northern part of the domain area receives more rainfall

than the southern part. However, there are minor variations shown between the model and the observed, which are between -1 and 1mm/day; thus it is considered insignificant.

The PRECIS model simulates nearly no rain in JJA, which is winter season; a time in which the basin does not receive any rainfall. The results from the model agree very well with CRU observed and, therefore the differences were considered insignificant because they were between -1 and 1mm/day.

The SON season is usually characterised by high temperatures, beginning of rain season and the PRECIS model closely matched the observed data with the pattern and variability of rainfall. However, differences noticed ranged between -1 and 2mm/day.

The season of DJF indicates some significant differences between PRECIS model and CRU observed because this is the wet season and highest rainfalls are recorded in the same season. The absolute differences show strong biases of up to 3mm/day. The differences may be attributed to errors in the model or observed data.

Validation of Temperature Results

The results from the PRECIS model were plotted for seasonal average temperature and compared with CRU observed temperature based on the same season and length of period. Figure 6.5 illustrates the comparisons based on the four seasons.

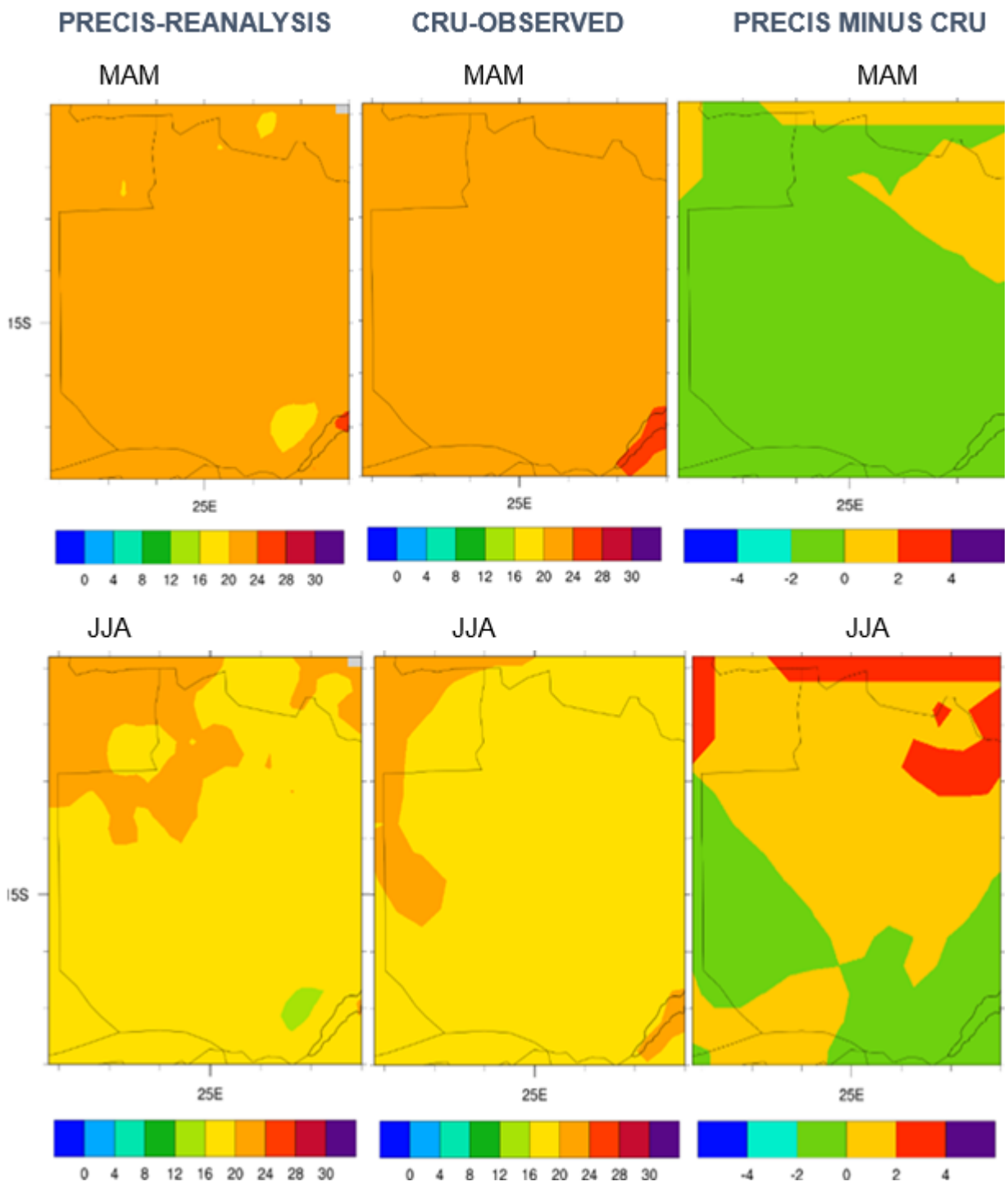

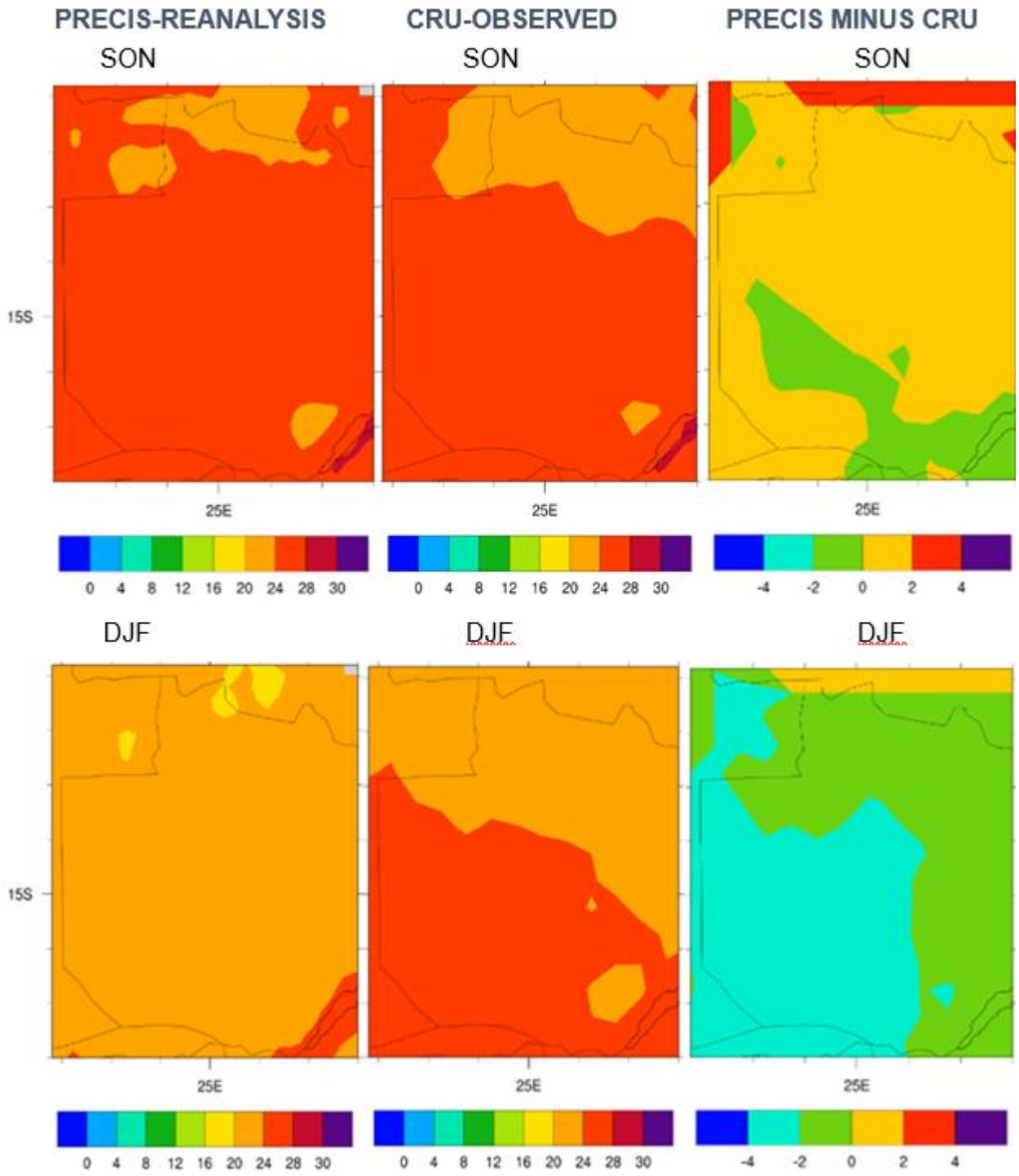

Figure 6.4 Comparison of PRECIS and observed temperature in ^{o}C

The PRECIS model also performed relatively well in simulating average temperatures in MAM with absolute differences ranging between -2 to 2 ^{o}C. The two plots match well even though minor differences exist.

The JJA season is equally well simulated as it is winter and has the lowest average temperature compared to the other three seasons. There are minor differences as the season shows some colder and warmer biases.

The SON and DJF are well-matched too, with minor differences that range between 0 and 2^{o}C. In general, PRECIS model can be concluded to simulate well and has demonstrated rear skill of modelling. However, there are some minor cold and warm biases that exist and in some cases they are more pronounced and requiring model bias estimation. The biases may be attributed to errors in either model outputs or observed data sets.

6.4.2 Time Series of Future Climate

Further analysis of the PRECIS model outputs was performed in order to determine the precipitation and temperature anomalies for only land points with reference to the (1975-2005) baseline monthly mean. The analysis was based on the 2020-2050 monthly time series under RCP4.5 and RCP8.5 future climate scenarios.

Precipitation and Temperature Anomalies

Precipitation and temperature anomalies were determined by firstly calculating the model baseline (1975-2005) multi-annual monthly means and subtracting this from the projected future monthly time series using Climatic Data Operators (CDO) commands in the Linux operating system.

Identification of Model Bias

Dynamic downscaling may include model biases that need to be identified and estimated (Baimoung et al. 2014). The PRECIS baseline temperature and precipitation time series were compared with the CRU observed time series for the

same period and further analysed for identification of the temperature and precipitation model biases. The operation was carried out with climate data operators in the Linux operating system with the assumption that the model biases were systematic. Figure 6.5 illustrates the monthly comparisons of PRECIS baseline and CRU observed temperature.

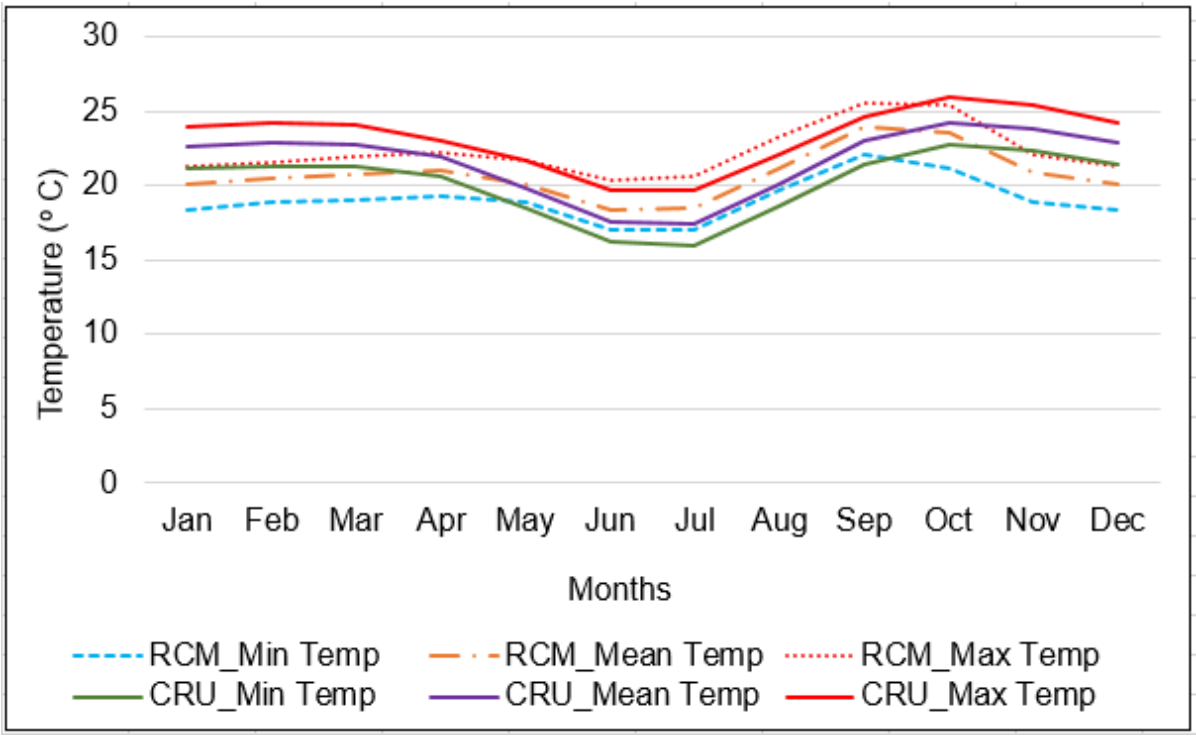

Figure 6.5 Monthly comparison of PRECIS baseline and CRU observed temperature

Figure 6.5 illustrates monthly comparisons of PRECIS baseline and CRU observed temperature which are similar in trend throughout the year with the lowest temperatures occurring in June and July as is the case in winter season for KRB and the highest temperatures occurring in September and October, which is the summer season of the basin.

However, the minor differences can be noticed in the magnitude between January and April where the PRECIS over-estimate temperatures while May to July indicate

a clear match in maximum, mean and minimum temperatures. The maximum temperatures also match very well from August to October except for December where the model tends to overestimate temperatures while the mean and minimum temperature have mismatches from August to December. In general, the PRECIS model significantly shows a similar trend with the CRU observed temperature except the magnitude where the model tends to over-estimate at the beginning and end of the year.

Similar comparisons were made for monthly PRECIS baseline precipitation and CRU observed precipitation and the results of the monthly comparisons are illustrated in Figure 6.6.

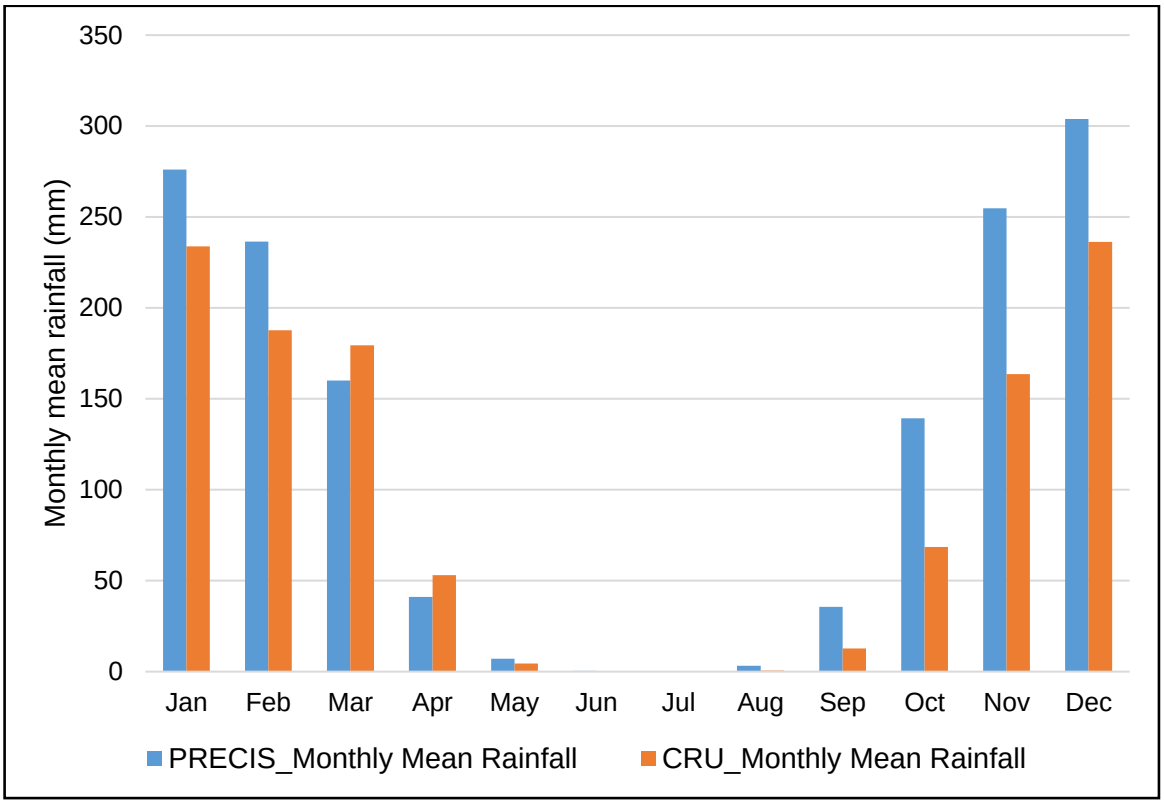

Figure 6.6 Comparison of PRECIS and CRU observed baseline monthly rainfall

Further comparisons were made for daily mean PRECIS baseline precipitation and CRU observed precipitation and the results of the daily mean comparisons are illustrated in Figure 6.7.

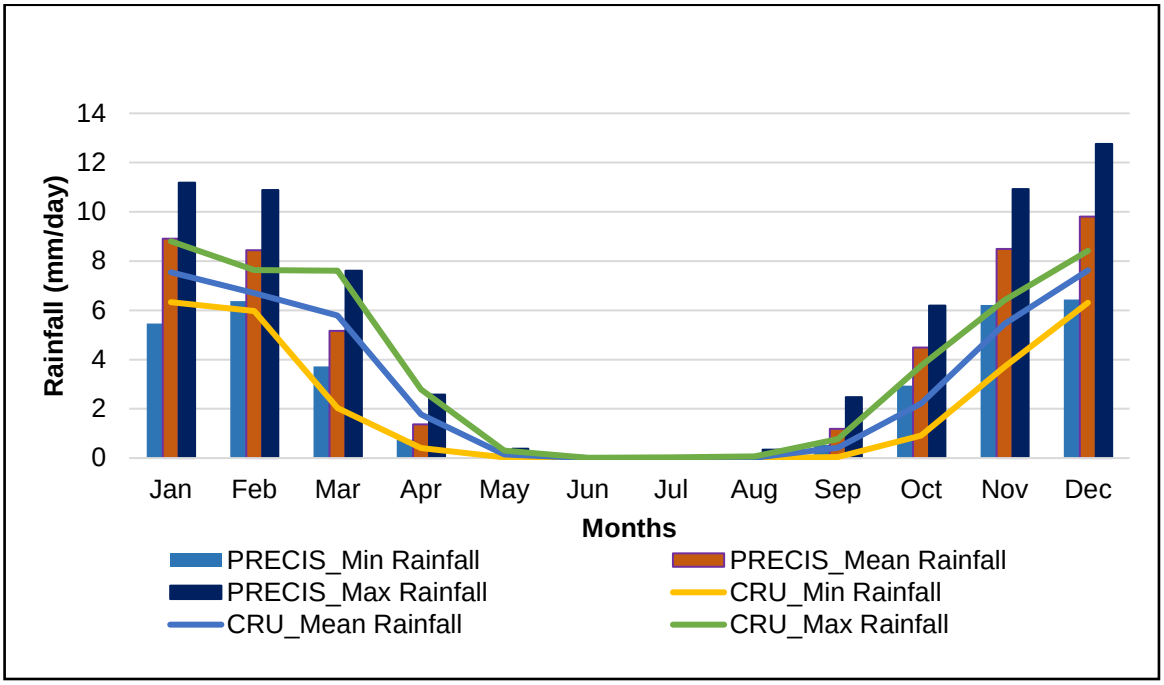

Figure 6.7 Comparison of daily PRECIS baseline and CRU rainfall in a month

The monthly mean and daily mean rainfall in Figure 6.6 and 6.7 respectively illustrates similar trend between the PRECIS baseline and CRU observed rainfall throughout the year. The differences are seen in the magnitudes where the model overestimates the maximum, mean and minimum daily rainfall for January to April and September to December while simulating no rainfall in May to August. In general, the model simulates rainfall with a similar trend with CRU observed when compared while overestimating the magnitude of rainfall in DJF and MAM.

In both cases of comparisons of PRECIS baseline and CRU observed temperature and precipitation, the model results agree well with observed results, especially in

trends with some minor biases that need to be identified. Further graphical comparison of climate variables for observed & model are listed on Appendix L.

Therefore, further analysis was performed in order to determine the monthly and daily PRECIS model biases for the baseline period and Figure 6.8 illustrates the Monthly precipitation model biases.

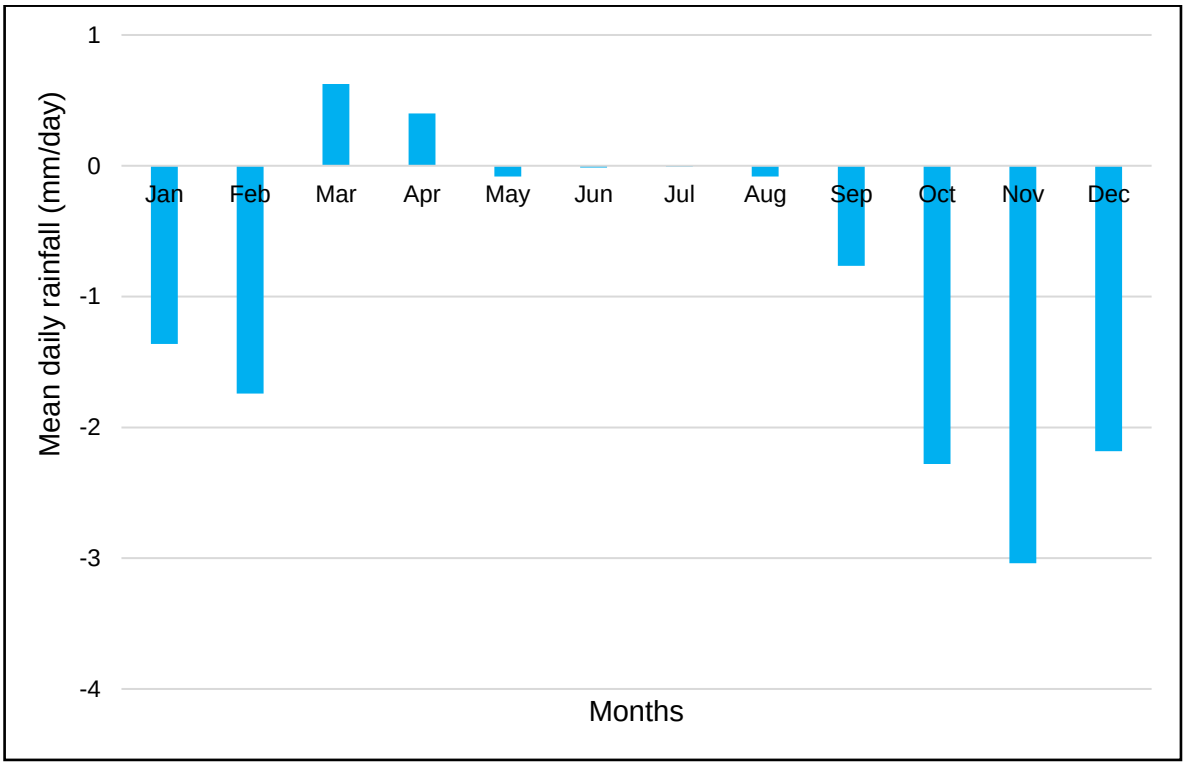

Figure 6.8 Monthly PRECIS Precipitation model biases

The positive biases in Figure 6.8 illustrates that the model was underestimating while negative biases show the model overestimation. The model overestimated in January, February, September, October, November and December while it underestimated in March and April. The period from May to August, the model biases are negligible as they are close to zero.

Similarly, the temperature monthly model biases were also determined for the same period and the results of monthly model biases are illustrated in Figure 6.9.

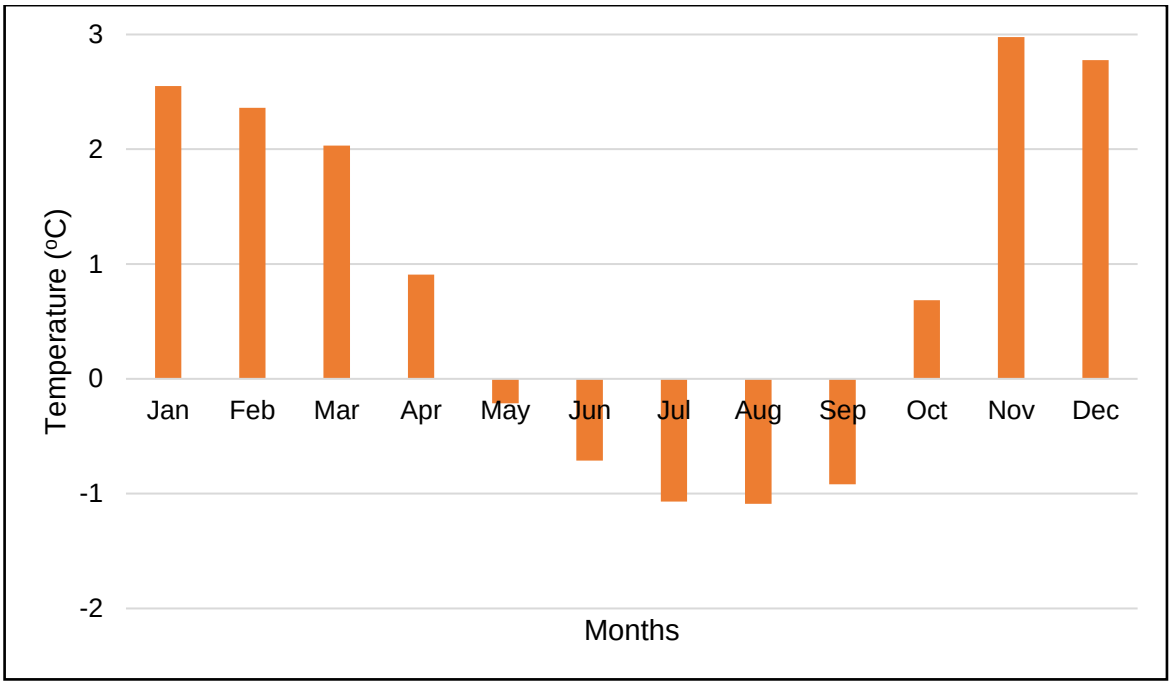

Figure 6.9 Monthly temperature PRECIS model biases

Figure 6.9 illustrates positive biases in January to April and October to December indicate that the model was underestimating temperatures while the negative biases in May to September indicate that the model was slightly overestimating the temperatures.

The model biases in Precipitation and temperature could be attributed to model physics such as convective schemes,topography,land surface and lateral boundary conditions. More over some biases may have also been inheried from the GCM. Its also important to acknowledge that the CRU observed data used for model evaluation may equally not be perfect because of the possible missing data and the few largely spaced stations within the study area.

The model performance in simulating precipitation and temperature was therefore found to be acceptable as the validation results and further graphical comparisons between the baseline for the model and observed results showed very similar trends despite minor biases in magnitude. In general, the results are evaluated to be useful for climate change impact studies. The PRECIS model average climate data are listed on Appendix E ,Table E1 and E2 and CRU observed average climate data is listed on Appendix F,Table F1 and F2.

6.4.3 Future Climate Change under RCP4.5 (2020-2050)

Analysis of the experiments for baseline and RCP4.5 climate scenarios were made with CFM a widely used method in climate change impact studies as described in section 2.1.2 and 6.2.3. The method was applied and impact change was quantified for the entire KRB. The future change in temperature and percentage change in rainfall were performed with Climate Data Operators (CDO) commands in the Linux operating system and plotted in ArcGIS in order to show spatial and temporal variability of precipitation and temperature based on the four seasons.

Prediction of Future Seasonal Rainfall

The seasonal rainfall change was analysed with reference to the RCM historical period, which was taken as baseline period and future period and the results are shown in Figure 6.10.

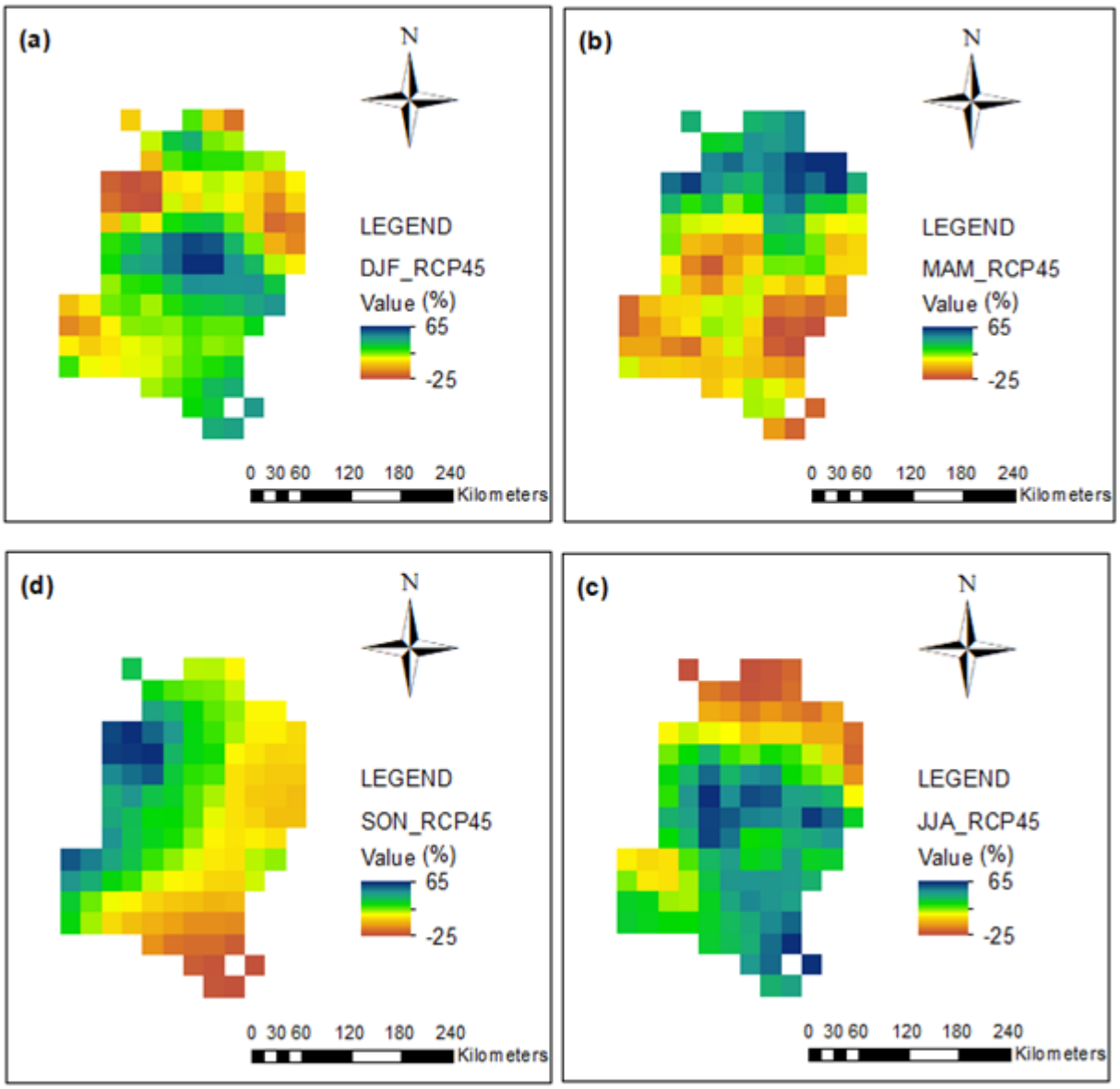

Figure 6.10 Predicted future seasonal rainfall based on RCP4.5

Figure 6.10 (a) shows a rainfall increase of 71% coverage area in DJF with the magnitude of 0<65%. Rainfall is predicted to increase in the middle part of the KRB and towards the south while reducing by 29% coverage area on the western and eastern parts of the basin. Figure 6.10 (b) shows a rainfall increase of 33% coverage area towards the north of the KRB while the rest of the 67% KRB area shows a significant reduction in the rainfall with the magnitude of -25% < 0. Figure 6.10 (c) shows an increase in rainfall with a magnitude of 65% > 0 and 77% coverage area

in the middle and towards the south of the basin while 23% coverage area in the northern parts and the southeast shows a decrease in rainfall with a magnitude of -25% < 0. Figure 6.10 (d) shows 37% coverage area of KRB will receive less rainfall with magnitude of -25% > 0 while the other 63% will receive slightly more rainfall with the magnitude of 65% > 0.

In general, 33-77% coverage area of the KRB will have a seasonal rainfall increase with the magnitude of 65% > 0 while 23-67% coverage area of the KRB will have a seasonal rainfall decrease with a magnitude of -25% > 0. Therefore, the future seasonal rainfall will have more coverage area for the increased rainfall than the decreased rainfall. However, its magnitude will vary depending on the monthly, seasonal and annual time scales. There is considerable spatial and temporal variability across the basin, which needs to be considered when planning for water resources.

Prediction of Future Seasonal Temperature

The temperature change was analysed with reference to the RCM historical period, which was the baseline period and future period and the results are shown in Figure 6.11.

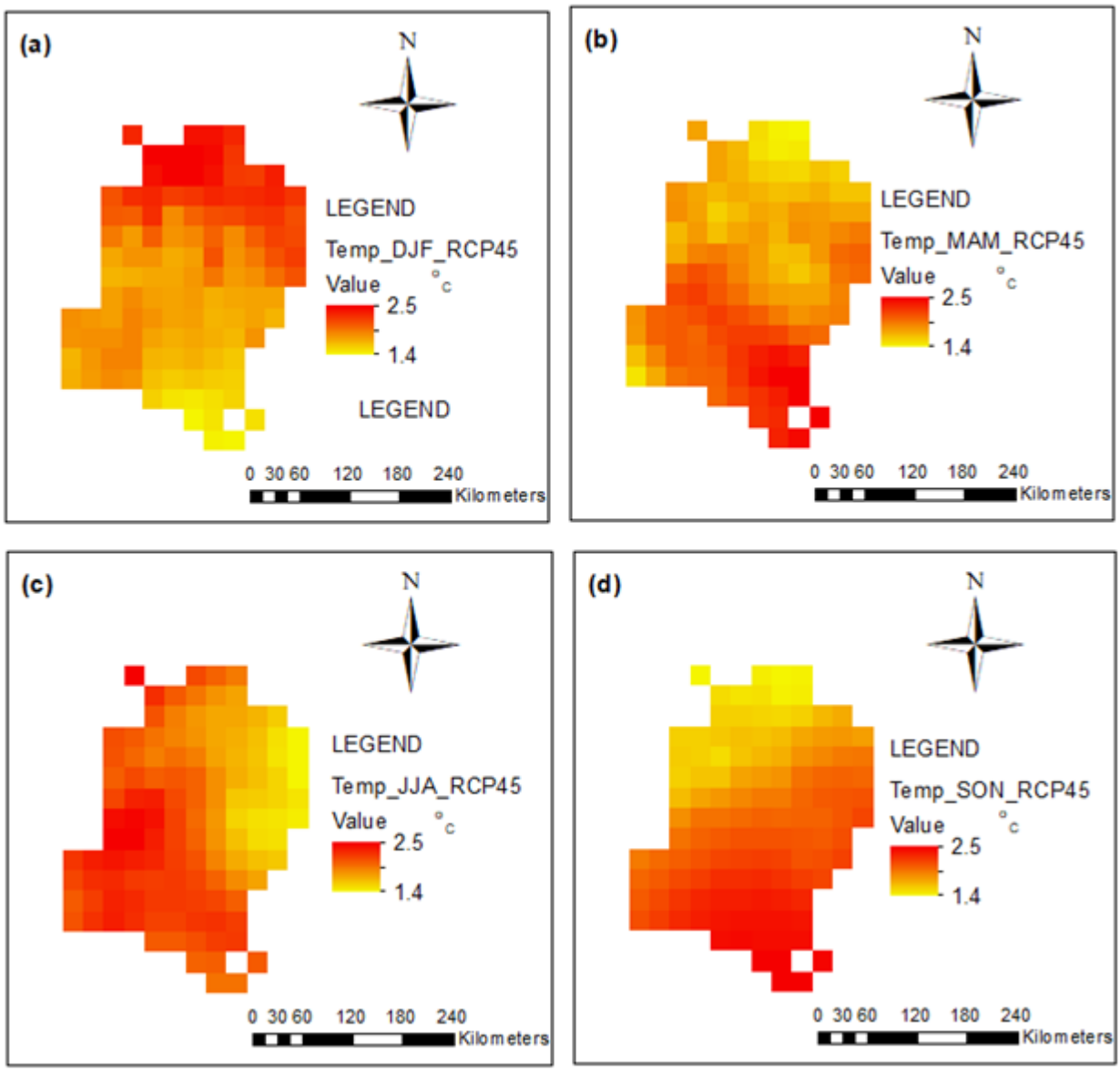

Figure 6.11 Predicted future seasonal temperature based on RCP4.5

Figure 6.11 (a) shows a considerable increase in temperatures towards the north of the KRB while a small increase in temperatures is predicted in the southern parts for the season of DJF. The MAM season in Figure 6.11 (b) is predicted with a small increase in temperature towards the north while the southern parts of the basin are predicted with a considerable temperature increase. Figure 6.11(c) shows a small increase in temperature in the western part of the basin while maintaining a considerable increase in all parts of the basin.

Figure 6.11 (d) shows a different pattern in SON where the northeastern part of the basin has a small increase in temperature while the rest of the basin has a considerable increase in temperature. In general, there is an increase in temperatures across the KRB in all the seasons. The increase varies from 1.4 ^{o}C to 2.5^{o}C across the basin with the highest increase predicted in SON.

6.4.4 Future Climate Change under RCP8.5 (2020-2050)

Analysis of the experiments for baseline and RCP8.5 climate scenarios were made with CFM as described in section 2.1.2 and 6.2.3. The method was applied and impact change quantified for the entire KRB. The future absolute change in temperature and percentage change in rainfall were then plotted to show temporal and spatial viability based on the seasons.

Prediction of Future Rainfall

The rainfall change was analysed for the historical period, which was the baseline period and future period and the results are shown in Figure 6.12.

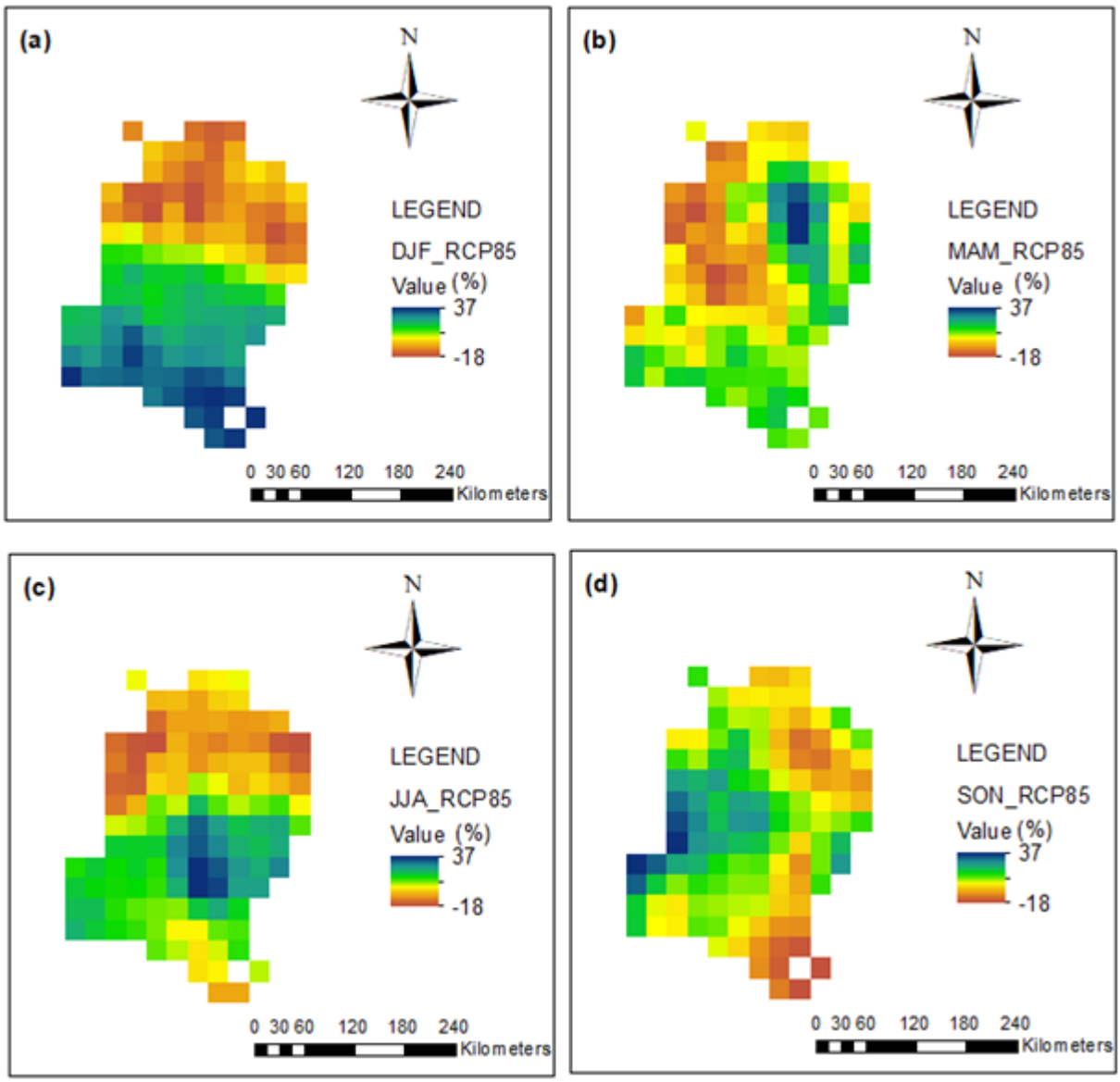

Figure 6.12 Predicted future seasonal rainfall based on RCP8.5

Figure 6.12 (a) shows a seasonal increase in rainfall towards the south and a considerable reduction towards the north of the KRB for DJF. The coverage area of KRB with increased rainfall is 58% with a magnitude of 0 < 37% while the area with reduced rainfall is 42% with the magnitude of -18% < 0.

Figure 6.12 (b) for MAM shows a rainfall reduction with a magnitude of -18% < 0 in the northern and eastern parts with 47% coverage area of the basin while 53% of

coverage area in the southern and western parts show an increase in rainfall with the magnitude of 0 < 37%. Figure 6.12 (c) shows JJA with a significant reduction in rainfall magnitude of -18% < 0 towards the north and the south end with 51% coverage area of the KRB while the rest of the 49% coverage area indicates an increase in rainfall with a magnitude of 0 < 37%. Figure 6.12 (d) shows SON reduction of rainfall with 48% coverage area and a magnitude of -18% < 0 in the northern, western and southern parts while the 52% coverage area in the eastern part and a few isolated areas show a rainfall increase with a magnitude of 0 < 37%.

The PRECIS model predicts that rainfall is likely to significantly increase in magnitude and coverage area in the season of DJF. The general rise in rainfall is predicted to increase coverage varying from 49% to 58% while the coverage area under decreased rainfall will vary from 51% to 42%. The increase of rainfall in DJF may cause flooding in some of the flood-prone areas and thus adaptation and mitigation strategies may be required.

Prediction of Future Temperature

The temperature change factor was determined with reference to the baseline period and the results are shown in Figure 6.13.

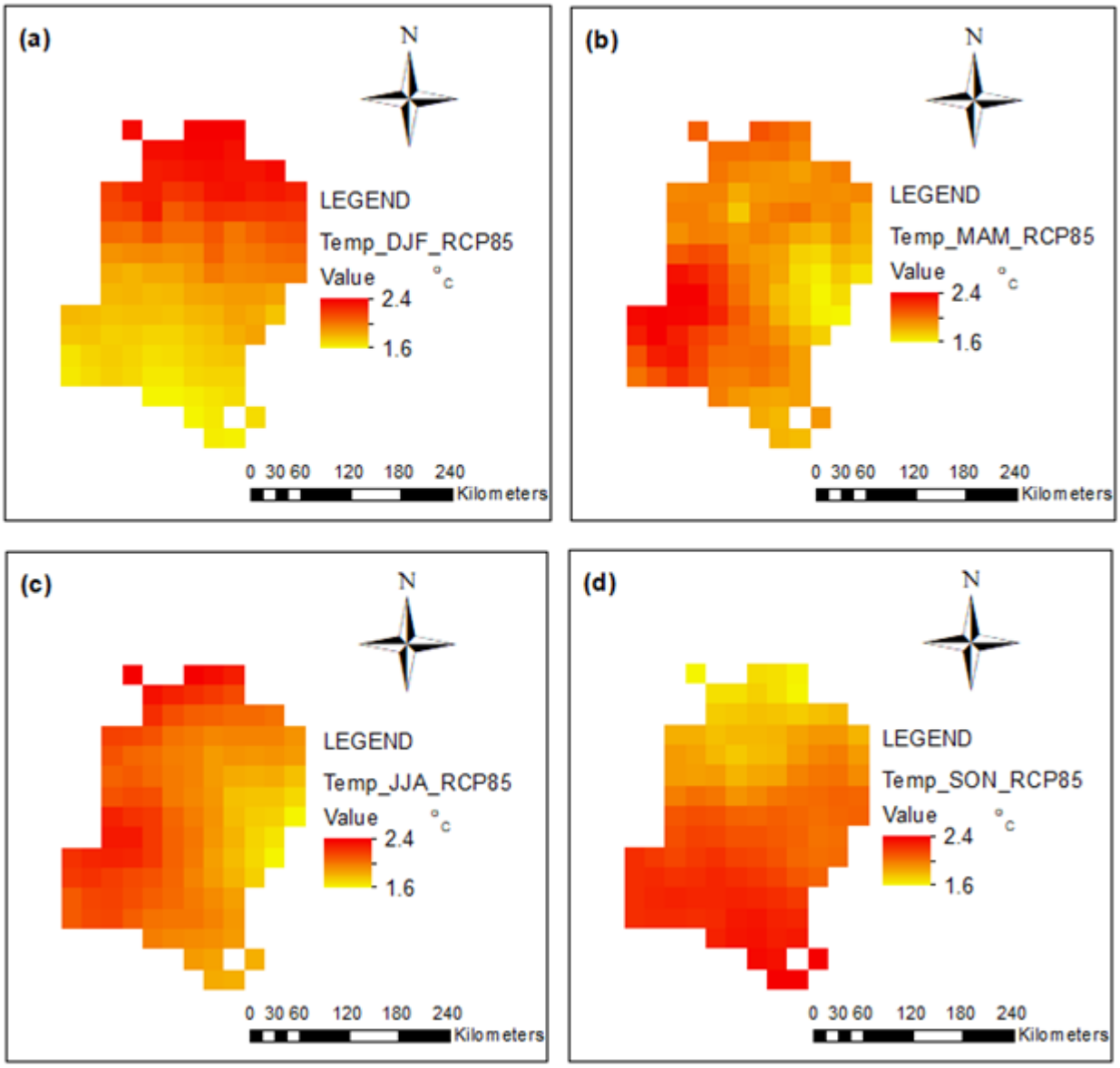

Figure 6.13 Predicted future seasonal temperature based on RCP8.5

Figure 6.13 (a) shows a similar pattern with climate scenarios under RCP4.5 with a considerable increase in temperature towards the north of the KRB while a small increase in temperatures is predicted in the southern parts for the season of DJF. The MAM season in Figure 6.13 (b) is predicted with a small increase in temperature towards the west while the southeast parts of the basin are predicted with a considerable temperature increase.

Figure 6.13 (c) shows a small increase in temperature in the western part of the basin while maintaining a considerable increase in all other parts of the basin. Figure 6.13 (d) shows a different pattern in SON where the northern part of the KRB has a small increase in temperature, with the rest of the basin having a considerable increase in temperature.

In general, there is an increase in temperatures across the KRB in all the seasons. The increase varies from 1.6^{o}C to 2.4^{o}C with the highest increase predicted in SON.

6.5 Conclusions

The PRECIS model has shown to be reliable as most of the results obtained are credible and comparable to the CRU observed climate data. The model skill is therefore, suitable to apply in climate change impact quantification. The prediction of future rainfall under RCP4.5 scenario indicate that rainfall will slightly increase in coverage area varying from 33% to 77% with magnitude varying from 65% to 0 while coverage areas with a decrease in rainfall will vary from 67% to 23% with magnitude varying from -25% to 0 in the four seasons of the KRB.

Therefore, much of the KRB will be under increased rainfall and less under decreased rainfall. There is a general rise in temperature for all seasons varying from 1.4^{o}c to 2.5^{o}c across the KRB and the season of SON is predicted to have the highest temperatures.

The PRECIS model predicts that rainfall under RCP8.5 is likely to significantly increase in magnitude and coverage area in the season of DJF. The general

increase in rainfall is predicted to increase by coverage area varying from 49% to 58% and magnitude varying from 0 to 37% while the coverage area under decreased rainfall will vary from 51% to 42% and magnitude will vary from 0 to -18%. The increase of rainfall in DJF may cause flooding in some of the flood-prone areas and adaptation and mitigation strategies may be required.

Further results under the same scenario also show increased temperatures ranging from 1.6^{o}c to 2.4^{o}c across the KRB, which may require appropriate design of adaptation and mitigation strategies. The results are in agreement and within the global temperature projections (Vuuren, 2014, 2011; Meinshausen et al. 2010).

It was, however, noticed that some model biases were apparent at validation for DJF and MAM seasons and monthly comparisons. The PRECIS model results would, therefore, need to be bias-corrected in order to improve accuracy before it can be used in hydrological modelling.

Further studies need to be done to include the use of more regional climate models for downscaling a more comprehensive set of HadCM3-based future scenarios for the creation of an ensemble. The RCM outputs will need to be bias corrected before their they can be used as in puts for hydrological modelling. The PRECIS model results were therefore only used for quantification of climate change impact in precipitation and temperature across the KRB in this chapter.

In order to determine PRECIS model's performance, the results were subjected to further analysis in chapter seven with six statistically downscaled bias-corrected

GCMs acquired for the same study area and time slice. Investigations and modelling of climate change impacts were performed in Chapter seven, with a specific focus on catchment water balance.

CHAPTER 7 : MODELLING IMPACT OF CLIMATE CHANGE ON CATCHMENT WATER BALANCE

7.1 Introduction

Hydrology and Water resources in catchments are already being affected by climate change in many forms that include rising spacial temporal variability,water balance changes which have implications on water and food security among many (Uniyal et al. 2015). Catchment water management seeks to optimise catchment water balance in order to secure water supplies for human health and human socio-economic development based on hydrological science (Zhang & Wurbs, 2018; Zhou et al. 2015). Management options can be developmed from Water balance modelling coupled with field experiments as it hences understanding of the hydrological cycle components (Zhang, 2002).

In order to evaluate and assess climate change impact on water balance components for KRB, six statistically downscaled bias-corrected GCM projections were acquired and used as inputs in SWAT model for hydrological modelling to determine the impact under RCP4.5 and RCP8.5 climate scenarios.

The assessment of the impact of climate change on hydrology and water resources in the KRB was performed to enhance integrated water resources management. Therefore, this chapter is focused on evaluating the impact of climate change on the catchment water balance, more specifically rainfall, water yield and runoff variables for different time scales in the KRB.

7.2 Materials and Methods

7.2.1 Description of the GCMs

ACCESS1-0

The Australian Community Climate and Earth System Simulator (ACCESS) is a coupled climate model, developed at the Centre for Australian Weather and Climate Research (CAWCR), which is a partnership of the Australian Bureau of Meteorology (BoM) and the Commonwealth Scientific and Industrial Research Organisation (CSIRO) working with different universities in Australia (Lewis & Karoly, 2014). It is a coupled Model Intercomparison Project Phase 5 (CMIP5) of the historical extension experiment and ensemble of r2i1p1(model realisation). The ACCESS1-0 is the atmosphere-only version with a grid spacing of 3.75◦Lon x 2.5◦ Lat horizontally and 38 vertical levels. The model represents physical processes that include: Precipitation, surface energy exchange, clouds, boundary layer processes and radiation (Ackerley & Dommenget, 2016).

CNRM-CM5

Centre National de Recherches Météorologiques (CNRM-CM5) is a Coupled Atmosphere, Ocean General Circulation Model (AOGCMs) which includes the atmospheric model ARPEGE-Climat (v5.2), the ocean model NEMO (v3.2), the land surface scheme and the sea ice model GELATO (v5) coupled through the OASIS (v3) system. The former version of the model, CNRM-CM3, was used in Phase 3 of the CMIP project and the released simulations are found on the CMIP3 database. Several studies undertaken on CMIP3 database were analysed with CNRM-CM3 and the results on a large scale circulation were considered reasonable (Decharme & Se, 2013).

IPCL-CM5A-LR

The IPSL-CM4 is a general circulation model developed at the Institute Pierre Simon Laplace (IPSL) and contributed to CMIP3. The model couples the atmosphere, land surface model to an ocean–sea ice mode (Denvil et al. 2013). The IPCL-CM5A-LR model used for CMIP5 projects constitutes the pre-industrial control simulations with boundary conditions of tropospheric greenhouse gases and aerosol concentrations (Persechino et al. 2013).

MIROC5

Model for Interdisciplinary Research on Climate (MIROC) is the latest version of the atmosphere-ocean general circulation model developed in partnership with the research community in Japan. MIROC5 is a newer version produced based on MIROC3.2 with many of the schemes replaced in atmospheric, ocean, land, sea ice components and control experiment (Masahiro et al. 2010).

MPI-ESM-MR

Max-Planck-Institute Earth System Model (MPI-ESM) comprises the coupled general circulation models for the atmosphere, ocean and the subsystem models for the land and vegetation and the marine biogeochemistry. MPI-ESM-MR model contributes to several climate change experiments through the coupled Model Intercomparison Project Phase 5 (CMIP5). The experiments are mostly based on the representative pathways (RCP) scenarios and/or the conceptualised forcing of CO2 only or the forcings dependant of observations (Giorgetta et al. 2013).

MRI-CGCM3

Meteorological Research Institute Coupled Global Climate Model (MRI-CGCM3) is a new and upgraded Meteorological Research Institute (MRI), previously climate

model MRI-CGCM2 series. The model forms part of the MRI's earth system model MRI-ESM1 and consists of atmosphere, land, aerosol and ocean-ice components. The model is used to perform basic experiments for pre-industrial control, historical and climate responsiveness (Yukimoto et al. 2012). Table 7.1 shows the summary of GCMs used in the study.

Table 7.1 Summary of GCMs used in the study

GCM No	GCM Name	Developer	Resolution Lon x Lat degrees
1	ACCESS 1-0	Commonwealth Scientific and Industrial Research Organisation–Bureau of Meteorology, Australia	1.9 x 1.2
2	CNRM-CM5	Centre National de Recherches Météorologiques, Centre, France.	1.4 x 1.4
3	IPCL-CM5A-LR	Institute Pierre Simon Laplace, France	3.7 x 1.9
4	MIROC5	Centre for climate research system(The University of Tokyo), National Institute for Environmental Studies and Frontier Research Center for Global Change (JAMSTEC), Japan	1.4 x 1.4
5	MPI-ESM-MR	Max Planck Institute for Meteorology, Germany	1.9 x 1.9
6	MRI-CGCM3	Meteorological Research Institute, Japan	1.4 x 1.4

7.2.2 GCM Projections and Data Source

The six GCMs in Table 7.1 were obtained from the NASA Earth Exchange (NEX) Global Daily Downscaled Projections (NEX-GDDP). The NEX-GDDP dataset consist of downscaled global climate scenarios produced from the General Circulation Model (GCM) runs performed through the Coupled Model

Intercomparison Project Phase 5 (CMIP5) (Taylor et al. 2012). The GCM runs were conducted over two representative concentration pathways (RCPs), namely RCP4.5 and RCP8.5 (Meinshausen et al. 2010). The CMIP5 GCM runs were produced to support the Fifth Assessment Report of the Intergovernmental Panel on Climate Change (IPCC AR5). The datasets were chosen because they provide a set of global, high resolution, bias-corrected climate change projections that can be used to evaluate climate change impacts on processes that are sensitive to finer-scale climate gradients and the effects of local topography on climate conditions (Thrasher et al. 2015).

The six GCMs covered the period 2020 to 2050 and the historical experiment that was conducted from 1975-2005 for each model. The historical run was taken as baseline because it was found to be reasonably accurate to replicate the main current climate effects in the KRB.

Every climate projection was downscaled at a spatial resolution of 0.25^{o} x 0.25^{o} (about 25km x 25km) (Thrasher et al. 2015).. The analysis of rainfall, water yield and runoff changes in the entire river basin was done at different time scales. An ensemble mean of six GCMs was used due to the significant benefits of relying on the many model outputs (Liu et al. 2012; Wilby & Harris, 2006).

7.2.3 Prediction of Changes in Hydrology & Water Resources

In order to predict changes in hydrology and water resources, the GCMs outputs on the global scale require downscaling into inputs of hydrological model on a regional or local scale (River et al. 2016; Farzan et al. 2013). This is done to improve the accuracy of the results because all model outputs may have biases that need

corrections. In view of the aforementioned, spatial downscaling and bias correction of GCM, outputs are a requirement prior to their use in regional impact studies (Farzan et al. 2013). Downscaling GCM outputs are widely performed through dynamic and statistical methods. The six GCMs under analysis in this study were statistically downscaled and bias-corrected for hydrological modelling at a regional scale.

7.2.4 Modelling Climate Change Impact Using SWAT

The GCM outputs were statistically downscaled to the region and used as input data to SWAT hydrological model. Statistical downscaling is mostly used as a conduit for linking GCM outputs with hydrological models due to insignificant computing resources required and can incorporate observations into method.

However, there is uncertainty in modelling impact of climate change on water resources, which starts with socio-economic storylines, future climate scenarios and actual impact modelling (Murphy & Ro, 2006). Hydrological models, therefore, provide the means for relating climate change to water resources by simulating the hydrological processes in river basins. SWAT is a hydrological model commonly used in simulating climate change effects (Wang et al. 2012; Arnold et al. 2009). SWAT simulates major components of the hydrological processes on a daily time step and a continuous watershed scale (Neitsch et al. 2005).

Daily solar radiation, relative humidity and wind speed were generated with the SWAT weather generator based on statistical information. The calibrated SWAT model (Described in chapter 5) was then used to simulate rainfall, water yield and

runoff water balance components for the KRB. The simulation was based on three climate scenarios namely;baseline period, RCP4.5 and RCP8.5.

In this study, land use and land cover were kept constant during SWAT simulations for future periods under RCP4.5 and RCP8.5, and therefore, climate change impact was the only factor considered to influence catchment water balance.

7.3 Results and Discussion

7.3.1 Comparisons of Means for PRECIS, CRU,GCM Ensemble and Observed Climate Data

The GCMs ensemble were further averaged and used to compare with observed data, for the same historical period for validation. The focus was rainfall and temperature data obtained from the Zambia Meteorological Department (ZMD), which was observed from five weather stations in the KRB for the same period (1975-2005).

Figure 7.1 indicates the location of weather stations in the basin where temperature and rainfall data were observed.

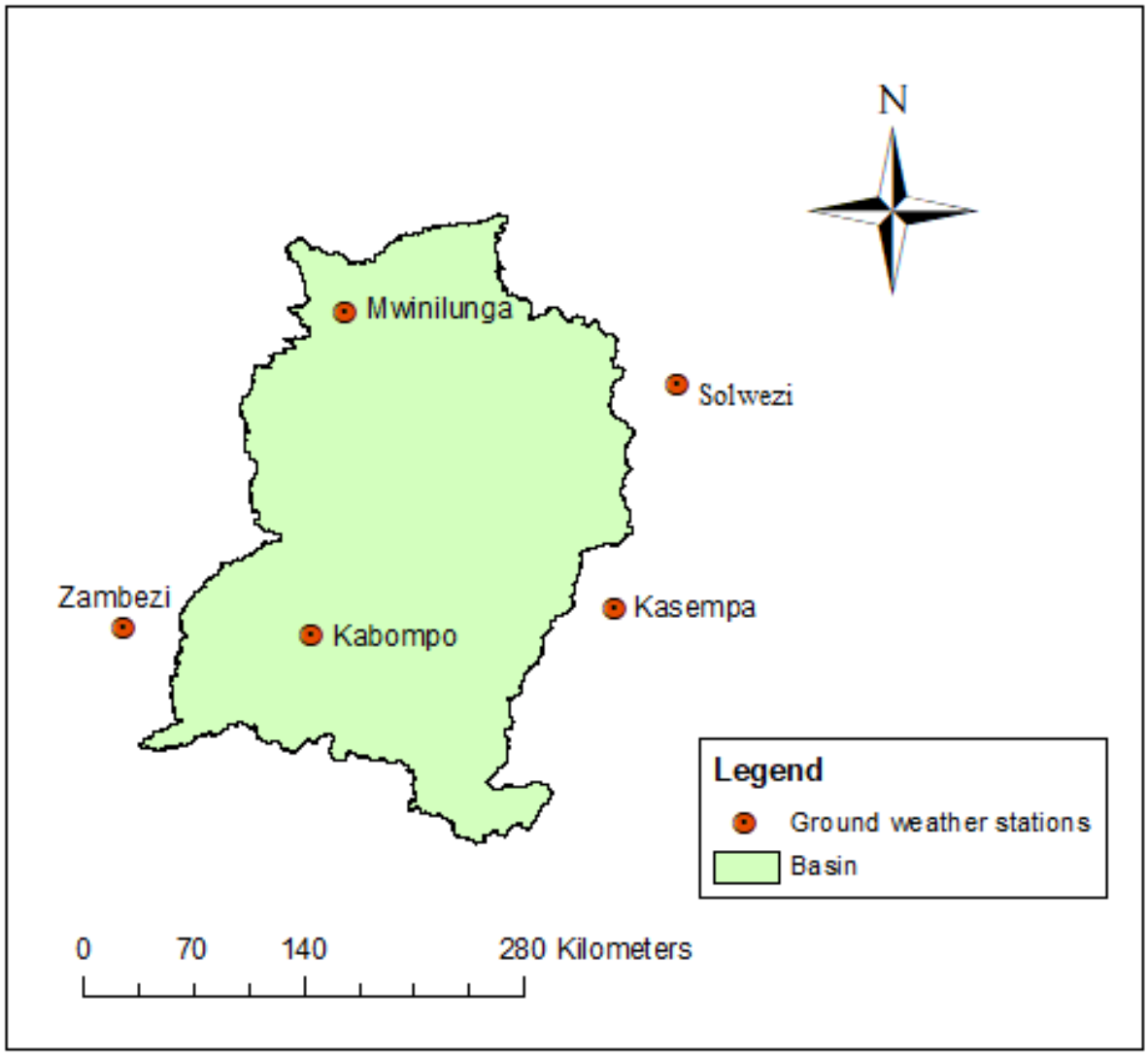

Figure 7.1 Location of weather stations

Figure 7.1 indicates location of weather stations that are sparsely distributed with a ground resolution of approximately 150km. The basin has an inadequate number of stations to represent the weather or climate of the area effectively. Some stations such as Zambezi, Kasempa and Solwezi may not have direct influence because they are slightly outside the basin.

The ground observed climate data,averaged GCM ensemble results and CRU data were then compared with PRECIS validation results from chapter six. The

comparison was made to confirm if the dynamic downscaled results (through PRECIS) and the statistically downscaled (GCM ensemble) match and to check the performance of the model. The climate variables compared and analysed were temperature and precipitation based on the same period.

Figure 7.2 illustrates the comparisons of temperature from PRECIS,CRU,GCM Ensemble and ground observed data.

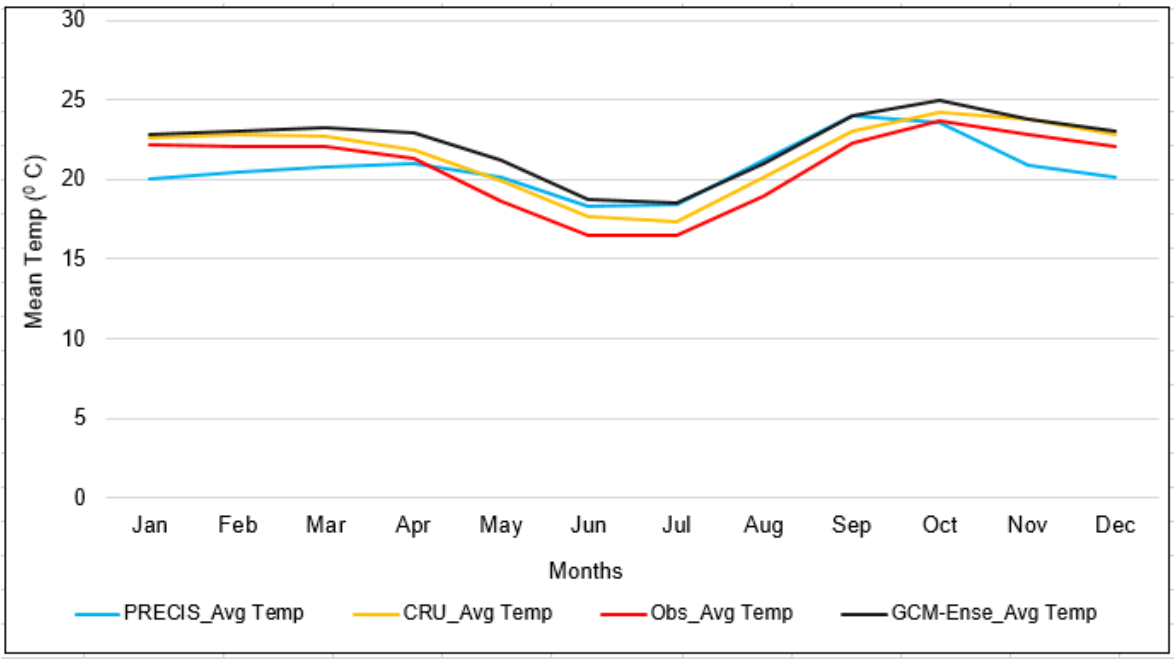

Figure 7.2 Comparisons of average monthly temperature

Figure 7.2 illustrates a very similar trend of average monthly temperatures from PRECIS, CRU,ground observed and GCM ensemble. The average temperatures range from 20 ^{o}C to 23 ^{o}C between January to April before falling to between 16 ^{o}C to 18 ^{o}C in June and July which are the coldest months and thereafter rise in September and October to between 24 ^{o}C to 26 ^{o}C which is the summer in the basin. However there is a slight mismatch between PRECIS and the other three at the

beginning and the end of the year. This could be attributed to some biases in the model.

Figure 7.3 illustrates the comparisons of rainfall from PRECIS,CRU,GCM Ensemble and ground observed data.

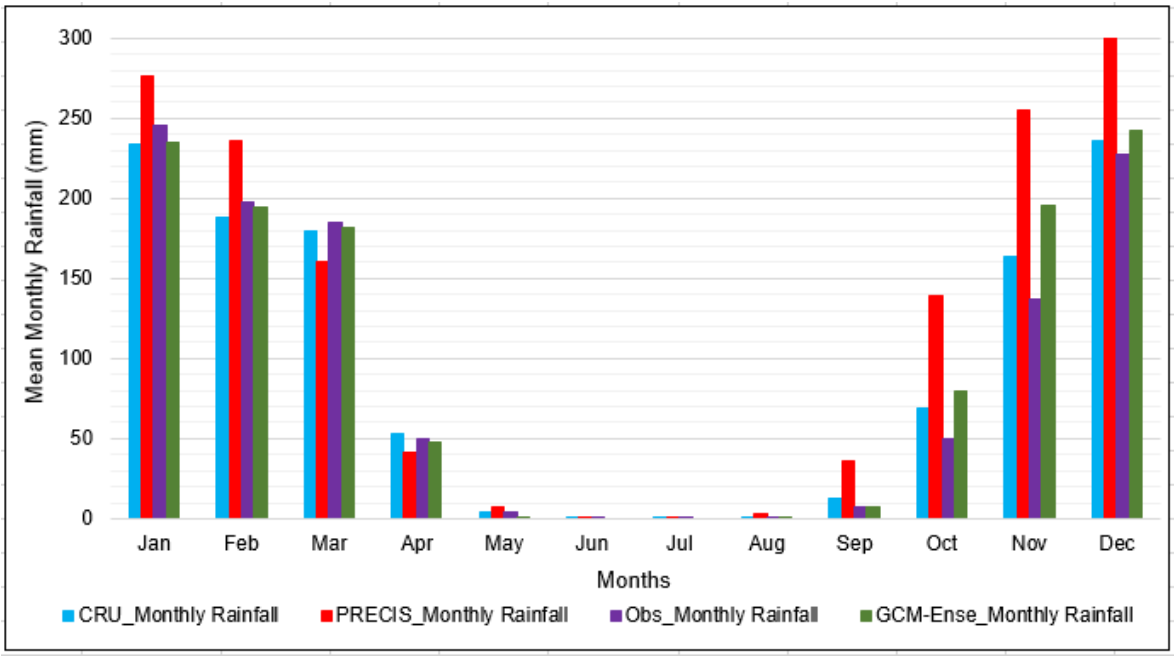

Figure 7.3 Comparisons of average monthly rainfall

Figure 7.3 illustrates similar trend of the average monthly rainfall from PRECIS,CRU,ground observed and GCM ensemble. There is however an over estimation of rainfall by PRECIS between January to February and September to December which are typically rain season months. The model matches very well in the rest of the months. The over estimation could be attributed to model biases.

In general PRECIS model results can be described to have a very similar trend with other data sources and matched relatively well for temperature while rainfall showed some mismatches. The PRECIS model results for RCP4.5 and RCP8.5 could not

be used for hydrological modelling because they need accuracy improvement. The PRECIS output were only used for Quantifying climate change impact in terms of coverage area and magnitude as described in chapter six. Therefore only GCM ensemble data was analysed in the subsequent sections.

The temperature and rainfall from GCM ensemble and ground observed was then plotted on the same graph to show the temporal variability across the basin. Figure 7.4 illustrates temporal variability of rainfall and temperature across the basin

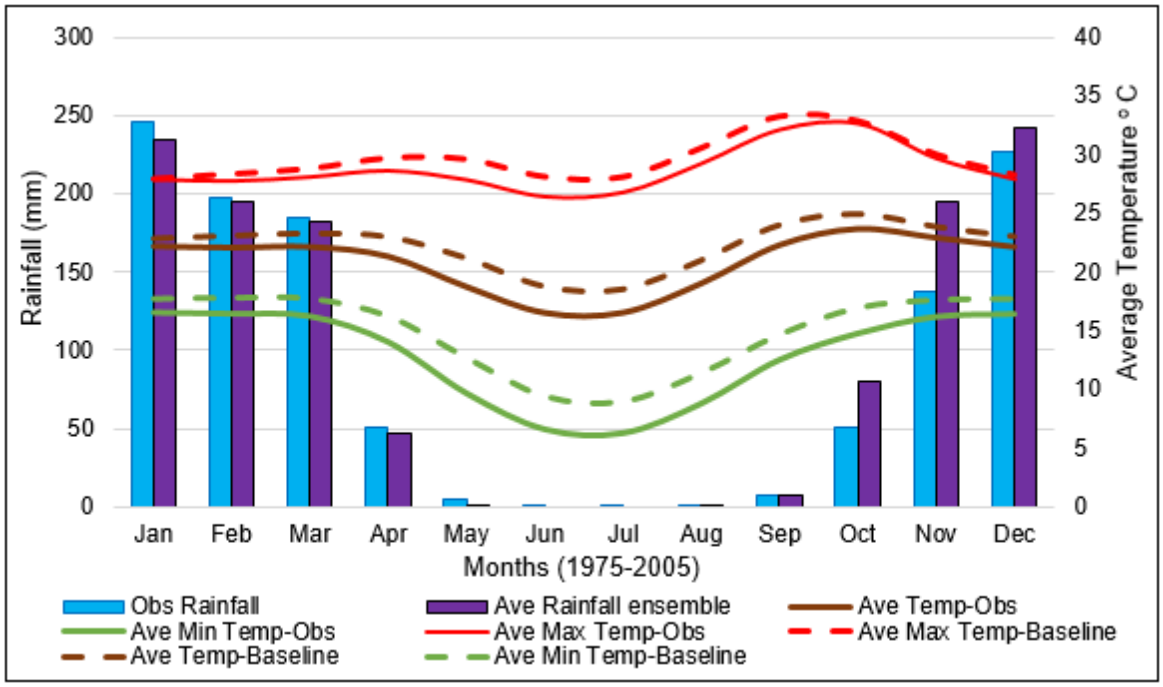

Figure 7.4 Comparisons of temp and rainfall for observed and ensemble means

Figure 7.4 illustrates a good match between GCM ensemble means and observed rainfall except for October and November, where there is a notable mismatch. The baseline temperature is slightly overestimated when compared to the observed temperature for maximum, minimum and average temperatures. However, the baseline was still found suitable for determining the change factor for future

temperatures because the regime is the same and the differences show only some uncertainties in GCMs.

The rainfall ensemble was further subjected to a trend analysis to determine its suitability for hydrological impact studies. A correlation efficiency was determined between the observed and the ensemble mean rainfall data sets. The results in Figure 7.5 illustrates a correlation efficiency of 96%, which confirmed the reliability of the average ensemble mean for use in hydrological impact studies.

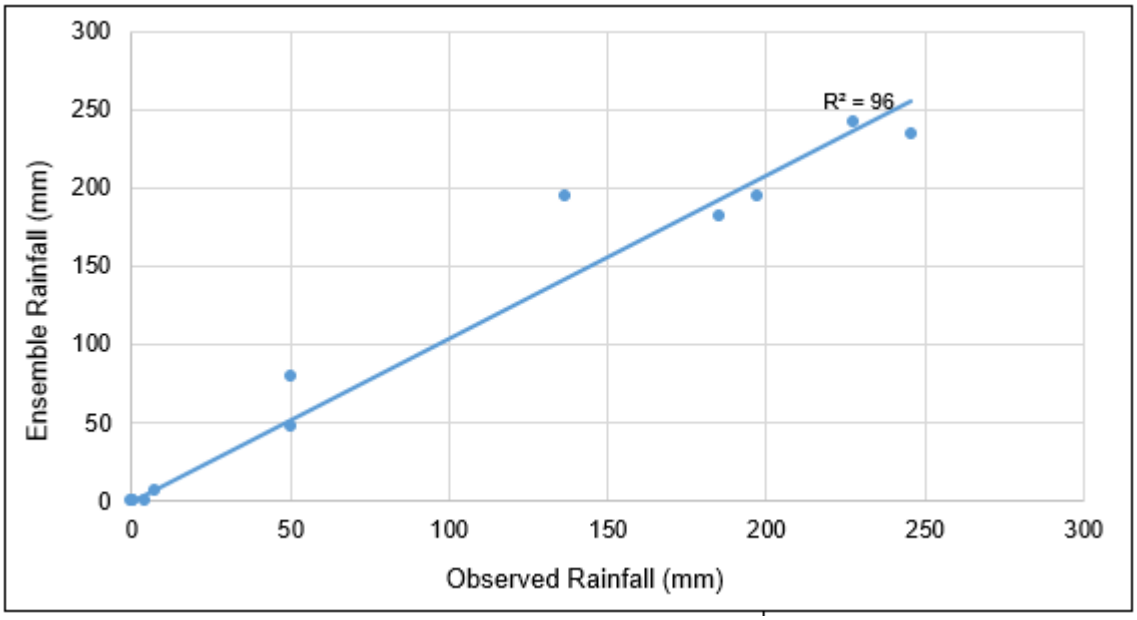

Figure 7.5 Monthly observed Vs ensemble baseline rainfall

The graph in Figure 7.5 shows a good correlation efficiency at 96% and therefore it can be used confidently to determine the ensemble mean for climate change analysis. The baseline ensemble mean was used as the baseline in the current research for climate change impact analysis.

7.3.2 Impact of Climate Change on Catchment Water Balance

The results from six GCM projections that were simulated by SWAT highlighted variations in increased and decreased water balance components in all the months under review for the KRB. The variations were also reflected in all the seasons except for June, July and August (JJA) season where no rainfall was simulated. However, the increases in rainfall, water yield and runoff were larger under RCP8.5 than the RCP4.5 climate scenarios, perhaps because RCP8.5 is a high Greenhouse Gas (GHG) emission scenario compared to RCP4.5, which is a medium GHG emission scenario.

The highest rainfall increases were simulated by Access1-0 under RCP8.5 when compared to any of the remaining five GCMs while the same GCM also simulated the lowest rainfall under RCP4.5 amongst the six GCMs. This could be due to different responses of various GCMs to the same climate scenarios and therefore creates fundamental uncertainties in climate change projections (Li & Jin, 2017; Stone et al. 2003). Thus, models have various baseline climates when compared and have different sensitivities to changes in emission scenarios (Carolina et al. 2003). The SWAT model was analysed for sensitivity to the two scenarios representing the climate change at two various spatial scales that are physically related.

SWAT model results are summarised for the baseline period 1975-2005, RCP4.5 and RCP8.5 for the period 2020-2050. The rainfall, water yield and runoff are investigated at monthly, seasonal and annual time scales.

Further evaluation of the SWAT simulated GCMs ensemble was performed and the mean was determined. The results are illustrated in Figure 7.6 as a simulation ensemble.

.

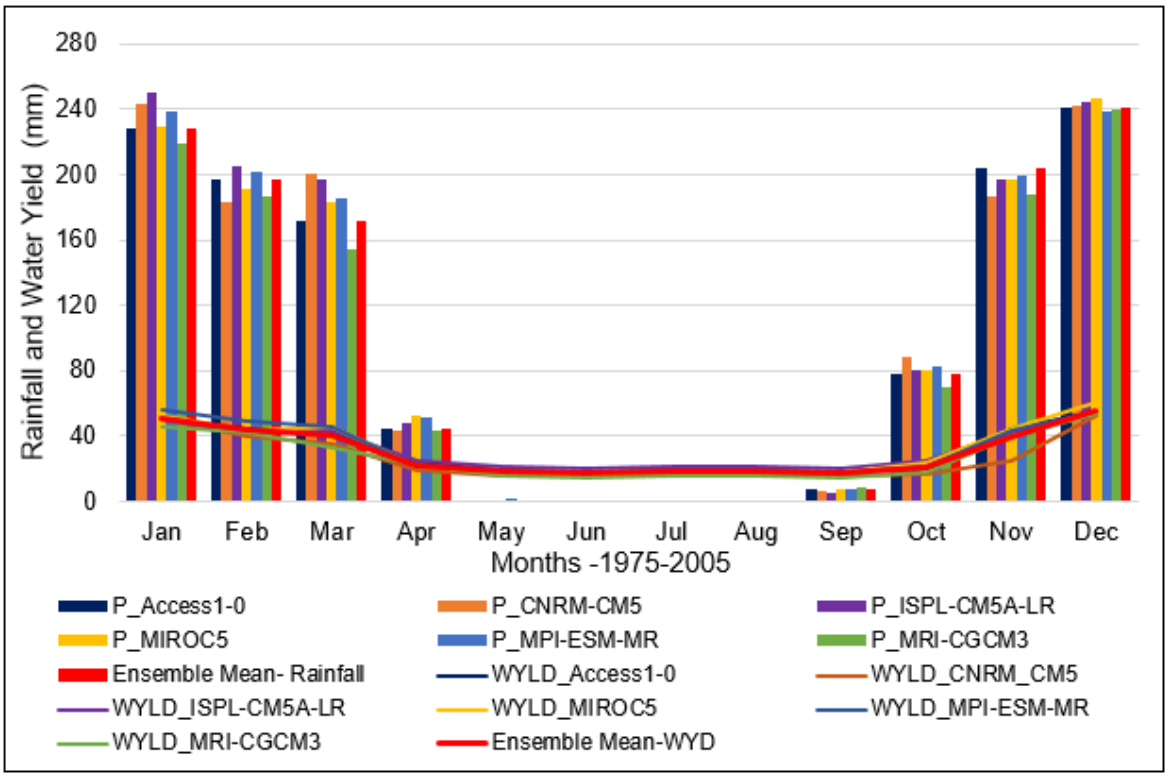

Figure 7.6 Simulated ensemble and the mean for baseline rainfall and water yield

The SWAT simulated ensemble and the mean for baseline rainfall (P) and water yield (WYLD) in Figure 7.6 show minor variations and indicates the highest rainfall of 200-250mm occuring in January and December with P_ISPL-CM5A-LR showing the highest rainfall in January exceeding the remaining five. The simulations also show that rainfall for February, March and April occurs in a decreasing order before finally ending in May where there is insignificant rainfall. Figure 7.6 further indicates no simulation for rainfall in June and July but insignificant rainfall is simulated in August and September while for October, November and December rainfall is simulated in an increasing order.

The water yield is a direct response to the rainfall in the basin and the SWAT model simulates the highest water yield in January and December with 55-60mm from the ensemble GCMs. The water yield decreases as rainfall reduces but maintains above 15mm in May to September when there is either no rainfall or negligible. The Water yield rises again from October to December due to rainfall increase. In general, the SWAT simulated rainfall and water yield based on six GCMs show a consensus with insignificant uncertainties.

The ensemble runoff simulations and their calculated mean were also plotted with ensemble rainfall to further compare it between the individual GCMs and analyse the impact and uncertainty. The results are illustrated in Figure 7.7.

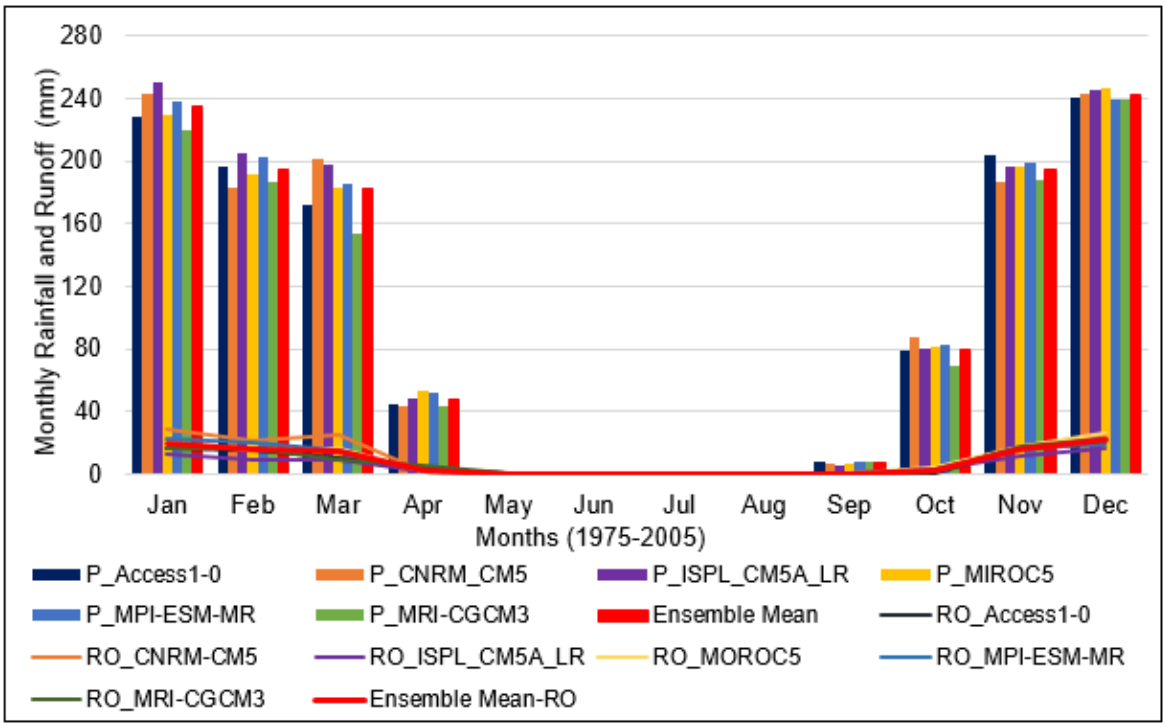

Figure 7.7 Simulated ensemble and the mean for baseline rainfall and runoff

The SWAT simulated ensemble and the mean for baseline rainfall (P) and runoff (RO) in Figure 7.7 show minor variations in the rain season indicating uncertainty and differences in model skill. The ensemble runoff is slightly higher in January, February, March, November and December when rainfall is also high and tend to decrease with decreasing rainfall occurring in April, September and October. The model simulates no runoff from May to the end of August, which is when rainfall is also absent. The streamflow is composed of base flow mainly coming from the water yield shown in Figure 7.6. Runoff also rises from September to December as a direct response to rainfall. The runoff simulated from CNRM-CM5 output gives the highest runoff of 29mm in January while ISPL-CM5A-LR output gave the lowest runoff of 12mm in the same period. Generally, SWAT simulated runoff based on six GCMs shows a consensus with insignificant uncertainties and variations.

Further comparisons were made between monthly rainfall and actual evapotranspiration (ET) of the SWAT simulated ensemble with their calculated mean. The results are illustrated in Figure 7.8.

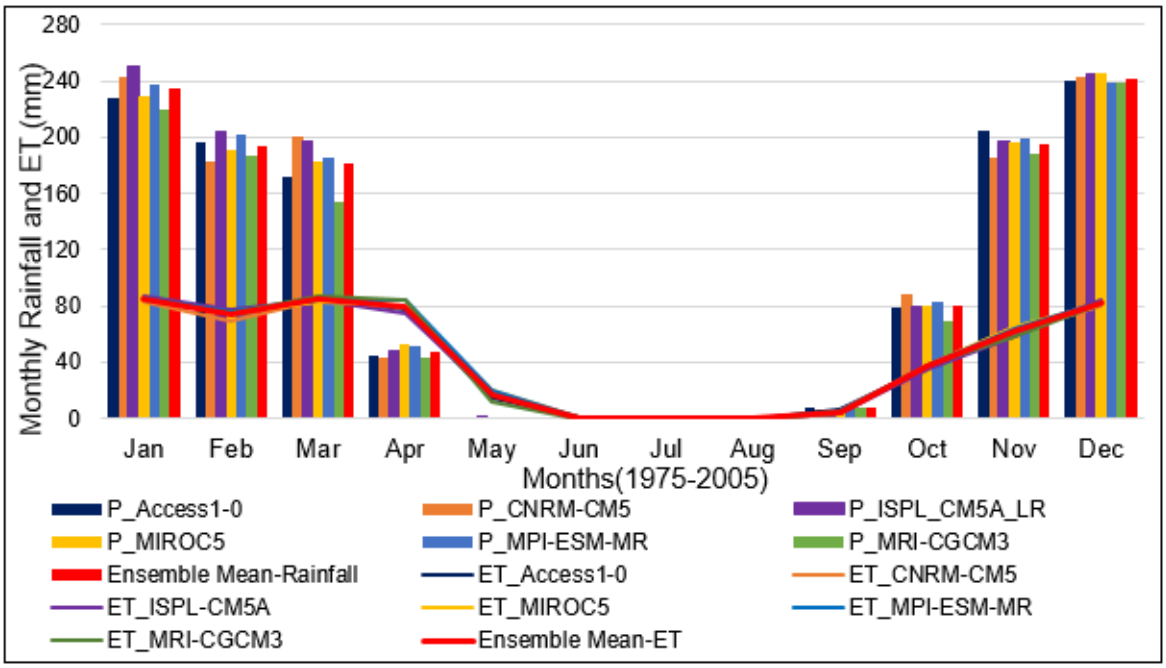

Figure 7.8 Simulated ensemble and the mean for baseline monthly ET

The SWAT simulated ensemble and the mean for baseline evapotranspiration (ET) in Figure 7.8 indicate no variation and ET ranged from 87-74mm for the period January to April, which is also the rain season. Furthermore, temperatures are generally low as shown in Figure 7.4, while from April to May and June there is a sharp decrease. ET further decreases to zero or insignificant between June to September before gently rising to 81mm in December; this is as a result of the rise in temperature. The June, July and August (JJA) season is characterised with low temperatures as it is winter and temperatures begin to rise in September. In general, the SWAT simulated ET based on six GCMs and shows a consensus with insignificant variations.

7.3.3 Baseline Seasonal Catchment Water Balance

The seasons for the Kabompo River Basin are defined as December, January and February (DJF), which is the typical rain season, March, April and May (MAM) is the

autumn, June, July and August (JJA) is the winter season and September, October and November (SON) is the summer season. Seasonal changes in catchment water balance are useful for planning of agricultural production, tourism, environmental flow concessions, water supply, industrial development and hydropower generation. The baseline seasonal changes of the catchment water balance were plotted to show variability. Figure 7.9 illustrates the results of a seasonal water balance.

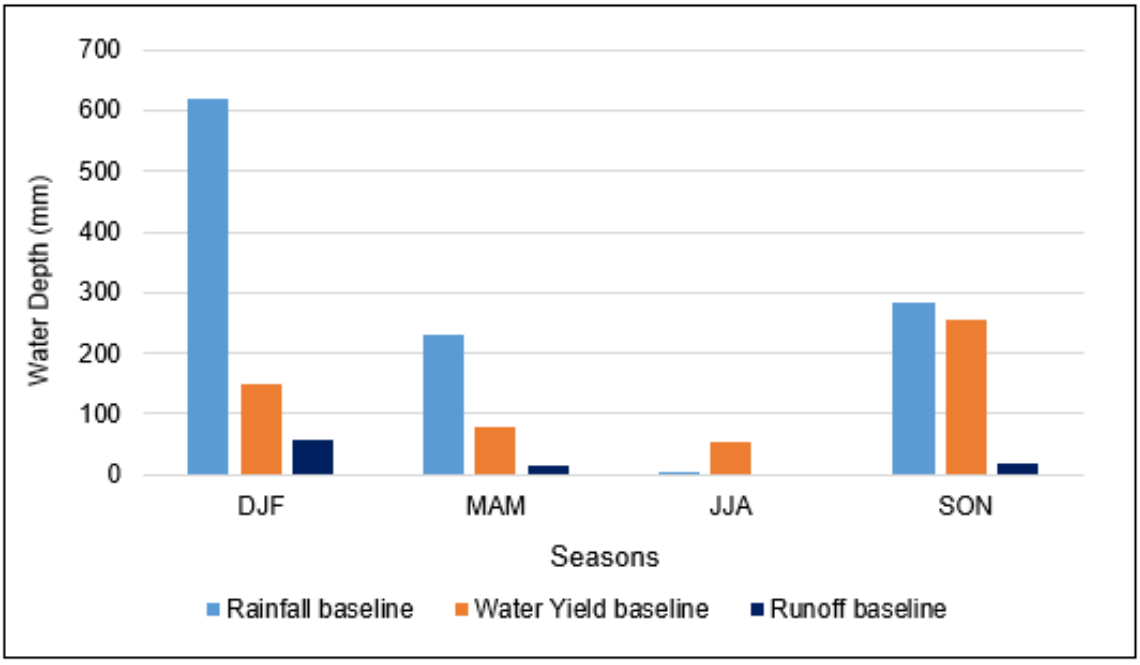

Figure 7.9 Seasonal water balance of the baseline period

Figure 7.9 shows the highest seasonal rainfall (620mm) and the highest runoff (58mm) recorded in DJF while the highest water yield of 256mm was recorded in SON. The SON season receives the second-largest rainfall followed by MAM and JJA when no rain is recorded. DJF shows the second-highest water yield followed by MAM and the lowest is recorded in JJA. SON and MAM show 18mm and 16mm runoff, respectively, with JJA having no rainfall and runoff, although it has a considerable water yield. This is the baseline flow regime analysed for a 31-year-

period (1975-2005) and a control period that shall be used for analysing change with future scenarios.

7.3.4 Future Changes in Catchment Water Balance under RCP4.5

The GCM ensemble was analysed under the RCP4.5 for the period 2020-2050 in order to detect the change signal and to quantify the magnitude of change for the catchment water balance components. The study focused on rainfall and water yield with runoff. Runoff was separated to show its contribution in water yield and its relationship with rainfall. Different time scales were considered under this emission scenario, which included annual, monthly and seasonal across the basin. This was done to understand the occurrences of the changes with their magnitude.

Monthly Changes

Figure 7.10 shows the individual GCM monthly changes in water balance as simulated by SWAT. Figure 7.10 also indicates the individual GCM monthly changes in water balance as simulated by SWAT.

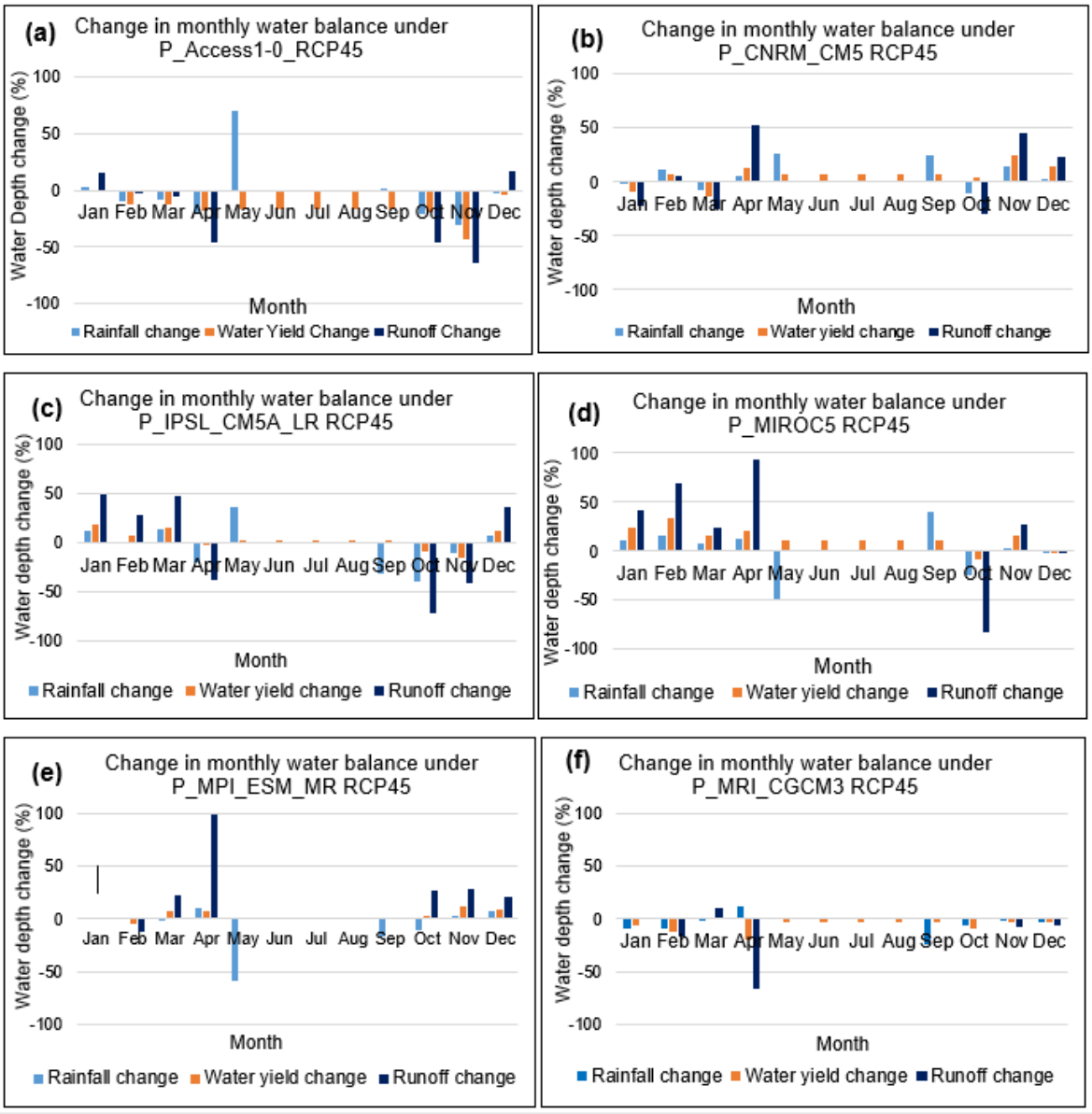

Figure 7.10 Monthly changes in catchment water balance under RCP4.5

Figures 7.10 (a) and (f) illustrate the predicted decrease of rainfall, water yield and runoff in all the months except for January and April. The highest decrease (30%) is predicted in November, as shown in Figure 7.10 (a). Figure 7.10 (d) shows a moderate increase in rainfall and water yield in all the months except October. Figures 7.10 (e), (c) and (b) indicate moderate decreases and increases of rainfall and water yield. The results of GCM ensemble show uncertainty because various GCMs responded differently to external forcing.

In order to obtain an overview of the average change for the entire basin, further analysis using a Change Factor Methodology (CFM), one of the most widely used methods in climate change impact studies (Trzaska & Schnarr, 2014; Anandhi *et al*. 2011), was performed between the GCM ensemble mean under RCP4.5 and the baseline ensemble mean. Figure 7.11 illustrates the results of the average monthly changes in rainfall,water yield and runoff under RCP4.5.

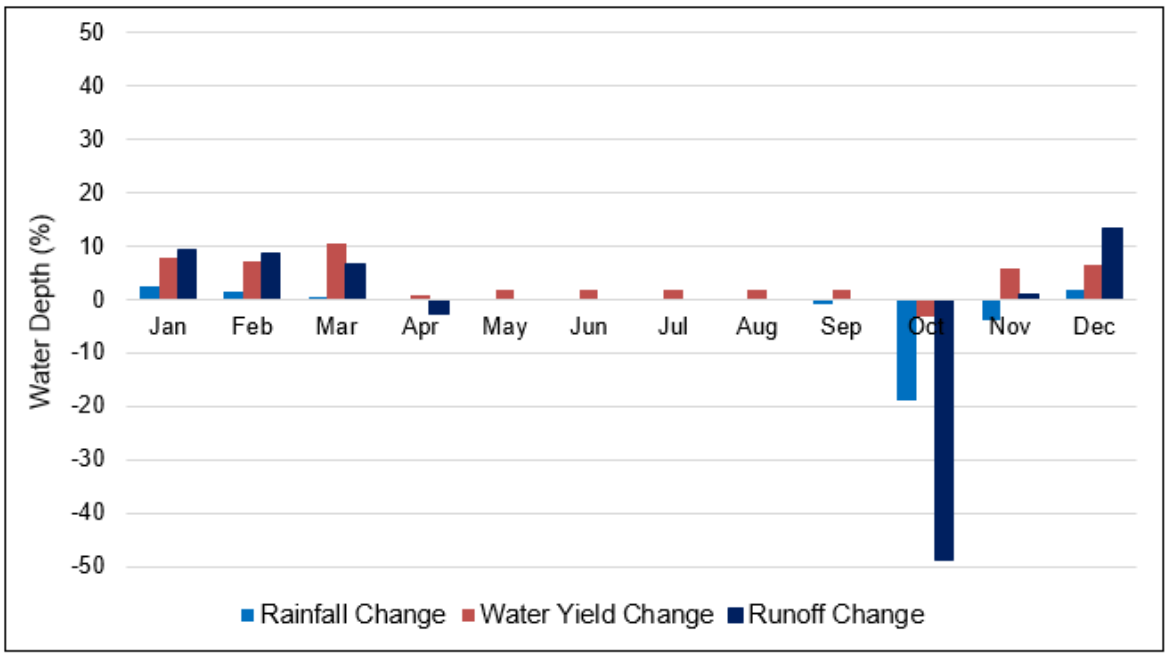

Figure 7.11 Average monthly changes under RCP4.5

The GCM ensemble mean, shown in Figure 7.11, indicates a slight increase in the monthly rainfall for December, January, February and March while October and November show a significant decrease. The water yield and runoff when compared with a baseline ensemble also show a slight increase.

The results clearly show that monthly rainfall, water yield and runoff have increased in December, January, February and March while rainfall decreased by 19% and 4% in October and November, respectively. The high rainfall increase of 3% is

predicted in January, followed by 2% in February and December. The highest monthly water yield is predicted to be 10% and 8% in March and January, respectively, while the highest runoff is predicted to be 13% in December followed by 9% in January and February. There is a slight increase in water yield between April and September.

Seasonal Changes

The seasons have also been altered with changes in catchment water balance. Figure 7.12 illustrates the seasonal changes in rainfall, water yield and runoff.

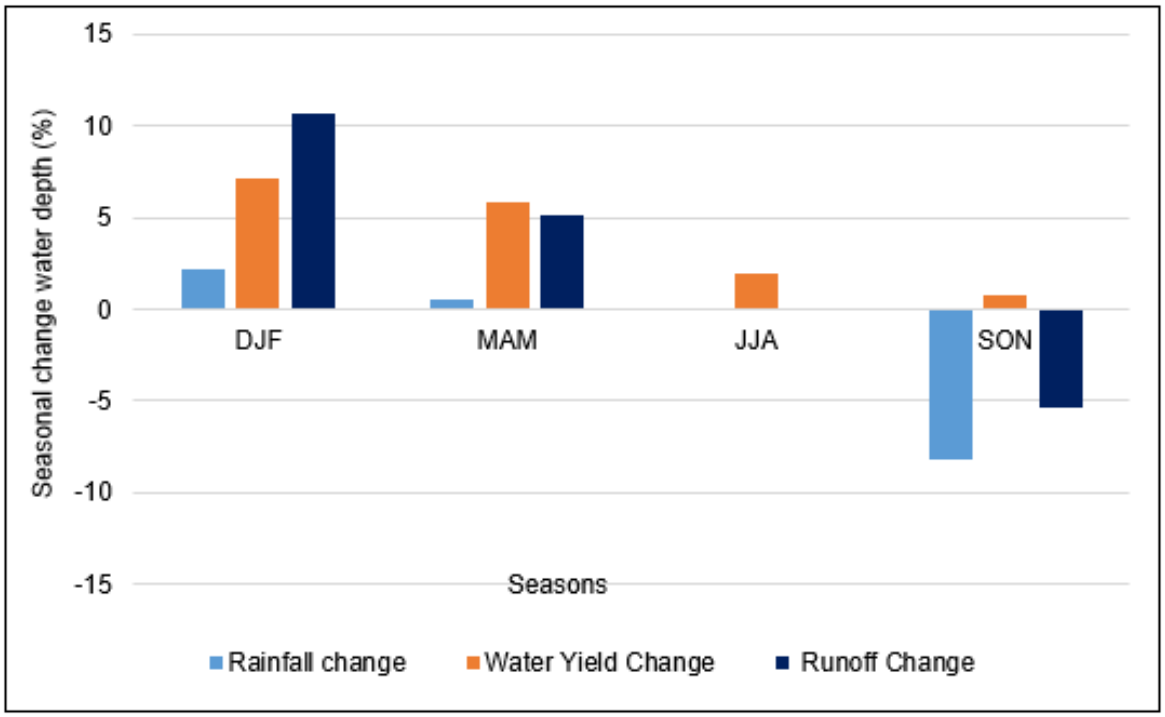

Figure 7.12 Seasonal changes under RCP4.5

Figure 7.12 illustrates that rainfall in DJF will increase by 2% across the basin while water yield will increase by 7% and runoff by 11%. Rainfall and water yield will increase in MAM by 1% and 6%, respectively, while runoff increases by 5%. In JJA no rainfall and runoff are predicted while water yield is predicted to increase by 2%. The SON season is predicted with a rainfall decrease of 8% while runoff also

decreases by 5% and water yield will slightly increase by 1%. This decrease may lead to seasonal drought requiring major interventions. In general, the Figure shows that there will be insignificant changes in rainfall while keeping runoff with considerable changes.

Annual Changes

The annual changes under RCP4.5 for the next period (2020-2050) indicate that rainfall will decrease by 1%, while water yield and runoff will increase by 5% and 6%, respectively. Table 7.2 shows the summary of results for the changes in the ensemble mean.

Table 7.2 Annual changes under RCP 4.5

Water Balance Component	Future Annual Variable(mm)	Baseline Annual Parameter(mm)	Change (mm)	Change (%)
Rainfall	1175	1184	-8.	-1
Water Yield	381	362	18	5
Runoff	99	93	6	6

The results under RCP4.5 predict that runoff in DJF will have a considerable increase of 11% while the changes in the rest of the seasons in rainfall and other hydrological variables are generally insignificant throughout the period. The annual rainfall shows an insignificant reduction of 1% and a small increase of 5% in water yield while runoff increased by 6%. The results also show that the RCP4.5 and baseline periods are almost the same with only a few minor differences.

7.3.5 Future Changes in Catchment Water Balance under RCP8.5

Further analysis was perfomed on GCM ensemble under the RCP8.5 for the period 2020-2050 to evaluate the change through quantification of change in the water balance components. The SWAT simulations were considered under monthly,

seasonal and annual time scales across the basin in order to analyse the variability of changes with their magnitude.

Monthly Changes

Figure 7.13 illustrates the monthly changes in catchment water balance for individual GCMs as simulated by SWAT.

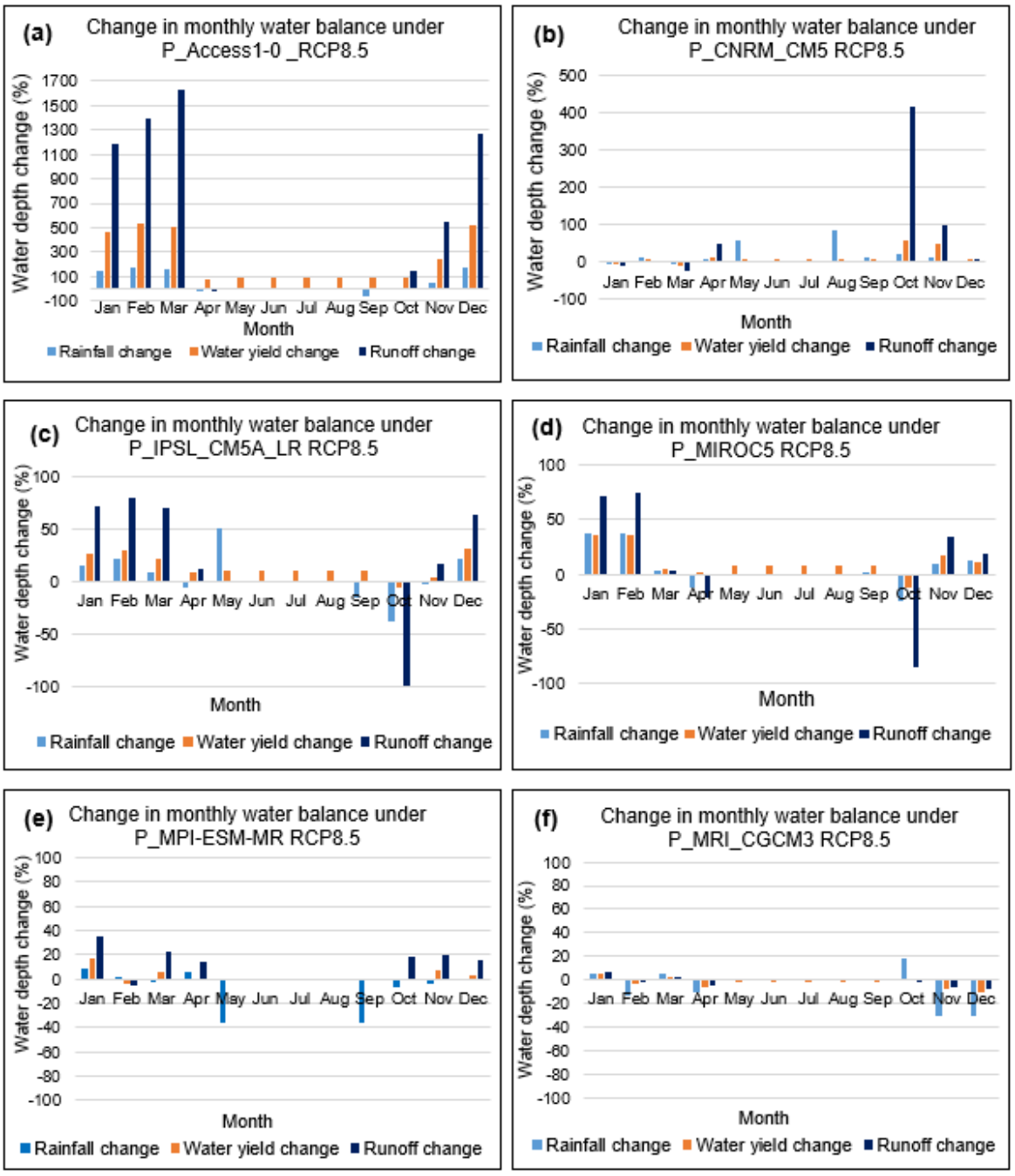

Figure 7.13 Monthly changes in catchment water balance under RCP8.5

Figure 7.13 (a) shows the P- Access 1-0 with the highest increase in rainfall, water yield and runoff in January, February, March, November and December when compared with the other five GCMs. The increase in rainfall ranges from 3-180% while water yield and runoff range from 83-534% and 153-1628%, respectively. The results show significant differences with the remaining five GCMs. Figure 7.13 (b) indicates P-CNRM-CM5 with a decrease in rainfall, water yield and runoff for January and March while showing a moderate increase in the water balance components in February, November, December and April. The largest runoff increase of 416% is predicted in October and the remaining months of May, June, July, August and September have insignificant rainfall and water yield, with no runoff predictions.

Figure 7.13 (c) shows P-IPSL-CM5A-LR with a moderate increase in the water balance for January, February, March and December while October and November shows a decrease. The increase in rainfall and runoff ranges from 8-50% and 12-80%, respectively, while water yield ranges from 4-31%; predicting the largest decrease in rainfall and runoff in October at 39% and 99%, respectively. There is a reasonable water yield increase of 10% from May to September but without rainfall and runoff, perhaps due to a contribution of baseflow. Figure 7.13 (d) shows P-MIROC5 with a similar trend to Figure 7.13 (c) where there is a moderate increase in water balance for the same months while April and October have a decrease. There is also a slight increase in water yield from May to August. Figure 7.13 (e) shows P-MPI-ESM-MR with March, September, October and November to have a decrease of 3-36% in rainfall while January, February and April show an increase in

rainfall, water yield and runoff. The Figure also shows an increase in water yield and runoff for March, November and December while also showing a notable decrease in water yield from May to September. Figure 7.13 (f) shows P-MRI-CGCM3 with a considerable decrease of rainfall in April, December, November and February in the order of 25%, 16%, 13% and 7%. Furthermore, the Figure shows that January, March, September and October have an increase in rainfall, water yield and runoff while May to August has a decrease in water yield and no rainfall and runoff is predicted.

There are considerable differences in GCM results, which can be attributed to uncertainty emanating from external forcing, downscaling and modelling processes. The results from GCM P-Access1-0 show a significant increase in catchment water balance, which is far above the remaining five GCMs for the future period. There are also wide variations in the five GCMs and this could be due to uncertainties regarding the aforementioned. Therefore, six GCM results show no consensus when compared to Figure 7.13.

In order to obtain an overview of the average change for the entire basin, further analysis was performed between the GCM ensemble mean under RCP8.5 and the baseline ensemble mean. Figure 7.14 illustrates the results of average monthly changes in rainfall,water yield and runoff under RCP8.5.

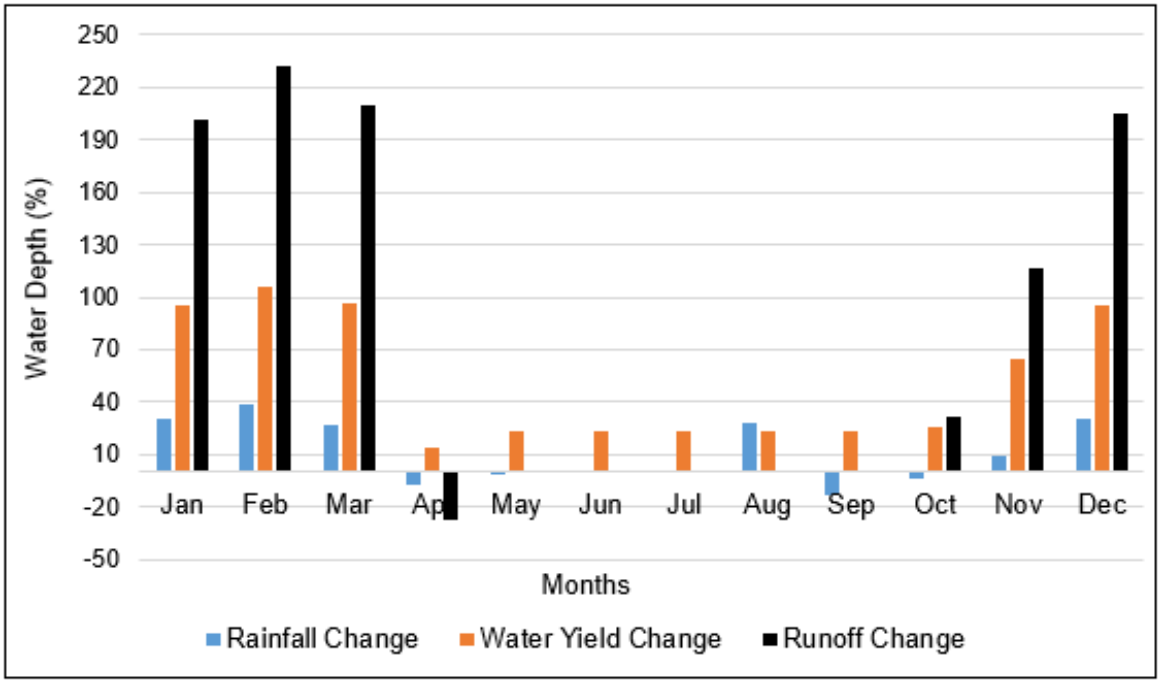

Figure 7.14 Average monthly changes under RCP8.5

The results in Figure 7.14 clearly show that the monthly water balance will significantly increase in November, December, January, February and March. Rainfall and runoff will increase between 9% and 39% and 31% and 232%, respectively. Rainfall is expected to decrease in October, September, May and April by approximately 1-13%. The highest rainfall increase is 39%, predicted in February, followed by 31% in December and January. A total of 27% is predicted in March and 9% predicted in November. The highest monthly water yield and runoff is predicted to be 106% and 232% in February. The lowest decrease in runoff is predicted in April, with 27%. In May, June, July, August and September no runoff is predicted, although an increase of 23-26% in water yield might occur.

Seasonal Changes

The seasonal water balance varies from season to season. The DJF season is predicted to have the highest water balance followed by MAM, SON and JJA. Figure 7.15 illustrates the seasonal changes in rainfall, water yield and runoff.

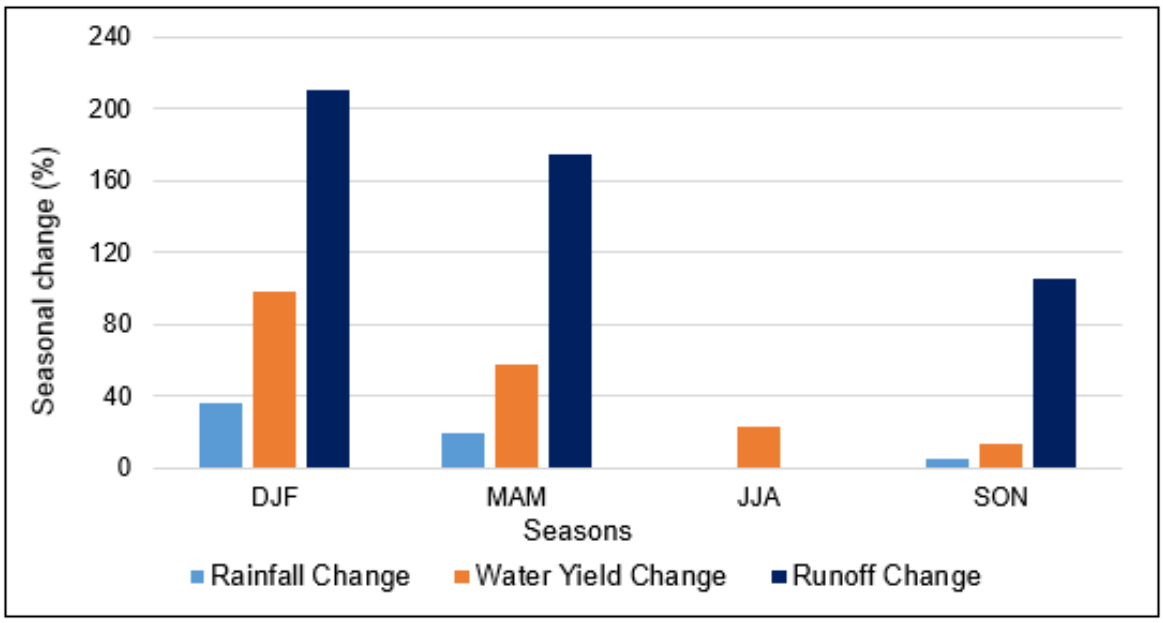

Figure 7.15 Seasonal changes under RCP8.5

Figure 7.15 shows a significant increase of runoff in DJF at 211% while predicting 174% rise in MAM and 105% in SON, with no runoff in JJA. The figure also shows a 98% increase in water yield for DJF followed by 58% in MAM, 23% in JJA and 14% in SON. The increase in rainfall is predicted at 36% in DJF followed by 20% in MAM and 5% in SON. The JJA season is predicted with no rain, as is the case with the current basin scenario.

Annual Changes

The annual changes under RCP8.5 for the period 2020-2050 show that the annual water balance will increase in general. Rainfall will increase by 19% and the water

yield and runoff will increase by 40% and 65%, respectively. Table 7.3 shows the annual changes.

Table 7.3 Annual changes under RCP 8.5

Water Balance Component	Future Annual Variable (mm)	Baseline Annual Parameter (mm)	Change (mm)	Change (%)
Rainfall	1466	1184	282	19
Water Yield	604	362	241	40
Runoff	264	93	171	65

The results under RCP8.5 predict a general increase in the annual water balance. Annual rainfall and runoff will increase by 19% and 65%, respectively while the annual water yield will increase by 40%. The general annual increase in the water balance may be attributed to the high emission scenarios under RCP8.5. The general rise in the annual water balance may culminate into floods and high storage of groundwater.

7.3.6 Analysis of Water Balance under RCP4.5 and RCP8.5

Comparisons and summary were made for the catchment water balance under the two climate scenarios. Figure 7.16 illustrates the results of the seasonal water balance under RCP4.5 and RCP8.5.

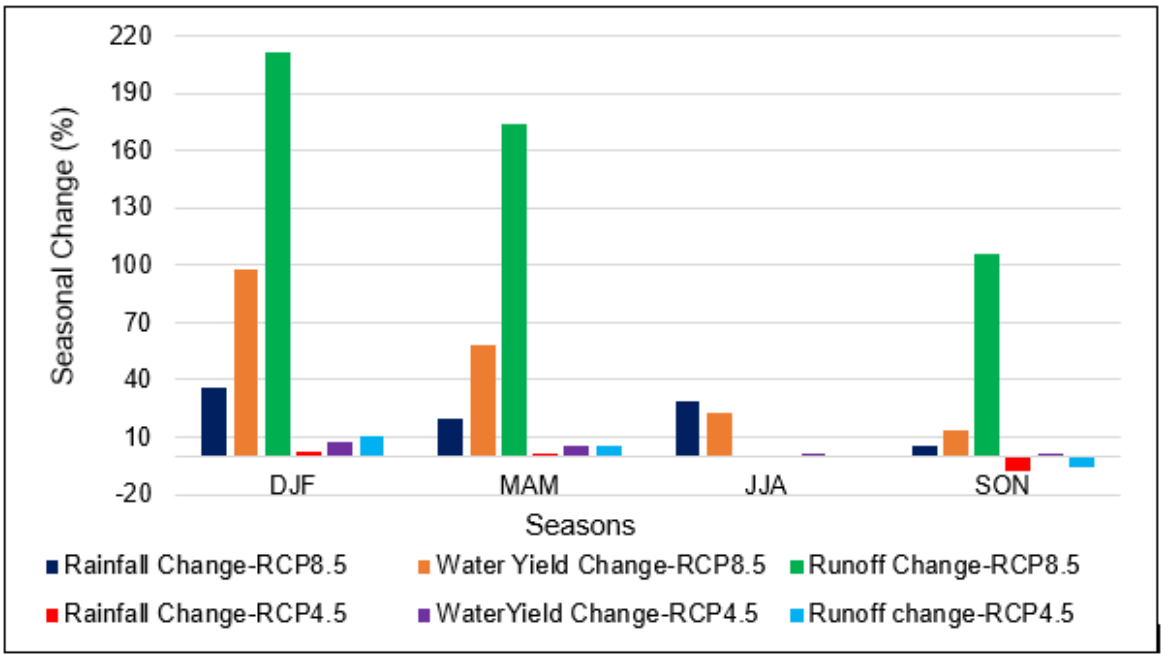

Figure 7.16 Comparisons of seasonal water balance under RCP4.5 and RCP8.5.

The comparison of the seasonal water balance in Figure 7.16 shows no consensus between the two future climate scenarios. The water balance components analysed under RCP8.5 is much more than that of the RCP4.5. The seasonal rainfall changes under RCP8.5 range between 5% and 35%, while RCP4.5 does not show any significant seasonal changes except for an 8% decrease in SON. The Figure also shows that the catchment water balance under RCP4.5 will have insignificant variations with the baseline catchment water balance. Another analysis was performed to compare and contrast the annual catchment water balance. The results are shown in Table 7.4.

Table 7.4 Annual water balance changes

Water Balance Component	RCP4.5 Annual Change (%)	RCP8.5 Annual Change(%)
Rainfall	-1	19
Water Yield	5	40
Runoff	6	65

Table 7.4 shows that the annual changes in the water balance under RCP4.5 are insignificant and therefore, unlikely to alter the current water balance. The changes under RCP8.5 are significant and likely to increase the catchment water balance to unprecedented levels. Nevertheless, the scenario under RCP8.5 are characterised with high uncertainty due to non-consensus of the SWAT simulations that are based on the six GCMs. The data for simulated rainfall, runoff and water yield based on baseline,RCP4.5 and RCP8.5 is listed on Appendix I,J and K.

Therefore, in general, the future is predicted with two scenarios: The future catchment water balance without changes from the baseline but with increased water demand and the future water balance with a significant increase above the baseline with an excessive surplus.

7.4 Conclusion

The impact of climate change on the catchment water balance based on GCMs is different and depends on a temporal resolution and the climate scenarios. The monthly changes under RCP4.5 indicate a slight increase in monthly rainfall for December, January, February and March while October and November show a significant decrease. The water yield and runoff when compared with a baseline,

also show a slight increase. The results clearly show that monthly rainfall, water yield and runoff has increased in December, January, February and March while rainfall decreased by 19% and 4% in October and November, respectively. The highest rainfall increase of 3% is predicted in January, followed by 2% in February and December. The highest monthly water yield is predicted at 10% and 8% in March and January, respectively. The highest and lowest runoff is predicted at 13% in December and 50% in October. There is a slight increase in water yield between April and September. The overall changes in the monthly water balance are not significant in this scenario. The monthly changes under RCP8.5 show that the monthly water balance will significantly increase in November, December, January, February and March. Rainfall and runoff will increase between 9% and 39% and 31% and 232%, respectively. Rainfall is expected to decrease between 1% and 13% in October, September, May and April. The highest rainfall increase is 39%, predicted in February, followed by 31% in December and January. This is followed by 27% predicted in March and 9% in November. The highest monthly water yield and runoff is predicted at 106% and 232% in February, respectively. The lowest decrease in runoff is predicted in April with 27% while there is a no runoff prediction for May, June, July, August and September, although a 23-26% increase in water yield is possible.

The seasonal changes under RCP4.5 predict 11% seasonal runoff increase in DJF while the changes in the rest of the seasons in rainfall and water yield are generally insignificant throughout the period. The annual rainfall will reduce by 1% while water yield and runoff will increase by 5% and 6%, respectively. The individual GCM results show insignificant variations and a good overall consensus.

The catchment water balance under this scenario will not deviate considerably from the baseline and therefore the major concern would be to enhance the management of water resources due to the demand, which is likely to double by the end of the 31-year period for municipal water supply, environmental, industrial, agricultural, energy and mining sector. The evaluated impact under this scenario illustrates a status quo of water resources with the baseline period.

The seasonal changes under RCP8.5 scenario predict significant increases in water balance that has a strong likelihood of increasing catchment water balance. The seasonal increases of runoff at 211%, rainfall at 35% may indicate the occurrence of an excessive catchment water balance. The comparison of seasonal water balance under the two RCPs shows no consensus of the future climate scenarios. The water balance analysed under RCP8.5 is much more than that of the RCP4.5. The seasonal rainfall changes under RCP8.5 range from 5%-35% while RCP4.5 does not show any significant seasonal changes except for an 8% decrease in SON. The catchment water balance under RCP4.5 will have insignificant variations with the baseline catchment water balance.

Annual statistics under RCP8.5 show a significant increase of 65%, 40% and 19% in runoff, water yield and rainfall, respectively, while under RCP4.5 there is an annual reduction in rainfall of 1% and an increase in runoff and water yield of 6% and 5%, respectively. Generally, the RCP8.5 climate scenario shows high uncertainties of GCM simulations compared to the RCP4.5 climate scenario in the

KRB. The variability of individual GCMs is also wide and shows no good consensus under RCP8.5 as compared to the RCP4.5 results.

The six GCMs have demonstrated a rare skill in modelling climate change for KRB. There is a significant increase under RCP8.5 in the catchment water balance at monthly, seasonal and annual time scales. The prediction may call for preparedness in disaster mitigation and adaptation, review of policies, review of designs of hydraulic structures, flood mapping and awareness campaigns. Meanwhile, under RCP4.5, the evaluated catchment water balance at monthly, seasonal and annual time scales may also call for integrated water resources management of available water resources against a growing water demand in the KRB.

Further analysis on the evaluation of the impact of climate change on streamflow in order to inform the adaptation and mitigation strategies were performed in Chapter eight.

CHAPTER 8 : ASSESSMENT OF IMPACT OF CLIMATE CHANGE ON STREAMFLOW

8.1 Introduction

Assessment of the impact of climate change on the future streamflow regime is a prerequisite for water resources planning (Arnell et al. 2015; Kusangaya et al. 2014). Adequate and accurate information on temporal and spatial variability of streamflow is required, especially concerning water availability, quality and maintenance of environmental flows (Chien et al. 2013).

Prediction of future water resources under the projected climate scenarios is made using hydrological models with accuracy to simulate observed streamflow through calibration (Gupta et al. 1998). Streamflow prediction can be achieved using hydrological ensemble systems (Mainardi et al. 2014; Chien et al. 2013). Assessments of impact of climate change on hydrology and water resources come with many uncertainties.

The uncertainties can be attributed to emission scenarios, climate models, hydrological models and downscaling. Many times, uncertainties associated with climate models are larger than that of hydrological models or downscaling (Li & Jin, 2017; Velazquez, 2015). Uncertainty with hydrological prediction is better considered with an ensemble system than with a deterministic approach (Krysanova et al. 2018; Qin & Lu, 2014).

.

This chapter focuses on evaluating the impact of climate change on streamflow regime of the KRB in Zambia. The method involved the use of the SWAT calibrated model and GCM data described in Chapter seven. Land use and land cover were also kept constant during the SWAT simulations under the RCP4.5 and RCP8.5, with climate change being the only factor considered to be influencing streamflow regime.

The basin under RCP8.5 climate scenario shows no consensus based on individual GCMs. However, the simulated ensemble mean for the annual streamflow under RCP8.5 predicts an annual increase of 85%, while the ensemble mean for the annual streamflow under RCP4.5 predicts no annual change with the baseline streamflow on GCMs. The majority of simulations indicate that intra-annual and inter-annual streamflow variability will increase in the future under RCP8.5 by a considerable margin while reducing under RCP4.5 scenario when compared to the baseline scenario.

8.2 Materials and Methods

The study focussed on average monthly, seasonal and annual simulations rather than daily simulations because GCM's reliability decreases at higher frequency temporal scales (Anandhi et al., 2011b). The six downscaled bias-corrected GCM projections were used as input data in calibrated SWAT model described in chapter five to simulate monthly streamflow in m^3/s. The streamflow simulations were based on the baseline, RCP4.5 and RCP8.5 climate scenarios for each GCM projection.

The simulated streamflow was then used as an ensemble for evaluation based on monthly, seasonal and annual time scales.

8.2.1 Hydrological Statistics

In order to understand the future catchment hydrology of the KRB, flood frequency analysis was performed on simulated streamflow time series for each GCM (Yu et al, 2018; Ngongondo et al. 2013). Log Normal (LN) and Log Pearson type III (LP3) probability distributions with parameter estimation of mean moments (MM) were used for the analysis. Temporal variability of streamflow at the KRB outlet was analysed with a coefficient of variation for each GCM to determine the spread of the streamflow about the means. Therefore, intra-annual and inter-annual variability of the streamflow were determined.

Flow Duration Curves (FDC) were calculated to analyse the streamflow variability and the percentage flow exceedances (Mülle & Thompson, 2015; Ngongondo et al. 2013). Different factors affect the shape of the FDC. The rest of the methods and data used in this chapter is the same as described in chapter seven.

8.3 Results and Discussion

The SWAT simulated results, based on the six GCM projections, show considerable variations in monthly streamflow under RCP8.5, RCP4.5 and baseline climate scenarios. The SWAT simulated ensemble for streamflow under RCP8.5 shows much higher flows from Access1-0 than the remaining five GCMs, while the simulation ensemble for streamflow under RCP4.5 was within the same range with only a few minor differences. The simulations ensemble streamflow for baseline were found to be within similar range as the one under RCP4.5.

Therefore, the magnitude and regime of the simulated ensemble for streamflow under RCP4.5 does not significantly differ from the simulated ensemble for baseline streamflow suggesting that the hydrological variables, such as water yield, surface runoff, groundwater flow and interflow may be within the same range. Similar results (in Chapter seven) were obtained with rainfall simulation from the six ensemble member GCM projections where Access1-0 under RCP8.5 had a much higher rainfall amount than the remaining five GCMs.

Although RCP4.5 is a future medium climate scenario (Medium emissions of CO_2), the simulations have revealed that it will not result in any significant change in streamflow from the baseline period. Perhaps, it is due to the limited change in temperature under RCP4.5 in the basin, which has insignificant variations with the baseline. Figure 8.1 illustrates the temperature variability in the basin under the three climate scenarios.

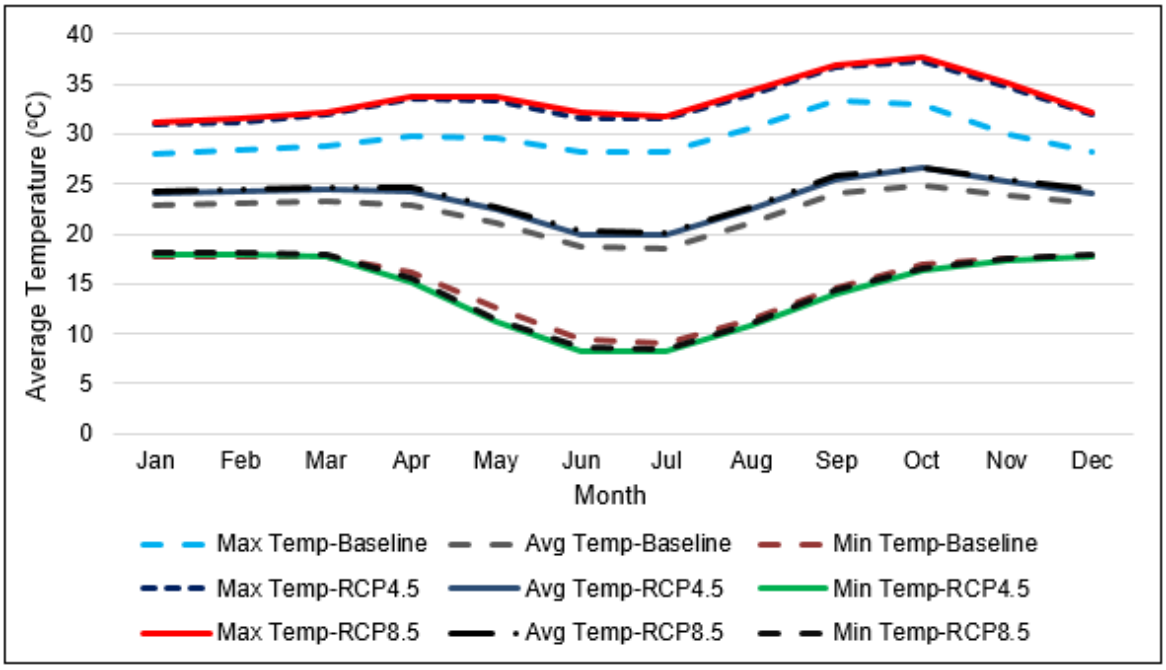

Figure 8.1 Baseline and future temperature variability

Figure 8.1 ilustrates a temperature rise of 1.5^{o}c under RCP8.5 which is close to RCP4.5 while the maximum temperature under baseline are far less. The temperature rise of 1.5^{o}c is quite significant as it comes with huge effects on evapotranspiration. Despite the increase in temperature, the pattern across the basin remains the same with winter season in June, July and August and summer season in September, October and November.

8.3.1 Simulated Streamflow under three Climate Scenarios

The different GCM projections were simulated using the SWAT model under the baseline, RCP4.5 and RCP8.5 climate scenarios to show variations and any possible similarity of patterns that may exist. Figures 8.2 (a), (b) and (c) illustrates the six-member simulation ensemble and their calculated mean for streamflow for the three climate scenarios.

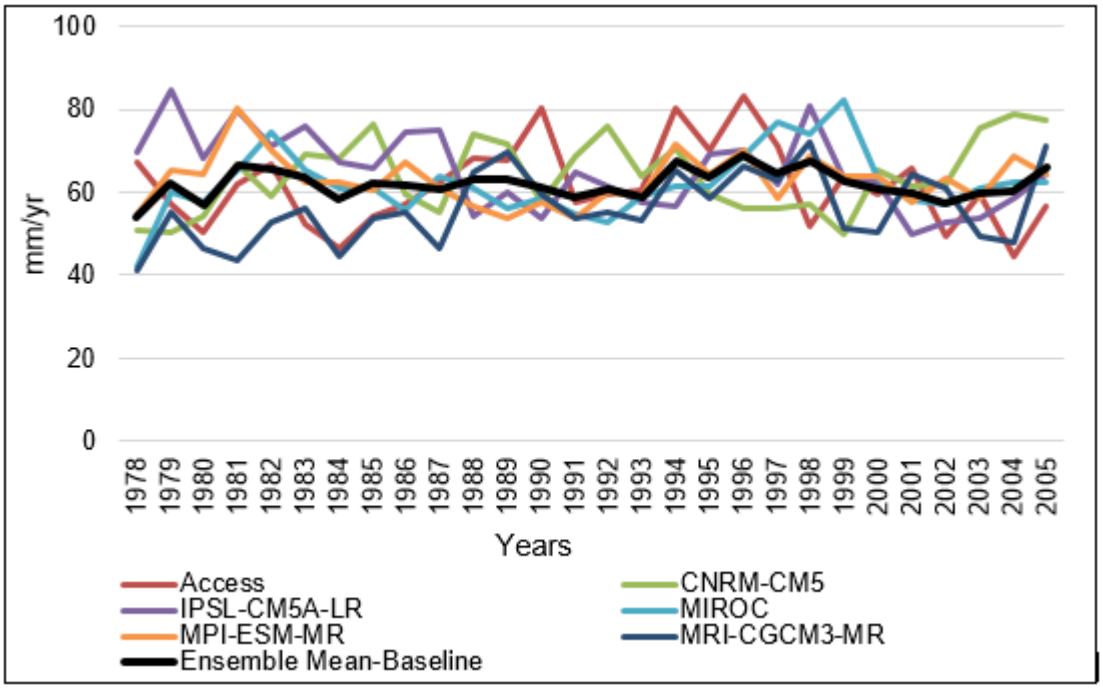

Figure 8.2 (a) Simulated ensemble and the mean for streamflow under baseline

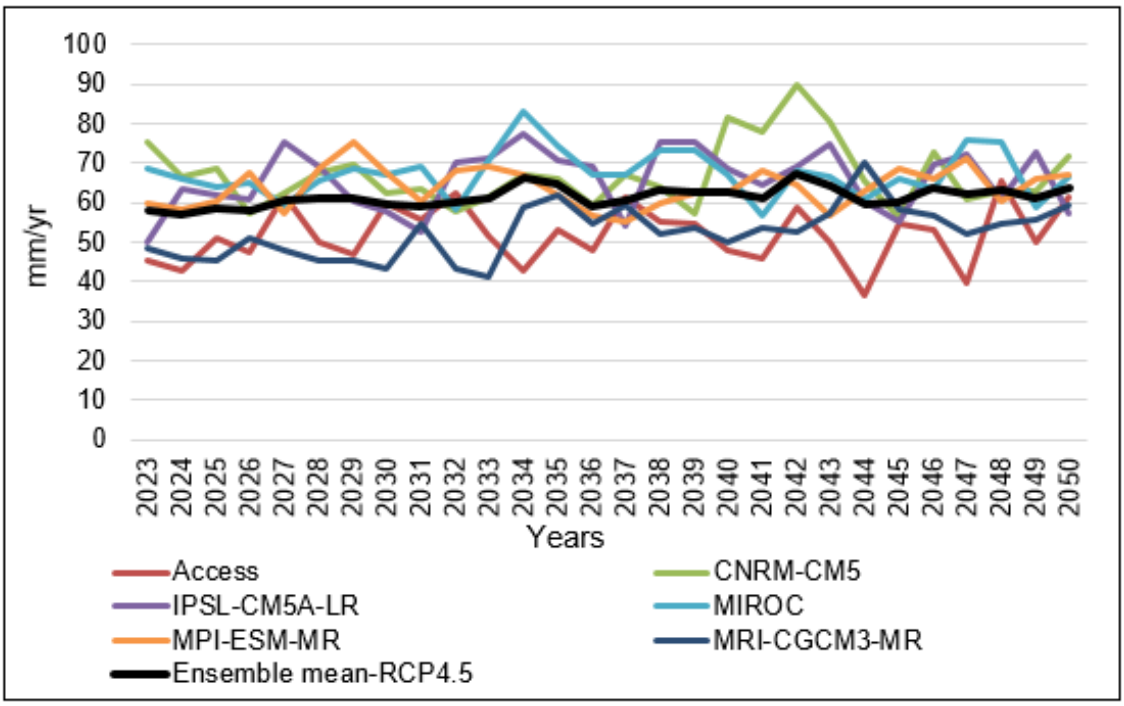

Figure 8.2 (b) Simulated ensemble and the mean for streamflow under RCP4.5

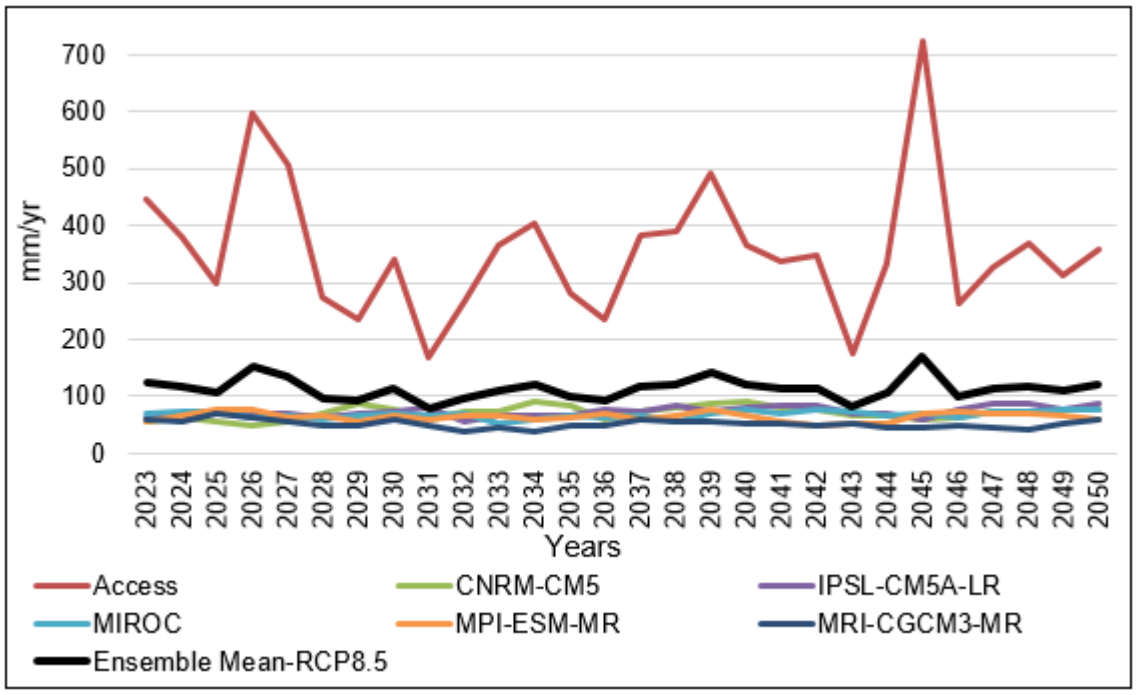

Figure 8.2 (c) Simulated ensemble and the mean for streamflow under RCP8.5

The simulated streamflow based on baseline and RCP4.5 in Figures 8.2 (a) and (b) show less variability compared to the mean. The figures also show a similar pattern

with the annual streamflow simulations that are in the same range of flow between 30-90mm/yr across the basin. However, Figure 8.2 (c) shows the simulated ensemble streamflow and the mean under RCP8.5 with significant differences as streamflow simulated under Access1-0 is higher and in the range of 168-725mm/yr across the basin with a different pattern, while the remaining five GCMs in Figure 8.2 (c) are within 30-90mm/yr with a pattern similar to Figure 8.2 (a) and (b). There is, therefore, a similarity of all the GCMs under the baseline and RCP4.5 climate scenarios. However, there is no similarity under RCP8.5, which is a high emission scenario with a high streamflow simulated based on Access1-0 in Figure 8.2 (c); the remaining five GCMs have similarities. The high streamflow simulated reflects the high rainfall simulated in chapter seven (Figure 7.11a) under the same GCM and RCP. Further more the differences in simulations may demonstrate uncertainty in GCMs that have various model skills (Hawkins & Sutton, 2009).

8.3.2 Monthly Streamflow Analysis

Figure 8.3 illustrates the SWAT simulated streamflow results for each of the GCM under baseline, RCP4.5 and RCP8.5 climate scenarios.

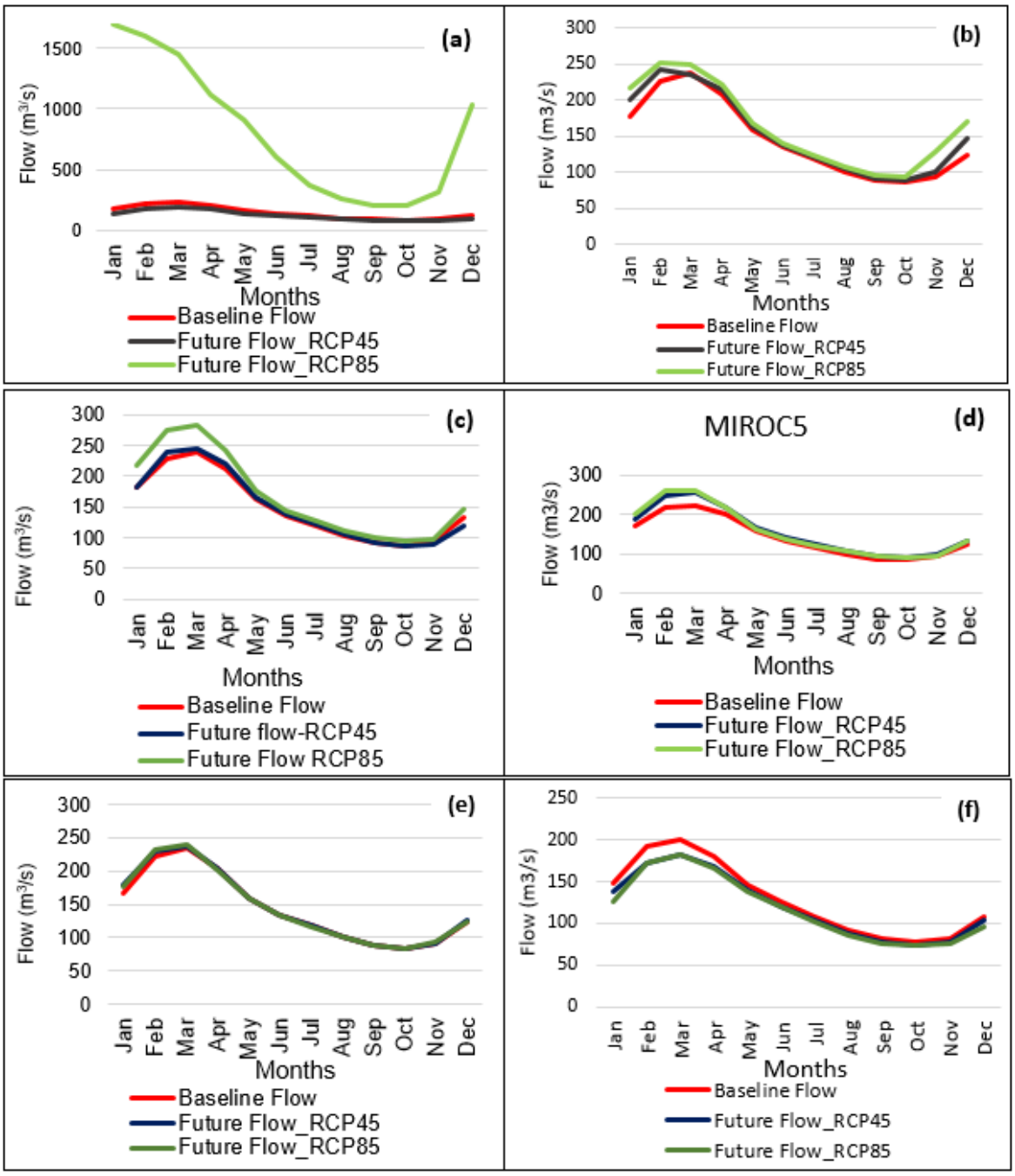

Figure 8.3 Streamflow simulations based on individual GCMs

Figure 8.3 (a) shows the monthly streamflow based on Access1-0 under RCP8.5 that has the highest magnitude of streamflow at 1696m^3/s compared to the baseline and RCP4.5. The highest simulated streamflow occurs in January, while in February and March the flow begins to recede and continues until August when perhaps it is only baseflow. The lowest flow of 204m^3/s is experienced in September and October

and thereafter begins to rise at a gentle slope up to November where the rise changes to a steep slope due to rainfall events that start at the end of September.

The peak baseline streamflow is shown as 224m^3/s occurring in March, while peak streamflow under RCP4.5 is illustrated as a peak streamflow of 187m^3/s occurring in the same month. The baseline streamflow is slightly higher than RCP4.5 throughout the year, predicting a decrease in RCP4.5 flow magnitude. The lowest flow for both baseline and RCP4.5 is 73m^3/s occurring in November. Figure 8.3 (a) also shows a shift in the peak flow occurrence when compared under the three scenarios. Peak flow under RCP8.5 is predicted to occur in January while for baseline and RCP4.5 it is in March. There is also a sharp rise in flow predicted under RCP8.5 from November to January, which may be the result from a high rainfall input beginning in October. Meanwhile, the baseline and RCP4.5 have a very negligible rise in the same period, suggesting an input of limited rainfall.

Figure 8.3 (b) shows the monthly simulated streamflow based on CNRM-CM under baseline, RCP4.5 and RCP8.5 scenarios compared with the baseline period. The streamflow simulations under the three climate scenarios have nearly the same flow regime with insignificant variations. However, the streamflow under RCP8.5 is slightly higher than RCP4.5, which is a bit higher than baseline flows between January to April and October to December. These are also months of rainfall in the KRB. The predictions generally show that the future period will not be very different from the baseline period.

Figure 8.3 (c) is the prediction of streamflow based on IPSL-CM5A-LR under RCP4.5 and RCP8.5 compared with the baseline period. The streamflow simulations have nearly the same flow regime with some differences between January and April. The streamflow under RCP8.5 is higher than both RCP4.5 and baseline streamflow that is almost matching throughout the year. The Figure also shows GCM predictions with insignificant variations between the three streamflows throughout the year except between January and April where there are apparent differences. These are also months of rainfall in the KRB. The predictions generally show that the future period will not vary significantly from the baseline with a slight streamflow rise between January to April under RCP8.5.

Figure 8.3 (d) shows the streamflow simulated based on MIROC under the baseline period, RCP4.5 and RCP8.5 scenarios. Figure 8.3 (d) shows the prediction of streamflow based on MIROC5 under RCP4.5 and RCP8.5 compared with the baseline period. The three-streamflow simulations have nearly the same magnitude and flow regime with some differences between January to April. The streamflow under RCP8.5 is slightly higher than RCP4.5, which is also higher than the baseline streamflow between January and April. Furthermore, the GCM predicts that there will be insignificant variations between the three streamflows from May to December. The predictions generally show that the future period will have minor differences from the baseline with a slight streamflow rise between January to April under RCP8.5 and RCP4.5.

Figure 8.3 (e) shows the streamflow simulated based on MPI-ESM-MR under the baseline period, RCP4.5 and RCP8.5. Figure 8.3 (e) illustrates the prediction of

streamflow based on MPI-ESM-MR under RCP4.5 and RCP8.5 compared with the baseline period. The streamflow simulations have the same flow regime with insignificant variations in magnitude between January and March. The predictions generally show that the future period will not have considerable differences from the baseline period.

Figure 8.3 (f) shows the streamflow simulated based on MPI-ESM-MR under the baseline, RCP4.5 and RCP8.5 climate scenarios compared with the baseline period. The streamflow simulations have nearly the same flow regime with some differences between January and May. The streamflow under the baseline is slightly higher than both RCP8.5 and RCP4.5 that are almost the same throughout the year. The GCM is also predicting that the future magnitude of streamflow will slightly reduce between May and December while considerable reductions will occur between January and April.

The majority of streamflow simulations based on the five GCMs predict a slight increase in streamflow while streamflow simulations based on Access1-0 predict a significant increase, while the streamflow simulation based on MRI-CGCM3-MR predicts a slightly less streamflow. The streamflow simulations based on the five GCMs are within the same range while streamflow simulation based on Access1-0 has a significant increase. Further analysis was, therefore, performed to construct the monthly simulated streamflow ensemble means based on the six GCMs under baseline, RCP4.5 and RCP8.5 climate scenarios. Figure 8.4 illustrateds the results of monthly ensemble mean streamflow.

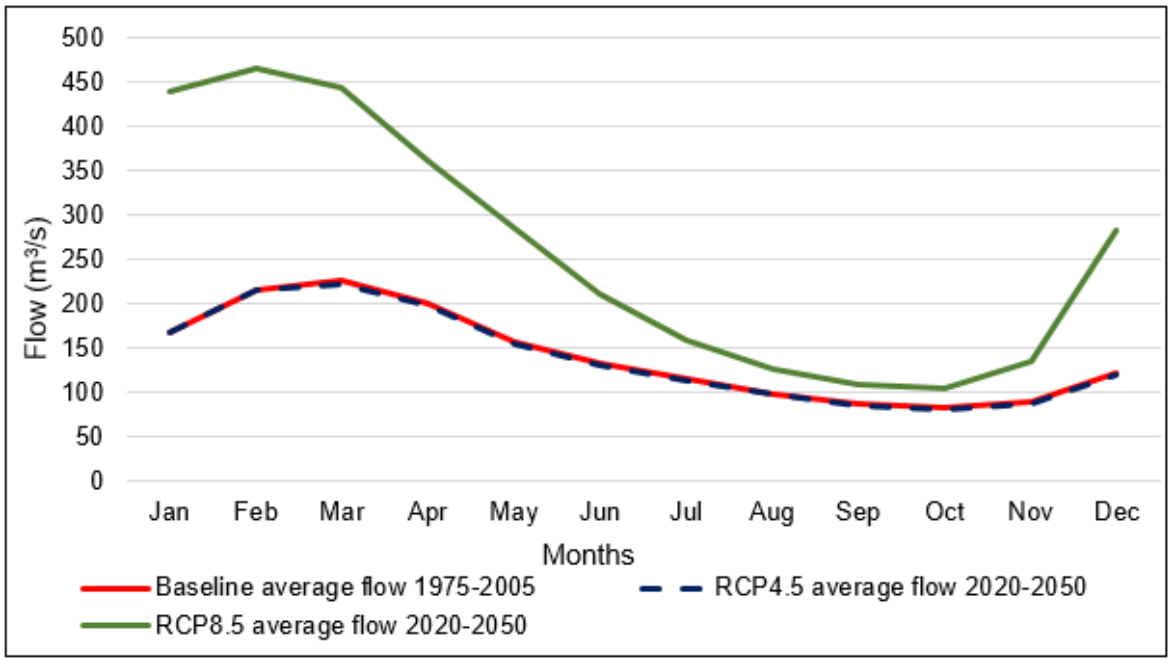

Figure 8.4 Monthly ensemble mean streamflow

The ensemble mean streamflow in Figure 8.4 predicts that baseline and RCP4.5 streamflow will have nearly the same magnitude and flow regime while the ensemble mean streamflow under RCP8.5 will be much higher in magnitude compared to the two ensemble mean streamflow that also includes a wide variation in flow regime. The ensemble mean peak flow under RCP8.5 is predicted to be 467m^3/s occurring in February while under RCP4.5 and baseline it is 224m^3/s, which occurs in March. The lowest base flow under RCP8.5 is predicted to be 106m^3/s occurring in October while under RCP4.5 and baseline periods it is 82m^3/s occurring in the same month.

The ensemble mean streamflow under RCP8.5 shows a sharp rise from November to January. Under RCP4.5 there is a moderate rise from November to January. The predictions from the ensemble mean streamflow indicate an increased magnitude of streamflow under RCP8.5, which may culminate into excessive streamflow of

most parts of the basin depending on the topography. RCP4.5 generally indicate the status quo of the flow regime and magnitude when compared with the baseline flow.

In order to determine the actual increase or decrease for the ensemble mean streamflow, a change factor methodology (CFM), one of the most widely used methods as described in chapter three was applied. Figure 8.5 illustrates the results of ensemble mean streamflow changes.

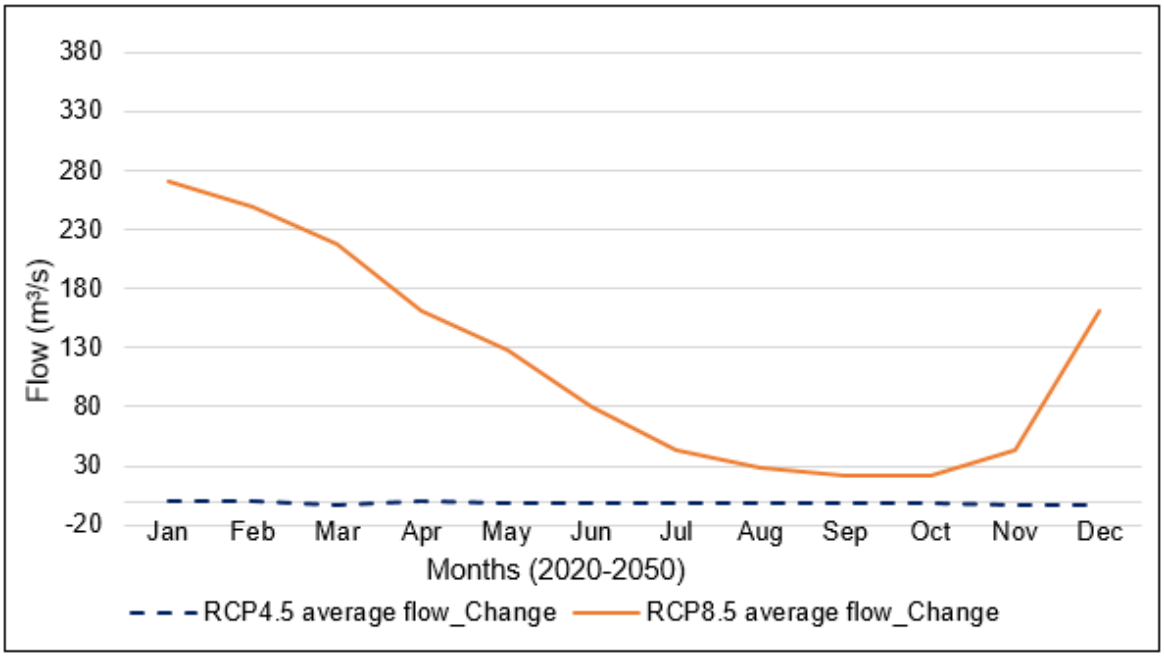

Figure 8.5 Ensemble mean streamflow changes

Figure 8.5 ilustrates the highest increase in streamflow of 270m^3/s under RCP8.5, which is much higher than the ensemble mean under RCP4.5. The increase in streamflow occurs in January while the lowest increase of 22m^3/s occurs in September and October and a sharp rise in increase starts from November to January. Another prediction is in flow regime where the peak flow is shown in January and recedes gently until September before rising again in November.

Meanwhile, the ensemble mean under RCP4.5 predicts no change in streamflow with the baseline period.

8.3.3 Seasonal Flow Analysis

The KRB experiences four seasons, namely December, January and February (DJF) the typical rain season, March, April and May (MAM) is autumn, June, July and August (JJA) is winter season and September, October and November (SON) the summer season. Streamflow varies depending on the season. DJF and MAM are also known as the wet seasons, while JJA and SON are known as the dry season. Future streamflow from GCM ensemble means was analysed based on the aforementioned seasons and the monthly future streamflow. A change factor was applied to the monthly streamflow and aggregated to seasonal streamflow. Figure 8.6 shows the seasonal comparisons between baseline, RCP4.5 and RCP8.5 streamflow and the changes per season.

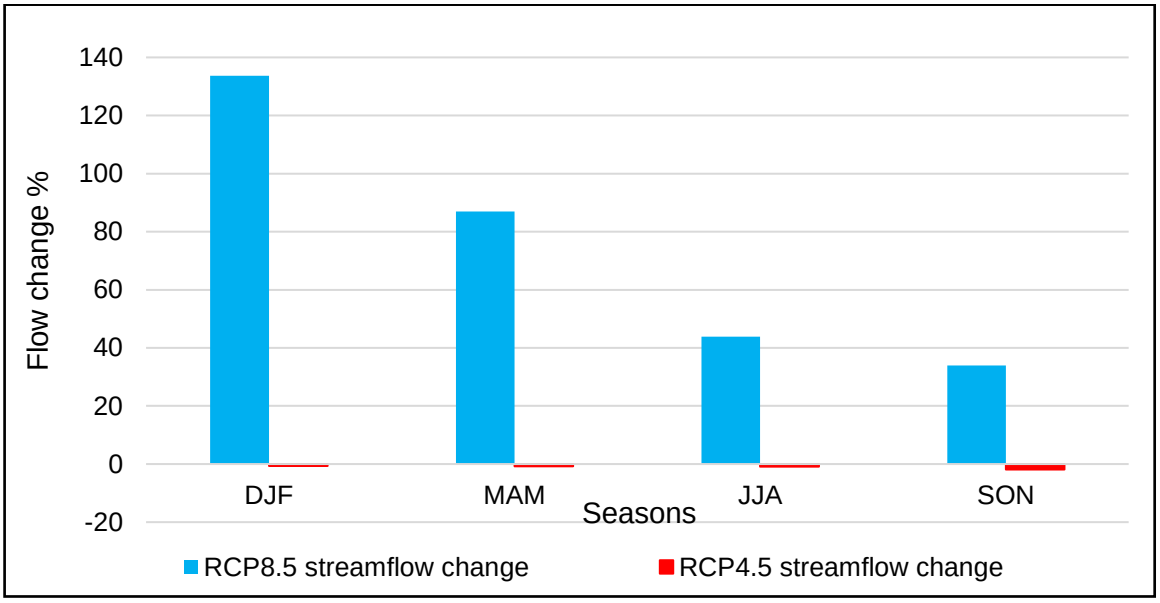

Figure 8.6 Comparisons of change in seasonal future streamflow

The seasonal streamflow in Figure 8.6 shows that under RCP4.5 streamflow will be reduced by -0.6% in DJF, -0.7% in MAM, -0.9% in JJA and -1.9% in SON. The seasonal streamflow will be slightly less than the baseline flow because all the seasons have been predicted with a negative magnitude; the highest occurrence in SON at -2% reduction. Therefore, the reduction in seasonal streamflow will need planning and management.

However, seasonal streamflow under RCP8.5 is apparently high for all the seasons, creating a huge change with baseline and RCP4.5 streamflow. The highest seasonal streamflow change in Figure 8.6 is predicted at 134% occurring in DJF, which is followed by 87% occurring in MAM. Thereafter 44% is predicted in JJA while the lowest predicted is 34% occurring in SON. This implies that DJF and MAM may experience excessive streamflows, while JJA that is a dry season may have a higher magnitude of streamflow constituting mostly base flow. SON may have streamflow, which will be predominately base flow because it is a dry season. All the percentage calculations are based on baseline data.

8.3.4 Intra-Annual Flow Analysis

The monthly streamflow simulated based on the six GCMs were plotted in Figure 8.7. The intra-annual variability shows a uniform pattern of streamflow indicating a significant correlation efficiency.

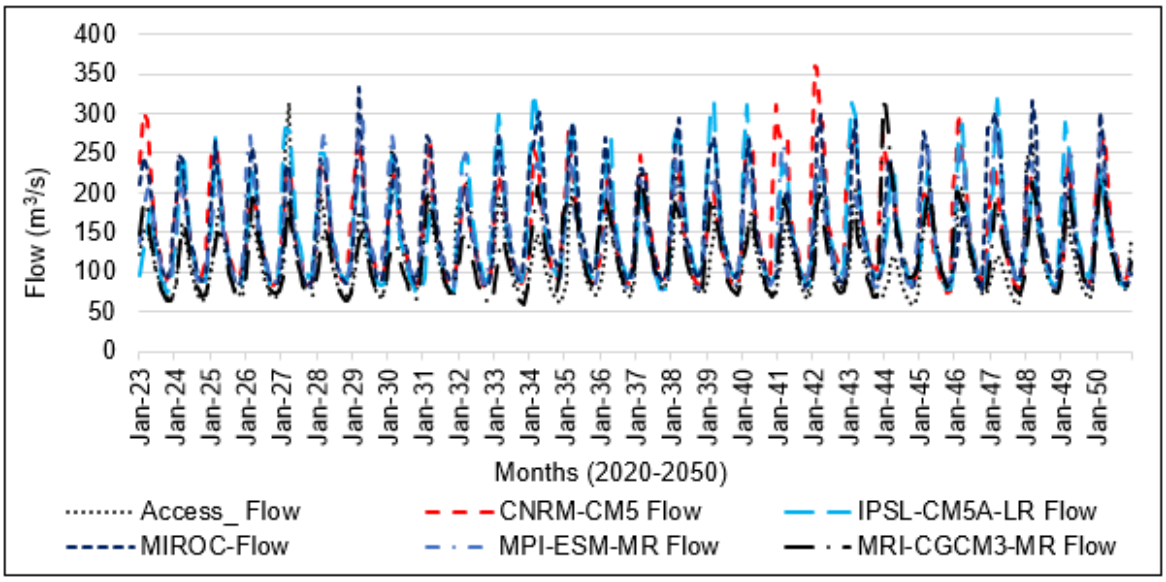

Figure 8.7 Intra-annual streamflow simulations based on six GCMs under RCP4.5

The monthly streamflow simulated based on RCP8.5 have significant differences between Access1-0 and the other five GCMs. Figure 8.8 shows the monthly streamflow from the six GCMs.

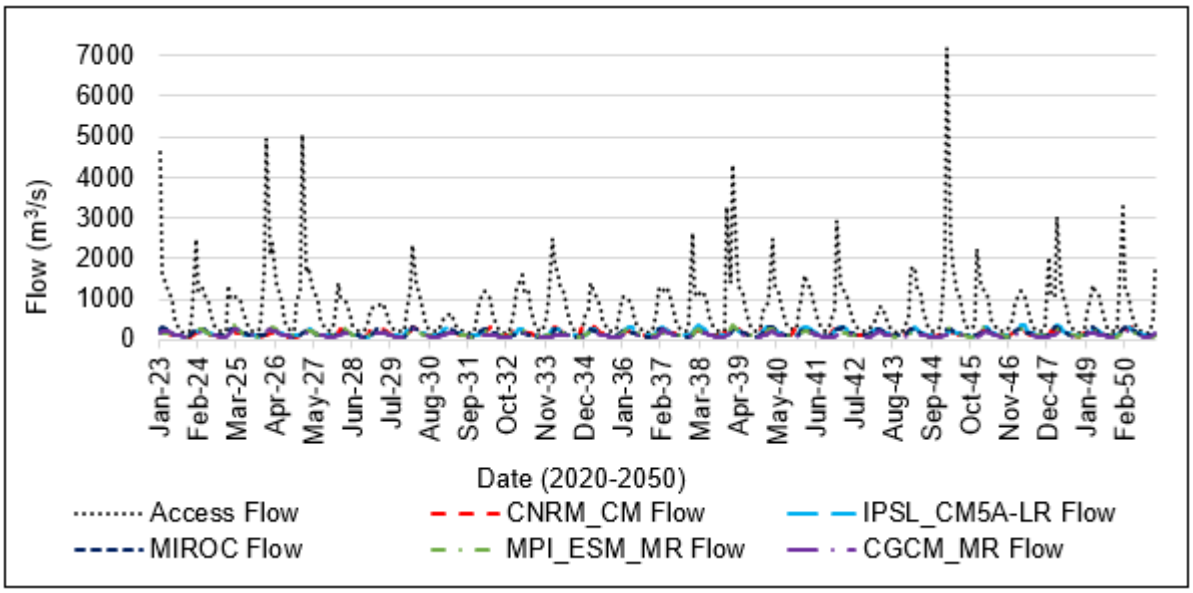

Figure 8.8 Monthly streamflow for six GCMs under RCP8.5

The simulated streamflow in Figure 8.8 shows that Access1-0 monthly streamflow is much higher than the majority, suggesting uncertainty and confirming that different

GCMs respond to external forcings differently. The simulations from the majority GCMs is similar and provides a uniform pattern throughout the projection period. The simulated monthly flows were aggregated to ensemble mean annual flows to analyse the annual variability. The result is shown in Figure 8.9.

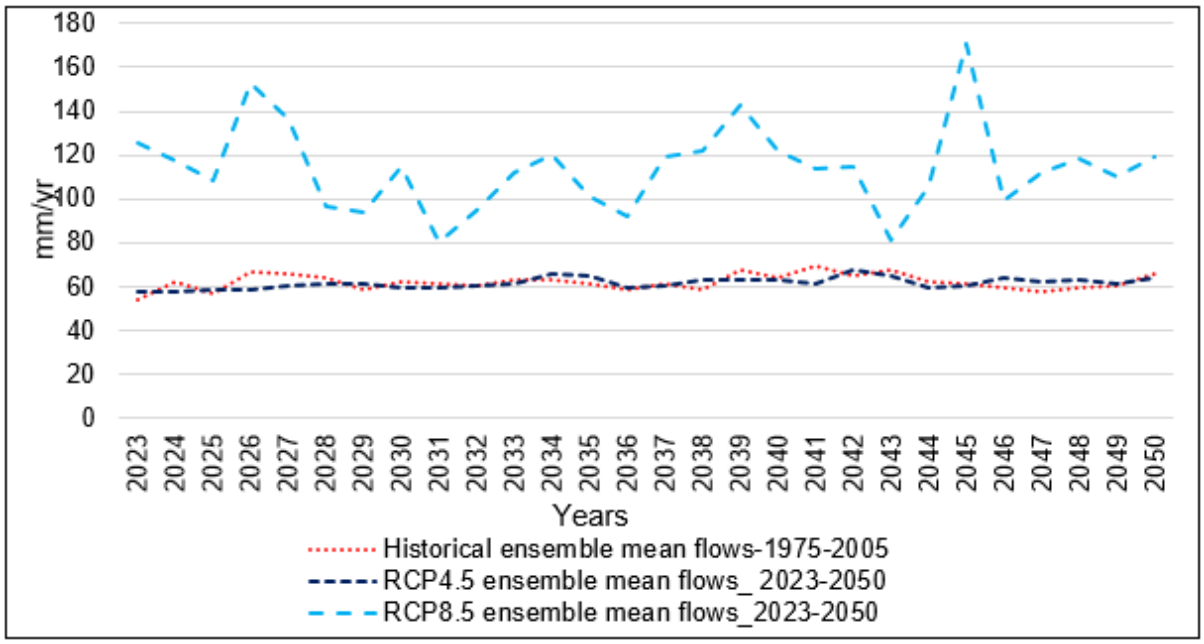

Figure 8.9 Ensemble mean annual flows

The ensemble mean annual flows are predicted to be higher under RCP8.5 than the ensemble means under RCP4.5 and baseline. Figure 8.9 shows that annual flows under RCP4.5 and baseline have insignificant differences in magnitude and regime. The ensemble mean annual streamflow under RCP8.5 predict an annual increase of 85% while the ensemble mean annual streamflow under RCP4.5 predicts no annual change with baseline streamflow.

8.3.5 Intra-Annual and Inter-Annual Streamflow Variability

Intra-annual variability of baseline streamflow predicted streamflow under RCP4.5 and RCP8.5 were determined for each GCM to determine the spread about the mean, which was quantified as the coefficient of variation (VC). While the inter-

annual variability was quantified as the CV; the mean of CVs for all GCMs. The averaged intra-annual variability under RCP4.5 is 0.397, which is lower than 0.399 of the six estimates of the intra-annual variability under baseline. Similarly, the averaged inter-annual variability under RCP4.5 is 0.112, which is also lower than 0.136 of the six estimates of the inter-annual variability under baseline. In addition, all the CVs, under RCP8.5 scenario, are lower than the CV under baseline scenario. Therefore, the majority of simulations indicate that intra-annual and inter-annual streamflow variability will decrease in the future under RCP4.5.

The averaged intra-annual variability under RCP8.5 is 0.510, which is higher than 0.399 of the six estimates of the intra-annual variability under the baseline. Similarly, the averaged inter-annual variability under RCP8.5 is 0.161, which is also higher than 0.136 of the six estimates of the inter-annual variability under baseline. Also, the majority of the CVs, under RCP8.5 scenario, are higher than the CVs under baseline scenario, except the CVs for MRI-CGCM3-MR. The estimated coefficient of variation for each GCM is listed on Appendix O,Table O1.

The majority of simulations indicate that intra-annual and inter-annual streamflow variability will increase in the future under RCP8.5 by a considerable margin. A graphical comparison of coefficient of variation for each GCM based on the climate scenario was made and revealed that both inter-annual and Intra-annual CVs were higher under RCP8.5 than the baseline and RCP4.5. Further information on simulated streamflow based on six GCM are listed on Appendix M,Table M1,M2,M3,M4,M5 and M6.

Figure 8.10 shows the comparison of CVs for the six GCMs.

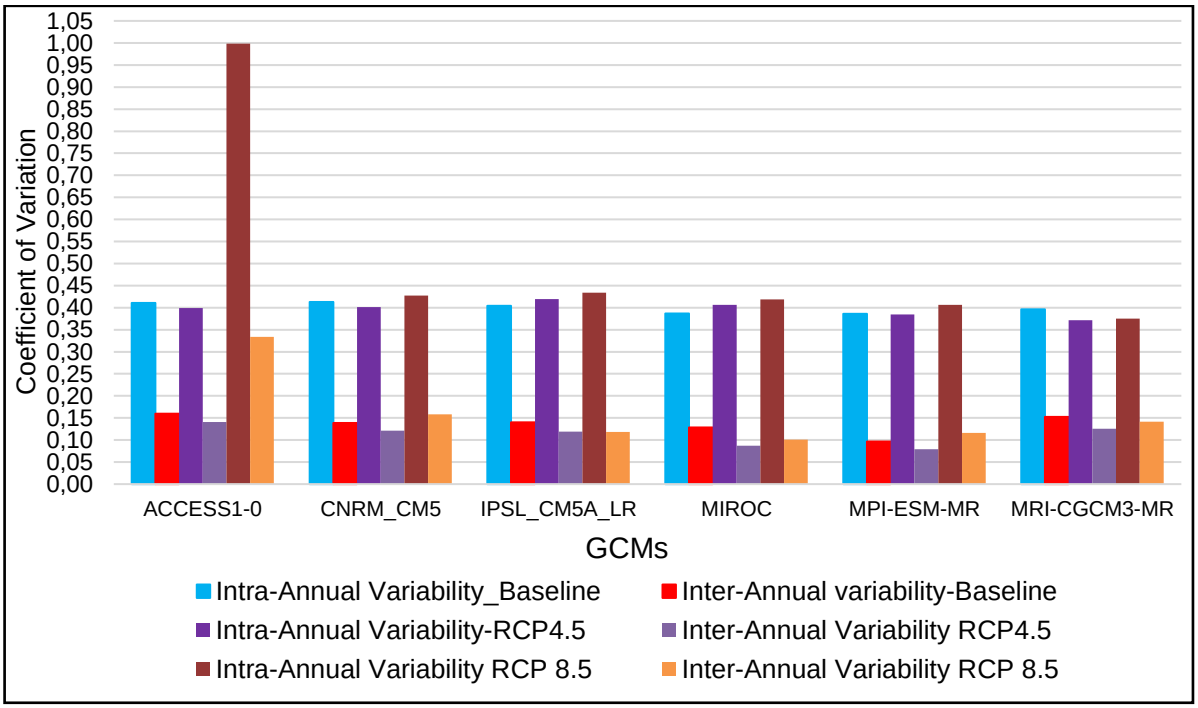

Figure 8.10 comparisons of CVs

Further analysis showed that the means of CVs based on climate scenario was still higher under RCP8.5 than both RCP4.5 and baseline. Table 8.1 shows the CV means.

Table 8.1 Mean CVs based on six GCMs

Climate	Mean (CV)	Mean (CV)
Baseline	0.399	0.136
RCP4.5	0.397	0.112
RCP8.5	0.510	0.161

The annual streamflow is significant and has been confirmed with the intra-annual and inter-annual variability of streamflow to increase under RCP8.5. Therefore, further analysis to determine the magnitude and frequency of its occurrence on a

monthly, seasonal and yearly basis is required and will be discussed in the next section.

8.3.6 Analysis of Flood Frequency in a changing Climate

A standard procedure for future flood frequency analysis has not yet been established and, therefore, it is a matter of research (Quintero et al. 2018). Two periods were used in the analysis to compare and determine the changes. The comparisons under future and baseline periods were considered with the assumptions of stationarity conditions for the two periods. This was due to the insignificant changes in climate variables for baseline and RCP4.5 for the period 2020-2050.

Annual maximum series (AMS) of peak discharges were selected for the baseline period (1975-2005) and future annual peak flows under RCP8.5 (2020-2050) for each GCM. Flood frequency analysis was performed on two different periods in order to quantify changes in frequency of occurrence and the magnitude of the peak discharges and their return period (Millington et al. 2011). The AMS data were further subjected to statistical analysis to estimate parameter values such as the location, dispersion (scale) and shape in order to determine the appropriate probability distribution to be applied.

In addition to the consideration of the choice of a distribution, the method of parameter estimation was also analysed to ensure reasonable, accurate results. Parameter estimation was determined through Method of Moments (MM), which is widely used in hydrology while Log Normal (LN) and Log Pearson type III (LP3) were found suitable probability distributions for flood frequency analysis.

All the GCMs simulated streamflow were analysed for flood frequency individually using the frequency factor method (Chow, 2007) and is applicable to many probability distributions used in hydrological frequency analysis. The predicted peak streamflow based on Access 1-0 under the RCP8.5 have clearly shown a shift of the frequency and an increase in peak streamflow in the future increasing the potential severity of flooding. Figure 8.11 shows the comparative results of the analysis for the future and baseline periods.

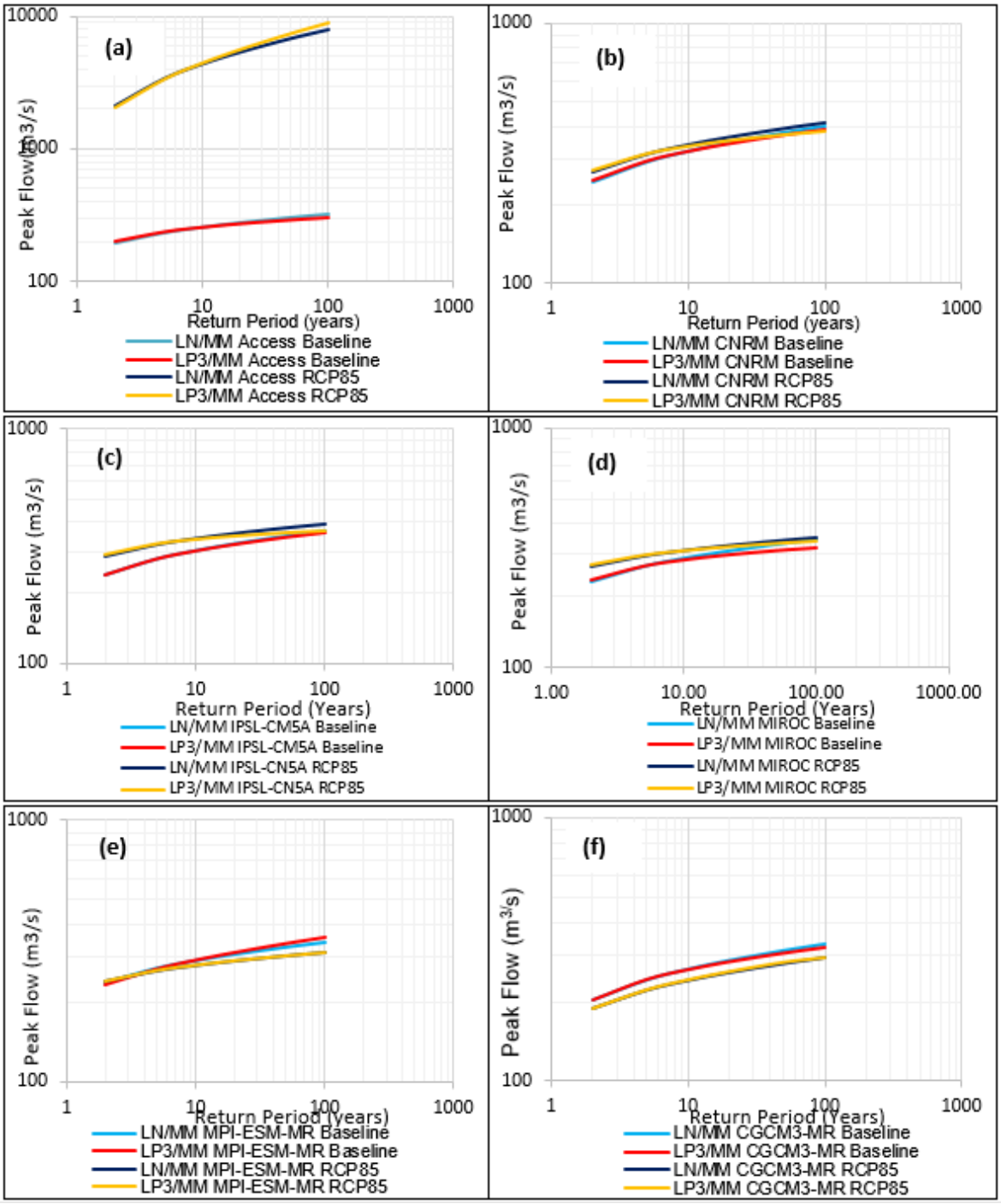

Figure 8.11 Comparisons of flood frequency curves for two periods

Figure 8.11 (a) shows the probability distribution based on Access1-0, which indicates an increase of 97% and 96% in future peak floods with a return period of 50 years under LP3/MM and LN/MM, respectively. Figure 8.11 (b) shows the probability distribution based on CNRM-CM, which indicates no increase under

LP3/MM, while under LN/MM shows an increase of 4% for the future peak floods. Figure 8.11 (c) shows the probability distribution based on IPSL-CM5A-LR, which indicates a 4% and 8% increase under LP3/MM and LN/MM, respectively for the future peak floods.

Figure 8.11 (d) shows probability distribution based on MIROC Probability distribution, which indicates a 7% and 4% increase under LP3/MM and LN/MM, respectively for the future peak floods. Figure 8.11 (e) shows the probability distribution based on MPI-ESM-MR with a 12% and 9% decrease under LP3/MM and LN/MM, respectively for the future floods. Figure 8.11 (f) shows probability distribution based on CGCM3-MR with an 8% and 11% decrease under LP3/MM and LN/MM, respectively for the future peak floods. The percentages were calculated based on the future period with a return period of 50 years.

The probability distributions predicted under Access1-0 generally show severe future peak flood while the majority GCMs predict an increase of 4-8% magnitude of flood with a return period of 50 years. There is also a generally low magnitude of floods predicted with some insignificant variation in frequencies at 2, 5 and 20 return periods among the majority GCMs. However, the flood frequency at 50 and 100 year return periods show some considerable variations in the magnitudes for all the GCMs. This could be attributed to the uncertainties in GCMs and the assumptions in flood frequency analysis. The ranked simulated streamflow for six GCMs is listed on Appendix N,Table N1.

The magnitude of an extreme event is related to its frequency of occurrence. The bigger the magnitude, the longer the frequency of occurrence. The estimated flood frequencies confirm the concept as all peak flows also have higher return periods. The longest return period calculated from the data can only be double the period of the length of the baseline data, therefore, the data under analysis could only be used to estimate peak discharge with return periods not exceeding 60 years as the projected period is 2020-2050.

However, 60 years can only be well extrapolated when the calculation includes 100 years to project the return periods. It is not enough to only estimate the flood magnitude with its frequency of occurrence but also analyse the streamflow regime with percentages of flow being equalled or exceeded. Therefore, further analysis was performed with flow duration curves.

8.3.7 Variability of streamflow under Flow Duration Curves

The streamflow variation for the KRB was further analysed with Flow Duration Curves (FDC) that was calculated to show how flow is distributed over a period of 30 years. FDC shows the relationship between magnitude of streamflow and its frequency of daily, weekly, monthly streamflow or an interval for a particular river basin (Vogel & Fennessey, 1996; Searcy, 1969).

Six-member simulated ensemble monthly streamflow was analysed under baseline, RCP4.5 and RCP8.5 climate scenarios. The ensemble monthly streamflow was analysed for FDC in order to determine the basin characteristics under various climate scenarios as projected by the GCMs. Figure 8.12 indicates the baseline FDCs for all the GCM ensemble streamflow with the calculated average ensemble.

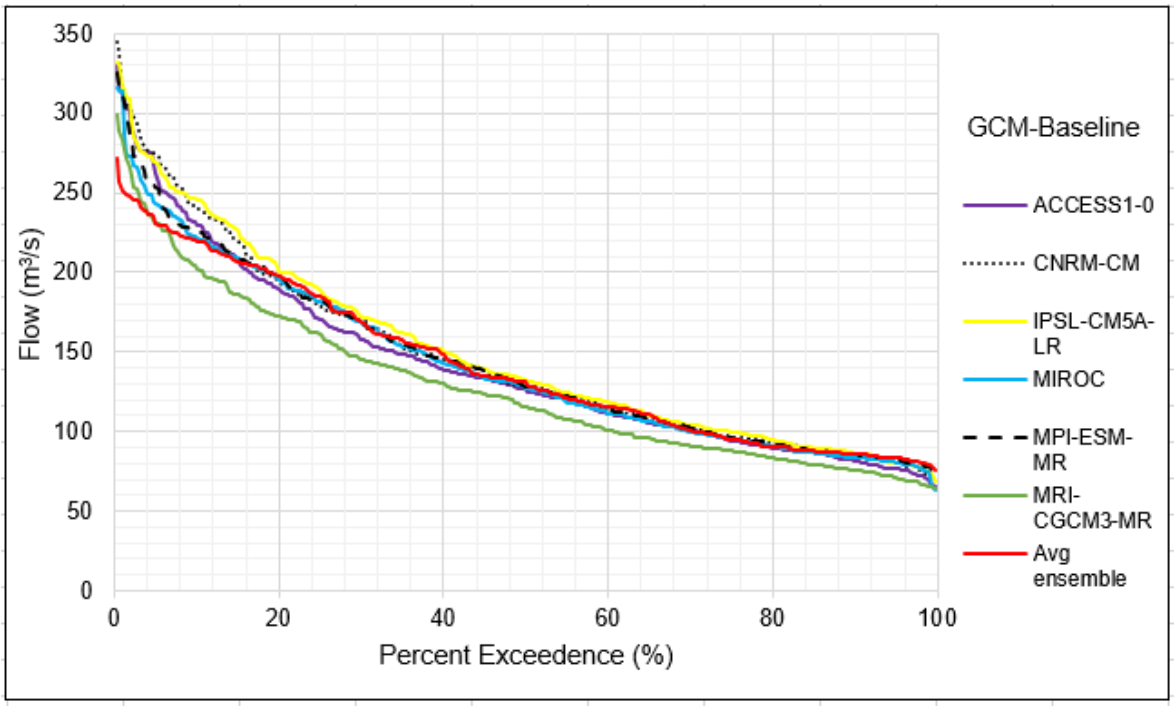

Figure 8.12 Flow duration curves for ensemble streamflow under baseline period

Figure 8.12 shows the simulated ensemble FDCs plotted for the baseline period with the average ensemble. There is minor variation between the average ensemble and the GCM streamflow. All the curves exhibit gentle slopes characterising the basin to have a significant contribution of base flow (spring sources of water) and with the capacity to sustain the low flows throughout the year.

The steep slope of the curves for Q10 characterise the flood regime of the basin, which is perhaps precipitated by rainfall. However, the high flows, Q10, are characterised by a steep slope, while the low flows, Q70, are characterised by flat curves. The lowest flow that is equalled or exceeded at 100% time is 66m3/s, which is available throughout the year. This is also known as Q100. The flow between Q0 and Q10 are considered as high flows that are only available for a small proportion of time in a year, while flows between Q10 and Q70 are medium-range flows. Flows

from Q70 to Q100 are the low flows that are available most of the times. Moving further to the right of the graph, flows from Q95 to Q100 are also considered as drought flows. The FDC analysis was extended to monthly ensemble streamflow under RCP4.5 with the calculated average ensemble. Figure 8.13 shows the ensemble streamflows with its calculated average based on RCP 4.5.

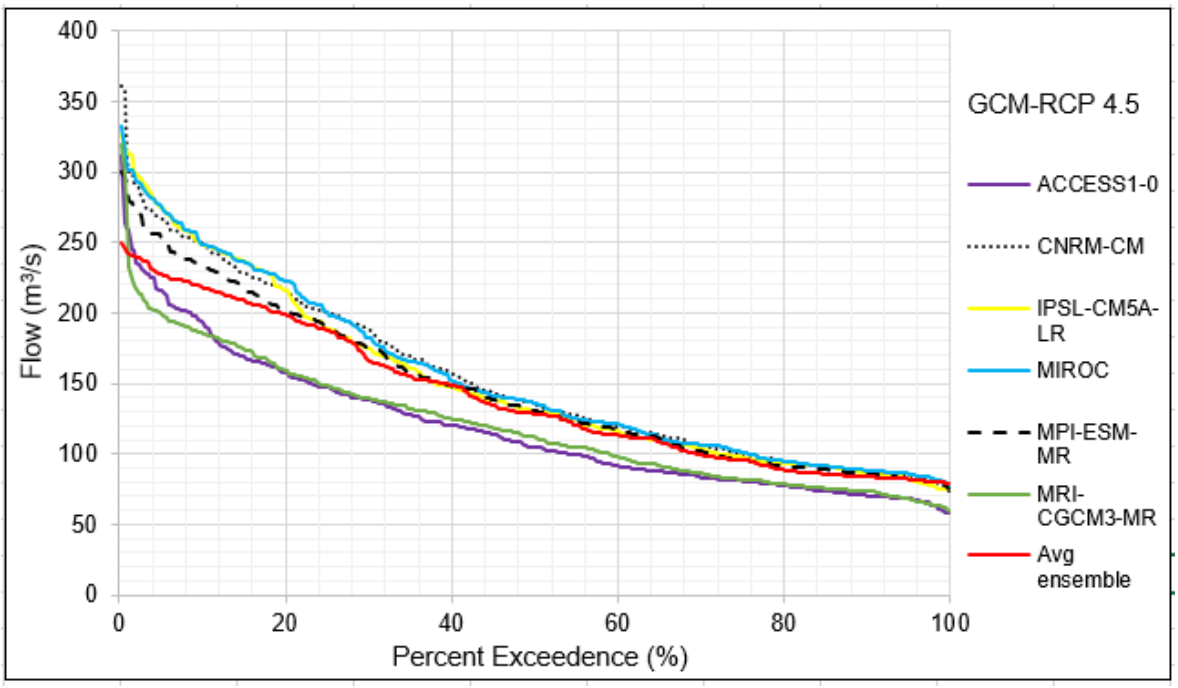

Figure 8.13 Flow duration curves for ensemble streamflow under RCP45

Figure 8.13 shows ensemble streamflow with its average under RCP 4.5 which does not significantly differ from ensemble stream under baseline in Figure 8.12. The FDCs in Figure 8.13 have the slopes and trend that are considerably gentle, reflecting the same basin characteristics as shown in Figure 8.12. The high flows are represented by Q0 to Q4 where there is a steep slope indicating flood regime. The flow may only be available for a very short time in the year reducing the probability of flooding. Flows between Q4 and Q60 are medium-range, while low flows occur between Q60 and Q100. In general, the basin will have more low flows

under this climate scenario with less likelihood of floods. There is a high probability that low flows may result in drought flows.

Further analysis of simulated ensemble FDC and the calculated average was performed under RCP 8.5 scenario. Figure 8.14 shows the ensemble FDC with its calculated average based on RCP 4.8.

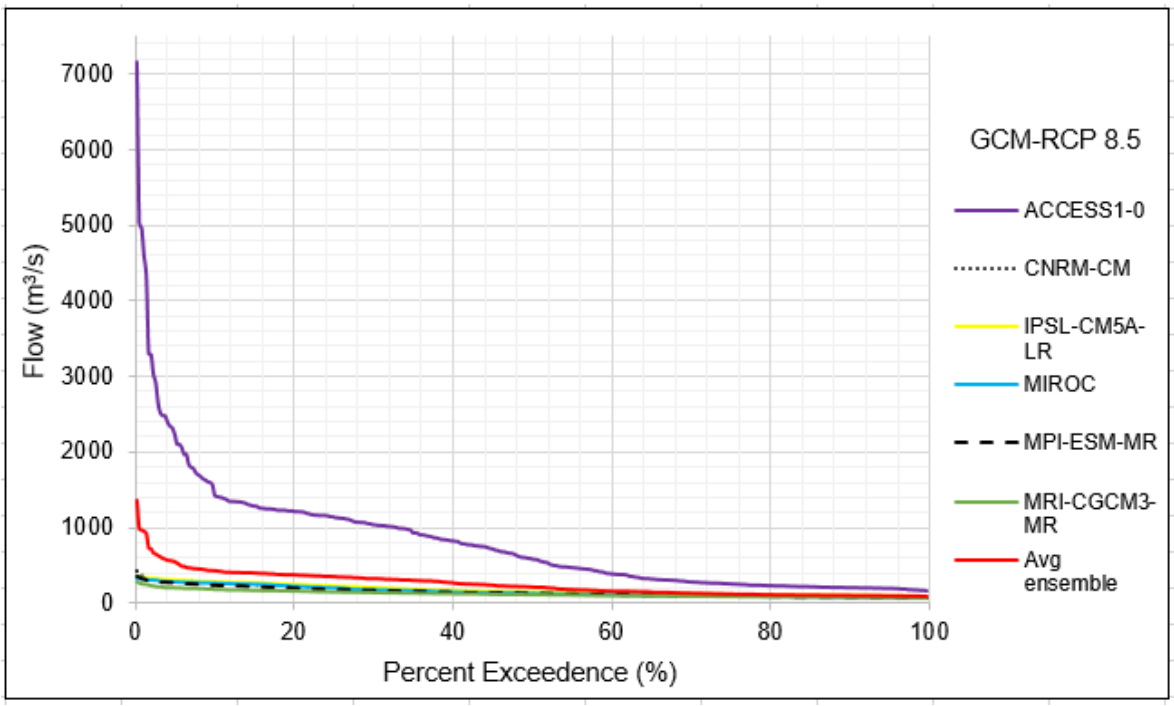

Figure 8.14 Flow duration curves for ensemble streamflow under RCP8.5

Figure 8.14 show a simulated ensemble FDC with its average under RCP8.5 that has wide differences between Access1-0 and the other five GCMs showing no consensus. The variation between the average ensemble and individual FDC is considerable. The FDC analysed from Access1-0 simulated streamflow can be divided into very steep slope, gentler slope and very flat slopes.

The Q0 to Q10 is a very steep slope indicating the flood regime and is considered a high flow section, which could last for 10% of the time in a year. The slope indicates

the possibility of serious floods with Q4 flows considered as severe floods. The medium-range flows are between Q10 and Q70, which has a gentler slope while low flows are between Q70 and Q100 where the slope is very flat. The basin is predicted to experience severe floods under this climate scenario that may require comprehensive preparedness.

The majority of GCMs have consensus and are generally flat slopes and not different from the climate scenario under RCP4.5. There is no likelihood of floods even for flows between Q0 and Q4. The two responses (From Access1-0 and the five GCMs) are at a variance, therefore, further analysis was performed between the average ensemble baseline and RCP 8.5 to find the future percentage increase in flows. Figure 8.15 shows the future percentage increase in FDC under RCP 8.5.

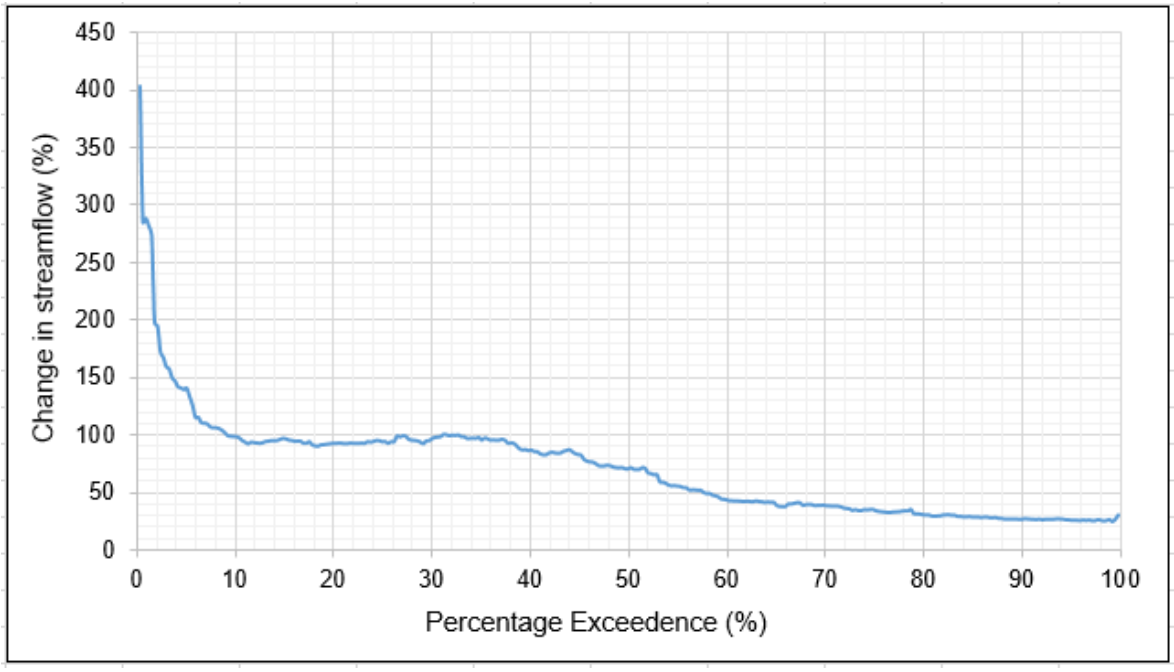

Figure 8.15 FDC for percentage change in average ensemble under RCP8.5

Figure 8.15 refers to the percentage change in average ensemble streamflow under RCP8.5. The three sections in the FDC are still eminent as very steep, gentler and

very flat. There is a very steep slope between Q0 and Q10 which is predicted to increase the basin flows by 100% - 400% for the basin. This may signify high probability of severe floods to occur for about 10% of the time in a year.

The flood regime is most likely to be characterised by high-intensity rainfall. The Q10 to Q70 has a gentle slope, which has medium-range flows expected to increase by 25% - 100% while the Q70 to Q100 is a very flat slope with low flows. The percentage increase in lowest flow is estimated at 25% and is the flow equalled or exceeded throughout the year. The overview result predicts that the basin under this scenario will experience severe floods with an increased magnitude of streamflow throughout the year.

8.4 Conclusion

Evaluation of climate change impact on streamflow is critical for water quantification, streamflow variability and water balancing. The basin under RCP8.5 for the period 2020-2050 climate scenario shows no consensus amongst the ensemble GCMs. However, the majority GCMs (four out of six) indicate 4-8% increase in streamflow predicted in flood frequency analysis with significant changes in monthly, seasonal and annual flow regime and magnitude. The majority of simulations indicate that intra-annual and inter-annual streamflow variability will increase in the future under RCP8.5 by a considerable margin. There is also a significant increase in seasonal streamflow that ranges from 134 - 34% analysed from the simulated ensemble under RCP8.5.

The Flow Duration Curves have also confirmed that the peak flows are between Q0 and Q10 where there is an increase of high flows by 100% - 400%. The predicted flows at Q10 occur for about 10% of the time in a year. Therefore, the high flows (floods) are likely to last for one month and two weeks before subsiding. In addition, the basin has sufficient low flows expected to increase by 25% at Q95 with 95% time of occurrence.

The basin under RCP4.5 for the period 2020-2050 climate scenario is predicted with insignificant changes in monthly, seasonal and annual flow regime and magnitude. The predictions suggest that the magnitude and temporal streamflow variability will not vary from the baseline magnitude and flow regime. Therefore, RCP4.5 future climate scenario does not significantly translate into a changed streamflow for the basin whether simulated as individual GCMs or ensemble mean. The result is almost the same with minor differences. The predicted excessive streamflow under RCP8.5 needs comprehensive planning for adaptation and mitigation strategies, while streamflows predicted under RCP4.5 will require effective management of water resources in the basin. This should be reviewed in order to consider the ever-increasing water demand and other impacts such as water quality, rainfall intensity not investigated under this study.

Future studies need to focus on RCP4.5 for the period 2050-2090 and RCP8.5 for the period 2050-2090 in order to assess any possible climate change impact on streamflow that would arise from the scenarios. It is also advisable to increase the number of GCMs projections to find a better consensus in uncertainty.

CHAPTER 9 : CONCLUSION AND RECOMMENDATIONS

9.1 Introduction

The status of the water resources availability and its linkage to climate variability revealed that there was paucity of hydro-meteorological data, a high occurrence of floods and droughts, uneven distribution of water resources across the basin and increasing temperatures across the ZRB altering the hydrology and water resources of the KRB. Climate change in the basin becomes an enormous additional pressure on water resources. The challenges called for immediate interventions to contribute to finding a lasting solution.

In a bid to address the situation, the research undertaken focused on finding solutions, which were based on the KRB to determine their appropriateness for the local conditions. The major research findings to the challenges in the KRB and the ZRB include:

- The use of gridded climate data (CFSR) in data-scarce Southern Africa to become an alternative to the traditional ground observed data from hydrometeorological stations.
- Generation of high-resolution climate scenarios for quantification of impact across the KRB identified areas for immediate interventions.
- Assessment of current and future water balance to facilitate the planning of water resources under climate change which has begun to impact the KRB.
- Evaluation of streamflow in the basin for analysis of hydrological flow regime under the current and future scenarios and enhance IWRM.

The detailed research findings are elaborated on in the following sections.

9.2 Hydrological Modelling with Alternative Technology.

The SADC countries in the Southern African region similar to many developing countries have challenges of paucity of hydro-meteorological data making it difficult to effectively assess water resources with high accuracy. Alternatives and other options were, therefore, explored in the research and alternative technology was applied with gridded climate data (CFSR) that proved to be reliable and perhaps recommended alternative in data-scarce regions. The quantitative statistics showed that the alternative technology results were good and may be used in catchments with similar characteristics.During the research, it was noted that automatic calibration and validation with SWAT-CUP SUFI-2 was effective and efficient as it was less time-consuming in producing optimum calibrated parameters. The Southern African region has particularly been a data-scarce region, which has hampered research on a large scale, but with the use of alternative technology, water resources would be well assessed and effective water resources management can be envisaged.

The assessment of water resources using alternative technology in the KRB showed that spatial distribution of water yield has uneven distribution with some areas of the basin appearing to be under water stress. Other areas have excess water, which tends to flow out of the basin due to underutilisation and limited water conservation structures. The estimated water resources provide an insight into the water balance of the basin where various water demands from different water use sectors can be assessed. The mean annual water yield ranges from 362mm to 1011mm across the

basin and forms part of the green water that can be used to enhance agricultural productivity in order to improve the livelihood and reduce the poverty levels of the people in the communities. The KRB was assessed with a good potential for harnessing water resources where more than half of the generated runoff appears to leave the basin unutilised.

9.3 PRECIS Evaluation of Climate Change Impacts

The PRECIS (RCM) model proved reliable as most of the results obtained were found to be credible after the validation process that was done with the CRU observed data. The PRECIS is a sufficient model skill to suitably apply with confidence in modelling future climate scenarios.

The prediction of future rainfall under RCP4.5 for the period 2020-2050 scenario indicates that rainfall will increase with a coverage area varying from 33% to 77% with a magnitude of 0 < 65% while coverage areas with a decrease in rainfall will vary from 23% to 67% with magnitudes of -25% < 0 in the four seasons of the KRB. Although much of KRB will be under increased rainfall and less will be under decreased rainfall, the annual rainfall does not significantly differ from the baseline period. There is a general rise in temperature for all seasons varying from 1.4 ^{o}C to 2.5 ^{o}C across the KRB and the season of SON is predicted to have the highest temperatures.

The PRECIS model predicts that rainfall under RCP8.5 for the period 2020-2050 is likely to significantly increase in magnitude and coverage area in the season of DJF. The general rise in rainfall is predicted to increase by coverage area varying from

49% to 58% and the magnitude varying from 0% to 37%. The coverage area under decreased rainfall will vary from 51% to 42% and the magnitude varying from 0% to -18%. The increase of rainfall in DJF may cause flooding in the flood-prone areas and thus adaptation and mitigation strategies may be required. Further results under the same scenario also show increased temperatures ranging from 1.6ºC to 2.4ºC across the KRB. It was, however, noticed that model biases were apparent at validation for DJF and MAM seasons and monthly comparisons that will in future need bias-correction especially if required for hydrological modelling.

In general, the PRECIS model predicts an increase in rainfall and temperature in selected areas while predicting a decrease in other areas within the same basin under both RCP4.5 and RCP8.5 climate scenarios. Even though the increases are predicted under RCP4.5, the annual rainfall will insignificantly change from the baseline period. The increase and decrease in precipitation and temperature predicted are in both magnitude and coverage areas of the basin. Further investigations may be required for detailed and accurate quantification of the increase and decrease of the climatic variables

Furthermore, a single RCM would not represent the local region well because of the uncertainties that exist in the GCM, downscaling and the hydrological model. Future studies need to include the use of more regional climate models for downscaling a more comprehensive set of HadCM3-based future scenarios in order to create an ensemble for prediction and detailed accurate quantification of impact.

9.4 Evaluation of Impact of Climate Change on Water Balance

The impact of climate change on the catchment water balance based on GCMs is different and depends on temporal resolution and the climate scenarios. The monthly changes under RCP4.5 indicate a slight increase in monthly rainfall for December, January, February and March while October and November show a significant decrease. The water yield and runoff when compared with a baseline also show a slight increase. The results clearly show that monthly rainfall, water yield and runoff has increased in December, January, February and March while rainfall decreased by 19% and 4% in October and November, respectively. The highest rainfall increase of 3% is predicted in January, followed by 2% in February and December. The highest monthly water yield is predicted to be 10% and 8% in March and January, respectively. The highest and lowest runoff is predicted to be 13% in December and 50% in October. There is a slight increase in water yield between April and September.

The overall changes in the monthly water balance are not significant in this scenario. The monthly changes under RCP8.5 show that the monthly water balance will significantly increase in November, December, January, February and March. Rainfall and runoff will increase between 9% and 39% and 31% and 232%, respectively. Rainfall is expected to decrease in October, September, May and April between 1% and 13%. The highest rainfall increase is 39%, predicted in February, followed by 31% in December and January. A 27% prediction is set for March and 9% predicted in November. The highest monthly water yield and runoff is predicted at 106% and 232% in February, respectively. The lowest decrease in runoff is

predicted in April with 27% while May, June, July, August and September are predicted with no runoff but 23-26% increase in water yield.

The seasonal changes under RCP4.5 predict 11% seasonal runoff increase in DJF, while the changes in the rest of the seasons in rainfall and water yield are generally insignificant throughout the period. The annual rainfall will reduce by 1% while water yield and runoff will increase by 5% and 6%, respectively. The individual GCM results show insignificant uncertainties and a good consensus. The catchment water balance under this scenario will not deviate considerably from the baseline and therefore the major concern would be to enhance management of water resources because of the demand, which is likely to double by the end of the 31 year period for municipal water supply, environmental, industrial, agricultural, energy sector and mining sector. The evaluated impact under this scenario gives a status quo of water resources with the baseline period.

The seasonal changes under RCP8.5 scenario predict significant increases in water balance that has a strong likelihood of increasing the catchment water balance. The seasonal increases of runoff at 211%, rainfall at 35% may indicate an occurrence of excessive catchment water balance. The comparison of seasonal water balance under the two RCPs shows no consensus of the future climate scenarios. The water balance analysed under RCP8.5 is significantly more than that of the RCP4.5. The seasonal rainfall change under RCP8.5 range from 5%-35% while RCP4.5 does not show any significant seasonal changes except for an 8% decrease in SON. The catchment water balance under RCP4.5 will have insignificant variations with the baseline catchment water balance.

Annual statistics under RCP8.5 show a significant increase of 65%, 40% and 19% in runoff, water yield and rainfall, respectively. On the other hand, under RCP4.5 there is an annual reduction in rainfall of 1% and an increase in runoff and water yield of 6% and 5%, respectively. Generally, RCP8.5 climate scenario shows high uncertainties of GCMs simulations than RCP4.5 climate scenario in the KRB. The variability of individual GCMs is also wide and shows no good consensus under RCP8.5, compared to RCP4.5 results.

The six GCMs have demonstrated a rare skill in modelling climate change for the KRB. There is a significant increase under RCP8.5 in the catchment water balance at monthly, seasonal and annual time scales. The prediction may call for preparedness in disaster mitigation and adaptation, review of policies, review of designs of hydraulic structures, flood mapping and awareness campaigns. Meanwhile, under RCP4.5 the evaluated catchment water balance at monthly, seasonal and annual time scales may also require integrated water resources management of available water resources against a growing water demand in the KRB.

9.5 Analysis of Impact of Climate Change on Streamflow

Evaluation of climate change impact on streamflow is critical for water quantification, temporal and spatial variability and water balancing. The basin under RCP4.5 for the period 2020-2050 climate scenario is predicted with insignificant changes in monthly, seasonal and annual flow regime and magnitude. The predictions suggest that the magnitude and temporal streamflow variability will not vary from the baseline

magnitude and flow regime. Therefore, RCP4.5 future climate scenario does not significantly translate into a changed streamflow for the basin whether simulated as individual GCMs or ensemble mean; the result is almost the same with minor differences.

The basin under RCP8.5 climate scenario shows no consensus amongst the ensemble GCMs. However, the majority GCMs (four out of six) indicate a 4-8% increase in streamflow predicted in flood frequency analysis with significant changes in monthly, seasonal and annual flow regime and magnitude. The majority of simulations indicate that intra-annual and inter-annual streamflow variability will increase in the future under RCP8.5 by a considerable margin. There is also a significant increase in seasonal streamflow that ranges between 134 - 34% analysed from the streamflow simulated ensemble mean.

The Flow Duration Curves have also confirmed that the peak flows are between Q0 and Q10 where there a predicted increase of 100% - 400% in high flows. The predicted flows at Q10 occur for about 10% of the time in a year. This means that the high flows (floods) are likely to last for one month and two weeks before subsiding. Also, the basin has sufficient low flows expected to increase by 25% at Q95 with 95% time of occurrence.

9.6 General Research Findings

The analysis of hydrology and water resources under RCP4.5 climate scenario showed that results from PRECIS (RCM) experiments, assessment and evaluation of the impact of climate change on the catchment water balance and streamflow

would insignificantly vary from the historical baseline period. There is agreement of the results that indicate rainfall, water yield, runoff, streamflow to be within the baseline period.

However, the analysis of hydrology and water resources under RCP8.5 climate scenario show that results from PRECIS (RCM) experiments, assessment and evaluation of the impact of climate change on the catchment water balance and streamflow will significantly vary from the (historical) baseline period. There is consensus of the results that indicate a seasonal, monthly and annual increase in rainfall, water yield, runoff, streamflow when compared with the baseline period.

Predicted floods under RCP8.5 need comprehensive planning for adaptation and mitigation strategies while streamflow predicted under RCP4.5 will require effective management of water resources in the basin. This needs to be reviewed and should consider the ever-increasing water demand and other impacts such as water quality, rainfall intensity not investigated under this study.

9.7 Recommendations for Future Research

The future climate change impact studies need to focus on RCP4.5 and RCP8.5 for the period 2050-2090 to assess and evaluate any possible future impact on hydrology and water resources that would arise from the scenarios. It is also advisable to conduct research based on an increased number of GCM projections to find a better consensus in uncertainty.

The PRECIS experiment results need to be bias-corrected and further analysed in detail to be used as input data for hydrological modelling to enable future researchers to derive an in-depth understanding of the local hydrological processes. The results can then be compared with other downscaled, bias-corrected GCMs.

The PRECIS experiments were conducted on a domain area covering almost the entire Zambezi River Basin, with Eswatini and parts of South Africa included. Therefore, much of the Southern African region is included and the data generated for the region is useful for further research in other areas of the region. Group research may be arranged to analyse the future hydrology and water resources of the region.

REFERENCES

Abbaspour, K., Rouholahnejad, E., Vaghefi, S., Srinivasan, R., Yang, H., & Kløve, B. (2015). A continental-scale hydrology and water quality model for Europe : Calibration and uncertainty of a high-resolution large-scale SWAT model. *Journal of Hydrology*,*524*,733–752. https://doi.org/10.1016/j.jhydrol.2015.03.027

Abbaspour, K C, Vaghe, S. A., Yang, H., & Srinivasan, R. (2019). Global soil , landuse , evapotranspiration , historical and future weather databases for SWAT Applications, *Scientific Data* 6, 263:1–11. https://doi.org/10.1038/s41597-019-0282-4

Abbaspour, Karim C, Faramarzi, M., & Rouholahnejad, E. (2010). Hydrological Modeling of Alberta Using Swat Model,*Report* 1–83. https://albertawater.com/docs-work/projects-and-research/dynamics-of-albertas-water-supply/83-hydrological-modeling-of-alberta-using-swat-model-1 (Accessed on 12 March 2019)

Adedeji, O., Reuben, O., & Olatoye, O. (2014). Global Climate Change, *Journal of Geoscience and Environment Protection*,2, (April) 114-122. http://dx.doi.org/10.4236/gep.2014.22016

Akhtar, M., Ahmad, N., & Booij, M. J. (2008). The impact of climate change on the water resources of Hindukush-Karakorum-Himalaya region under different glacier coverage scenarios. *Journal of Hydrology*, *355*(1–4), 148–163. https://doi.org/10.1016/j.jhydrol.2008.03.015

Alias, N. E., & Takara, K. (2012). Probability Distribution for Extreme Hydrological Values-Series in the Yodo Probability Distribution for Extreme Hydrological Values-Series in the Yodo River Basin,*PhD Dissertation*,Civil and Earth Resources Engineering, Kyoto University, Japan.

Amede, T., Desta, L. T., Harris, D., Kizito, F., & Xueliang, C. (2014). The Chinyanja Triangle in the Zambezi River Basin , Southern Africa : Status of , and Prospects for , Agriculture , Natural Resources Management and Rural Development. *IWMI Books, International Water Management Institute, number 208759, November.* DOI: 10.22004/ag.econ.208759.

Anandhi, A., Frei, A., Pierson, D. C., Schneiderman, E. M., Zion, M. S., Lounsbury, D., & Matonse, A. H. (2011a). Examination of change factor methodologies for climate change impact assessment. *Water Resources Research* 47, W03501: 1–10. https://doi.org/10.1029/2010WR009104.

Andréassian, V., Moine, N. Le, Perrin, C., Ramos, M. H., Oudin, L., Lerat, J., … Oudin, L. (2012). HAL Id : hal-00737778 All that glitters is not gold : the case of calibrating hydrological models.*Hydrological processes*,26,2206-2010. https://doi.org/10.1002/hyp.9264

Arnold, J., Moriasi, D. ., Gassman, P. Abbaspour, K. ., White, M. ., Srinivasan, R. Griensven, A. Van. (2012). Swat: Model Use, Calibration, And Validation, *Transactions of the Asabe 55*(4), 1491–1508. American Society of Agricultural and Biological Engineers ISSN 2151-0032.

Baimoung, Oki, Chevarahuprok, Boonlert, Yuttaphan, Aphantree, A., & Manoon. (2014). Bias correction techniques for meteorological data of A2 scenario climate model output in Chao Phraya River Basin of Thailand. *Hydrological Research Letters*, 8 (1):71-76. https://doi.org/10.3178/hrl.8.71

Beck, L., & Bernauer, T. (2011). How will combined changes in water demand and climate affect water availability in the Zambezi river basin? *Global Environmental Change*, *21*(3), 1061–1072. https://doi.org/10.1016/j.gloenvcha.2011.04.001

Builfuss, R and Santos David dos (2001). Patterns Of Hydrological Change In The Zambezi Delta, Mozambique. Working Paper #2 Program for the Sustainable Management of Cahora Bassa Dam and the Lower Zambezi: https://www.researchgate.net/publication/313679710_Patterns_of_Hydrological_Change_in_the_Zambezi_Delta_Mozambique.(accessed on 3 March 2019)

Beilfuss, R. (2012). A Risky Climate for Southern African Hydro. *International Rivers, Berkely*, (September), 1–46. http://climenews.com/letoltes/zambezi_climate_report_final.pdf.(accessed on 15 January 2018).

Bell, J. E., Brown, C. L., Conlon, K., Herring, S., Kunkel, K. E., Lawrimore, J., … Uejio, C. (2018). Changes in extreme events and the potential impacts on human health. *Journal of the Air & Waste Management Association*, *68*(4), 265–287. https://doi.org/10.1080/10962247.2017.1401017.

Bergström, s., Carlsson, B., Gardelin, M., Lindström, G., Petterson, A., & Rummukainen, M. (2001). Climate change impacts on runoff in Sweden - Assessments by global climate models, dynamical downscalling and hydrological modelling. *Climate Research*, *16*(2), 101–112. https://doi.org/10.3354/cr016101

Bergström, S. (2006). Experience from applications of the HBV hydrological model from the perspective of prediction in ungauged basins. *The Swedish Meteorological and Hydrological Institute*, SE-601 76 Norrköping, Sweden *IAHS-AISH Publication*, (307), 97–107. https://iahs.info/uploads/dms/13603.08-97-107-21-BERGSTROM.pdf. Accessed on 12 January 2019)

Botha J. F and Cloot, A. H (2004). Deformations and the Karoo aquifers of South Africa. *Advances in Water Resources, 27*,(4) April, 383–398. https://doi.org/10.1016/j.advwatres.2004.02.014

Bosilovich, M., Akella, S., Coy, L., Cullather, R., Draper, C., Gelaro, R., … Suarez, M. (2015). MERRA-2 : Initial Evaluation of the Climate. *NASA Technical Report Series on Global Modeling and Data Assimilation*, *43*(September), 139. https://doi.org/NASA/TM–2015-104606/Vol. 43

Butts, M., & Graham, D. (2005). Flexible Integrated Watershed Modeling with MIKE SHE. *Watershed Models*, (May 2015), 245–271. https://doi.org/10.1201/9781420037432.ch10

Cain, M., Gilbert, A., Hawkins, E., & Forster, P. (2019). Climate sensitivity : how much warming results from increases in atmospheric carbon dioxide (CO 2)?, 3400. *Royal Meteorological Society.* https://doi.org/10.1002/wea.3400

Callaway, J. M. (2004). Adaptation benefits and costs: how important are they in the Global policy picture and how can We estimate them? *Global Environmental Change, 14*, 273–284.

Casanueva, A., Kotlarski, S., Herrera, S., Fischer, A. M., Kjellstrom, T., & Schwierz, C. (2019). Climate projections of a multivariate heat stress index : the role of downscaling and bias correction. *Geosci. Model Dev.* 12, 3419–3438. https://doi.org/10.5194/gmd-12-3419-20193419–3438.

Cessford, F., & Burke, J. (2005). Inland Water: Background Research Paper produced for the South Africa. *Water Management*, (October), 1–27.

Chen, J., Brissette, F. P., & Leconte, R. (2011). Uncertainty of downscaling method in quantifying the impact of climate change on hydrology. *Journal of Hydrology*, *401*(3–4), 190–202. https://doi.org/10.1016/j.jhydrol.2011.02.020

Chen, S., & Roads, J. O. (1999). Global to regional simulations of California wintertime precipitation,(December). *Journal Of Geophysical Research*, Vol. 104, No. D24, Pages 31,517-31,532 https://doi.org/10.1029/1998JD200043

Chien, H., Yeh, P. J., & Knouft, J. H. (2013). Modeling the potential impacts of climate change on streamflow in agricultural watersheds of the Midwestern United States. *Journal of Hydrology*, *491*, 73–88. https://doi.org/10.1016/j.jhydrol.2013.03.026

Christos, Chalkias, Nikolaos Stathopoulos, K. K. and E. K., & Additional. (2016). Chapter 4. Applied Hydrological Modeling with the Use of Geoinformatics: *Theory and Practice.* http://dx.doi.org/10.5772/62824

Claassen, M. (2013). Integrated Water Resource Management in South Africa. *International Journal of Water Governance*, *1*(3), 323–338. https://doi.org/10.7564/13-IJWG12

Daggupati, P., Yen, H., White, M. J., Srinivasan, R., Arnold, J. G., Keitzer, C. S., & Sowa, S. P. (2015). Impact of model development , calibration and validation decisions on hydrological simulations in West Lake Erie Basin. *Hydrological processes*, Vol 29, (26) 5307-5320. https://doi.org/10.1002/hyp.10536

Davis-Reddy, C. L., & Vincent, K. (2017). *CC Handbook For Southern Africa Climate 2 nd Edition Lead Authors*. https://www.csir.co.za/sites/default/files/Documents/SADC Handbook_Second Edition_full report.pdf. (Accessed on 19 february 2019)

Decker, M., Brunke, M. A., Wang, Z., Sakaguchi, K., Zeng, X., & Bosilovich, M. G. (2012). Evaluation of the reanalysis products from GSFC, NCEP, and ECMWF using flux tower observations. *Journal of Climate*, *25*(6), 1916–1944. https://doi.org/10.1175/JCLI-D-11-00004.1

Desmond, O., Mukolwe, E., William, H., Haleh, K., Kevin, O., Fernandez, B., … Pablo, R. (1997). United nations, International Decade for Natural Disaster Reduction (IDNDR) Early Warning Programme Report on Early Warning for Hydrometeorological Hazards including Drought. May be accessed on the IDNDR web site: http://www.idndr.org

Devia, G. K., Ganasri, B. P., & Dwarakish, G. S. (2015). A Review on Hydrological Models. *Aquatic Procedia*, *4* (Icwrcoe), 1001–1007. https://doi.org/10.1016/j.aqpro.2015.02.126

Dile, Y. T, & Srinivasan, R. (2014). Evaluation of CFSR climate data for hydrologic prediction in data-scarce watersheds: An application in the blue nile river basin. *Journal of the American Water Resources Association*, *50* (5). https://doi.org/10.1111/jawr.12182

Dingman, L.. *Chapter1-2,*Introduction To Hydrological Science & Basic Hydrologic Concepts. In *Physical Hyrology.* 2nd ed. Upper Saddle River, N.J. : Prentice Hall, New Jersey,USA.2002, pp 646

Djebou C., D. S., & Singh, V. P. (2017). Impact of climate change on the hydrologic cycle and implications for society. *Environment and Social Psychology*, *1*(1). https://doi.org/10.18063/esp.2016.01.002

Dosio, A., & Jürgen, H. (2016). Climate change projections for CORDEX - Africa with COSMO - CLM regional climate model and differences with the driving global climate models. *Climate Dynamics*, *46* (5), 1599–1625. https://doi.org/10.1007/s00382-015-2664-4

Euroconsult Mott MacDonald (2008).Integrated Water Resources Zambezi River Basin Implementation Plan for the Management Strategy and SADC-WD/. http://www.zambezicommission.org/sites/default/files/clusters_pdfs/Zambezi%20River_Basin_IWRM_Strategy_ZAMSTRAT.pdf.(Accessed on 10 April 2018)

Farmer, W. & Richard, V. (2016). On the deterministic and stochastic use of hydrologic models. *Water Resour. Res.*, 52, 1–15. https://doi.org/10.1002/2016WR019129.

Farzan, K., Wang, G., Silander, J., Wilson, A. M., Allen, J. M., Horton, R., & Anyah, R. (2013). Statistical downscaling and bias correction of climate model outputs for climate change impact assessment in the U . S . northeast. *Global and Planetary Change, 100, 320–332.* https://doi.org/10.1016/j.gloplacha.2012.11.003

Fatichi, S., Vivoni, E., Fatichi, S., Vivoni, E. R., Ogden, F. L., Ivanov, V. Y., … Tarboton, D. (2016). An overview of current applications , challenges , and future trends in distributed process-based models in hydrology An overview of current applications , challenges , and future trends in distributed process-

based models in hydrology. *Journal Of Hydrology*, *537* (March), 45–60. https://doi.org/10.1016/j.jhydrol.2016.03.026

Feigenwinter I, Kotlarski S, Casanueva A, Fischer AM, Schwierz C, Liniger MA, (2018): Exploring quantile mapping as a tool to produce user-tailored climate scenarios for Switzerland.*Technical Report MeteoSwiss*, 270, 44 pp.

Fekete, B. M., Vörösmarty, C. J., & Grabs, W. (2002). High-resolution fields of global runoff combining observed river discharge and simulated water balances. *Global Biogeochemical Cycles, 16(3), 15-1-15–10*. https://doi.org/10.1029/1999gb001254

Ferrise, R., Moriondo, M., & Bindi, M. (2011). Probabilistic assessments of climate change impacts on durum wheat in the Mediterranean region.*Nat. Hazards Earth Syst. Sci.*11,1293–1302. https://doi.org/10.5194/nhess-11-1293-2011

Flato, G., Marotzke, J., Abiodun, B., Braconnot, P., Chou, S. C., Collins, W., … Rummukainen, M. (2013). IPCC AR5. WG1. Chap. 9. Evaluation of Climate Models. *Climate Change 2013: The Physical Science Basis. Contribution of Working Group I to the Fifth Assessment Report of the Intergovernmental Panel on Climate Change*, 741–866. https://doi.org/10.1017/CBO9781107415324

Fowler, H. J., Blenkinsop, S., & Tebaldi, C. (2007). Review Linking climate change modelling to impacts studies: recent advances in downscaling techniques for hydrological modelling. *Int. J. Climatol.* 27:(September)1547–1578. https://doi.org/10.1002/joc

Fuka, D. R., Walter, M. T., Macalister, C., Degaetano, A. T., Steenhuis, T. S., & Easton, Z. M. (2014). Using the Climate Forecast System Reanalysis as weather input data for watershed models. *Hydrological Processes*, *28* (22), 5613–5623. https://doi.org/10.1002/hyp.10073

Ganamala Kalpalatha and P. Sundar Kumar (2017). A Case Study on Flood Frequency Analysis, *International Journal of Civil Engineering and Technology*, 8(4), 2017, pp. 1762-1767.

Gao, H., Tang, Q., Shi, X., Zhu, C., & Bohn, T. (2010). Chapter 6, Water budget record from Variable Infiltration Capacity (VIC) model. *Algorithm Theoretical Basis Document for Terrestrial Water Cycle Data Records*, (Vic), 120–173. Retrieved from.http://scholar.google.com/scholar?hl=en&btnG=Search&q=intitle:Water+

Budget+Record+from+Variable+Infiltration+Capacity+(+VIC+)+Model#2

Gassman, P. P. W., Reyes, M. M. R., Green, C. C. H., & Arnold, J. J. G. (2007). The Soil and Water Assessment Tool : historical development, applications, and future research directions. *Transactions of the ASAE*, *50*(4), 1211–1250. https://doi.org/10.1.1.88.6554.

Gettelman, A and Rood, R. B. (2016a)*Book Chapter 4,Essence of a Climate Model*. Demistifying Climate Models, Earth Systems Data and Models, Bernd Blasius, Carl von Ossietzky, William Lahoz, *Kjeller,* Dimitri P. Solomatine,*Ed. UNESCO—IHE Institute for Water Education,* Springer, *Delft, The Netherland.* 2016**.**Volume 2, pp 37-57**.**

Gettelman, A., & Rood, R. B. (2016b). Demystifying Climate Models. *Earth Systems Data and Models*,2, DOI 10.1007/978-3-662-48959-8271

Giorgi, F.; Hewitson, B.; Arritt, R.; Gutowski, W.; Knutson, T.; Landsea, C.; and et al. 2001."Regional Climate Information—Evaluation and Projections". Geological and Atmospheric Sciences Publications. ed. J. T. Houghton, Y. Ding, D. J. Griggs, M. Noguer, P. J. vad der Linden, X. Dai, K. Maskell, C. A. Johnson. Cambridge: Cambridge University Press, administrator of Iowa State University Digital Repository,USA.2001,110,pp583-638.This book chapter is available at Iowa State University Digital Repository: http://lib.dr.iastate.edu/ge_at_pubs/110 (accessed on 10 January 2020).

Goosse H., P.Y. Barriat, W. Lefebvre, M. F. L. and V. Z.. Chapter 3 . Modelling the climate system. Introduction to climate dynamics and climate modeling*. Online textbook available at http://www.climate.be/textbook.* 2010 pp. 59–86 (accessed on 6 February 2020)

Grusson, Y. (2017). Testing the SWAT Model with Gridded Weather Data of Different Spatial Resolutions, (January). *Water 2017*, 9, 54 https://doi.org/10.3390/w9010054

Gupta, H. V., Sorooshian, S., & Yapo, P. O. (1998). Toward improved calibration of hydrologic models : Multiple and noncommensurable measures of information, *Wat Resour Res*, *34*,(4) 751–763. https://doi.org/10.1029/97WR03495.

Guzman, J. A., Moriasi, D. N., Gowda, P. H., Steiner, J. L., Starks, P. J., Arnold, J. G., & Srinivasan, R. (2015). A model integration framework for linking SWAT and MODFLOW. *Environmental Modelling and Software*, *73*, 103–116.

https://doi.org/10.1016/j.envsoft.2015.08.011

Hamududu, Byman H., & Killingtveit, Å. (2016). Hydropower production in future climate scenarios; the case for the Zambezi River. *Energies, 9(7)*. https://doi.org/10.3390/en9070502

Hamududu, Byman Hikanyona. (2012). Impacts of Climate Change on Water Resources and Hydropower Systems in central and southern Africa. *PhD Dissertation*,Norwegian University of Science and Technology,Norway http://hdl.handle.net/11250/242354 (accessed on 10 June 2018).

Handmer, J., Honda, Y., Kundzewicz, Z. W., Arnell, N., Benito, G., Hatfield, J., … Yamano, H. (2012). Changes in impacts of climate extremes: Human systems and ecosystems. *Managing the Risks of Extreme Events and Disasters to Advance Climate Change Adaptation: Special Report of the Intergovernmental Panel on Climate Change*, *9781107025*, 231–290. https://doi.org/10.1017/CBO9781139177245.007

Hawkins, B. Y. E. D., & Sutton, R. (2009). The Potential To Narrow Uncertainty in Regional Climate Predictions. *American Meteorological Society*. (August). https://doi.org/10.1175/2009BAMS2607.1

Hay, L, Robert L., A. W., & Leavesley, G. (2000). a Comparison of Delta Change and Downscaled Gcm Scenarios. *Journal Of The American Water Resources Association*, *36*(2), 387–397. https://doi.org/10.1111/j.1752-1688.2000.tb04276.x

Hosseinzadehtalaei, P. (2017). Uncertainty assessment for climate change impact on intense precipitation : how many model runs do we need ?, *Int. J. Climatol.* 37 (Suppl.1): 1105–1117.https://doi.org/10.1002/joc.5069

Hundecha, Y., Sunyer, M. A., Lawrence, D., Madsen, H., Willems, P., Bürger, G., … Yücel, I. (2016). Inter-comparison of statistical downscaling methods for projection of extreme flow indices across Europe. *Journal of Hydrology, 541*(August), 1273–1286. https://doi.org/10.1016/j.jhydrol.2016.08.033

IPCC. (2007). Climate change 2007: the physical science basis. *Intergovernmental Panel on Climate Change*, *446*(7137), 727–728. https://doi.org/10.1038/446727a.

IPCC, 2013: Climate Change 2013: The Physical Science Basis. Contribution of Working Group I to the Fifth Assessment Report of the Intergovern- mental

Panel on Climate Change [Stocker, T.F., D. Qin, G.-K. Plattner, M. Tignor, S.K. Allen, J. Boschung, A. Nauels, Y. Xia, V. Bex and P.M. Midgley (eds.)]. Cambridge University Press, Cambridge, United Kingdom and New York, NY, USA, 1535 pp

IPCC. (2014). Climate Change 2014 Synthesis Report Summary Chapter for Policymakers. *Ipcc*, 31. https://doi.org/10.1017/CBO9781107415324

Ipsos. (2015).Business daily. Zambia set to deepen power cuts after drought, 2015. Ipsos Kenya Acorn House,97 James Gichuru Road, Lavington, Nairobi, Kenya.

Javan, K., Saleh, F. N., & Shahraiyni, H. T. (2013). The Influences of Climate Change on the Runoff of Gharehsoo River Watershed. *American Journal of Climate Change*, *02*(04), 296–305. https://doi.org/10.4236/ajcc.2013.24030

Jeziorska, J., & Niedzielski, T. (2018). Applicability of TOPMODEL in the mountainous catchments in the upper Nysa Kłodzka river basin (SW Poland). *Acta Geophysica*, *66*(2), 203–222. https://doi.org/10.1007/s11600-018-0121-6

Jo, M., Carolyn, N., Dixon, K. W., & Adams-smith, D. (2019). Evaluation and improvement of tail behaviour in the cumulative distribution function transform downscaling method, *Int J Climatol.*;39 (December 2018), 2449–2460. https://doi.org/10.1002/joc.5964

Johansson, B., Andreasson, J., & Jansson, J. (2003). Satellite data on snow cover in the HBV model. Method development and evaluation. *Hydrology*, *90*(90), 32.

Jones, R G, M Noguer, D C Hassell, D Hudson, S Wilson, G Jenkins, and J F B Mitchell. 2004. “Generating High Resolution Climate Change Scenarios Using PRECIS,”.https://www.uncclearn.org/sites/default/files/inventory/undp17.pdf (Accessed on 13 March 2019).

Kalnay, E.; Kanamitsu, M.; Kistler, R.; Collins, W.; Deaven, D.; Gandin, L.; Iredell, M.; Saha, S.; White, G.; Woollen, J. Zhu, Y.; Chelliah, M.; Ebisuzaki, W.; Higgins, W.; Janowiak, J.; MoK.C., C. Ropelewski, Wang, J.; Leetmaa, A.; Reynolds, R.; Jenne, R. and J. D. (1995). Kalnay_1996_Ncep_Reanalysis.Pdf. *Bulletin of the American Meteorological Society*. Retrieved from https://journals.ametsoc.org/doi/10.1175/1520-0477%281996%29077%3C0437%3ATNYRP%3E2.0.CO%3B2

Kaluarachchi, J. J.& Smakhtin, V. U. (2008). Climate change impacts on hydrology and water resources of the Upper Blue Nile River Basin, Ethiopia. Colombo, Sri

Lanka: *International Water Management Institute*. 27p (IWMI Research Report 126)

Kapangaziwiri, E., Mokoena, M. P., Kahinda, J. M., & Hughes, D.A(2013). *ECOMAG:* An Evaluation for Use in South Africa. *WRC Report No*.,1-59. TT 555/13. ISBN 978-1-4312-0408-3

Katz, R. W., Parlange, M. B., & Naveau, P. (2002). Statistics of extremes in hydrology. *Advances in Water Resources* 25 (2002) 1287–1304. https://ral.ucar.edu/projects/extremes/Extremes/awr.pdf. (Accessed on 13 March 2018)

Keller, F, A. van Ulden, B. van den Hurk and Lenderink G (2007). A study on combining global and regional climate model results for generating climate scenarios of temperature and precipitation for the Netherlands.*Clim Dyn (2007)* 29:157–176. https://doi.org/10.1007/s00382-007-0227-z.

Khan, N., Shahid, S., Ahmed, K., & Ismail, T. (2018). Performance Assessment of General Circulation Model in Simulating Daily Precipitation and Temperature Using Multiple Gridded Datasets. *Water 2018*, 10, 1793;1-18. https://doi.org/10.3390/w10121793

Kim, J., Choi, J., Choi, C., & Park, S. (2013). Impacts of changes in climate and land use/land cover under IPCC RCP scenarios on streamflow in the Hoeya River Basin, Korea. *Science of the Total Environment*. https://doi.org/10.1016/j.scitotenv.2013.02.005

Kistler, R., Kalnay, E., Collins, W., Saha, S., White, G., Woollen, J., … Fiorino, M. (2001). The NCEP-NCAR 50-year reanalysis: Monthly means CD-ROM and documentation. *Bulletin of the American Meteorological Society*, *82*(2), 247–267. https://doi.org/10.1175/1520-0477(2001)082<0247:TNNYRM>2.3.CO;2

Kling, H., Stanzel, P., & Preishuber, M. (2014). Impact modelling of water resources development and climate scenarios on Zambezi River discharge. *Journal of Hydrology: Regional Studies*, *1*. https://doi.org/10.1016/j.ejrh.2014.05.002

Krinner G., Collins, M., R. Knutti, J. Arblaster, J.-L. Dufresne, T. Fichefet, P. Friedlingstein, X. Gao, W.J. Gutowski, T. Johns, , M. Shongwe, C. Tebaldi, A.J. Weaver and M. Wehner, 2013: Long-term Climate Change: Projections, Commitments and Irreversibility. In: Climate Change 2013: *The Physical Science Basis. Contribution of Working Group I to the Fifth Assessment Report of the*

Intergovernmental Panel on Climate Change [Stocker, T.F., D. Qin, G.-K. Plattner, M. Tignor, S.K. Allen, J. Boschung, A. Nauels, Y. Xia, V. Bex and P.M. Midgley (eds.)]. Cambridge University Press, Cambridge, United Kingdom and New York, NY, USA.

Kusangaya, S., Warburton, M. L., Archer van Garderen, E., & Jewitt, G. P. W. (2014). Impacts of climate change on water resources in southern Africa: A review. *Physics and Chemistry of the Earth, Parts A/B/C*, *67–69*, 47–54. https://doi.org/10.1016/j.pce.2013.09.014

Lian-yi, G. U. O., Qian, G. A. O., Zhi-hong, J., & Li, L. (2018). ScienceDirect Bias correction and projection of surface air temperature in LMDZ multiple simulation over central and eastern China. *Advances in Climate Change Research*, *9*(1), 81–92. https://doi.org/10.1016/j.accre.2018.02.003

Loliyana, V., & Patel, P. L. (2014). Calibration and Validation of Hydrologic Model for Yerli sub-catchment Calibration and Validation of Hydrologic Model for Yerli sub-catchment (Maharashtra,India). *Ish - Hydro 2014 International*,1-12.

Manase, G. (2010). Impact of Climate Change on Water in Southern Africa: Research on Climate Change and Water Resources in Southern Africa Report Prepared for the *Council for Scientific and Industrial Research and The Southern African Development Community (SADC)*. Cli (Vol. ISBN 978-9).

McCabe, G.J., and Markstrom, S.L. (2007), A monthly water-balance model driven by a graphical user interface: *U.S. Geological Survey* Open-File report 2007-1088, 6 p.

Meinshausen, M, Smith, S. J., Calvin, K., Daniel, J. S., Kainuma, M. L. T., & Lamarque, J. (2010). The RCP Greenhouse Gas Concentrations and their Extensions from 1765 to 2300, *Climatic Change* (2011) 109:213–241 DOI 10.1007/s10584-011-0156-z

Ministry of Energy and Water Development (2008). Zambia Integrated Water Resources Management and Water Efficiency,Implementation Plan, 182.Volume 1, Main report (2007-2030).

Molod, A., Takacs, L., Suarez, M., & Bacmeister, J. (2015). Development of the GEOS-5 atmospheric general circulation model: Evolution from MERRA to MERRA2. *Geoscientific Model Development*, *8*(5), 1339–1356. https://doi.org/10.5194/gmd-8-1339-2015

Moss, R. H., Edmonds, J. A., Hibbard, K. A., Manning, M. R., Rose, S. K., Vuuren, D. P. Van, … Wilbanks, T. J. (2010). The next generation of scenarios for climate change research and assessment. *Nature*, *463*(7282), 747–756. https://doi.org/10.1038/nature08823

Mülle, M.F.; Thompson, S.E (2015). Stochastic or statistic? Comparing flow duration curve models in ungauged basins and changing climates. *Hydrol Earth Syst Sci Discuss*, *12*, 9765–9811 https://doi.org/ 10.5194/hessd-12-9765-2015

Murthy, C. (2012) Climate change and catchment hydrology, 63–70. Book Chapter 10. Irish Climate Analysis and Research Unit (ICARUS), Department of Geography, National University of Ireland, Maynooth, Ireland. Available on http://mural.maynoothuniversity.ie/4890/1/CM_Climate_Change.pdf (accessed 10 January 2019)

Naidoo, S.(2013). Forests and Climate Change Working Paper 12 Forests, Rangelands and Climate Change in Southern Africa Forests,*Rangelands and Climate Change in Southern Africa*. Available on http://www.fao.org/3/a-i2970e.pdf. (Accessed on 20 August 2019)

Ndiritu, J. G. (2009). *Automatic Calibration of the Pitman Model Using*. *Report to the Water Research Commission.* School of Civil and Environmental Engineering University of the Witwatersrand,Johannesburg,South Africa

Neitsch, S. L., Arnold, J. G., Kiniry, J. R., & Williams., J. R. (2005). Soil and Water Assessment Tool User's Manual Version 2005. *Diffuse Pollution Conference Dublin*, 494.

Ngongondo, C.; Li, L.; Gong, L.(2013). Flood frequency under changing climate in the Upper Kafue River Basin, Southern Africa: a large scale hydrological model application. *Stoch Environ Res Risk Assess*, *27*, 1883–1898. https://doi.org/10.1007/s00477-013-0724-z

Niang, I., O.C. Ruppel, M.A. Abdrabo, A. Essel, C. Lennard, J. Padgham, and P. Urquhart, 2014: [Barros, V.R., C. B. F., D.J. Dokken, M.D. Mastrandrea, K.J. Mach, T.E. Bilir, M. Chatterjee, K.L. Ebi, Y.O. Estrada, R.C. Genova, B. G., & E.S. Kissel, A.N. Levy, S. MacCracken, P.R. Mastrandrea, and L. L. W. (2014). *Africa. In: Climate Change 2014: Impacts, Adaptation, and Vulnerability. Part B: Regional Aspects. Contribution of Working Group II to the Fifth Assessment Report of the Intergovernmental Panel on Climate Change*.

Niekerk Van et al. (2010). Chapter 4.The State of Public Science in the SADC Region.https://pdfs.semanticscholar.org/5da1/0038aa9d14c567c054c9d69e8e6cdeabf780.pdf (Accessed on 28 July 2018)

Odry, J. (2017). Comparison of Flood Frequency Analysis Methods for Ungauged Catchments in France. Geosciences 2017, 7(3), 88. https://doi.org/10.3390/geosciences7030088

Pierce, D. W., Cayan, D. R., Maurer, E. P., Abatzoglou, J. T., & Hegewisch, K. C. (2015). Improved Bias Correction Techniques for Hydrological Simulations of Climate Change. *Journal of Hydrometeorology*, *16*(6), 2421–2442. https://doi.org/10.1175/JHM-D-14-0236.1

Pitman, V. W., & Bailey, A. K. (2005). Water Resources Of South Africa, 2012 Study (WR2012),WRSM/Pitman Theory Manual. WRC Report No. TT 690/16.

Pletterbauer, F., Melcher, A., & Graf, W. (2018)**,**Climate Change Impacts in Riverine Ecosystems,. Riverine Ecosystem Management, *Aquat. Ecol Series*, 8,203–223. https://doi.org/10.1007/978-3-319-73250-3_11

Qin, X. S., & Lu, Y. (2014). Study of Climate Change Impact on Flood Frequencies: A Combined Weather Generator and Hydrological Modeling Approach*. *Journal of Hydrometeorology*, *15*(3), 1205–1219. https://doi.org/10.1175/jhm-d-13-0126.1

Randall, D.A., R.A. Wood, S. Bony, R. Colman, T. Fichefet, J. Fyfe, V. Kattsov, A. Pitman, J. Shukla, J. Srinivasan,R.J.Stouffer, A. Sumi and K.E.Taylor,(2007). Chapter 8. Cilmate Models and Their Evaluation. In: *Climate Change 2007*: The Physical Science Basis. Contribution of Working Group I to the Fourth Assessment Report of the *Intergovernmental Panel on Climate Change* [Solomon, S., D. Qin, M. Manning, Z. Chen, M. Marquis, K.B. Averyt, M.Tignor and H.L. Miller (eds.)]. Cambridge University Press, Cambridge, United Kingdom and New York, NY, USA.. https://www.ipcc.ch/site/assets/uploads/2018/02/ar4-wg1-chapter8-1.pdf (Accessed on 4 February 2019)

Refsgaard, J. C., & Storm, B. (1996). Distributed Hydrological Modelling.Chapter 3, In *Construction,Calibration and Validation of hydrological Models* (Vol. 22). https://doi.org/10.1007/978-94-009-0257-2

Riedy, C. (2011). *Climate Change*, *979*, 1–15. Institute for Sustainable Futures,

University of Technology Sydney,Australia.

Rienecker, M. M., Suarez, M. J., Todling, R., Bacmeister, J., Takacs, L., Liu, H.-C., Nielsen, J. E. (2008). The GEOS-5 Data Assimilation System-Documentation of Versions 5.0. 1, 5.1. 0, and 5.2. 0. *NASA Technical Report*, *27*(December), 118 pp.

River, D., Park, N., Basheer, A. K., Lu, H., Omer, A., Ali, A. B., & Abdelgader, A. M. S. (2016). Impacts of climate change under CMIP5 RCP scenarios on the streamflow in the Dinder River and ecosystem habitats in Dinder National Park , Sudan,. *Hydrol. Earth Syst. Sci., 20,* (August) *1331–1353, 2016* https://doi.org/10.5194/hess-20-1331-2016

Rockstrom, J., & Falkenmark, M. (2006). The New Blue and Green Water Paradigm: Breaking New Ground for Water Resources Planning and Management. *Journal of Water Resources Planning and Management, 132*(3), 129–132. https://doi.org/10.1061/(ASCE)0733-9496(2006)132:3(129)

Rodell, M., Houser, P. R., Jambor, U., Gottschalck, J., Mitchell, K., Meng, C. J., … Toll, D. (2004). The Global Land Data Assimilation System. *Bulletin of the American Meteorological Society*, *85*(3), 381–394. https://doi.org/10.1175/BAMS-85-3-381

Rouholahnejad, E., Abbaspour, K. C., Srinivasan, R., Bacu, V., & Lehmann, A. (2014). Water resources of the Black Sea Basin at high spatial and temporal resolution. *American Geophysical Union*, *50*(7), 5866–5885. https://doi.org/10.1002/2013WR014132.

Saha, S., Moorthi, S., Pan, H. L., Wu, X., Wang, J., Nadiga, S.,Goldberg, M. (2010). The NCEP climate forecast system reanalysis. *Bulletin of the American Meteorological Society*, *91*(8), 1015–1057. https://doi.org/10.1175/2010BAMS3001.1

Sandu, M.-A., & Virsta, A. (2015). Applicability of MIKE SHE to Simulate Hydrology in Argesel River Catchment. *Agriculture and Agricultural Science Procedia*, *6*, 517–524. https://doi.org/10.1016/j.aaspro.2015.08.135

SARDC. (2007). The Zambezi: Action on climate change to advance sustainable development in the Zambezi Basin. Zambezi newsletter (Vol. 7 (3)). https://www.sardc.net/imercsa/zambezi/zambezi/eng/documents/v7n3.pdf (Accessed on 12 January 2018)

Schulze R, E. (2000). Modelling Hydrological responses to land use and climate change: Southern Africa perspective, *AMBIO: A Journal of the Human Environment* 29(1), 12-22, (1 February 2000). https://doi.org/10.1579/0044-7447-29.1.12.

Simmons, A., Uppala, S, Dee, D., & Kobayashi, S. (2006). 17713-Era-Interim-New-Ecmwf-Reanalysis-Products-1989-Onwards, Newsletter Number 110 – Winter 2006/07 25-35. https://doi.org/10.21957/pocnex23c6

Sivaramanan, S. (2015). Global Warming and Climate change , causes , impacts and mitigation Global Warming and Climate change causes , impacts and mitigation, (September). Environmental Impact Assessment unit, Environmental Management & Assessment division, Central Environmental Authority, Battaramulla, Sri Lanka. https://doi.org/10.13140/RG.2.1.4889.7128

Southern African Development Community (SADC). (2014). Climate Change Adaptation: Perspectives for the Southern African Development Community (SADC), Report No. 1 for The Long Term Adaptation Scenarios Flagship Research Program (LTAS) 1 (1), 1–76.

Sukereman, A. (2015). The Needs for Integrated Water Resource Management (IWRM) Implementation Progress Assessment in Malaysia. *International Journal of Innovation, Management and Technology*, *5*(6). https://doi.org/10.7763/ijimt.2014.v5.563

Tan, Mou Leong, Gassman, P. W., & Cracknell, A. P. (2017). Assessment of Three Long-Term Gridded Climate Products for Hydro-Climatic Simulations in Tropical River Basins. *Water, 9(3),* 229,1-24. https://doi.org/10.3390/w9030229

Teodoru, C. R., Nyoni, F. C., Borges, A. V, Darchambeau, F., Nyambe, I., & Bouillon, S. (2015). Dynamics of greenhouse gases (CO_2,CH4,N_2O) along the Zambezi River and major tributaries, and their importance in the riverine, *Biogeosciences,12,2431–2453*. https://doi.org/10.5194/bg-12-2431-2015

Thorpe, A. J. (2005). Climate Change Prediction, A challenging scientific problem, *Institute of Physics*,2005,1-16. https://www.iop.org/publications/iop/archive/file_52051.pdf .(Accessed on 10 February 2019)

Thrasher, B., Maurer, E. P., McKellar, C. &, & Duffy, P. B. (2015). NASA Earth Exchange Global Daily Downscaled Projections (NEX-GDDP) 1 . Intent of

This Document and POC.https://nex.nasa.gov/nex/static/media/other/NEX-GDDP_Tech_Note_v1_08June2015.pdf (accessed on 20 January 2019)

Tomy, T., & Sumam, K. S. (2016). Determining the Adequacy of CFSR Data for Rainfall-Runoff Modeling Using SWAT. *Procedia Technology*, *24*, 309–316. https://doi.org/10.1016/j.protcy.2016.05.041

Trenberth, K. E. (n.d.). Water Cycles and Climate Change, Chapter DOI: HB_GlobalEnvChange_30 from : Book Title: Global Environmental Change Kevin (October 2011), 1–6. http://www.cgd.ucar.edu/staff/trenbert/trenberth.papers/Hydrological%20cycle Springer.pdf (Accessed on 27 August 2018)

Trzaska, S., & Schnarr, E. (2014). A Review of Downscaling Methods for Climate Change Projections. African and Latin American Resilience to Climate Change (ARCC). *United States Agency for International Development by Tetra Tech ARD*, (September), 1–42. https://doi.org/10.4236/ojog.2016.613098

Uniyal,Jha,& Verma, (2015). Assessing Climate Change Impact on Water Balance Components of a River Basin Using SWAT Model. *Water Resour Manage* (October) 29:4767–4785. https://doi.org/10.1007/s11269-015-1089-5

Uppala, S. M., Kållberg, P. W., Simmons, A. J., Andrae, U., da Costa Bechtold, V., Fiorino, M., … Woollen, J. (2005). The ERA-40 re-analysis. *Quarterly Journal of the Royal Meteorological Society*, *131*(612), 2961–3012. https://doi.org/10.1256/qj.04.176

USAID,(2011). Climate Change Adaptation in Southern Africa Climate Change Adaptation in Southern Africa. http://www.usaid.gov/sites/default/files/documents/1865/Agency%20Climate%20Change%20Adaptation%20Plan%202012.pdf. (Accessed on 26 May 2019)

Vavrus, S. J., Notaro, M., & Lorenz, D. J. (2015). Interpreting climate model projections of extreme weather events. *Weather and Climate Extremes*, *10*, 10–28. https://doi.org/10.1016/j.wace.2015.10.005

Vuuren, D. P. Van, Edmonds, J., Kainuma, M., Riahi, K., Nakicenovic, N., Smith, S. J., & Rose, S. K. (2011). The representative concentration pathways : an overview. *Climatic Change (2011)* 109:5–31 https://doi.org/10.1007/s10584-011-0148-z

Walker, S., & Road, E. (2000). The value of hydrometric information in water

resources management and flood control, *Meteorol. Appl.* 7, 387–397.

Wang, Y.; Jiang, R.; Xie, J.; Zhao, Y.; Yan, D., and Yang, S., 2019. Soil and water assessment tool (SWAT) model: A systemic review. In: Guido-Aldana, P.A. and Mulahasan, S. (eds.), Advances in Water Resources and Exploration. *Journal of Coastal Research, Special Issue* No. 93, pp. 22–30. https://doi.org/10.2112/SI93-004. ISSN 0749-0208.

Westenbroek, M. S., Kelson, V. a., Dripps, W. R., Hunt, R. J., & Bradbury, K. R. (2010). SWB — A Modified Thornthwaite-Mather Soil-Water- Balance Code for Estimating Groundwater Recharge. *U.S. Geological Survey Techniques and Methods 6-A31*, 60.

Wheater, H. S. (2008). Modelling hydrological processes in arid and semi-arid areas : an introduction to the workshop Rain Fall-Run Off Modelling. *Cambridge University Press*. pp 1-20. https://doi.org/10.1017/CBO9780511535734.002

White, P. G. (2014). A Review of Climate Change Model Predictions and Scenario Selection for impacts on Asian Aquaculture Strengthening Adaptive Capacities to the Impacts of Climate Change in Resource poor Small-scale Aquaculture and Aquatic resources-dependent Sector in the,*AquaClimate*(December 2013).

Wiston, M., & Km, M. (2018). *Journal of Climatology & Weather Weather Forecasting* : From the Early Weather Wizards to Modern-day Weather Predictions, *6*(2). https://doi.org/10.4172/2332-2594.1000229

World Meteorological Organisation (WMO) (2000). Guidelines On Performance Assessment Of Public Weather Services On Performance Assessment. *WMO/TD No. 1023*

World Bank.(2010)The Zambezi River Basin–A multi-sector investment opportunity analysis, The World Bank, 1818 H Street NW, Washington, DC 20433, USA. 1,1-204. http://documents.worldbank.org/curated/en/724861468009989838/Summary-report (accessed 12 October 2018)

Worqlul, A. W., Yen, H., Collick, A. S., Tilahun, S. A., Langan, S., & Steenhuis, T. S. (2017). Evaluation of CFSR, TMPA 3B42 and ground-based rainfall data as input for hydrological models, in data-scarce regions: The upper Blue Nile Basin, Ethiopia. *Catena*. https://doi.org/10.1016/j.catena.2017.01.019

Woyessa Ye. WE Welderufael, JDM Kinyua, G. K. & O. T. (2011). *Land-Water*

Linkages : Agent-Based Modelling Of Land Use And Its Impact On Water Resources. *WRC REPORT NO. 1753/1/10* .ISBN 978-1-4312-0083-2

Water Research Commission(WRC). (2011). The Impact of climate change on vulnerable water resources in Southern Africa. *Water Research Commission (South African)*.

Young, T., Tucker, T., Galloway, M., & Manyike, P. (2010).Climate change and health in SADC region: Review of the current state of knowledge (September). SADC: climate change and health synthesis report. http://www.sead.co.za/downloads/climate-change-2010.pdf (Accessed on 20 April 2018)

Yu & Boer, G (2014). Climate sensitivity and response. Climate *Dynamics (2003)* 20: 415–429.https://doi.org/10.1007/s00382-002-0283-3

ZAMCOM, SADC, & SARDC. (2015). *Zambezi Environmental Outlook 2015*. https://www.sardc.net/en/southern-african-news-features/sadc-launches-zambezi-environment-outlook-2015/. (Accessed on 20 January 2018).

Zhang Lu, Walker, G.R and Dawes,W.R.(2002). Water balance modelling: concepts and applications. In: McVicar, T.R., Li Rui, Walker, J., Fitz- patrick, R.W and Liu Changming (eds),*Regional Water and Soil Assessment for Managing Sustainable Agriculture in China and Australia,ACIAR Monograph* No.84,31-47

Zhang, Y., & Wurbs, R. (2018). Long-term changes in river system hydrology in Texas. *Proceedings of the International Association of Hydrological Sciences*, *379*(2006), 255–261. https://doi.org/10.5194/piahs-379-255-2018

Zhang, Z., Wang, S., Sun, G., McNulty, S. G., Zhang, H., Li, J., … Strauss, P. (2008). Evaluation of the MIKE SHE model for application in the Loess Plateau, China. *Journal of the American Water Resources Association*, *44*(5), 1108–1120. https://doi.org/10.1111/j.1752-1688.2008.00244.

Zhou S , Y. Huang1 , Y. Wei2 , and G. Wang (2015). Socio-hydrological water balance for water allocation between human and environmental purposes in catchments. *Hydrol. Earth Syst. Sci.*19, 3715–3726. https://doi.org/10.5194/hess-19-3715-2015.

APPENDICES

KABOMPO SUB BASIN AREAS

Table A1 Kabompo Sub Basin Areas

OBJECTID	GRIDCODE	Subbasin	Area(m^2)	Lat	Long_	Elev (m)	HydroID
1	1	1	63579.95	-11.3806	25.18377	1463.335	300001
2	2	2	45390.55	-11.5219	25.10548	1473.125	300002
3	3	3	19323.41	-11.5097	24.95059	1433.159	300003
4	4	4	103482.8	-11.3582	24.89257	1421.378	300004
5	5	5	47814.22	-11.6103	24.90114	1436.008	300005
6	6	6	3760.768	-11.5219	24.77727	1396.928	300006
7	7	7	77613.52	-11.4656	24.32713	1440.53	300007
8	8	8	72465.03	-11.6362	24.68304	1415.187	300008
9	9	9	84112.66	-11.6733	24.2763	1410.541	300009
10	10	10	25182.24	-11.6418	24.47135	1375.395	300010
11	11	11	61748.32	-11.7591	25.07484	1478.835	300011
12	12	12	113801.8	-11.7518	25.30728	1464.831	300012
13	13	13	103026.4	-11.8615	24.53206	1377.523	300013
14	14	14	64545.13	-11.9354	24.25341	1383.223	300014
15	15	15	28160.21	-12.0576	24.4417	1321.338	300015
16	16	16	58936.17	-12.0834	24.15118	1389.75	300016
17	17	17	4382.355	-12.164	24.35005	1257.316	300017
18	18	18	40601.93	-12.1589	24.52508	1370.926	300018
19	19	19	73103.56	-12.0025	25.14522	1358.588	300019
20	20	20	50885.74	-12.0679	25.34372	1303.205	300020
21	21	21	105117	-11.9491	25.56487	1361.105	300021
22	22	22	120188.3	-11.9948	25.79111	1376.132	300022
23	23	23	65201.82	-12.2354	24.11805	1387.343	300023
24	24	24	17334.24	-12.2315	24.37895	1268.188	300024
25	25	25	38896.59	-12.2186	25.13931	1215.071	300025
26	26	26	51298.78	-12.2789	25.28675	1242.645	300026
27	27	27	103244.8	-12.0871	24.95832	1343.755	300027
28	28	28	2657.062	-12.3483	25.09153	1147.192	300028
29	29	29	45778	-12.2814	25.53345	1279.665	300029
30	30	30	95972.32	-12.242	25.80674	1349.695	300030
31	31	31	179436.4	-12.0895	24.76562	1361.089	300031
32	32	32	34079.73	-12.429	25.04065	1189.347	300032
33	33	33	81838.9	-12.3098	23.89711	1379.108	300033
34	34	34	48053.07	-12.4314	24.03031	1348.813	300034

Continuation

OBJECTID	GRIDCODE	Subbasin	Area (m^2)	Lat	Long_	Elev(m)	HydroID
35	35	35	40424.53	-12.4718	25.62409	1243.327	300035
36	36	36	62201.26	-12.4848	25.7832	1278.09	300036
37	37	37	131854.1	-12.6171	25.89602	1275.63	300037
38	38	38	47549.03	-12.6163	25.43348	1195.523	300038
39	39	39	90121.21	-12.7943	25.51913	1213.612	300039
40	40	40	132308.2	-12.5074	25.29228	1217.791	300040
41	41	41	18402.37	-12.7955	25.26621	1169.044	300041
42	42	42	47431.58	-12.7117	24.08919	1223.72	300042
43	43	43	89079.24	-12.6247	24.23877	1243.186	300043
44	44	44	138037.9	-12.9268	25.85462	1282.524	300044
45	45	45	233706.9	-12.5869	24.84915	1195.906	300045
46	46	46	29918.53	-12.8405	25.12502	1151.706	300046
47	47	47	43924.15	-12.8885	24.8565	1149.62	300047
48	48	48	8036.874	-12.9299	25.00803	1129.501	300048
49	49	49	954.8258	-12.982	24.99226	1113.298	300049
50	50	50	110497.1	-12.9804	25.28131	1205.73	300050
51	51	51	277463.4	-12.6171	24.5009	1218.583	300051
52	52	52	89971.11	-13.0998	24.86564	1146.735	300052
53	53	53	125151.2	-12.8735	24.00373	1189.751	300053
54	54	54	75941.21	-12.957	24.23842	1167.898	300054
55	55	55	40767.18	-13.0146	24.46019	1162.639	300055
56	56	56	62500.25	-13.0853	24.56562	1143.07	300056
57	57	57	50228.02	-13.0304	24.36421	1167.339	300057
58	58	58	10076	-13.27	24.51355	1121	300058
59	59	59	154443.8	-13.1546	25.41084	1243.972	300059
60	60	60	148351.8	-13.3151	25.47141	1236.836	300060
61	61	61	35380.03	-13.3257	24.24879	1116.533	300061
62	62	62	51145.76	-13.3138	24.37561	1115.821	300062
63	63	63	49442.68	-13.4664	24.01384	1122.993	300063
64	64	64	101437.3	-13.3098	24.08748	1132.385	300064
65	65	65	46021.93	-13.3758	23.82899	1127.22	300065
66	66	66	58224.7	-13.4233	23.91349	1126.446	300066
67	67	67	3866.734	-13.6183	24.11594	1091.82	300067
68	68	68	48440.8	-13.5685	24.2778	1118.46	300068
69	69	69	93934.49	-13.5116	23.70847	1115.01	300069

Continuation

OBJECTID	GRIDCODE	Subbasin	Area(m^2)	Lat	Long_	Elev (m)	HydroID
70	70	70	28533.82	-13.712	23.78701	1101.52	300070
71	71	71	204848	-13.6094	25.35805	1195.983	300071
72	72	72	68857.38	-13.8496	25.30425	1169.624	300072
73	73	73	323.4512	-13.8958	25.07187	1130.644	300073
74	74	74	96949.54	-13.6459	25.01333	1157.368	300074
75	75	75	156993.9	-13.4928	24.54138	1161.762	300075
76	76	76	47841.42	-13.7916	24.61259	1174.327	300076
77	77	77	187206.1	-13.484	24.8921	1168.075	300077
78	78	78	715.3194	-13.8907	24.80445	1106.288	300078
79	79	79	87364.02	-13.6533	24.56673	1178.531	300079
80	80	80	15771.75	-13.8605	23.66189	1085.621	300080
81	81	81	76638.65	-13.9956	24.97415	1154.748	300081
82	82	82	55040.26	-13.8008	23.86521	1107.777	300082
83	83	83	15535.92	-13.8986	24.31186	1126.461	300083
84	84	84	2362.408	-13.9472	24.34335	1107.062	300084
85	85	85	35722.59	-14.0347	24.44879	1146.746	300085
86	86	86	15418.66	-13.9358	24.75144	1127.238	300086
87	87	87	62329.25	-14.0316	25.22399	1167.326	300087
88	88	88	79561.95	-13.7991	24.08362	1112.385	300088
89	89	89	3322.033	-14.0025	23.86162	1074.05	300089
90	90	90	111890.1	-14.0299	24.15123	1126.751	300090
91	91	91	80597.99	-14.0729	24.59157	1157.913	300091
92	92	92	9206.361	-13.9596	23.5962	1074.101	300092
93	93	93	40659.34	-13.9881	23.74844	1083.599	300093
94	94	94	48183.41	-14.1907	24.40428	1168.802	300094
95	95	95	56955.09	-14.134	23.95988	1114.854	300095
96	96	96	183462.6	-13.6613	23.52309	1097.212	300096
97	97	97	30978.67	-14.0891	23.56777	1068.078	300097
98	98	98	6299.159	-14.1249	23.44076	1052.917	300098
99	99	99	156107.6	-14.2118	24.85418	1175.663	300099
100	100	100	45741.01	-14.2311	25.24412	1168.814	300100
101	101	101	29081.06	-14.1803	23.338	1048.66	300101
102	102	102	289973	-14.5382	25.15933	1194.233	300102

APPENDIX B THE EXTRACTED BASIN FROM MOSAIC DEM

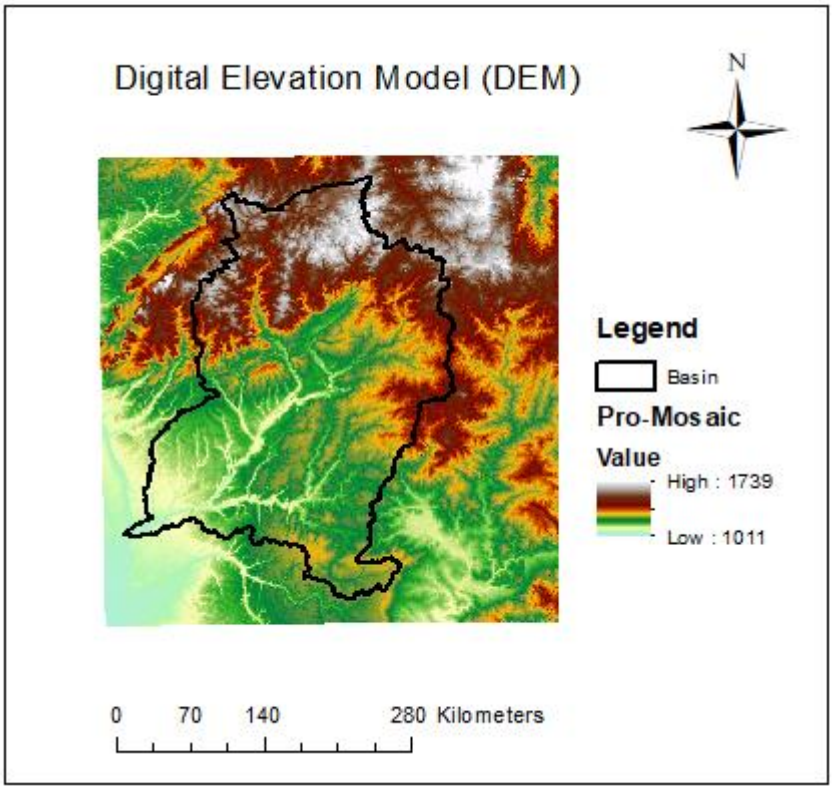

Figure B1 The extracted basin from mosaic DEM

APPENDIX C CALIBRATION AND VALIDATION DATA

Table C1 Calibration flow data 1982-1997

Month	Year	Flow(m^3/s)	Month	Year	Flow(m^3/s)
1	FLOW_OUT_1_1982	226.19	41	FLOW_OUT_5_1985	185.82
2	FLOW_OUT_2_1982	394.87	42	FLOW_OUT_6_1985	114.73
3	FLOW_OUT_3_1982	499.22	43	FLOW_OUT_7_1985	100.77
4	FLOW_OUT_4_1982	294.65	44	FLOW_OUT_8_1985	83.73
5	FLOW_OUT_5_1982	193.85	45	FLOW_OUT_9_1985	64.93
6	FLOW_OUT_6_1982	130.12	46	FLOW_OUT_10_1985	51.77
7	FLOW_OUT_7_1982	107.17	47	FLOW_OUT_11_1985	58.64
8	FLOW_OUT_8_1982	89.66	48	FLOW_OUT_12_1985	82.60
9	FLOW_OUT_9_1982	74.15	49	FLOW_OUT_1_1986	148.78
10	FLOW_OUT_10_1982	72.13	50	FLOW_OUT_2_1986	369.06
11	FLOW_OUT_11_1982	96.17	51	FLOW_OUT_3_1986	590.37
12	FLOW_OUT_12_1982	243.16	52	FLOW_OUT_4_1986	514.67
13	FLOW_OUT_1_1983	242.08	53	FLOW_OUT_5_1986	229.52
14	FLOW_OUT_2_1983	348.73	54	FLOW_OUT_6_1986	133.52
15	FLOW_OUT_3_1983	342.85	55	FLOW_OUT_7_1986	113.01
16	FLOW_OUT_4_1983	410.28	56	FLOW_OUT_8_1986	96.89
17	FLOW_OUT_5_1983	197.96	57	FLOW_OUT_9_1986	71.55
18	FLOW_OUT_6_1983	134.94	58	FLOW_OUT_10_1986	80.14
19	FLOW_OUT_7_1983	116.30	59	FLOW_OUT_11_1986	159.69
20	FLOW_OUT_8_1983	99.68	60	FLOW_OUT_12_1986	203.54
21	FLOW_OUT_9_1983	82.09	61	FLOW_OUT_1_1987	265.22
22	FLOW_OUT_10_1983	84.02	62	FLOW_OUT_2_1987	607.29
23	FLOW_OUT_11_1983	132.87	63	FLOW_OUT_3_1987	579.70
24	FLOW_OUT_12_1983	132.59	64	FLOW_OUT_4_1987	328.67
25	FLOW_OUT_1_1984	202.70	65	FLOW_OUT_5_1987	169.09
26	FLOW_OUT_2_1984	234.08	66	FLOW_OUT_6_1987	133.24
27	FLOW_OUT_3_1984	279.38	67	FLOW_OUT_7_1987	112.97
28	FLOW_OUT_4_1984	206.92	68	FLOW_OUT_8_1987	94.92
29	FLOW_OUT_5_1984	118.28	69	FLOW_OUT_9_1987	74.04
30	FLOW_OUT_6_1984	80.92	70	FLOW_OUT_10_1987	71.03
31	FLOW_OUT_7_1984	73.73	71	FLOW_OUT_11_1987	64.32
32	FLOW_OUT_8_1984	63.10	72	FLOW_OUT_12_1987	90.32
33	FLOW_OUT_9_1984	50.82	73	FLOW_OUT_1_1988	184.33
34	FLOW_OUT_10_1984	47.55	74	FLOW_OUT_2_1988	350.38
35	FLOW_OUT_11_1984	61.20	75	FLOW_OUT_3_1988	567.42
36	FLOW_OUT_12_1984	132.59	76	FLOW_OUT_4_1988	458.26
37	FLOW_OUT_1_1985	199.51	77	FLOW_OUT_5_1988	165.31
38	FLOW_OUT_2_1985	385.37	78	FLOW_OUT_6_1988	118.32
39	FLOW_OUT_3_1985	396.12	79	FLOW_OUT_7_1988	100.60
40	FLOW_OUT_4_1985	491.89	80	FLOW_OUT_8_1988	82.65

Month	Year	Flow(m^3/s)	Month	Year	Flow(m^3/s)
81	FLOW_OUT_9_1988	64.89	121	FLOW_OUT_1_1992	160.46
82	FLOW_OUT_10_1988	52.79	122	FLOW_OUT_2_1992	206.55
83	FLOW_OUT_11_1988	77.00	123	FLOW_OUT_3_1992	175.70
84	FLOW_OUT_12_1988	100.88	124	FLOW_OUT_4_1992	209.93
85	FLOW_OUT_1_1989	223.17	132	FLOW_OUT_12_1992	98.66
86	FLOW_OUT_2_1989	415.46	133	FLOW_OUT_1_1993	138.43
87	FLOW_OUT_3_1989	291.40	134	FLOW_OUT_2_1993	227.49
88	FLOW_OUT_4_1989	417.26	135	FLOW_OUT_3_1993	546.93
89	FLOW_OUT_5_1989	163.30	136	FLOW_OUT_4_1993	625.22
90	FLOW_OUT_6_1989	104.33	137	FLOW_OUT_5_1993	241.32
91	FLOW_OUT_7_1989	91.38	138	FLOW_OUT_6_1993	127.95
92	FLOW_OUT_8_1989	76.32	139	FLOW_OUT_7_1993	99.64
93	FLOW_OUT_9_1989	57.08	140	FLOW_OUT_8_1993	83.52
94	FLOW_OUT_10_1989	52.24	141	FLOW_OUT_9_1993	71.95
95	FLOW_OUT_11_1989	54.92	142	FLOW_OUT_10_1993	62.57
96	FLOW_OUT_12_1989	80.49	143	FLOW_OUT_11_1993	76.32
97	FLOW_OUT_1_1990	152.10	144	FLOW_OUT_12_1993	108.12
98	FLOW_OUT_2_1990	330.37	145	FLOW_OUT_1_1994	315.78
99	FLOW_OUT_3_1990	228.52	146	FLOW_OUT_2_1994	472.39
100	FLOW_OUT_4_1990	350.16	147	FLOW_OUT_3_1994	381.66
101	FLOW_OUT_5_1990	197.98	148	FLOW_OUT_4_1994	169.40
102	FLOW_OUT_6_1990	109.23	149	FLOW_OUT_5_1994	122.80
103	FLOW_OUT_7_1990	88.24	150	FLOW_OUT_6_1994	95.32
104	FLOW_OUT_8_1990	75.82	151	FLOW_OUT_7_1994	91.16
105	FLOW_OUT_9_1990	58.24	152	FLOW_OUT_8_1994	79.01
106	FLOW_OUT_10_1990	52.83	153	FLOW_OUT_9_1994	57.05
107	FLOW_OUT_11_1990	47.92	154	FLOW_OUT_10_1994	47.20
108	FLOW_OUT_12_1990	83.91	155	FLOW_OUT_11_1994	49.66
109	FLOW_OUT_1_1991	296.85	156	FLOW_OUT_12_1994	81.92
110	FLOW_OUT_2_1991	569.34	157	FLOW_OUT_1_1995	122.76
111	FLOW_OUT_3_1991	459.59	158	FLOW_OUT_2_1995	270.07
112	FLOW_OUT_4_1991	360.48	159	FLOW_OUT_3_1995	370.92
113	FLOW_OUT_5_1991	176.19	160	FLOW_OUT_4_1995	174.89
114	FLOW_OUT_6_1991	126.48	161	FLOW_OUT_5_1995	91.16
115	FLOW_OUT_7_1991	100.34	162	FLOW_OUT_6_1995	71.04
116	FLOW_OUT_8_1991	79.58	163	FLOW_OUT_7_1995	63.89
117	FLOW_OUT_9_1991	58.94	164	FLOW_OUT_8_1995	55.98
118	FLOW_OUT_10_1991	54.90	165	FLOW_OUT_9_1995	43.77
119	FLOW_OUT_11_1991	77.55	166	FLOW_OUT_10_1995	39.77
120	FLOW_OUT_12_1991	108.58	167	FLOW_OUT_11_1995	47.81

Month	Year	Flow(m^3/s)
168	FLOW_OUT_12_1995	83.10
169	FLOW_OUT_1_1996	127.24
170	FLOW_OUT_2_1996	193.51
171	FLOW_OUT_3_1996	370.55
172	FLOW_OUT_4_1996	247.71
173	FLOW_OUT_5_1996	111.28
174	FLOW_OUT_6_1996	89.50
175	FLOW_OUT_7_1996	73.87
176	FLOW_OUT_8_1996	60.55
177	FLOW_OUT_9_1996	47.92
178	FLOW_OUT_10_1996	38.29
179	FLOW_OUT_11_1996	47.72
180	FLOW_OUT_12_1996	86.14
181	FLOW_OUT_1_1997	197.45
182	FLOW_OUT_2_1997	273.61
183	FLOW_OUT_3_1997	299.29
184	FLOW_OUT_4_1997	265.27
185	FLOW_OUT_5_1997	131.52
186	FLOW_OUT_6_1997	89.20
187	FLOW_OUT_7_1997	73.25
188	FLOW_OUT_8_1997	61.12
189	FLOW_OUT_9_1997	49.69
190	FLOW_OUT_10_1997	45.27
191	FLOW_OUT_11_1997	56.25
192	FLOW_OUT_12_1997	129.50

Table C2 Validation flow data 1998-2005

Month	Year	Flow(m^3/s)	Month	Year	Flow(m^3/s)
1	FLOW_OUT_1_1998	386.47	41	FLOW_OUT_5_2001	209.41
2	FLOW_OUT_2_1998	468.08	42	FLOW_OUT_6_2001	141.82
3	FLOW_OUT_3_1998	667.99	43	FLOW_OUT_7_2001	123.12
4	FLOW_OUT_4_1998	532.80	44	FLOW_OUT_8_2001	106.62
5	FLOW_OUT_5_1998	205.48	45	FLOW_OUT_9_2001	85.15
6	FLOW_OUT_6_1998	134.59	46	FLOW_OUT_10_2001	67.43
7	FLOW_OUT_7_1998	118.39	47	FLOW_OUT_11_2001	98.78
8	FLOW_OUT_8_1998	99.94	48	FLOW_OUT_12_2001	137.05
9	FLOW_OUT_9_1998	75.18	49	FLOW_OUT_1_2002	210.41
10	FLOW_OUT_10_1998	64.58	50	FLOW_OUT_2_2002	371.31
11	FLOW_OUT_11_1998	66.74	51	FLOW_OUT_3_2002	330.15
12	FLOW_OUT_12_1998	114.23	52	FLOW_OUT_4_2002	343.36
13	FLOW_OUT_1_1999	290.55	53	FLOW_OUT_5_2002	192.63
14	FLOW_OUT_2_1999	466.68	54	FLOW_OUT_6_2002	139.63
15	FLOW_OUT_3_1999	584.77	55	FLOW_OUT_7_2002	120.64
16	FLOW_OUT_4_1999	556.84	56	FLOW_OUT_8_2002	95.10
17	FLOW_OUT_5_1999	189.07	57	FLOW_OUT_9_2002	76.50
18	FLOW_OUT_6_1999	130.37	58	FLOW_OUT_10_2002	64.66
19	FLOW_OUT_7_1999	114.59	59	FLOW_OUT_11_2002	76.91
20	FLOW_OUT_8_1999	92.93	60	FLOW_OUT_12_2002	112.42
21	FLOW_OUT_9_1999	71.25	61	FLOW_OUT_1_2003	308.27
22	FLOW_OUT_10_1999	64.96	62	FLOW_OUT_2_2003	371.56
23	FLOW_OUT_11_1999	70.74	63	FLOW_OUT_3_2003	503.20
24	FLOW_OUT_12_1999	112.83	64	FLOW_OUT_4_2003	640.35
25	FLOW_OUT_1_2000	146.60	65	FLOW_OUT_5_2003	224.73
26	FLOW_OUT_2_2000	205.92	66	FLOW_OUT_6_2003	142.78
27	FLOW_OUT_3_2000	490.56	67	FLOW_OUT_7_2003	122.07
28	FLOW_OUT_4_2000	316.97	68	FLOW_OUT_8_2003	102.61
29	FLOW_OUT_5_2000	140.27	69	FLOW_OUT_9_2003	77.36
30	FLOW_OUT_6_2000	102.63	70	FLOW_OUT_10_2003	62.98
31	FLOW_OUT_7_2000	88.00	71	FLOW_OUT_11_2003	73.83
32	FLOW_OUT_8_2000	75.06	72	FLOW_OUT_12_2003	128.87
33	FLOW_OUT_9_2000	59.88	73	FLOW_OUT_1_2004	246.94
34	FLOW_OUT_10_2000	47.64	74	FLOW_OUT_2_2004	330.86
35	FLOW_OUT_11_2000	63.80	75	FLOW_OUT_3_2004	539.94
36	FLOW_OUT_12_2000	186.16	76	FLOW_OUT_4_2004	588.97
37	FLOW_OUT_1_2001	410.44	77	FLOW_OUT_5_2004	245.69
38	FLOW_OUT_2_2001	695.32	78	FLOW_OUT_6_2004	151.02
39	FLOW_OUT_3_2001	762.00	79	FLOW_OUT_7_2004	126.37
40	FLOW_OUT_4_2001	637.08	80	FLOW_OUT_8_2004	106.58

Continuation

Month	Year	Flow(m^3/s)
81	FLOW_OUT_9_2004	80.63
82	FLOW_OUT_10_2004	69.82
83	FLOW_OUT_11_2004	80.75
84	FLOW_OUT_12_2004	144.55
85	FLOW_OUT_1_2005	411.07
86	FLOW_OUT_2_2005	523.88
87	FLOW_OUT_3_2005	390.02
88	FLOW_OUT_4_2005	409.26
89	FLOW_OUT_5_2005	200.84
90	FLOW_OUT_6_2005	141.52
91	FLOW_OUT_7_2005	124.81
92	FLOW_OUT_8_2005	104.85
93	FLOW_OUT_9_2005	81.48
94	FLOW_OUT_10_2005	64.63
95	FLOW_OUT_11_2005	62.71
96	FLOW_OUT_12_2005	102.96

APPENDIX D

Table D1 Gridded Rainfall from CFSR

SUBB	STATION	WLATITUDE	WLONGITU	WELEV	YRS	PCPMM1	PCPMM2	PCPMM3	PCPMM4	PCPMM5	PCPMM6	PCPMM7	MM8	PCPMM9	PCPMM10	PCPMM11	PCPMM12	MAPMM
1	114s253e	-11.3964	25.3125	1501	32	277.466	249.039	256.42	60.8631	3.36389	0.025803	0.057828	0.00	4.73544	32.2603	178.079	282.257	1344.567
2	114s250e	-11.3964	25	1410	32	334.878	293.076	298.811	70.711	3.20376	0.187245	0.09023	0.00	6.90159	44.4727	210.024	338.246	1600.602
3	114s250e	-11.3964	25	1410	32	334.878	293.076	298.811	70.711	3.20376	0.187245	0.09023	0.00	6.90159	44.4727	210.024	338.246	1600.602
4	114s250e	-11.3964	25	1410	32	334.878	293.076	298.811	70.711	3.20376	0.187245	0.09023	0.00	6.90159	44.4727	210.024	338.246	1600.602
5	117s250e	-11.7086	25	1483	32	365.747	313.601	310.731	72.0825	3.76757	0.177187	0.081432	0.00	8.03466	44.3009	226.975	355.514	1701.012
6	114s247e	-11.3964	24.6875	1355	32	347.408	298.733	295.399	69.3838	3.08105	0.301266	0.032723	0.00	7.40099	49.882	214.704	349.21	1635.536
7	114s244e	-11.3964	24.375	1503	32	311.026	267.181	265.132	64.2399	3.10302	0.216132	0.02135	0.02	6.80626	48.8126	200.922	323.261	1490.746
8	117s247e	-11.7086	24.6875	1447	32	346.494	295.549	291.211	64.6052	3.37781	0.100288	0.049406	0.00	8.57462	47.6361	219.432	342.618	1619.647
9	117s244e	-11.7086	24.375	1390	32	301.783	260.255	262.243	61.5128	2.99552	0.063461	0.028002	0.00	7.99821	48.5738	209.621	316.5	1471.574
10	117s244e	-11.7086	24.375	1390	32	301.783	260.255	262.243	61.5128	2.99552	0.063461	0.028002	0.00	7.99821	48.5738	209.621	316.5	1471.574
11	117s250e	-11.7086	25	1483	32	365.747	313.601	310.731	72.0825	3.76757	0.177187	0.081432	0.00	8.03466	44.3009	226.975	355.514	1701.012
12	117s253e	-11.7086	25.3125	1532	32	329.516	289.267	288.94	70.5882	4.0643	0.127995	0.109273	0.00	6.37856	34.6582	210.833	322.893	1557.376
13	117s247e	-11.7086	24.6875	1447	32	346.494	295.549	291.211	64.6052	3.37781	0.100288	0.049406	0.00	8.57462	47.6361	219.432	342.618	1619.647
14	120s244e	-12.0208	24.375	1240	32	291.615	248.939	254.425	57.7877	2.79545	0	0.055951	0.00	8.19511	39.4336	196.747	296.423	1396.417
15	120s244e	-12	24.375	1240	32	291.615	248.939	254.425	57.7877	2.7954	0	0.0559	0.00	8.1951	39.4336	196.747	296.423	1396
16	120s241e	-12.0208	24.0625	1404	32	300.556	260.358	266.453	62.3701	2.93761	0.134969	0.071025	0.00	8.83147	51.2744	221.308	309.26	1483.555
17	120s244e	-12.0208	24.375	1240	32	291.615	248.939	254.425	57.7877	2.79545	0	0.055951	0.00	8.19511	39.4336	196.747	296.423	1396.417
18	120s244e	-12.0208	24.375	1240	32	291.615	248.939	254.425	57.7877	2.79545	0	0.055951	0.00	8.19511	39.4336	196.747	296.423	1396.417
19	120s250e	-12.0208	25	1401	32	321.113	268.09	258.642	53.2117	2.70895	0.090176	0.053752	0.00	5.77166	24.5614	173.788	300.448	1408.479
20	120s253e	-12.0208	25.3125	1373	32	306.71	263.064	246.761	51.9158	2.80779	0.107101	0.111312	0.00	4.31082	20.577	164.253	284.461	1345.079
21	120s256e	-12.0208	25.625	1366	32	307.834	272.216	238.01	45.2025	2.50698	0.155193	0.073814	0.06	3.61082	18.7076	155.325	283.745	1327.446
22	120s259e	-12.0208	25.9375	1419	32	332.28	301.676	249.823	43.6456	2.93616	0.134271	0.034869	0.05	2.99144	17.9492	152.534	308.24	1412.296
23	123s241e	-12.333	24.0625	1419	32	299.145	255.552	255.547	54.5917	2.59852	0.058633	0.020546	0.00	7.57027	39.4852	206.43	296.296	1417.295
24	123s244e	-12.333	24.375	1240	32	280.409	233.941	231.285	43.9972	2.10191	0	0.038248	0.00	6.96057	25.2656	167.791	267.907	1259.697
25	123s250e	-12.333	25	1154	32	268.634	217.681	195.536	34.7767	1.41183	0.055093	0.029397	0.00	3.82108	12.8336	124.279	237.192	1096.25
26	123s253e	-12.333	25.3125	1232	32	264.515	216.922	185.615	32.3522	1.53559	0.079447	0.034547	0.00	2.42026	12.5298	118.773	231.072	1065.849
27	120s250e	-12.0208	25	1401	32	321.113	268.09	258.642	53.2117	2.70895	0.090176	0.053752	0.00	5.77166	24.5614	173.788	300.448	1408.479
28	123s250e	-12.333	25	1154	32	268.634	217.681	195.536	34.7767	1.41183	0.055093	0.029397	0.00	3.82108	12.8336	124.279	237.192	1096.25
29	123s256e	-12.333	25.625	1270	32	283.44	236.591	192.783	31.6458	1.50984	0.08744	0.034332	0.02	2.33234	12.9829	118.198	245	1124.623
30	123s259e	-12.333	25.9375	1331	32	298.818	264.823	208.78	32.604	1.7484	0.146771	0.019097	0.06	2.74583	13.1523	118.836	272.416	1214.148
31	120s24	-	24	1401	32	310	258	253	52	2	0	0	0.00	7	30	179	299	1392

SUBB	STATION	WLATITUD	WLONGIT	WELEV	Yrs	PCPMM1	PCPMM2	PCPMM3	PCPMM4	PCPMM5	PCPMM6	PCPMM7	MM8	PCPMM9	PCPMM10	PCPMM11	PCPMM12	MAPMM
32	123s250e	-12.333	25	1154	32	268.634	217.681	195.536	34.7767	1.41183	0.055093	0.029397	0.00	3.82108	12.8336	124.279	237.192	1096.25
33	123s238e	-12.333	23.75	1382	32	328.22	285.66	279.251	61.589	2.68832	0.147253	0	0.00	7.08185	51.1648	234.448	329.814	1580.064
34	123s241e	-12.333	24.0625	1419	32	299.145	255.552	255.547	54.5917	2.59852	0.058633	0.020546	0.00	7.57027	39.4852	206.43	296.296	1417.295
35	123s256e	-12.333	25.625	1270	32	283.44	236.591	192.783	31.6458	1.50984	0.08744	0.034332	0.02	2.33234	12.9829	118.198	245	1124.623
36	123s259e	-12.333	25.9375	1331	32	298.818	264.823	208.78	32.604	1.7484	0.146771	0.019097	0.06	2.74583	13.1523	118.836	272.416	1214.148
39	126s256e	-12.6453	25.625	1218	32	297.487	247.154	189.891	28.1901	1.30833	0.168389	0.050318	0.02	1.59353	12.2032	116.21	260.334	1154.612
40	126s253e	-12.6453	25.3125	1207	32	285.101	230.866	187.129	27.9263	1.41621	0.0725	0.018024	0.02	1.45783	11.8082	112.541	240.464	1098.817
41	126s253e	-12.6453	25.3125	1207	32	285.101	230.866	187.129	27.9263	1.41621	0.0725	0.018024	0.02	1.45783	11.8082	112.541	240.464	1098.817
42	126s241e	-12.6453	24.0625	1224	32	291.12	240.417	221.525	35.865	1.3013	0	0	0.00	6.14626	23.9805	163.612	269.459	1253.426
43	126s244e	-12.6453	24.375	1231	32	296.112	239.666	213.601	32.5204	1.2413	0	0.028217	0.00	6.20481	17.513	147.274	263.44	1217.601
44	130s259e	-12.9575	25.9375	1315	32	311.298	273.714	214.491	32.432	1.92148	0.343645	0.103641	0.08	1.56024	12.9865	123.644	292.968	1265.545
45	126s250e	-12.6453	25	1214	32	278.743	226.657	191.124	31.2589	1.67745	0.063461	0	0.00	3.21186	11.4442	117.446	235.652	1097.278
46	130s250e	-12.9575	25	1120	32	337.481	276.482	234.275	37.4349	2.1212	0.056595	0.034815	0.00	2.92999	17.1352	139.826	290.835	1338.612
47	130s250e	-12.9575	25	1120	32	337.481	276.482	234.275	37.4349	2.1212	0.056595	0.034815	0.00	2.92999	17.1352	139.826	290.835	1338.612
48	130s250e	-12.9575	25	1120	32	337.481	276.482	234.275	37.4349	2.1212	0.056595	0.034815	0.00	2.92999	17.1352	139.826	290.835	1338.612
37	126s259e	-12	25.9375	1280	32	286.887	248.944	192.937	28.5104	1.4066	0.1917	0.0754	0.08	1.8937	11.395	108.785	260.351	1141
38	126s253e	-12.6453	25.3125	1207	32	285.101	230.866	187.129	27.9263	1.41621	0.0725	0.018024	0.02	1.45783	11.8082	112.541	240.464	1098.817
49	130s250e	-12.9575	25	1120	32	337.481	276.482	234.275	37.4349	2.1212	0.056595	0.034815	0.00	2.92999	17.1352	139.826	290.835	1338.612
50	130s253e	-12.9575	25.3125	1208	32	352.475	294.31	232.302	34.8849	1.93559	0.096452	0.025427	0.03	1.22539	16.8013	140.693	307.985	1382.76
51	126s244e	-12.6453	24.375	1231	32	296.112	239.666	213.601	32.5204	1.2413	0	0.028217	0.00	6.20481	17.513	147.274	263.44	1217.601
52	130s250e	-12.9575	25	1120	32	337.481	276.482	234.275	37.4349	2.1212	0.056595	0.034815	0.00	2.92999	17.1352	139.826	290.835	1338.612
53	130s241e	-12.9575	24.0625	1188	32	298.079	240.748	195.688	25.1402	0.684875	0.015986	0	0.00	4.80883	17.3042	136.599	261.632	1180.7
54	130s244e	-12.9575	24.375	1171	32	326.47	259.556	217.298	28.8691	1.1037	0	0	0.00	4.98851	17.5284	141.202	279.577	1276.593
55	130s244e	-12.9575	24.375	1171	32	326.47	259.556	217.298	28.8691	1.1037	0	0	0.00	4.98851	17.5284	141.202	279.577	1276.593
56	130s247e	-12.9575	24.6875	1103	32	338.593	268.875	236.38	35.3407	2.1142	0	0	0.00	4.0985	18.9096	143.726	289.871	1337.908
57	130s244e	-12.9575	24.375	1171	32	326.47	259.556	217.298	28.8691	1.1037	0	0	0.00	4.98851	17.5284	141.202	279.577	1276.593
58	133s244e	-13.2697	24.375	1074	32	312.88	249.019	209.437	27.4613	0.975546	0	0.021297	0.03	3.71612	18.6379	131.733	276.035	1229.943
59	133s253e	-13.2697	25.3125	1240	32	366.605	305.465	244.515	35.7387	1.65331	0.156856	0.067002	0.03	1.33099	18.901	145.797	326.304	1446.567
60	133s256e	-13.2697	25.625	1267	32	372.647	313.757	247.67	36.9226	1.86805	0.195131	0.062656	0.03	1.47607	17.7174	148.367	337.529	1478.24
61	133s244e	-13.2697	24.375	1074	32	312.88	249.019	209.437	27.4613	0.975546	0	0.021297	0.03	3.71612	18.6379	131.733	276.035	1229.943
62	133s244e	-13.2697	24.375	1074	32	312.88	249.019	209.437	27.4613	0.975546	0	0.021297	0.03	3.71612	18.6379	131.733	276.035	1229.943
63	136s241e	-13	24.0625	1097	32	278.762	231.819	193.523	25.0446	0.668	0.0207	0.019	0.06	2.2457	19.064	124.379	257.253	1132

SUBB	STATION	WLATITUDE	WLONGITU	WELEV		PCPMM1	PCPMM2	PCPMM3	PCPMM4	PCPMM5	PCPMM6	PCPMM7		PCPMM9	PCPMM10	PCPMM11	PCPMM12	MAPMM
64	133s241e	-13.2697	24.0625	1110	32	297.42	239.01	196.04	23.64	0.75	0.04	0.02	0.00	3.47	18.37	129.47	259.17	1167.38
65	133s238e	-13.2697	23.75	1143	32	278.54	228.41	186.65	25.12	0.63	0.07	0.02	0.00	2.57	19.36	134.39	247.04	1122.82
66	133s241e	-13.2697	24.0625	1110	32	297.42	239.01	196.04	23.64	0.75	0.04	0.02	0.00	3.47	18.37	129.47	259.17	1167.38
67	136s241e	-13.582	24.0625	1097	32	278.76	231.82	193.52	25.04	0.67	0.02	0.02	0.06	2.25	19.06	124.38	257.25	1132.86
68	136s244e	-13.582	24.375	1094	32	268.65	215.61	180.78	23.31	0.74	0.00	0.03	0.07	2.08	16.35	111.59	242.38	1061.59
69	136s238e	-13.582	23.75	1125	32	287.38	237.18	198.81	25.87	0.63	0.02	0.03	0.02	1.71	21.67	129.84	261.96	1165.11
70	136s238e	-13.582	23.75	1125	32	287.38	237.18	198.81	25.87	0.63	0.02	0.03	0.02	1.71	21.67	129.84	261.96	1165.11
71	136s253e	-13.582	25.3125	1174	32	295.39	238.89	192.82	24.26	1.11	0.07	0.13	0.00	1.16	13.04	111.74	270.58	1149.20
72	139s253e	-13.8942	25.3125	1192	32	252.92	201.08	156.71	18.89	0.87	0.00	0.15	0.00	1.29	9.69	86.93	227.67	956.20
73	139s250e	-13.8942	25	1176	32	246.01	195.99	154.95	18.93	0.67	0.04	0.06	0.00	1.68	11.13	86.20	221.81	937.48
74	136s250e	-13.582	25	1200	32	276.55	218.92	181.19	23.37	1.00	0.04	0.09	0.03	1.58	12.83	104.41	247.99	1067.99
75	136s247e	-13.582	24.6875	1113	32	265.08	210.00	174.45	23.67	0.87	0.02	0.05	0.05	1.68	13.97	104.20	235.13	1029.17
76	139s247e	-13.8942	24.6875	1072	32	243.42	195.24	154.03	20.63	0.61	0.00	0.05	0.02	1.51	12.47	88.52	213.94	930.45
77	136s250e	-13.582	25	1200	32	276.55	218.92	181.19	23.37	1.00	0.04	0.09	0.03	1.58	12.83	104.41	247.99	1067.99
78	139s247e	-13.8942	24.6875	1072	32	243.42	195.24	154.03	20.63	0.61	0.00	0.05	0.02	1.51	12.47	88.52	213.94	930.45
79	136s247e	-13.582	24.6875	1113	32	265.08	210.00	174.45	23.67	0.87	0.02	0.05	0.05	1.68	13.97	104.20	235.13	1029.17
80	139s238e	-13.8942	23.75	1078	32	288.81	232.77	196.84	27.45	0.53	0.03	0.02	0.05	1.56	21.30	121.53	257.43	1148.31
81	139s250e	-13.8942	25	1176	32	246.01	195.99	154.95	18.93	0.67	0.04	0.06	0.00	1.68	11.13	86.20	221.81	937.48
82	139s238e	-13.8942	23.75	1078	32	288.81	232.77	196.84	27.45	0.53	0.03	0.02	0.05	1.56	21.30	121.53	257.43	1148.31
83	139s244e	-13.8942	24.375	1060	32	256.94	212.58	170.03	23.03	0.60	0.02	0.04	0.06	1.71	15.32	99.92	229.24	1009.48
84	139s244e	-13.8942	24.375	1060	32	256.94	212.58	170.03	23.03	0.60	0.02	0.04	0.06	1.71	15.32	99.92	229.24	1009.48
85	139s244e	-13.8942	24.375	1060	32	256.94	212.58	170.03	23.03	0.60	0.02	0.04	0.06	1.71	15.32	99.92	229.24	1009.48
86	139s247e	-13.8942	24.6875	1072	32	243.42	195.24	154.03	20.63	0.61	0.00	0.05	0.02	1.51	12.47	88.52	213.94	930.45
87	139s253e	-13.8942	25.3125	1192	32	252.92	201.08	156.71	18.89	0.87	0.00	0.15	0.00	1.29	9.69	86.93	227.67	956.20
88	139s241e	-13.8942	24.0625	1040	32	277.96	227.04	191.72	25.73	0.60	0.05	0.04	0.05	1.74	19.04	113.24	249.36	1106.56
89	139s238e	-13.8942	23.75	1078	32	288.81	232.77	196.84	27.45	0.53	0.03	0.02	0.05	1.56	21.30	121.53	257.43	1148.31
90	139s241e	-13.8942	24.0625	1040	32	277.96	227.04	191.72	25.73	0.60	0.05	0.04	0.05	1.74	19.04	113.24	249.36	1106.56
91	142s247e	-14.2064	24.6875	1195	32	268.02	224.06	173.30	22.90	0.74	0.03	0.04	0.05	1.98	13.30	95.86	234.99	1035.26
92	139s238e	-13.8942	23.75	1078	32	288.81	232.77	196.84	27.45	0.53	0.03	0.02	0.05	1.56	21.30	121.53	257.43	1148.31
93	139s238e	-13.8942	23.75	1078	32	288.81	232.77	196.84	27.45	0.53	0.03	0.02	0.05	1.56	21.30	121.53	257.43	1148.31

SUBB	STATION	WLATITUDE	WLONGITU	WELEV		PCPMM1	PCPMM2	PCPMM3	PCPMM4	PCPMM5	PCPMM6	PCPMM7		PCPMM9	PCPMM10	PCPMM11	PCPMM12	MAPMM
94	139s238e	-13.8942	23.75	1078	32	288.81	232.77	196.84	27.45	0.53	0.03	0.02	0.05	1.56	21.30	121.53	257.43	1148.31
95	142s244e	-14.2064	24.375	1134	32	270.51	228.13	181.75	23.75	0.61	0.04	0.08	0.02	1.74	15.88	100.86	237.03	1060.39
96	142s241e	-14.2064	24.0625	1121	32	276.15	227.06	184.76	24.79	0.49	0.02	0.06	0.03	1.70	17.50	102.63	242.99	1078.18
97	136s234e	-13.582	23.4375	1115	32	279.45	237.97	196.11	27.39	0.45	0.06	0.03	0.00	1.69	23.24	133.23	253.97	1153.59
98	142s234e	-14.2064	23.4375	1073	32	258.94	206.82	172.88	23.39	0.58	0.02	0.00	0.02	1.23	19.35	103.27	218.47	1004.98
99	142s250e	-14.2064	25	1132	32	269.57	226.41	166.62	21.29	0.76	0.00	0.09	0.04	1.77	11.68	93.46	238.48	1030.17
100	142s253e	-14.2064	25.3125	1166	32	262.31	215.69	159.09	20.11	0.84	0.02	0.11	0.04	1.43	8.74	87.66	234.09	990.13
101	142s234e	-14.2064	23.4375	1073	32	258.94	206.82	172.88	23.39	0.58	0.02	0.00	0.02	1.23	19.35	103.27	218.47	1004.98
102	145s253e	-14.5186	25.3125	1183	32	267.46	225.32	159.42	21.67	0.80	0.11	0.10	0.04	1.61	9.61	91.23	234.65	1012.03

APPENDIX E PRECIS (RCM) AVERAGE CLIMATE DATA 1975-2005

Table E1 PRECIS (RCM) average temperature data 1975-2005

	Temp °C		
Month	Min	Mean	Max
Jan	18.423	20.058	21.280
Feb	18.903	20.482	21.618
Mar	19.048	20.727	21.938
Apr	19.339	20.990	22.177
May	18.900	20.081	21.644
Jun	17.097	18.343	20.313
Jul	17.025	18.454	20.590
Aug	19.723	21.221	23.232
Sep	22.032	23.954	25.562
Oct	21.223	23.554	25.412
Nov	18.862	20.831	22.157
Dec	18.352	20.081	21.362

Table E2 PRECIS (RCM) average precipitation data 1975-2005

	Precip (mm/day)		
Month	Min	Mean	Max
Jan	5.46460	8.90510	11.18700
Feb	6.36850	8.44320	10.87900
Mar	3.71830	5.16270	7.60290
Apr	0.74941	1.37050	2.57330
May	0.14748	0.22789	0.38057
Jun	0.00823	0.01649	0.03720
Jul	0.00378	0.00889	0.01886
Aug	0.02104	0.10425	0.33863
Sep	0.53950	1.18790	2.47790
Oct	2.93520	4.49270	6.19000
Nov	6.21570	8.49070	10.92100
Dec	6.44120	9.80540	12.75100

APPENDIX F CRU (OBSERVED) DATA 1975-2005

Table F1 CRU Temperature (°C) data 1975-2005

Month	Min	Mean	Max
Jan	21.12900	22.60800	23.9840000
Feb	21.33200	22.84400	24.2190000
Mar	21.26500	22.75800	24.1350000
Apr	20.58400	21.89900	23.0900000
May	18.52900	19.86700	21.6520000
Jun	16.30000	17.63000	19.7290000
Jul	15.93500	17.38400	19.6840000
Aug	18.59700	20.13400	22.1190000
Sep	21.48400	23.03500	24.6810000
Oct	22.75500	24.23800	25.9840000
Nov	22.35800	23.80800	25.4420000
Dec	21.39700	22.85700	24.2580000

Table F2 CRU Precipitation 1975-2005

	Precip (mm/day)		
Month	Min	Mean	Max
Jan	6.33060	7.54300	8.80450
Feb	5.96430	6.70210	7.63380
Mar	2.03650	5.78690	7.61490
Apr	0.40194	1.76950	2.78050
May	0.03205	0.14657	0.30656
Jun	0.00000	0.00284	0.01161
Jul	0.00000	0.00137	0.03028
Aug	0.00000	0.02147	0.07128
Sep	0.04419	0.42190	0.77215
Oct	0.91093	2.21250	3.74910
Nov	3.70660	5.45260	6.41330
Dec	6.31090	7.62230	8.41710

APPENDIX G COMPARISON OF RAINFALL FOR REANALYSIS & BASELINE

Graphical rainfall comparison of reanalysis and baseline in mm/day.

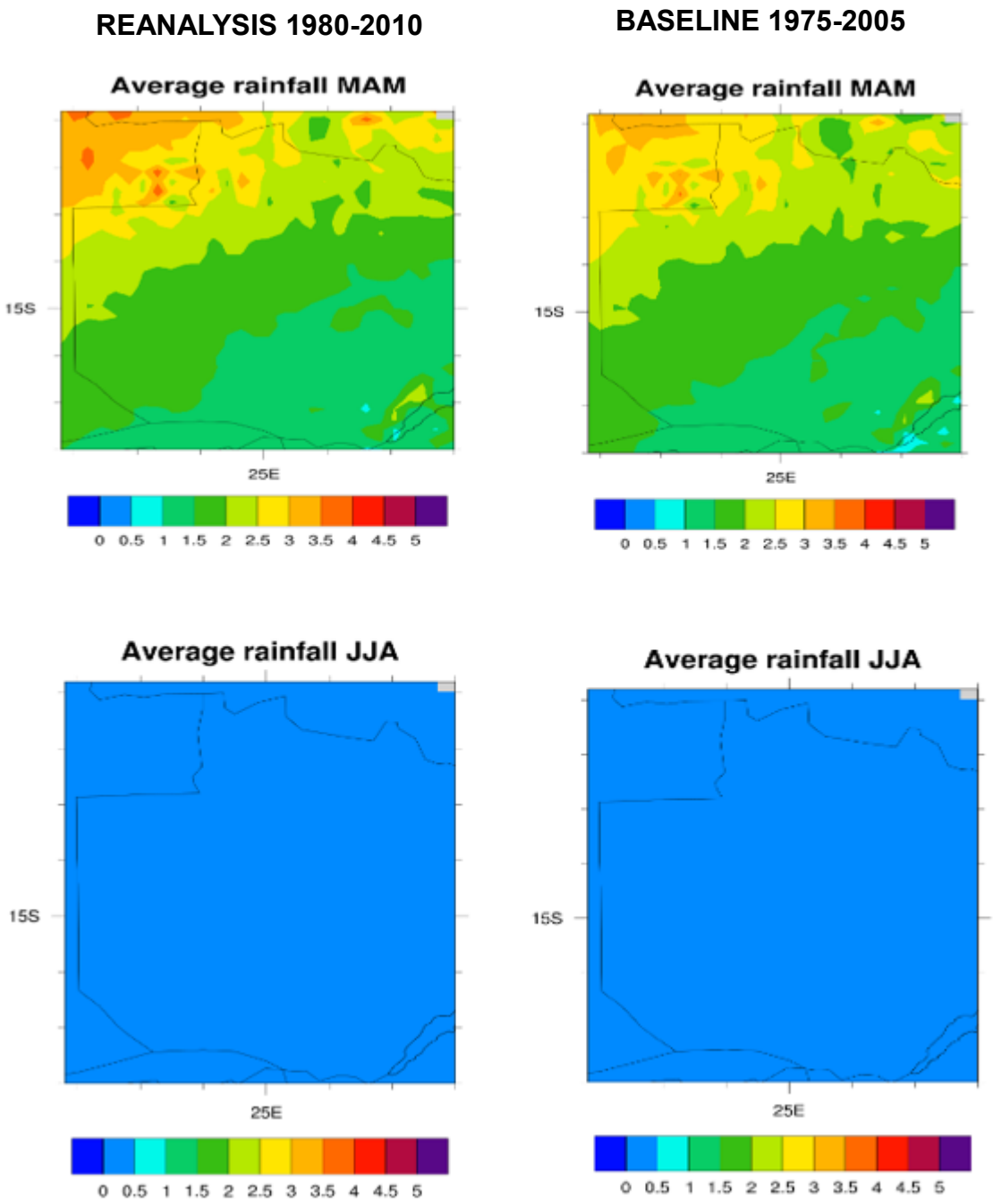

Figure G1 Graphical rainfall comparison of reanalysis & baseline for MAM & JJA

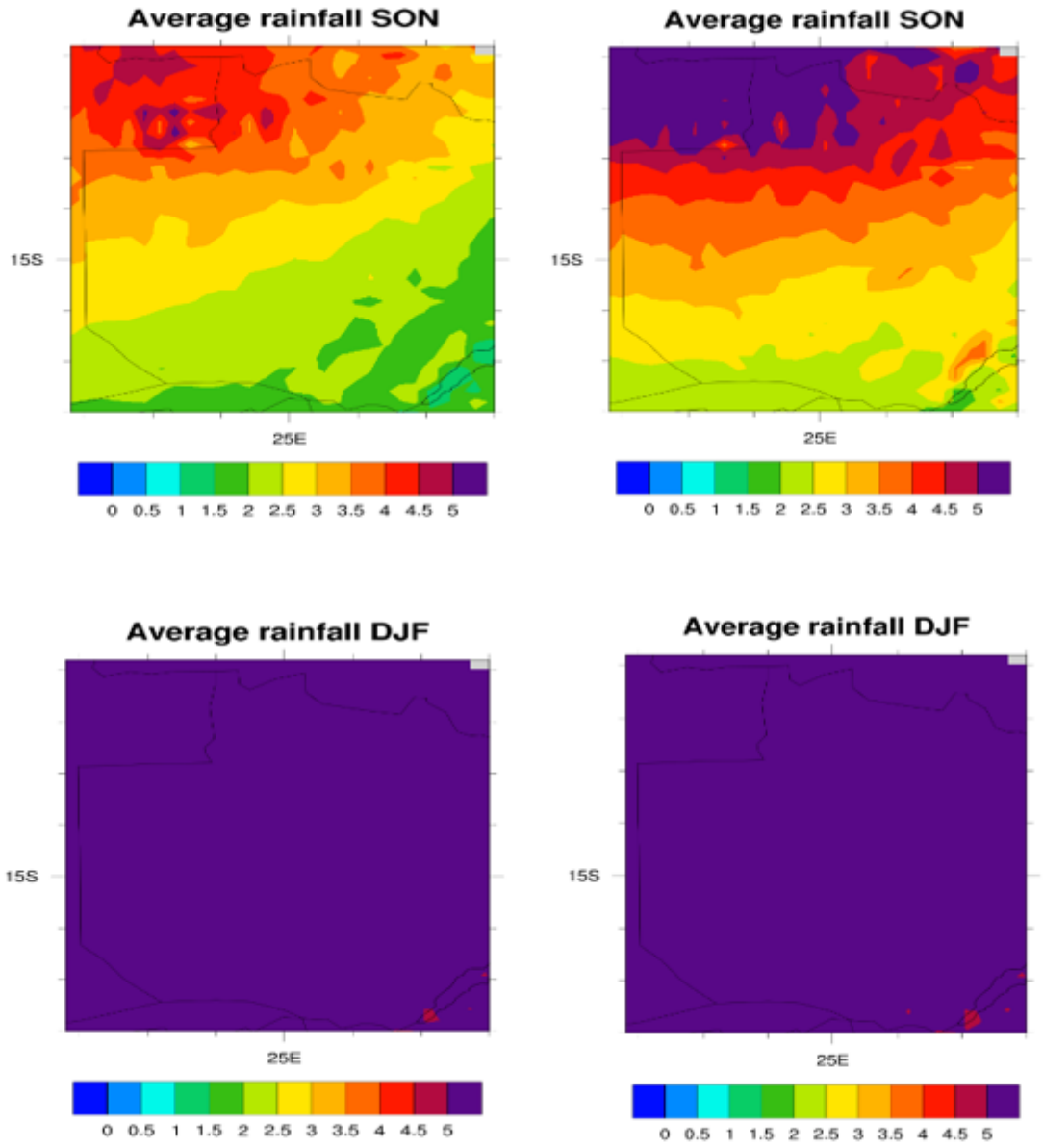

Figure G2 Graphical rainfall comparison of reanalysis & baseline for SON & DJF

APPENDIX H COMPARISON OF TEMPERATURE FOR REANALYSIS & BASELINE IN ^{O}C.

Graphical temperature comparison of reanalysis and baseline

TEMPERATURE

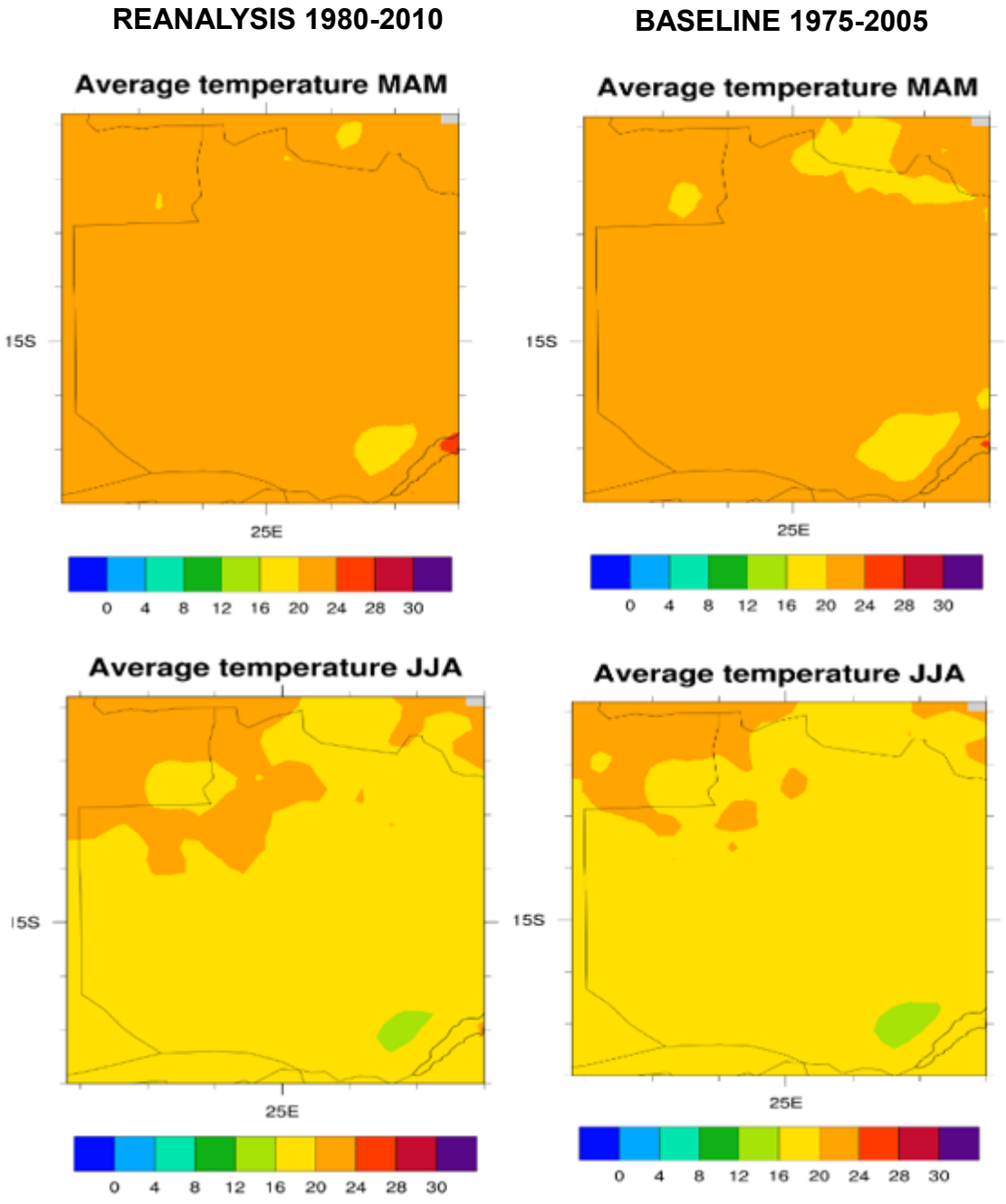

Figure H1 Graphical temp comparisons of reanalysis & baseline for MAM & JJA

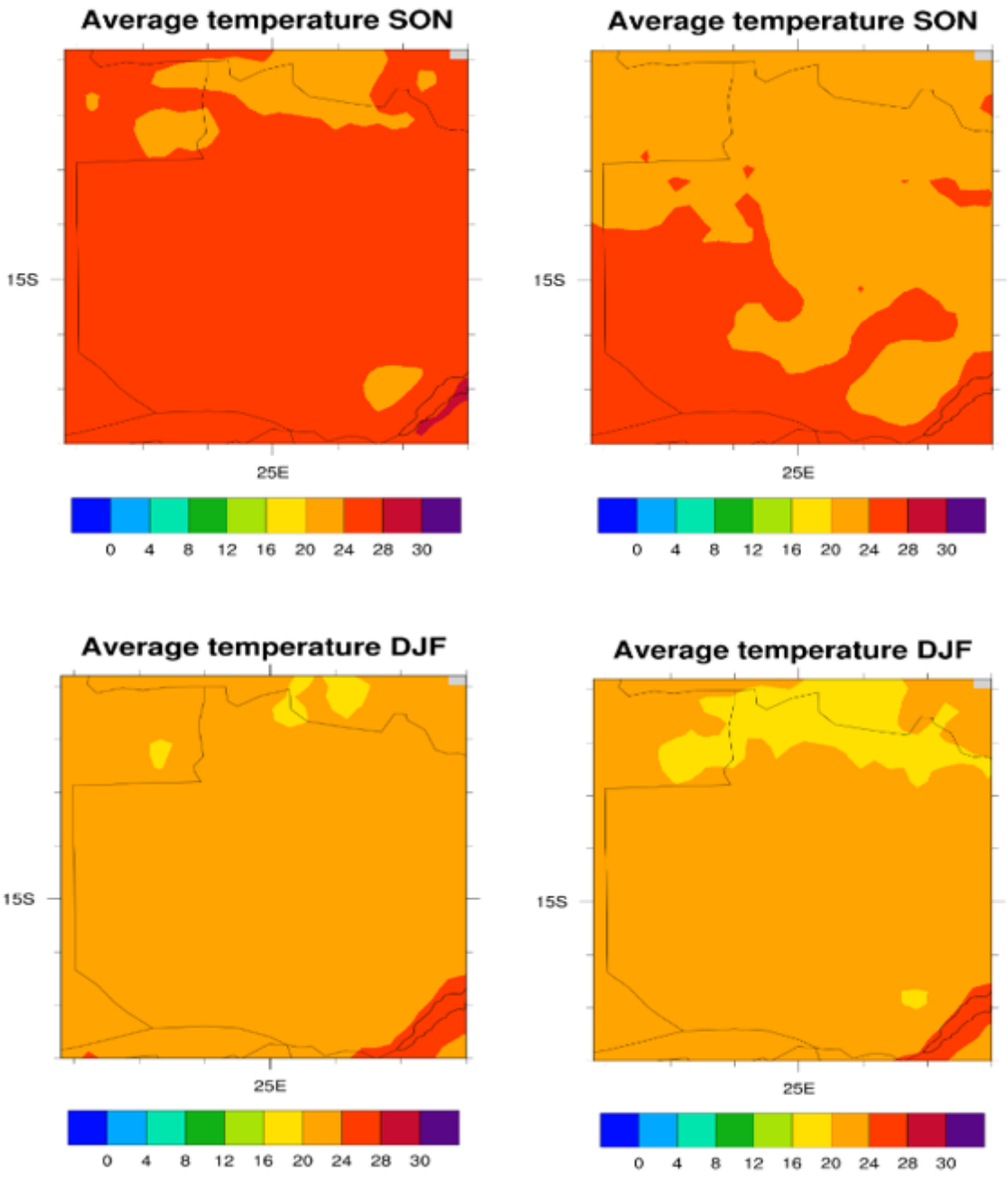

Figure H2 Graphical temp comparisons of reanalysis & baseline for SON & DJF

APPENDIX I SIMULATED RAINFALL FOR BASELINE AND RCP 4.5

Table I1 Simulated rainfall for baseline and RCP 4.5

Baseline	1975-2005		Rainfall(mm)			
Month	p_Access1-0	P_CNRM_CM5	p_ISPL_CM5A_LR	P_MIROC5	p_MPI-ESM-MR	P_MRI-CGCM3
Jan	228.52	242.75	250.31	229.88	238.07	219.4
Feb	196.82	183.34	204.73	191.56	202.16	187.04
Mar	171.62	201.02	197.09	182.72	185.69	154.2
Apr	44.22	43.85	47.84	52.77	51.65	43.93
May	0.36	0.5	0.52	0.96	1.28	0.57
Jun	0	0	0	0	0	0
Jul	0	0	0	0	0	0
Aug	0.06	0.01	0	0	0	0
Sep	7.46	6.78	5.76	7.29	7.62	8.44
Oct	78.44	88.02	79.8	80.85	82.38	69.63
Nov	204.17	186.14	196.92	196.44	199.16	187.99
Dec	240.81	242.53	244.86	246.33	238.86	239.52

RCP45	2020-2050		Rainfall(mm)			
Month	p_Access1-0	P_CNRM_CM5	p_ISPL_CM5A_LR	P_MIROC5	p_MPI-ESM-MR	P_MRI-CGCM3
Jan	234.23	239.16	280.1	254.62	238.84	198.94
Feb	178.06	204.19	207	220.85	203.11	170.23
Mar	157.02	184.96	224.73	196.12	184.06	152.14
Apr	35.2	46.1	38.39	59.86	56.9	48.98
May	0.61	0.63	0.71	0.49	0.53	0.57
Jun	0	0	0	0	0	0
Jul	0	0	0	0	0	0
Aug	0.23	0.01	0	0	0	0.05
Sep	7.56	8.48	3.94	10.18	6.39	6.46
Oct	61.8	78.93	48.25	60.66	73.62	64.95
Nov	142.16	213.66	175.64	202.16	204.79	185.59

Table I2 Simulated rainfall for RCP 8.5 (mm)

Month	p_Access1-0	P_CNRM_CM5	p_ISPL_CM5A_LR	P_MIROC5	p_MPI-ESM-MR	P_MRI-CGCM3
Jan	561.88	239.51	289.54	267.66	259.27	225.28
Feb	549.25	212.02	250	229.49	203.58	173.31
Mar	456.04	188.89	213.57	186.21	180.4	159.83
Apr	44.11	47.97	44.76	40.64	54.49	32.91
May	0	1.15	0.78	0.67	0.82	0.71
Jun	0	0	0	0	0	0
Jul	0	0	0	0	0	0
Aug	0	0.06	0	0	0	0.03
Sep	2.54	7.75	4.89	8.08	4.89	9.38
Oct	80.89	112.14	48.99	56.47	77.33	87.66
Nov	313.3	216.99	190.82	206.65	192.85	157.27
Dec	648.03	251.34	296.83	259.7	238.39	208.5

APPENDIX J SIMULATED RUNOFF FOR BASELINE

Table J1 Simulated runoff for baseline

		Runoff(mm)				
Baseline	1975-2005					
Month	p_Access1-0	P_CNRM_CM5	p_ISPL_CM5A_LR	P_MIROC5	p_MPI-ESM-MR	P_MRI-CGCM3
Jan	17	28.51	12.29	20.77	22.87	16.43
Feb	15.05	21.71	8.98	15.18	19.78	16.48
Mar	10.69	25.49	8.62	17.01	15.71	8.8
Apr	2.84	1.61	1.56	2.1	1.69	5.14
May	0	0	0	0	0	0
Jun	0	0	0	0	0	0
Jul	0	0	0	0	0	0
Aug	0	0	0	0	0	0
Sep	0	0	0	0	0	0.01
Oct	0.94	2.21	2.67	4.62	2.55	1.23
Nov	16.85	17.86	11.2	18.16	16.58	17.52
Dec	19.97	25.46	16.2	26.22	19.4	22.94

Table J2 Simulated runoff for RCP 4.5 and RCP 8.5 (mm)

RCP 4.5 (2020-2050)

RCP45	p_Access1-0	P_CNRM_CM5	p_ISPL_CM5A_LR	P_MIROC5	p_MPI-ESM-MR	P_MRI-CGCM3
Jan	19.69	22.23	18.34	29.46	22.62	16.6
Feb	14.73	22.84	11.5	25.67	17.34	13.64
Mar	10.05	18.98	12.7	21.18	19.26	9.75
Apr	1.55	2.45	0.98	4.08	3.77	1.73
May	0	0	0	0	0	0
Jun	0	0	0	0	0	0
Jul	0	0	0	0	0	0
Aug	0	0	0	0	0	0
Sep	0	0	0	0.03	0	0
Oct	0.51	1.56	0.77	0.81	3.25	0.38
Nov	6.03	25.99	6.63	22.98	21.35	16.14
Dec	23.46	31.28	21.97	25.55	23.55	21.69

RCP 8.5 (2020-2050)

Month	**p_Access1-0**	**P_CNRM_CM5**	**p_ISPL_CM5A_LR**	**P_MIROC5**	**p_MPI-ESM-MR**	**P_MRI-CGCM3**
Jan	217.77	26	21.04	35.75	30.97	23.36
Feb	224.16	22.31	16.11	26.63	18.85	14.34
Mar	184.76	19.07	14.68	17.57	19.29	11.46
Apr	2.71	2.37	1.75	1.67	1.94	0.52
May	0	0	0	0	0	0
Jun	0	0	0	0	0	0
Jul	0	0	0	0	0	0
Aug	0	0	0	0	0	0
Sep	0.22	0	0	0.02	0	0.01
Oct	2.38	11.41	0.02	0.7	3.01	1.13
Nov	108.76	35.24	13.09	24.55	19.9	10.92
Dec	274.27	27.07	26.41	31.06	22.47	15.13

APPENDIX K SIMULATED WATER YIELD FOR BASELINE

Table K1 Simulated water yield for baseline (mm)

Month	p_Access1-0	P_CNRM_CM5	p_ISPL_CM5A_LR	P_MIROC5	p_MPI-ESM-MR	P_MRI-CGCM3
Jan	50.64	49.97	50.59	52.58	56.2	45.91
Feb	44.88	39.43	42.24	43.37	49.31	42.13
Mar	40.68	35.71	43.5	45.4	45.47	32.73
Apr	23.42	19.03	24.77	21.81	21.82	22.87
May	18.97	15.71	21.27	18	18.57	15.49
Jun	18.35	15.25	20.65	17.36	18	15.02
Jul	19	15.79	21.38	17.97	18.64	15.55
Aug	19	15.8	21.39	17.98	18.64	15.56
Sep	18.39	15.3	20.69	17.41	18.05	15.08
Oct	20.74	16.61	25.38	23.36	21.89	17.47
Nov	44.4	25	41.7	44.22	43.62	39.41
Dec	55.19	53.15	54.81	61.11	54.57	53.33

Table K2 Simulated water yield for RCP 4.5 (mm)

Month	p_Access1-0	P_CNRM_CM5	p_ISPL_CM5A_LR	P_MIROC5	p_MPI-ESM-MR	P_MRI-CGCM3
Jan	49.97	56.35	59.65	64.83	56.22	43.19
Feb	39.43	53.18	45.26	58.06	46.75	36.93
Mar	35.71	48.03	50.3	52.57	48.89	33.19
Apr	19.03	23.5	24.14	26.2	23.57	18.45
May	15.71	18.96	21.77	19.87	18.65	14.97
Jun	15.25	18.41	21.15	19.28	18.06	14.49
Jul	15.79	19.06	21.9	19.96	18.7	15
Aug	15.8	19.06	21.91	19.96	18.7	15
Sep	15.3	18.46	21.19	19.37	18.1	14.53
Oct	16.61	21.73	23.31	21.39	22.38	15.86
Nov	25	53.83	35.37	50.97	48.72	38.32
Dec	53.15	66.64	61.62	61.02	59.83	51.29

Table K3 Simulated water yield for RCP 8.5 (mm)

Month	p_Access1-0	P_CNRM_CM5	p_ISPL_CM5A_LR	P_MIROC5	p_MPI-ESM-MR	P_MRI-CGCM3
Jan	284.59	60.16	64.3	71.59	65.69	51.61
Feb	284.61	53.21	54.88	59.09	47.72	38.57
Mar	244.71	48.84	53.15	47.99	48.28	35.63
Apr	42.76	23.49	26.78	21.97	21.53	16.65
May	37.09	19.31	23.34	19.39	18.55	15.36
Jun	35.99	18.69	22.62	18.82	17.89	14.89
Jul	37.26	19.35	23.43	19.49	18.52	15.41
Aug	37.27	19.35	23.44	19.49	18.52	15.41
Sep	36.22	18.73	22.67	18.89	17.93	14.94
Oct	40.21	33.28	23.71	20.59	22.08	17.66
Nov	155.15	64.19	43.33	51.78	46.76	31.41
Dec	344.73	63.42	71.54	67.63	56.37	43.29

APPENDIX L COMPARISON OF CLIMATE VARIABLES OBSERVED AND BASELINE

Table L1 comparison of climate variables observed and baseline

Rainfall 1975-2005			Temperature 1975-2005				GCM-Historical		
	Observed	Hist-Ensemble	Obs average	Obs Min	Obs Max		Max	Average	Min
Jan	245.59	234.82	22	17	28	Jan	28	23	18
Feb	197.47	194.28	22	16	28	Feb	28	23	18
Mar	185.01	182.06	22	16	28	Mar	29	23	18
Apr	50.42	47.38	21	14	29	Apr	30	23	16
May	4.17	0.70	19	10	28	May	30	21	13
Jun	0.41	0.00	16	7	26	Jun	28	19	9
Jul	0.00	0.00	16	6	27	Jul	28	19	9
Aug	0.45	0.01	19	9	29	Aug	31	21	11
Sep	7.23	7.23	22	12	32	Sep	33	24	15
Oct	50.18	79.85	24	15	33	Oct	33	25	17
Nov	136.89	195.14	23	16	30	Nov	30	24	18
Dec	227.23	242.15	22	16	28	Dec	28	23	18

APPENDIX M SIMULATED STREAMFLOW BASED ON SIX GCMs

Table M1 Simulated streamflow based on ACCESS1-0

Month	Historical	RCP45	RCP85
	m^3/s	m^3/s	m^3/s
Jan	169.82	128.06	1695.8
Feb	215.37	171.14	1605.48
Mar	224.08	186.87	1454.01
Apr	196.16	172.77	1115.9
May	155.40	140.62	903.479
Jun	131.18	119.36	600.682
Jul	114.13	102.16	364.675
Aug	98.46	87.20	256.661
Sep	87.32	77.08	209.018
Oct	83.21	73.00	203.85
Nov	90.75	72.90	317.618
Dec	124.35	93.19	1036.61

Table M2 Simulated streamflow based on P-CNRM-CM5

Month	Historical	RCP45	RCP85
	m^3/s	m^3/s	m^3/s
Jan	176.87	200.26	216.05
Feb	226.35	241.43	251.73
Mar	238.54	236.08	249.23
Apr	208.32	213.01	221.51
May	158.88	162.49	166.92
Jun	134.66	137.04	139.65
Jul	117.82	120.42	123.19
Aug	101.37	103.71	106.99
Sep	89.36	91.19	94.63
Oct	85.57	87.64	93.30
Nov	93.14	99.27	128.19
Dec	124.42	147.36	169.06

Table M3-M4 Simulated streamflow based on P-IPSL-CM5A-LR and P-MIROC5

Month	Historical	RCP45	RCP85
	m^3/s	m^3/s	m^3/s
Jan	183.26	181.86	218.58
Feb	227.49	240.18	275.04
Mar	238.30	246.05	282.32
Apr	211.78	220.89	241.83
May	162.86	165.01	176.61
Jun	136.79	138.03	144.79
Jul	119.71	121.24	127.94
Aug	103.25	104.45	112.21
Sep	91.51	92.10	99.66
Oct	87.62	86.56	94.73
Nov	95.01	89.88	98.41
Dec	133.77	119.15	146.30

	P-MIROC5		
Month	Historical	RCP45	RCP85
	m^3/s	m^3/s	m^3/s
Jan	170.36	187.04	201.95
Feb	216.50	245.46	260.81
Mar	223.11	254.42	259.32
Apr	198.52	219.10	216.36
May	156.27	166.21	163.13
Jun	133.34	139.26	137.61
Jul	116.39	122.14	121.30
Aug	99.66	105.37	105.01
Sep	87.50	92.76	92.69
Oct	83.69	88.05	87.82
Nov	94.13	97.86	94.28
Dec	123.04	130.81	130.54

Table M5 Simulated streamflow based on MPI-ESM-MR

Month	Historical	RCP45	RCP85
	m^3/s	m^3/s	m^3/s
Jan	167.53	180.26	175.86
Feb	222.36	228.40	233.01
Mar	235.71	236.41	239.39
Apr	203.88	204.85	202.65
May	158.58	158.95	157.85
Jun	134.64	134.92	134.21
Jul	117.49	117.90	117.28
Aug	100.58	101.02	100.65
Sep	88.62	88.79	88.30
Oct	84.16	84.41	83.60
Nov	90.77	91.81	94.23
Dec	122.64	125.48	123.15

Table M6 Simulated streamflow based on MRI-CGCM3-MR

Month	Historical	RCP45	RCP85
	m^3/s	m^3/s	m^3/s
Jan	147.92	137.82	126.60
Feb	192.44	171.97	173.10
Mar	200.22	181.51	182.70
Apr	181.26	167.47	167.13
May	146.47	140.09	138.35
Jun	125.14	120.73	118.89
Jul	107.84	103.29	101.40
Aug	92.37	88.12	86.56
Sep	81.36	77.73	76.41
Oct	77.37	73.27	72.92
Nov	81.11	77.56	76.47
Dec	108.59	104.00	95.01

APPENDIX N Table N1 Ranked simulated streamflow for six GCM

		Access		CNRM_CM5			IPSL_CM5A_LR			MIROC			MPI-ESM-MR			MRI-CGCM3-MR			
	Year	Hist	RCP45	RCP85	Hist	RCP45	RCP85	Hist	RCP45	RCP85	Hist	RCP45	RCP85	Hist	RCP45	RCP85	Hist	RCP45	RCP85
1	2023	312.2	153.8	4595	200	300.2	214.7	254	178.2	267.5	129.6	245.7	300.4	200.8	209.4	183.9	123.3	187.4	216.5
2	2024	263.9	151.4	2479	185	223.2	265.9	332.4	246.7	259.5	242.3	248.4	265.3	238.2	206.6	266.4	200.7	166.4	209.6
3	2025	260.2	190.2	1677	222	258.1	217	246.7	268.4	280.2	214.8	264.8	285.1	212.3	213.7	340	165.4	148.5	269
4	2026	235.4	162.3	4964	273	196.4	167.9	274.5	235	245.7	258.1	256.9	254	311.5	270.9	314.6	147.5	192.6	241.9
5	2027	230.1	312.2	5037	209	227.5	203.7	257.5	281.1	310	314.3	235.8	274.6	285.1	214.9	227.3	204.3	196.4	199.6
6	2028	227.1	197.3	1401	339	240.7	272.6	294.9	250.5	251.9	238.7	242.2	219.1	233.2	277.5	288.6	210.1	155.2	173
7	2029	225.3	176.6	923.9	240	268.2	319.6	278	220.2	272.9	199.9	332.4	279.5	241.4	299.8	199.2	147.4	153	165.7
8	2030	217.2	260.2	2319	298	241.3	310.5	249.8	246.1	254.3	213.7	246.6	301.9	210.9	273.8	255.7	214.2	134.3	283.7
9	2031	215.5	200.8	824.4	198	258.4	229.9	269.2	189	331.2	204.3	270.9	260.8	269.4	227.7	209.9	206.5	202.7	159.7
10	2032	214.2	212.6	1210	175	213.4	299.6	276.9	247.1	192.4	249.3	206.9	282.2	228.9	248.7	235.6	174.5	147.2	120.2
11	2033	212.6	194	1606	309	223.8	282.8	172.4	298.3	281.8	223.5	277.7	178.9	198.6	247.7	244.9	234.8	139.9	166
12	2034	205.1	194	1606	309	223.8	282.8	172.4	298.3	281.8	223.5	277.7	178.9	198.6	247.7	244.9	234.8	139.9	166
13	2035	202.1	214.2	1410	253	280.3	374.1	182.1	292.5	278	219.4	288.4	269.2	208.9	242.9	245.7	209.6	198.4	173.4
14	2036	200.8	183.3	1079	274	220.1	202.5	259	268.7	309.3	188.5	270.1	234.8	175.8	222.6	301.8	196.6	194.6	191.5
15	2037	197.3	225.3	2641	289	247.3	293.9	229.4	195.8	301.5	197.2	230.5	252.2	229.9	218.2	187.1	187.6	224.3	250.6
16	2038	194	227.1	3302	242	245.3	300.8	195.8	273.8	356.5	214.1	292.9	207.1	219.5	247.5	267.5	208.1	185.3	203
17	2039	194	217.2	4334	308	201.2	303.3	201.6	312.4	286.4	244.6	269.3	275.3	300.5	223.1	346.4	244.9	193.9	216.4
18	2040	190.2	163	2476	233	310.9	348.8	280.8	311.9	313.6	207.3	265.7	299.5	217.2	230.4	271.3	186.2	179.4	193.6
19	2041	184.5	167.6	1595	230	279.6	306.7	272.9	236.8	321.6	238.2	202.2	279.6	325.1	261.2	211.9	272.3	192	200.8
20	2042	183.3	235.4	2916	190	360.2	300.6	243.6	231.1	302.6	316.1	298.1	321.8	221.6	242.7	171.9	248.5	199.2	195
21	2043	176.6	202.1	814	238	273.1	223	330.9	313.9	272.3	267.4	291.5	271.9	287.1	196.3	186	299.3	297.4	199.9
22	2044	167.6	119.1	1798	162	253.3	254.8	249.5	230.2	300.8	286.2	239.1	264.8	242.3	240.5	177	172.2	319.8	168.3
23	2045	163	215.5	7163	263	200.6	244.7	229.8	227.5	226.9	243.6	276.2	257.2	256.9	269.7	317.1	185.3	207.1	146.5
24	2046	162.3	205.1	1339	221	300.1	226.2	182.8	286.3	313.9	209	281.3	252.8	205.4	256.4	290.7	232.8	202	194.9
25	2047	153.8	120.6	2058	222	237.4	286.8	210.7	318.2	345.6	189.1	301.6	269.5	251.9	291.1	258.6	265.7	189.6	153.2
26	2048	151.4	263.9	3029	345	226.4	257.5	190.9	215.7	348.2	251.4	315.8	324.1	221.7	236.5	275	186.3	213.5	144
27	2049	120.6	184.5	1343	301	251.3	322	208.6	289.9	273.1	225.9	225.8	317.7	316.9	256.3	242.3	167	203.2	170.6
28	2050	119.1	230.1	3290	310	272.5	304	261.5	233.1	341.1	249	301.9	300.2	230.6	269.2	207.6	277.5	219.7	203.8

APPENDIX O ESTIMATED COEFFICIENT OF VARIATION FOR EACH GCM

Table O1 Estimated coefficient of variation for each GCM

GCM	Access	CNRM CM5	IPSL CM5A LR	MIROC	MPI-ESM-MR	MRI-CGCM3-MR	Highest CV	Mean CV	Lowest CV
Scenario			**Historical**						
Intra-annual (CV)	0.410	0.413	0.404	0.387	0.386	0.396	0.	0.399	0.386
Inter-Annual (CV)	0.160	0.139	0.140	0.128	0.096	0.153	0.160	0.136	0.096
Scenario			**RCP4.5**						
Intra-annual (CV)	0.399	0.401	0.419	0.406	0.384	0.371	0.419	0.397	0.371
Inter-Annual (CV)	0.141	0.121	0.119	0.087	0.079	0.125	0.141	0.112	0.079
Scenario			**RCP8.5**						
Intra-annual (CV)	0.998	0.427	0.434	0.419	0.407	0.375	0.998	0.510	0.375
Inter-Annual (CV)	0.334	0.158	0.118	0.101	0.116	0.142	0.334	0.161	0.101